Advances in the reconstruction of temperature history, physiology and paleoenvironmental change: evidence from light stable isotope chemistry

A Thesis Submitted to the College of
Graduate Studies and Research
in Partial Fulfillment of the Requirements
for the Degree of Doctor of Philosophy
in the Department of Geological Sciences
University of Saskatchewan
Saskatoon

By

Christopher Martin Wurster

July 2005

Keywords: bat guano, deuterium, metabolic rate, otolith, paleoclimate, thermal behavior, stable carbon isotope, stable oxygen isotope, semi-arid

PERMISSION TO USE

In presenting this thesis in partial fulfillment of the requirements for a Postgraduate degree from the University of Saskatchewan, I agree that the Libraries of this University may make it freely available for inspection. I further agree that permission for copying of this thesis in any manner, in whole or in part, for scholarly purposes may be granted by the professor or professors who supervised my thesis work or, in their absence, by the Head of the Department or the Dean of the College in which my thesis work was done. It is understood that any copying or publication or use of this thesis or parts thereof for financial gain shall not be allowed without my written permission. It is also understood that due recognition shall be given to me and to the University of Saskatchewan in any scholarly use which may be made of any material in my thesis.

Requests for permission to copy or to make other use of material in this thesis in whole or part should be addressed to:

Head of the Department of Geological Sciences
University of Saskatchewan
Saskatoon, Saskatchewan (S7N 5E2)

ABSTRACT

The rationale of this study is to apply light stable isotope chemistry towards investigations that require temporally high-resolution data. High-resolution (or high sampling frequency) data sets, are critical for testing environmental and/or paleoenvironmental hypotheses that seek to explain processes occurring over rapid or short time intervals. The investigation of climate variation (e.g., seasonality, El Niño, deglaciation), animal migration and physiology, and disturbance ecology (e.g., fire, flooding) benefits from the recovery of proxy information at decadal to subannual resolutions. The type of material used also dictates a spatial scale. Herein are presented four studies that utilize high-resolution light stable isotope profiles with contrasting temporal and spatial scales.

The first study employs advances in three-dimensional computer-controlled micromilling to recover ~daily to weekly deposited carbonate from small (~1 cm) mollusc shells. $\delta^{18}O$ values from freshwater mollusc shells are predictably related to the local environment of growth using previously published temperature-fractionation relationships, providing a paleoclimate record of temperature and precipitation. The second study investigates variation in $\delta^{13}C$ values from *Aplodinotus grunniens* otoliths, for which high-resolution patterns were critical in assessing metabolic rate as the governing control. The third study employs high-resolution $\delta^{18}O$ and $\delta^{13}C$ values to determine chinook salmon (*Oncorhynchus tshawytscha*) seasonal and ontogenetic migration in Lake Ontario and its tributaries. Lastly, high-resolution δD and $\delta^{13}C$ values of chitin derived from Mexican free-tailed bat (*Tadarida brasiliensis*) guano are presented, providing a record of abrupt climate change. Thus, this thesis reports on promising new research avenues for paleoclimatology, paleoecology, and modern ecology.

ACKNOWLEDGEMENTS

Many people helped me to complete this body of work. I should begin by acknowledging my supervisor, Bill Patterson. I also wish to express many thanks to the rest of my examining committee, Kevin Ansdell, Keith Hobson, Chris Holmden, Len Wassenaar, and Peter Sauer for serving as the external. I feel fortunate to have had such wisdom at my disposal. I also thank Don Stewart, Don McFarlane, Jim Bowlby, and Tom Stewart as fellow collaborators.

I wish to express appreciation for comments, suggestions, and useful discussions by J. Brower J. Catterall, A. Deifendorf, E. Dufour, B. Eglington, Jixiang He, L. Ivany, M. Lachniet, K. Limburg, and A. Zazzo. I was also lucky enough to improve individual manuscripts in this thesis from reviews by S. Thorrold, David Dettman, Walter Dean, H. Foster and anonymous reviewers. Many thanks to P. Arnold, M. Cheatham, M. Kirby, T. Prokopiuk, J. Scott and I. González-Alvarez who gave much needed technical assistance, and Gerald L. Mackie, who provided species identification on the fingernail clams from Science Lake, and Peter Landre from the Cornell Cooperative Extension who kindly provided temperature and physical information on Keuka Lake. Carey Cox and Charles Faulkner from the University of Tennessee at Knoxville provided the material and helpful information on the site for chapter 3. Finally, I wish to express gratitude to Kathy and Martin Wurster for collecting water samples from Allegany State Park.

Much of this work was supported by competitive small grants to the student author, and has convinced me that such opportunities are essential. These include Geological Society of America Student Research Grants, a Karst Student Research Grant, a Syracuse University Graduate School Spring and Summer Research/Creative Project Grant, a Syracuse University John James Prucha Student Field Research Grant, a Syracuse University Graduate Summer Fellowship, a National Speleological Society Research Grant, and a Sigma Xi Student Research Grant. The National Oceanic and Atmospheric Administration (NOAA) award NA86RG0056 to the Research Foundation of the State University of New York for New York Sea Grant and a Sea Grant Scholarship Award supported chapter 4, and Sea Grant awarded a Thesis Completion Scholarship to help me finish this work.

DEDICATION

I wish to dedicate this work to my late mom Kathy. She always gave me the best in encouragement and support, and, together with my dad, gave me a love and curiosity of the living world, all the way from clams and fish to bats.

TABLE OF CONTENTS

LIST OF TABLES

LIST OF FIGURES

CHAPTER 1. GENERAL INTRODUCTION AND RATIONALE

The acquisition of light stable isotope profiles (e.g., δD, $\delta^{18}O$, $\delta^{13}C$, $\delta^{15}N$, $\delta^{34}S$) at high-resolution (i.e., high sampling frequency) benefits the investigation of environmental change that occurs over rapid and short time scales. The rationale of this study is to apply high-resolution light stable isotope profiles to problems at various spatio-temporal scales. Many fundamental environmental processes occur at time scales requiring high-resolution analysis. Seasonality, an important component of climate (Axelrod, 1992), and examination of annual or daily animal migration for example, require analysis on a subseasonal or even subdaily resolution on local to regional spatial scales (Elsdon and Gillanders, 2003). Climatic oscillations such as El Niño/ Southern Oscillation, and ecosystem disturbance (hurricanes/ flooding/ fire) also require study at annual resolution on regional spatial scales (Wang and Schimel, 2003; Tolimieri and Levin, 2004). Additionally, the study of physiological change, necessitates examination at ontogenetic and subseasonal scales (e.g., Schwarcz et al., 1998) over a very local spatial scale—that of the organism itself. On larger time scales over the geological record, abrupt climate and associated rapid ecosystem change separate stable climate modes (Rahmstorf, 2002). Analysis of such abrupt change is enabled by examining proxy information at high-resolution on local to global spatial scales (Clark et al., 2002). New technologies and techniques make it possible to gather this information.

Rapidly advancing technologies in stable isotope ratio mass spectrometry (SIRMS) and continuous-flow isotope ratio mass spectrometry (CF-IRMS) enable ever decreasing amounts of sample material to be analyzed for precise data, and faster sample throughput (Merritt and Hayes, 1994). These advances enable the derivation of ever-higher resolution records so long as analytical capabilities can be combined with advances in sampling techniques, such as the use of robotic microsampling (Dettman and Lohmann, 1995; Wurster et al., 1999), or sample-standard equilibration (Wassenaar and Hobson, 2000, 2003). Together, these improvements result in novel techniques that help solve

longstanding problems and develop new directions in studies utilizing light stable isotopic chemistry.

High-resolution light stable isotope techniques are applied to four individual investigations. Incorporated within each study is the development of proxies using advances in SIRMS and CF-IRMS and sampling protocol. In chapter 2, two modern bivalves, *Sphaerium simile* and *Dreissena polymorpha*, from two locales are micromilled to acquire subseasonal (to ~daily) $\delta^{18}O$ and $\delta^{13}C$ values. Measured $\delta^{18}O$ values can be compared to those predicted from temperature-fractionation relationships to determine if $\delta^{18}O$ values can be used as a predictor of past environments. Organisms were captured from two different sized drainage basins to compare spatial scales. Measurement of $\delta^{18}O$ and $\delta^{13}C$ values from as little as 20 µg carbonate was achieved using recent technological advances in robotic micromilling with three-dimensional sampling capabilities and SIRMS technology.

In chapter 3, robotic micromilling is used to capture the highest-resolution intra-otolith $\delta^{13}C$ values to date from freshwater drum (*Aplodinotus grunniens*) sub-fossil otoliths. Subseasonal and ontogenetic $\delta^{13}C$ values from these otoliths are essential to test the hypothesis that metabolic rate exerts the dominant control on intra-otolith $\delta^{13}C$ values.

In chapter 4, subseasonal and ontogenetic migration of chinook salmon (*Oncorhynchus tshawytscha*) in Lake Ontario are determined from $\delta^{18}O$ thermometry coupled with inferences from $\delta^{13}C$ values. Thermal histories of two chinook populations approximately a decade apart are coupled with a bioenergetic analysis to describe energetic changes in the Lake Ontario system. Thus the temporal scale of this study ranges from a decade to seasonal, and the spatial scale is the Lake Ontario system. Chapters 3 and 4 also use advances in robotic micromilling techniques and SIRMS technology.

In chapter 5, a high-resolution late Pleistocene/ early Holocene record of $\delta^{13}C$ and δD values is recovered from chitin derived from the guano of insectivorous bats. An abrupt onset of a new climate mode for the southwest United States is inferred. Thus a very different temporal and spatial scale is employed in this chapter relative to those described above. Abrupt climate change is inferred from a rapid rise in $\delta^{13}C$ and δD

values occurring over less than 100 radiocarbon years. Bats consumed insects over a large spatial scale, and these insects record riparian ecosystem changes related to climate fluctuations. In this chapter, emerging technologies in CF-IRMS that permit routine online high-temperature pyrolysis of organic compounds (Burgoyne and Hayes, 1998), and recent methodological advances to correct for non-exchangeable δD values of samples with the precision necessary for such a study are employed (Wassenaar and Hobson, 2000, 2003).

This thesis is written in a manuscript format where chapters 2 through 5 are formatted for publication in peer-reviewed journals. Three of these chapters (chapters 2, 3, and 4) are published.

Chapter 2 is published in the Journal of Paleolimnology by authors C. M. Wurster and W. P. Patterson, and is entitled "Seasonal variation in stable oxygen and carbon isotope values recovered from modern lacustrine freshwater molluscs: Paleoclimatological implications for sub-weekly temperature records." Journal of Paleolimnology 26(2): 205-218, and reprinted with kind permission of Springer Science and Business Media.

Chapter 3 is published in the Journal of Paleobiology by authors C. M. Wurster and W. P. Patterson and is entitled "Metabolic rate of late Holocene freshwater fish: evidence from $\delta^{13}C$ values of otoliths." Paleobiology 29(4): 492-505, and reprinted with kind permission of the Paleontological Society.

Chapter 4 is published in the Canadian Journal of Fisheries and Aquatic Sciences by authors C. M. Wurster, W. P. Patterson, D. J. Stewart, J. N. Bowlby, and T. J. Stewart and is entitled "Thermal histories, stress, and metabolic rates of Chinook salmon in Lake Ontario: evidence from intra-otolith $\delta^{18}O$ and $\delta^{13}C$ values." Canadian Journal of Fisheries and Aquatic Sciences 62(3): 700-713, and reprinted with kind permission of the National Research Council of Canada.

Chapter 5 is envisioned, with appropriate formatting changes, to be submitted to a high quality journal. A final chapter, chapter 6, is included as a general discussion, which links the themes of these separate chapters.

CHAPTER 2. Seasonal variation in stable oxygen and carbon isotope values recovered from modern lacustrine freshwater molluscs: Paleoclimatological implications for sub-weekly temperature records[1]

2.1 Introduction

Stable isotope values of accretionary biogenic carbonate have been used to evaluate paleoenvironmental conditions since the idea was first proposed by Harold Urey over 50 years ago (Urey, 1947). Environmental variables such as temperature and $\delta^{18}O_{(H_2O)}$ values have been derived from $\delta^{18}O_{(CaCO_3)}$ values from a variety of materials including molluscs (e.g., Dettman and Lohmann, 1993; Klein et al., 1996), corals (e.g., Linsley et al., 1994; Leder et al., 1996; Beck et al., 1997), ostracodes (e.g., Xia et al., 1997), and more recently fish otoliths (e.g., Kalish, 1991a,b; Patterson et al., 1993; Patterson, 1998). In addition to environmental records, these materials yield information on physiology (e.g., Wefer and Berger, 1991; Campana, 1999). $\delta^{13}C$ values likely record trophic position and/or metabolic rate, as well as the dissolved inorganic carbon (Tanaka et al., 1986; Schwarcz et al., 1998; Dettman et al., 1999). Recent technological advances permit microsampling of carbonate to obtain records with sub-annual (Dettman and Lohmann, 1995; Wurster et al., 1999) and even daily resolution (this paper). Therefore, micromilling of accretionary biogenic carbonate yields ontogenetic variation in $\delta^{18}O$ and $\delta^{13}C$ values that can be used to characterize the environment and physiology of the $CaCO_3$ secreting organism.

Well-preserved fossil accretionary biogenic carbonates are common in both geological and archaeological settings. These fossils can provide quantitative information on temperature variability in paleoclimate studies (e.g., Dettman and Lohmann, 1993;

[1] Wurster, C. M., and W. P. Patterson, 2001. Seasonal variation in stable oxygen and carbon isotope values recovered from modern lacustrine freshwater molluscs: Paleoclimatological implications for sub-weekly temperature records. Journal of Paleolimnology 26(2): 205-218. Reprinted with kind permission of Springer Science and Business media.

Steuber, 1996; Patterson, 1998). However, shell carbonate must be deposited at or near oxygen isotope equilibrium in order to differentiate between environmental and intrinsic organism variation. In this paper 'equilibrium' is defined as a reasonable temperature-fractionation relationship to the environmental variables (temperature and $\delta^{18}O_{(H_2O)}$ value) according to well-defined, empirically derived equations.

Disequilibrium precipitation has been reported for many biogenic carbonates, and is usually attributed to kinetic factors related to rapid growth (McConnaughey, 1989a,b; Rahimpour-Bonab et al., 1997). However, marine molluscs generally precipitate under equilibrium conditions (e.g., Wefer and Berger, 1991; Klein et al., 1996). Relatively few studies have focused on freshwater bivalves (Fastovsky et al., 1993). In the limited number of studies on $\delta^{18}O$ values of modern freshwater bivalves, some researchers have found equilibrium with the environment (Tevesz et al., 1996; Dettman et al., 1999), while other studies conclude disequilibrium precipitation (Fastovsky et al., 1993; von Grafenstein et al., 1999). Some of these studies consider whole shell growth, assume shell growth of the animal through the winter, and/or assume the variation in the $\delta^{18}O_{(H_2O)}$ value of the ambient water. High-resolution sampling provides a means to evaluate these assumptions, because seasonal patterns revealed by the micromilling of modern mollusc shells can be compared to seasonal meteorological records.

Sub-weekly variation in $\delta^{18}O_{(CaCO_3)}$ values are a function of changing $\delta^{18}O_{(H_2O)}$ values and temperature; therefore, variation in $\delta^{18}O_{(H_2O)}$ value related to individual storm events might be recorded in $\delta^{18}O_{(CaCO_3)}$ values if the hydrology of the basin responds to such storms. This provides a technique to evaluate paleostorminess if fossil shells from appropriate basins are analyzed. Storminess is an important component of climate and is often associated with the mean position of the circumpolar vortex (Lamb, 1995). However, only large destructive storms are usually preserved in paleo-records generally in the form of disrupted sediment (e.g., Lamb, 1995; Hass, 1996). Developing a means with which to evaluate the more subtle components of storms (such as temperature and origin of moisture) would be an important breakthrough in paleoclimate studies.

We present high-resolution $\delta^{18}O$ and $\delta^{13}C$ values from two modern lacustrine mollusc shells. These values are compared to predicted $\delta^{18}O_{(CaCO_3)}$ values in order to test whether

the carbonate was deposited in equilibrium with the environment. In addition, we examine the hypothesis that shells deposited in relatively small lake basins are more likely to record high-resolution perturbations in the $\delta^{18}O_{(H_2O)}$ value (including storminess), while larger lake basins with a relatively constant $\delta^{18}O_{(H_2O)}$ value throughout the year are appropriate for characterizing seasonality of temperature.

2.2 Methods

2.2.1 Study area, materials, and $\delta^{18}O_{(H_2O)}$ analysis

Science Lake is a small (1.4 hectares, 10 m deep) man-made lake located within Allegany State Park, New York on the Allegheny Plateau at 565 m elevation (Figure 2.1) Air temperatures were measured at a nearby weather station (460 m elevation). A 2-week running average is assumed to represent surface water temperature for the purpose of comparing high-resolution data. From March 1998-October 1999, surface water samples were collected approximately once a month from the north edge of the lake in Nalgene™ containers, and sealed until analyzed for $\delta^{18}O_{(H_2O)}$ values. Live fingernail-clams (*Sphaerium* sp., Sphaeriidae) were collected from the upper 6 cm of sediment from Science Lake (at less than 0.5 m water depth) on October 3, 1999. The specimen selected for stable isotope analyses was older than 1 year because 1 seasonal band was located. Younger specimens generally have higher growth rates (Jones et al., 1989), making a higher-resolution study possible.

Keuka Lake, located in central New York at 216 m elevation, is the third largest Finger Lake in surface area (4,700 hectares) and volume (Figure 2.1). Keuka Lake has a watershed of 45,070 hectares. Water temperature was measured 9 times in 1998 and 8 times in 1999 from April through December (Peter Landre, *Pers. Comm*.). Surface water samples were collected 9 times during 1998-1999 in high-density Nalgene™ containers, and sealed until analyzed for $\delta^{18}O_{(H_2O)}$ values (Table 2.1). Living zebra mussels (*Dreissena polymorpha*) aged 1-2 years, were collected on October 31, 1999 from a depth less than 0.5 m on the west central side of Keuka Lake (Figure 2.1).

$\delta^{18}O_{(H_2O)}$ values were determined using a Finnigan HDO-II water equilibration device

Table 2.1—Keuka lake $\delta^{18}O_{(H_2O)}$ values.

Location of Sample	Date of Sample	$\delta^{18}O_{(H_2O)}$ Value
Outlet	7/1/1998	-8.0
Outlet	7/16/1998	-8.1
Outlet	2/20/1999	-8.1
Outlet	7/27/1999	-7.8
Outlet	8/15/1999	-7.9
Outlet	9/5/1999	-7.5
Mid Lake	7/1/1998	-8.2
South End	7/1/1998	-8.0
South End	10/31/1999	-8.0
Average Value	------	-8.0±0.2

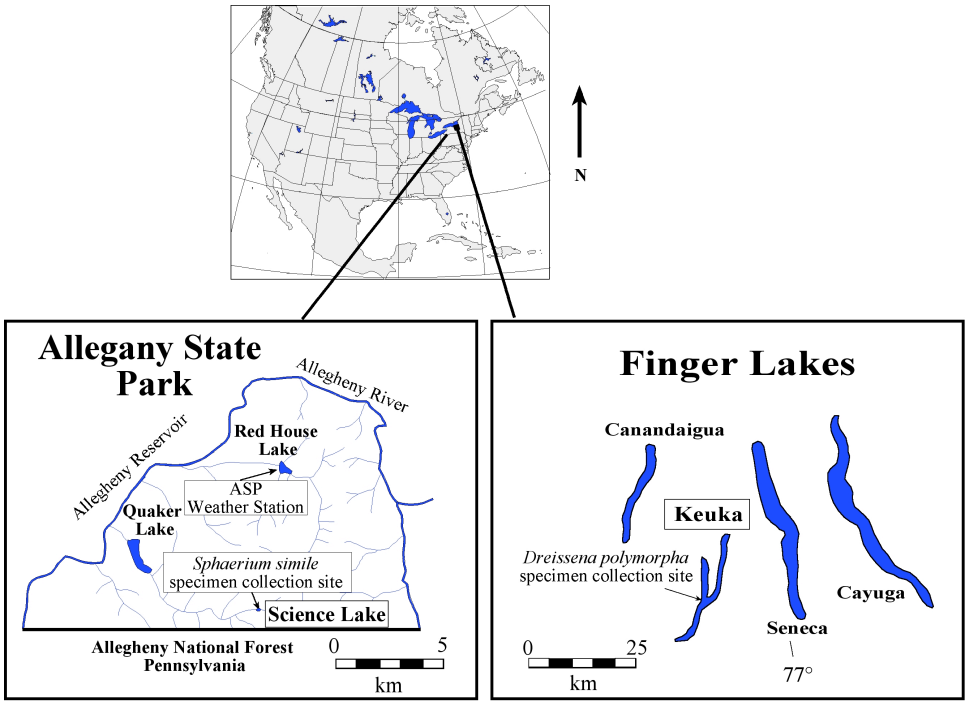

Figure 2.1—Study area of selected study molluscs.

The fingernail clam (*Sphaerium simile*) was collected on the north end of Science Lake, a small watershed located in Allegany State Park, New York. The zebra mussel (*Dreissena polymorpha*) was collected on the west-central side of Keuka Lake, New York (the third largest Finger Lake). Note the different scales of each location.

directly coupled to a Finnigan MAT 252 gas ratio mass spectrometer. Standard CO_2 gas is equilibrated with water samples for 6 hours at 25°C and then sequentially analyzed. Values are reported to ±0.1‰. Replicate analyses of water samples were within ±0.1‰.

2.2.2 High-resolution sampling and stable isotope analysis of carbonate

One valve from each mollusc was mounted to a computer-controlled micromilling stage. Three-dimensional coordinates were digitized in real-time using growth features as a guide. Using x-y-z coordinates it is possible to sample the whole valve without sectioning (Figure 2.2). A cubic spline best fit through the coordinates provides "smooth" digitized paths that accurately represent growth features, between which intermediate paths were interpolated. The computer-controlled stage moved along sample paths as a micro burr mills carbonate parallel to growth banding. Typical sample path widths are 20 μm, and typical depths are 40 μm. Care was taken not to mill below the prismatic layer into the nacreous layer which might represent precipitation at another time. A detailed description of the micromilling apparatus and methodology is presented in Wurster et al. (1999).

A fingernail clam (*Sphaerium simile*) from Science Lake was micromilled such that 175 consecutive carbonate samples were isolated over 5 mm of shell growth. $\delta^{18}O$ and $\delta^{13}C$ values were determined for 155 of these carbonate samples. Similarly, a zebra mussel from Keuka Lake was micromilled, yielding 277 individual carbonate samples over 14 mm of shell growth. A subset of 206 samples was analyzed for $\delta^{18}O$ and $\delta^{13}C$ values. Carbonate samples were roasted *in vacuo* for 1 hour at 200°C. Samples were analyzed using an automated carbonate preparation device. Individual samples of carbonate were analyzed with standard precision of ±0.08‰ (1σ). The minimum estimated sample mass was ~20 μg.

2.2.3 Calculation of predicted $\delta^{18}O_{(CaCO_3)}$

In order to calculate predicted $\delta^{18}O_{(CaCO_3)}$, the temperature and $\delta^{18}O_{(H_2O)}$ value must be known. Because water temperature closely tracks air temperature (e.g., McCombie, 1959; Edinger et al., 1968; Dingman, 1972; Webb, 1974; Livingstone and Lotter, 1998; Patterson, 1998), water temperatures for Science Lake were calculated from air

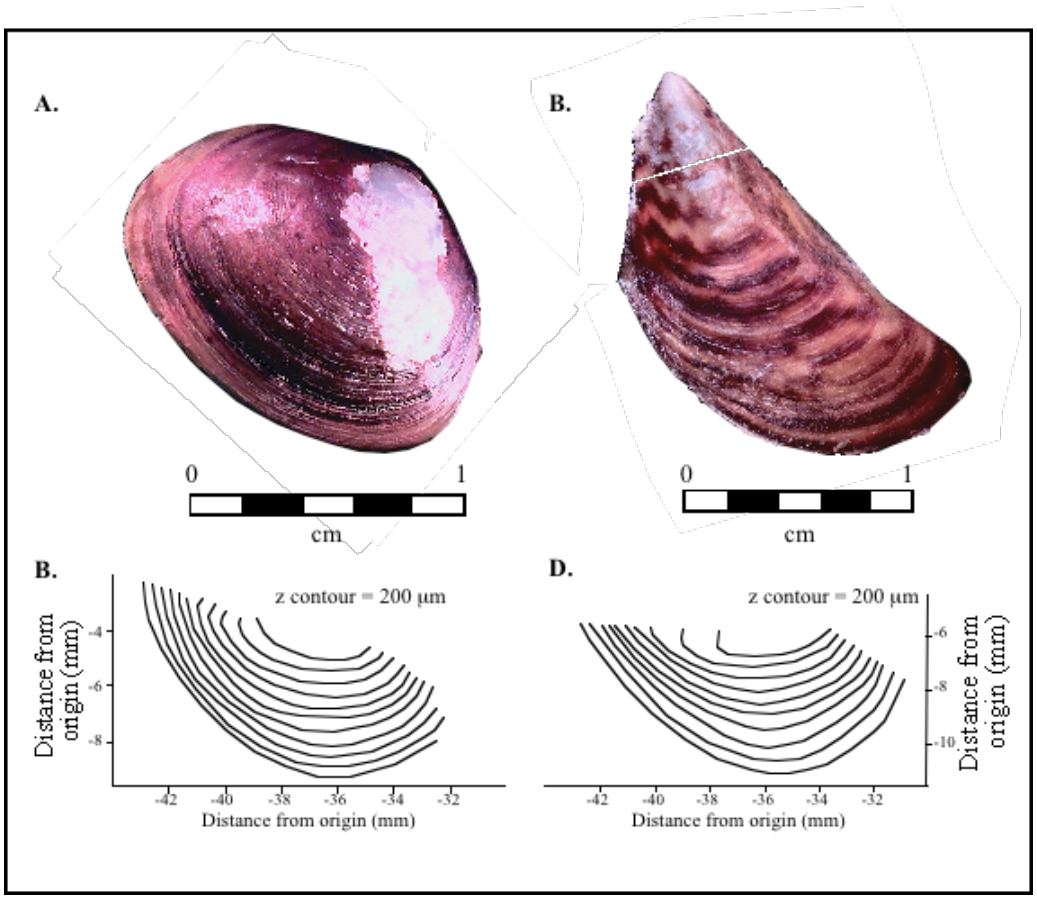

Figure 2.2—Digital images and path coordinates of study mollusc shells.

A. Digital image of the sampled *Sphaerium simile*; B. illustration of a portion of the morphology of *Sphaerium simile* determined using digital path coordinates C. Digital image of *Dreissena polymorpha*; D. illustration of a portion of the morphology of *Dreissena polymorpha* determined using digital path coordinates.

temperatures measured at the Allegany State Park (ASP) weather station (Figure 2.1). Air temperature variation is muted by the thermal inertia of water, therefore water temperature was estimated using a 2-week running average of air temperature.

Predicted equilibrium values were calculated from two empirical temperature-fractionation relationships published for aragonite. Grossman and Ku (1986) determined the relationship:

$$T(°C) = 20.6 - 4.34(\delta^{18}O_{(CaCO_3)} - \delta^{18}O_{(w)}) \quad (2.1)$$

where $\delta^{18}O_{(w)}$ is the $\delta^{18}O_{(H_2O)}$ relative to the VSMOW standard subtracted by 0.2‰ in order to relate to the VPDB standard. We use the modified equation derived by Dettman et al. (1999) from the tabulated data in Grossman and Ku (1986), which yields temperature directly from the fractionation factor.

$$10^3 \ln(\alpha) = 2.559(10^6 T(K)^{-2}) + 0.715 \quad (2.2)$$

where

$$\alpha = (1000 + \delta^{18}O_{(CaCO_3)} / 1000 + \delta^{18}O_{(H_2O)}) \text{ SMOW} \quad (2.3)$$

For comparative purposes, we also predict $\delta^{18}O$ values using the temperature-fractionation relationship developed by Patterson et al. (1993), specifically for aragonitic otoliths of freshwater fish.

$$10^3 \ln(\alpha) = 18.56(10^3 T(K)^{-1}) - 33.49 \quad (2.4)$$

where α is calculated as in equation (2.3). Equation (2.4) predicts values ~0.6‰ lower than equation (2.2) over the range of $\delta^{18}O_{(H_2O)}$ values and temperature discussed herein

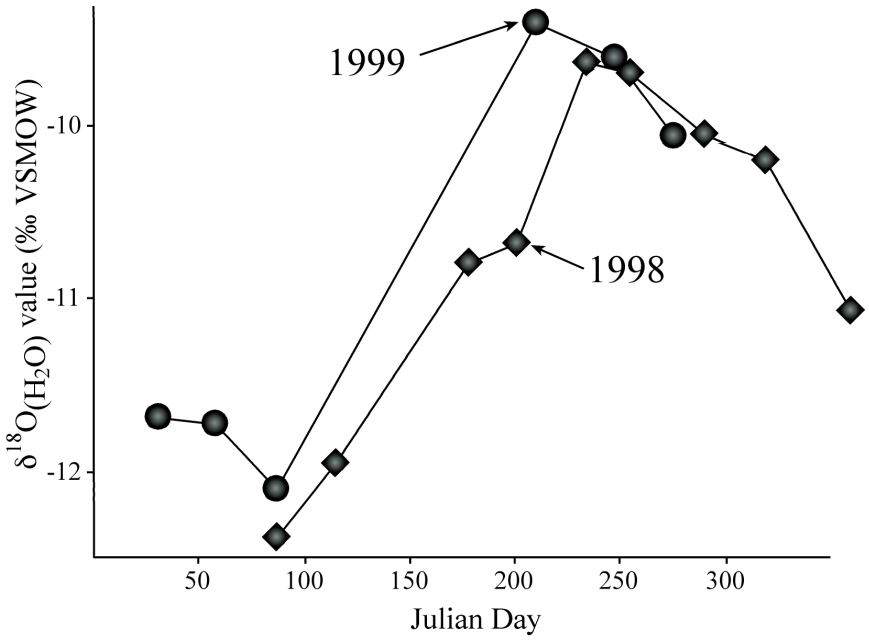

Figure 2.3—$\delta^{18}O_{(H_2O)}$ values measured from Science Lake.

Note that samples were not collected between March and July of 1999.

(for a given $\delta^{18}O_{(H_2O)}$ value, this corresponds to 2.5-3°C).

Because of the seasonal change in Science Lake $\delta^{18}O_{(H_2O)}$ values, daily $\delta^{18}O_{(H_2O)}$ values were interpolated using a cubic spline best fit to existing data in order to calculate daily $\delta^{18}O_{(CaCO_3)}$ value with which to more easily compare with the $\delta^{18}O_{(mollusc)}$ values. Individual storm events will not be tracked by this assumption, and more variation is expected. For Keuka Lake, $\delta^{18}O_{(H_2O)}$ values were relatively constant (Table 2.1).

2.3 Results

2.3.1 $\delta^{18}O_{(H_2O)}$ values of Science and Keuka Lake

Science Lake $\delta^{18}O_{(H_2O)}$ values range from –9.4 to –12.4‰$_{(VSMOW)}$ with each year (1998 and 1999) displaying a similar amplitude and pattern. In 1999, $\delta^{18}O_{(H_2O)}$ values were 0.2‰ higher than 1998 at both the seasonal minima and maxima (August and March, respectively). The total seasonal variation for this small lake and watershed in both 1998 and 1999 was 2.7‰. The $\delta^{18}O_{(H_2O)}$ value toward the end of March is low, and is suggestive of spring snowmelt.

Keuka Lake $\delta^{18}O_{(H_2O)}$ values are relatively constant at approximately –8.0‰$_{(VSMOW)}$ (Table 2.1). Approximately 75% of the annual water budget is derived from cool season precipitation with dominant inflow from the south and output through the northeastern branch, and a residence time of about 6 years (Michel and Kraemer, 1995). The isotope value of the lake is principally determined by variation in the ratio of winter/summer precipitation.

2.3.2 Molluscan $\delta^{18}O$ and $\delta^{13}C$ values

Micromilled carbonate $\delta^{18}O$ and $\delta^{13}C$ values for the fingernail clam from Science Lake exhibits a seasonal pattern (Figure 2.4). $\delta^{18}O_{(CaCO_3)}$ values range from –11.2 to –8.6‰$_{(VPDB)}$. A plateau with minor variation (0.3‰) from 9.3 to 10.1 mm averaged –8.9‰$_{(VPDB)}$. $\delta^{13}C$ values also show a seasonal pattern with a high degree of variability that ranges from –11.1 to –6.5‰$_{(VPDB)}$. $\delta^{13}C$ values are out of phase with $\delta^{18}O$ values, beginning to decrease at 8.8 mm. $\delta^{18}O$ values increase until 9.2 mm where they plateau, ultimately decreasing at 10 mm.

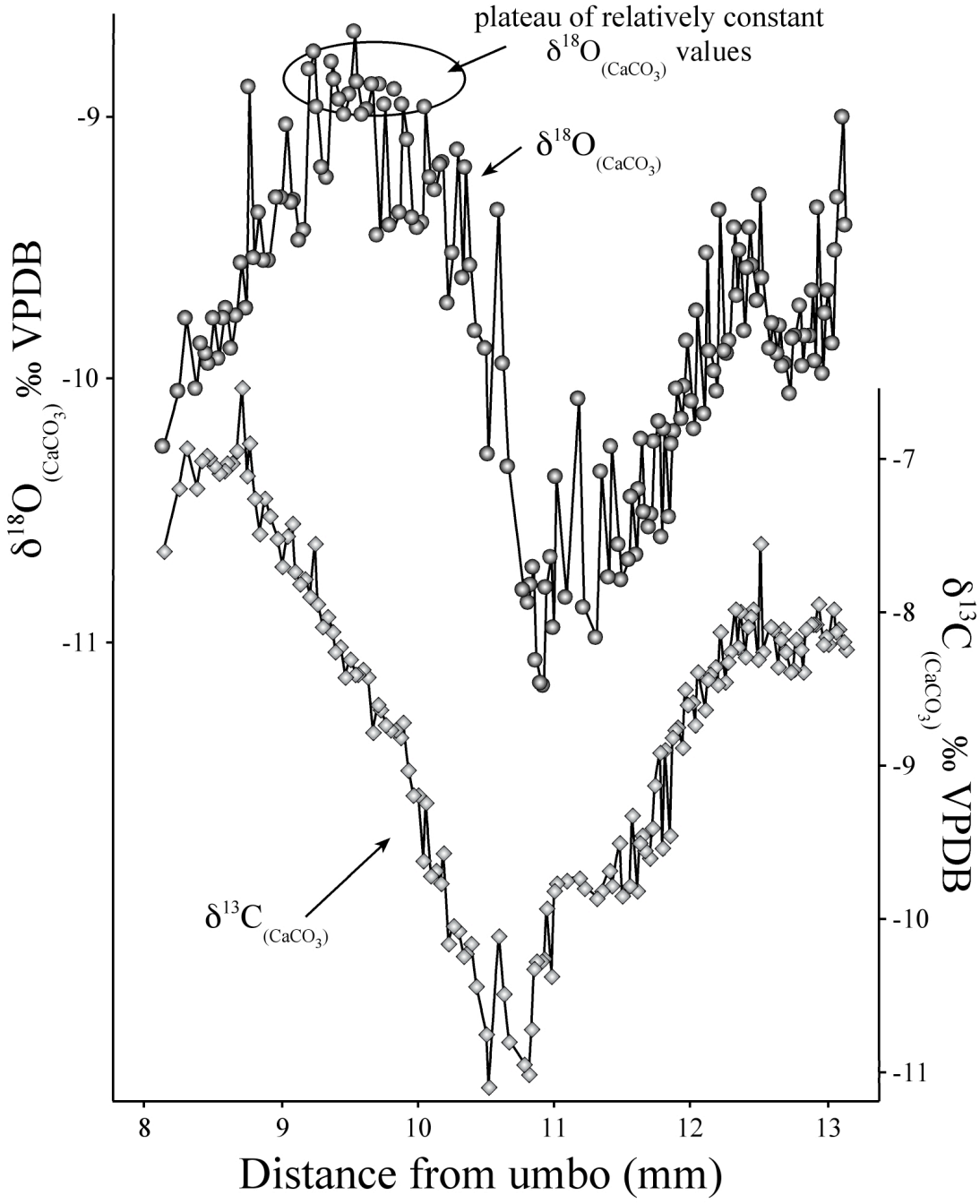

Figure 2.4—Intra-molluscan $\delta^{18}O_{(CaCO_3)}$ and $\delta^{13}C_{(CaCO_3)}$ values for a fingernail clam, (*Sphaerium simile*), collected from Science Lake in Allegany State Park, New York.

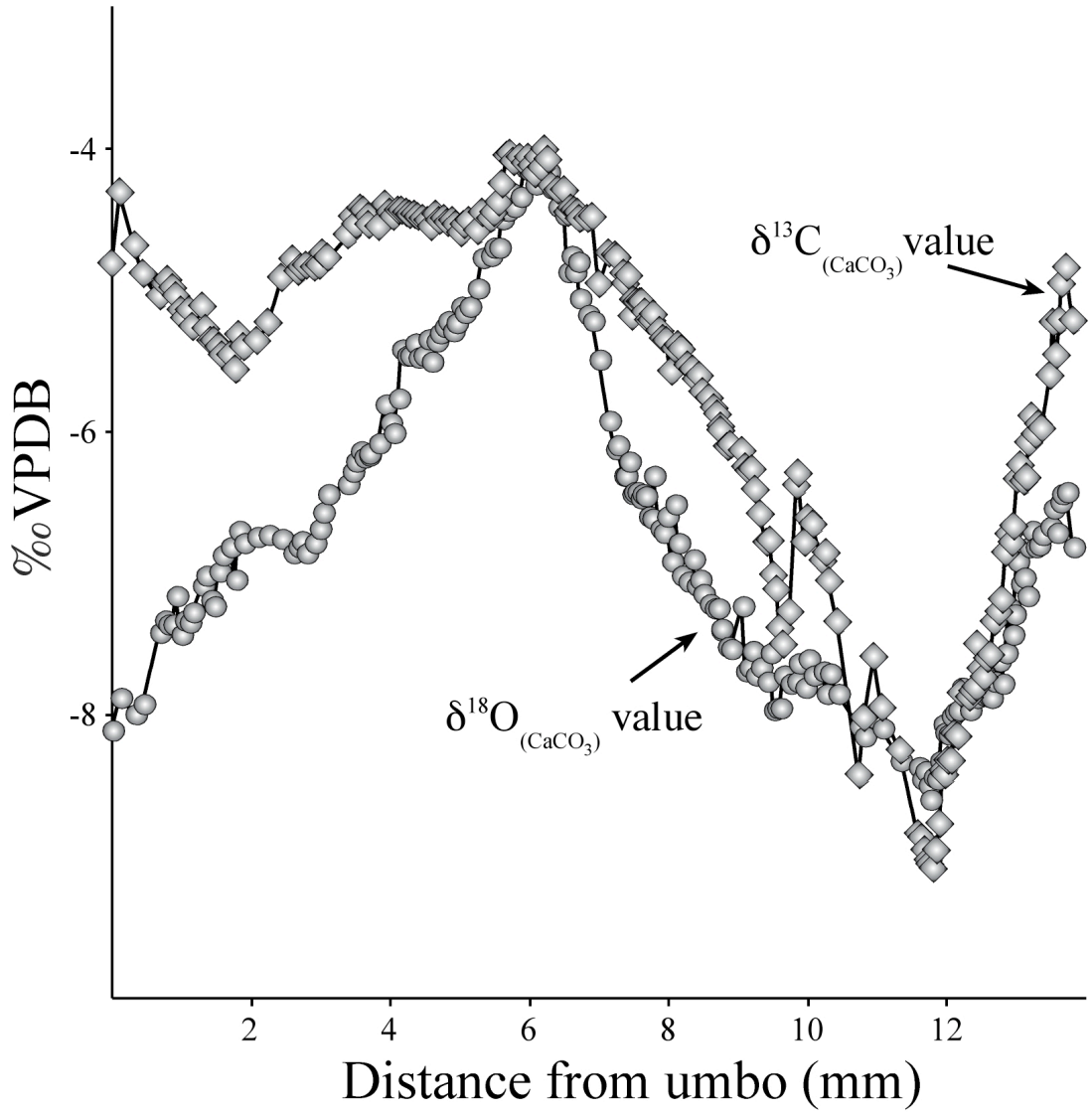

Figure 2.5—Intra-molluscan $\delta^{18}O_{(CaCO_3)}$ and $\delta^{13}C_{(CaCO_3)}$ values for a zebra mussel (*Dreissena polymorpha*), collected from Keuka Lake in central New York.

Although there is less of a degree of variability about a seasonal pattern than found for the fingernail clam, the zebra mussel still shows a seasonal pattern in both $\delta^{18}O_{(CaCO_3)}$ and $\delta^{13}C_{(CaCO_3)}$ values for less than two years of growth (Figure 2.5). The minimum $\delta^{18}O_{(CaCO_3)}$ value is –8.6‰$_{(VPDB)}$, whereas the maximum is –4.1‰$_{(VPDB)}$. $\delta^{13}C_{(CaCO_3)}$ values range from –4.0 to –9.1‰$_{(VPDB)}$ and are usually positively covaried with $\delta^{18}O_{(CaCO_3)}$ values ($r^2 = 0.67$); although $\delta^{13}C_{(CaCO_3)}$ values near the umbo negatively covary with $\delta^{18}O_{(CaCO_3)}$.

2.4 Discussion

2.4.1 Equilibrium fractionation of $\delta^{18}O_{(CaCO_3)}$

Figures 2.6 and 2.7 compare predicted and measured $\delta^{18}O_{(CaCO_3)}$ values for the fingernail clam and zebra mussel, respectively. Interestingly, there is a close correlation between the Science Lake fingernail clam's $\delta^{18}O_{(CaCO_3)}$ values and those predicted using equation (2.4). In contrast, the $\delta^{18}O_{(CaCO_3)}$ values of the zebra mussel from Keuka Lake are best predicted by equation (2.2). For the fingernail clam, $\delta^{18}O$ values appear to track high-resolution variability that includes the slight warming trend toward the end of 1999. It is also evident that the molluscan $\delta^{18}O_{(CaCO_3)}$ values show a much higher variation around a similar trend than do the predicted values. This may be due to unmeasured variation in the $\delta^{18}O_{(H_2O)}$ value. However, molluscan $\delta^{18}O_{(CaCO_3)}$ values still appear to be close to 0.25‰ lower than predicted values via equation (2.4) during the mid-summer. This can perhaps be explained by $\delta^{18}O_{(H_2O)}$ values, which were not measured during April, May, and June of 1999. If the seasonal pattern in $\delta^{18}O_{(H_2O)}$ values in 1999 was similar to that of 1998, a small "plateau" in $\delta^{18}O_{(H_2O)}$ value occurred during June-July that would not have been interpolated by a cubic spline (Figure 2.3). This would result in lower predicted $\delta^{18}O_{(CaCO_3)}$ values consistent with those measured in the mollusc.

The zebra mussel from Keuka Lake shows a pattern closely related to equilibrium values predicted using equation (2.2). Water temperatures were measured once a month from April to December and predicted $\delta^{18}O_{(CaCO_3)}$ values (using these temperatures) show

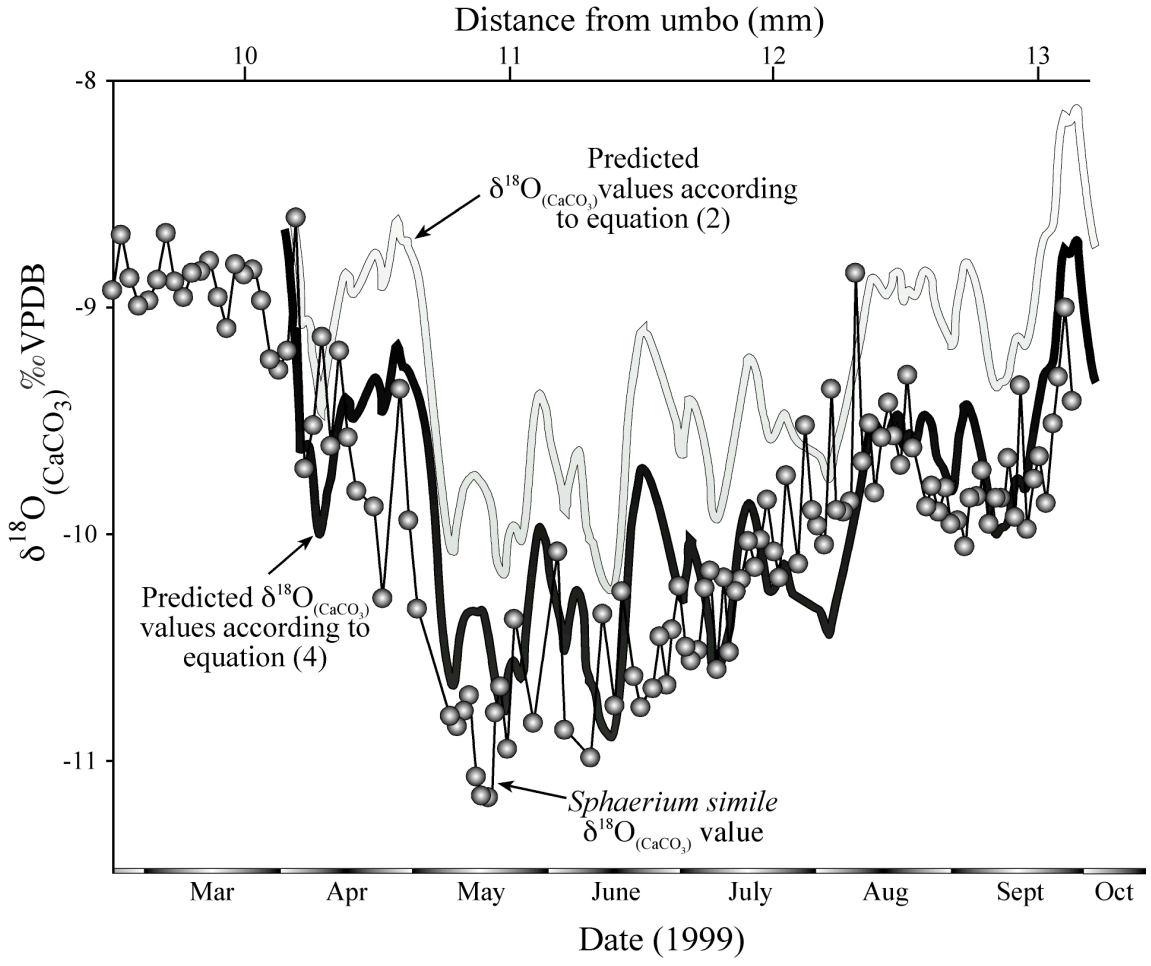

Figure 2.6—Comparison between predicted $\delta^{18}O_{(CaCO_3)}$ values and analyzed molluscan $\delta^{18}O_{(CaCO_3)}$ values for *Sphaerium simile*.

Molluscan $\delta^{18}O_{(CaCO_3)}$ values were expanded along the x-axis so that the oldest sample from the outer edge matched the date of collection (October 3, 1999), and the minimum $\delta^{18}O_{(CaCO_3)}$ value matched the minimum predicted $\delta^{18}O_{(CaCO_3)}$ value occurring in early April, 1999. No attempt was made to account for seasonal changes in the deposition rate of carbonate.

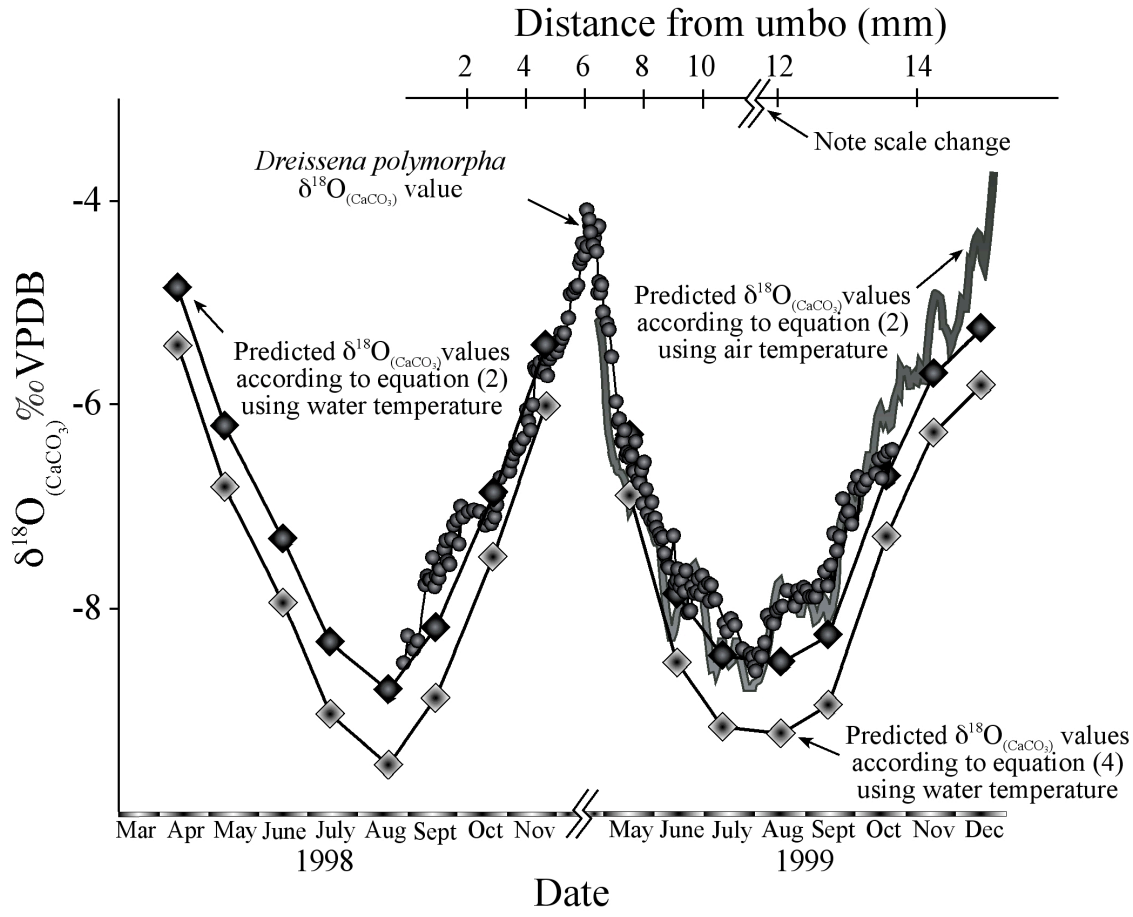

Figure 2.7—Comparison between predicted $\delta^{18}O_{(CaCO_3)}$ values and analyzed molluscan $\delta^{18}O_{(CaCO_3)}$ values for *Dreissena polymorpha*.

In order to satisfactorily compare the data and account for seasonal changes in the deposition of carbonate, different growth scales were used. A different growth scale was used from the umbo to the minimum $\delta^{18}O_{(CaCO_3)}$ value and from the minimum $\delta^{18}O_{(CaCO_3)}$ value to last sample. In order to show a more detailed comparison, predicted $\delta^{18}O_{(CaCO_3)}$ values determined using air temperature from Rochester and equation (2.2) are also shown. Note that the scale was not changed for the date axis, however November through March are omitted because predicted $\delta^{18}O_{(CaCO_3)}$ values could not be determined for these months.

a good general correlation, but do not display some of the more detailed patterns. In a further test of equilibrium precipitation, we also compare $\delta^{18}O_{(CaCO_3)}$ values predicted from equation (2.2) using air temperature from Rochester, NY (the nearest WMO weather station to the study site), which displays some of the more detailed variation (Figure 2.7). Winter $\delta^{18}O_{(CaCO_3)}$ values could not be accurately predicted because water temperatures were not measured during the winter and air temperature goes well below the minimum 0°C temperature for freshwater. The zebra mussel may produce carbonate throughout the winter because a minimum $\delta^{18}O_{(CaCO_3)}$ value of –4‰$_{(VPDB)}$ corresponds to a temperature of 2°C using equation (2.2). This is a reasonable minimum temperature estimate for Keuka Lake because minimum freshwater temperature would lie in the range 0-4°C.

Equation (2.2) predicts $\delta^{18}O_{(CaCO_3)}$ values more positive than those calculated using equation (2.4). Inorganic aragonite analyzed by Tarutani et al. (1969) was found to have a $\delta^{18}O_{(CaCO_3)}$ value 0.6‰ more positive than calcite precipitated at 25°C. If it is assumed that the slope of the fractionation relationship is the same as the inorganic calcite temperature-fractionation relationship of Kim and O'Neil (1997), an estimated fractionation equation for inorganic aragonite can be calculated applying Kim and O'Neil's (1997) revised acid fractionation factor, enriched by 0.6‰ for calcite-aragonite (Campana, 1999). This estimated inorganic aragonite fractionation relationship is indistinguishable from the Patterson et al. (1993) equation (Campana, 1999), suggesting that equation (2.4) predicts $\delta^{18}O_{(CaCO_3)}$ values more in accordance with that predicted by inorganic equilibrium precipitation of aragonite. This compares favorably with several studies of the calcite shells of marine molluscs whose $\delta^{18}O$ values appear to be in equilibrium according to inorganic calcite temperature-fractionation relationships (e.g., Wefer and Berger, 1991; Rahimpour-Bonab, 1997).

Several workers have reported $\delta^{18}O_{(CaCO_3)}$ values for modern freshwater bivalves, although most of these studies have focused on patterns of seasonal variation or of validating schlerochronological methods and have not directly measured the $\delta^{18}O_{(H_2O)}$ value (e.g., Krantz et al., 1987; Jones and Quitmyer, 1996; Veinott and Cornett, 1996). A few studies have attempted to determine whether freshwater bivalve carbonate is

deposited in oxygen isotope equilibrium with the environment; however, no consensus was reached. Some recent studies have concluded disequilibrium (Fastovsky et al., 1993; von Grafenstein et al., 1999), while Dettman et al. (1999) using methodology similar to that in this study, concluded that equilibrium precipitation occurs according to the modified Grossman and Ku (1986) temperature-fractionation relationship for aragonite. Our data suggest that *Sphaerium simile* from Science Lake appears to precipitate $\delta^{18}O_{(CaCO_3)}$ values according to Patterson et al. (1993), while *Dreissena polymorpha* precipitates $\delta^{18}O_{(CaCO_3)}$ values in agreement with Grossman and Ku (1986).

We propose two possible mechanisms for this apparent discrepancy. One possibility is that the environmental variables were not properly estimated. Although possible, this is unlikely because a consistent summer temperature offset of 2.5-3°C must then occur. Furthermore, studies have shown a direct correlation between air temperature and water temperature (e.g., McCombie, 1959; Edinger et al., 1968; Dingman, 1972; Webb, 1974; Livingstone and Lotter, 1998). We also find a close correlation between Rochester air temperature and Keuka Lake temperature (Figure 2.7). $\delta^{18}O_{(H_2O)}$ values for Science Lake display a distinct seasonal component, and water temperature likely responds to atmospheric temperature variation as well. It is possible that because *Sphaerium simile* burrows into the sediment that this species records parameters of a different environment. However, consistently lower temperatures and/or an increase in $\delta^{18}O_{(H_2O)}$ values within the sediment (compared to the open water) would have to occur. Furthermore, a consistent offset of ~0.6‰ would have to occur for this species to fit the Patterson et al. (1993) aragonite temperature-fractionation relationship. Because fresh, oxygenated water is required for *Sphaerium simile* to respire, it is likely that water exchange between sediment and overlying water column would maintain temperature equality between the two systems.

The second, and more favored hypothesis, is that there is a familial difference in the aragonite temperature-fractionation relationship. We suggest that Unionidae and Dreissenidae may have consistent 'vital effects', while Sphaeriidae may precipitate aragonite more in accord with estimated inorganic aragonite equilibrium. Both bivalve groups can therefore be used to accurately predict temperature and/or $\delta^{18}O_{(H_2O)}$ values. There is support for this hypothesis in some recent studies.

A study by von Grafenstein et al. (1999) measured temperature, $\delta^{18}O_{(H_2O)}$, and $\delta^{13}C_{(DIC)}$ at different depths throughout the year. Predicted $\delta^{18}O_{(CaCO_3)}$ values calculated from the empirically derived calcite temperature-fraction equation of Friedman and O'Neil (1977) were compared to measured $\delta^{18}O_{(CaCO_3)}$ values of different species of ostracodes and one bivalve for the purpose of assessing 'vital' effects. *Psidium* (Sphaeriidae) was found to be approximately 0.86±0.17‰$_{(VPDB)}$, more positive than that predicted by the Friedman and O'Neil's (1977) calcite equation, which is similar to Kim and O'Neil (1997) inorganic calcite temperature-fractionation relationship under these conditions. However, *Psidium* sp. precipitates an aragonite shell. If predicted $\delta^{18}O$ values are recalculated using equation (2.4), it would appear to be much closer to predicted values. The remaining ~0.2‰ offset may be related to the moderating effect of whole shell sampling. The only other study that has looked at $\delta^{18}O_{(CaCO_3)}$ values from modern *Sphaerium* finds that this genus predicts a mean $\delta^{18}O_{(CaCO_3)}$ value 0.6‰ more negative than the mean value for a Unionid shell sampled from the same location and which deposited carbonate during the same time (Tevesz et al., 1996). The authors attributed the contrast to potential winter growth differences and/or 'vital effects'. We find evidence against winter growth and for 'equilibrium' fractionation of $\delta^{18}O_{(CaCO_3)}$ values for *Sphaerium*.

Fastovsky et al. (1993) also report disequilibria for freshwater bivalve $\delta^{18}O$ values. They measured $\delta^{18}O_{(CaCO_3)}$ values of *Elliptio complanata* 1-3‰ lower than predicted values. An error in the treatment of the $\delta^{18}O_{(H_2O)}$ value within Grossman and Ku's (1986) equation resulted in predicted $\delta^{18}O_{(CaCO_3)}$ values 0.2‰ more positive (Dettman et al., 1999). If the tabulated $\delta^{18}O_{(CaCO_3)}$ value is averaged to represent the growing season and compared to predicted $\delta^{18}O_{(CaCO_3)}$ value from equation (2.4), the average offset is just 0.1‰ for two of three bivalves analyzed. The third bivalve still exhibits a 0.7‰ offset. Dettman et al. (1999) describe how misconceptions of spatial and temporal resolution in shell material might lead to erroneous interpretations for these Unionids. Dettman et al. (1999) used methodology similar to ours, demonstrating that $\delta^{18}O_{(CaCO_3)}$ values of several species of Unionids are deposited close to values predicted using equation (2.2). It is clear that further studies are required to resolve this issue.

2.4.2 Comparison of molluscan seasonal $\delta^{18}O_{(CaCO_3)}$ variation

There is a distinct difference in the degree of variability about the seasonal patterns of $\delta^{18}O_{(CaCO_3)}$ between the fingernail clam and the zebra mussel. We propose that this is a function of the water budget of the different lakes, in particular the residence time and input to volume ratio. The relatively constant seasonal $\delta^{18}O_{(H_2O)}$ value of Keuka Lake is a function of a 6-year residence time and the greater size of the drainage basin that integrates individual precipitation events (Table 2.1). As a result, the zebra mussel seasonal pattern in $\delta^{18}O_{(CaCO_3)}$ values is predominately a function of temperature (Figure 2.7).

In contrast, the fingernail clam from Science Lake displays significant variation about the seasonal pattern in $\delta^{18}O_{(CaCO_3)}$ values, that we interpret to be related to untracked variation in the $\delta^{18}O_{(H_2O)}$ value (Figure 2.6). These results highlight the importance of knowledge of paleo-hydrology in interpreting isotope data. In small basins such as Science Lake, it may be possible to de-convolve secular trends in storminess and seasonal temperature variation. However, changes in a lake size or residence time may affect the seasonal pattern without, necessarily, a corresponding atmospheric change.

Another distinct difference in seasonal variability between $\delta^{18}O_{(CaCO_3)}$ values of the fingernail clam and the zebra mussel is winter growth. $\delta^{18}O$ values from the fingernail clam from Science Lake suggest that the organism does not accrete $CaCO_3$ during the winter months. A plateau in $\delta^{18}O_{(CaCO_3)}$ values occurs between 9.3-10.1 mm averaging –8.9‰$_{(VPDB)}$, while values peak at –8.6‰$_{(VPDB)}$ (Figure 2.4). It is not possible to accurately define the growth cessation point because water temperature was not continually monitored; however, a reasonable estimation can be constructed using the 2-week running average of air temperature, which appears to correspond well with the brief warming period toward the end of the fall. The highest value –8.6‰$_{(VPDB)}$ corresponds to a temperature of 10°C, the same temperature estimated by Krantz et al. (1987) for the marine bivalve *Spisula* and for *Aplodinotus grunniens* fish otoliths (Patterson et al., 1993). If the average "plateau" value of –8.9‰$_{(VPDB)}$ is taken to correspond to the growth cessation point, then a temperature of ~12°C is estimated, which is in agreement with the results of Dettman et al. (1999) for 3 species of Unionids. The zebra mussel apparently

grows well into the winter, recording a maximum $\delta^{18}O_{(CaCO_3)}$ value of –4.1‰$_{(VPDB)}$, which corresponds to a minimum temperature of 2°C according to equation (2.2). Neumann et al. (1993) found virtually no winter shell growth for zebra mussels by applying a negative exponential growth equation in winter months, and tentatively suggested that this might be a function of a growth cessation point and/or inadequate food supply. This study presents evidence that shell material does accrete during the winter months in Keuka Lake via $\delta^{18}O_{(CaCO_3)}$ values taken from a zebra mussel; however, at a much reduced rate when compared to summer growth. Therefore, these results are not necessarily different from those found by Neumann et al. (1993).

2.4.3 Molluscan $\delta^{13}C$ values

Because dissolved inorganic carbon (DIC) isotope values ($\delta^{13}C_{(DIC)}$) were not measured, fractionation of carbon into the $CaCO_3$ shell can only be estimated based on seasonal variation in $\delta^{13}C_{(DIC)}$ in other aquatic systems. $\delta^{13}C_{(CaCO_3)}$ values in both specimens decrease during the summer. However, it is likely that the $\delta^{13}C$ value of the DIC increased with productivity during the summer (e.g., Atekwana and Krishnamurthy, 1998; Dettman et al., 1999; von Grafenstein et al., 1999). $\delta^{13}C_{(CaCO_3)}$ values presented here are on average several per mil more negative and show a greater seasonal range (–7 to –12‰$_{(VPDB)}$ and –4.0 to –9.1‰$_{(VPDB)}$) than are reported for lakes (e.g., von Grafenstein et al., 1999). Additionally, covariation with $\delta^{18}O_{(CaCO_3)}$ values suggest that there is a non-linear temperature effect on metabolic processes because the temperature influence on inorganic aragonite-HCO_3^- carbon is insignificant (Romaneck et al., 1992).

2.4.4 Geological and archaeological implications

The tremendous abundance of fossil molluscs in archaeological and geological records presents exceptional opportunities for deriving geochemical and paleoclimate information from $\delta^{18}O_{(CaCO_3)}$ and $\delta^{13}C_{(CaCO_3)}$ values. $\delta^{13}C_{(CaCO_3)}$ values appear to be related to physiological variables such as metabolic activity, trophic position, and/or reproduction, which may have significant implications for evolutionary and physiological studies, for both extant and extinct species. High-resolution techniques are necessary to

uncover seasonal and ontogenetic variation in $\delta^{18}O_{(CaCO_3)}$ values on sub-daily time scales, which are predictably related to the temperature and $\delta^{18}O_{(H_2O)}$ value.

Using the seasonal pattern in $\delta^{18}O_{(CaCO_3)}$ values from fossil shells it may be possible to evaluate changes in storminess and/or temperature seasonality. Variation about the seasonal pattern in $\delta^{18}O_{(CaCO_3)}$ value in small lake basins is probably a result of individual storm perturbations. We present further evidence of a shutdown temperature in a temperate mollusc (below this temperature, carbonate no longer accretes, whereas above this temperature carbonate accretes). This shutdown temperature (10°C-12°C) is in agreement with other findings both on an intraclass (e.g., Krantz et al., 1987; Dettman et al., 1999) and interphylla level (Patterson et al., 1993). A known temperature of skeletal growth cessation would permit a discrete calculation of $\delta^{18}O_{(H_2O)}$ value at that time of year (Patterson et al., 1993; Patterson, 1998). If the seasonal variation in $\delta^{18}O_{(H_2O)}$ value can be determined, discrete calculation of temperature for the remainder of the growing season can be defined. While this approach has been used successfully in studies of fish otoliths (Smith and Patterson, 1994; Patterson, 1998), the relative abundance of fossil mollusc material suggests even greater opportunities for studies of paleolimnology, paleoclimatology, and paleoecology.

Because the zebra mussel continued to accrete carbonate during the winter, it provides the opportunity to track the full range of seasonality in high-latitudes. For such a study, $\delta^{18}O_{(H_2O)}$ values would be estimated assuming a minimum temperature of water in a temperate setting (0-4°C). Lastly, the growth rate of many molluscs, coupled with the technology for high-resolution partitioning of $CaCO_3$, has application toward season-of-capture information, which is important for the establishment of seasonal occupation of archaeological sites (Casteel, 1976).

2.5 Conclusions

A high-resolution record was recovered from two species of temperate modern lacustrine molluscs to investigate their suitability for recovering paleoenvironmental records on daily to weekly time scales. *Sphaerium simile* and *Dreissena polymorpha* yield $\delta^{18}O$ values calculated from environmental parameters. Relatively short-term temperature variability, such as a warming trend toward the end of 1999 is faithfully

recorded. This finding is in agreement with a recent report of equilibrium oxygen isotope fractionation in several species of temperate freshwater Unionidae molluscs, and in contrast with evidence indicating oxygen isotopic disequilibria in other species of freshwater molluscs. However, we find evidence for familial differences in the temperature-fractionation equation. The *Sphaerium simile* sampled from Science Lake apparently produced $\delta^{18}O_{(CaCO_3)}$ values more in accord with the temperature-fractionation relationship of Patterson et al. (1993), rather than Grossman and Ku's (1986) equation. Conversely, the zebra mussel from Keuka Lake was found to be in equilibrium with Grossman and Ku's (1986) temperature-fractionation relationship. Further study is needed to better delineate subtle differences and mechanisms in freshwater molluscan fractionation of stable oxygen isotopes. Nonetheless, the seasonal pattern in the $\delta^{18}O_{(CaCO_3)}$ values is a powerful tool for interpreting climates of the past.

We have shown that the seasonal pattern of $\delta^{18}O_{(CaCO_3)}$ value is significantly influenced by the organism's environment. For example, a greater degree of variation about a seasonal trend is found in the mollusc from a small watershed environment. This is probably due to increased sensitivity of the watershed to day-to-day variation in temperature, in addition to $\delta^{18}O_{(H_2O)}$ variability resulting from input of storm water. Selection of an appropriate watershed makes it be possible to evaluate secular changes in storminess, an important characteristic of climate. Conversely, interpretation of temperature seasonality is best accomplished using a large watershed that provides a relatively predictable seasonal variation in $\delta^{18}O_{(H_2O)}$ value.

High-resolution $\delta^{18}O_{(CaCO_3)}$ and $\delta^{13}C_{(CaCO_3)}$ values have widespread implications for paleoenvironmental and physiological studies. Climatic and geochemical information can be determined from $\delta^{18}O$ values, while trophic condition, metabolic rate, and/or reproduction systematics may be derived from $\delta^{13}C$ values.

Chapter 3. Metabolic rate of late Holocene freshwater fish: evidence from $\delta^{13}C$ values of otoliths[2]

3.1 Introduction

Stable isotope analyses of otoliths provide a wealth of information for ecology, geology, and archaeology (e.g., Degens, 1978; Campana, 1999; Patterson and Smith, 2002). Because $\delta^{18}O_{(CaCO_3)}$ values of fish otoliths are in equilibrium with the environment, they are useful in reconstructing environmental temperatures and/or $\delta^{18}O_{(H_2O)}$ values (Kalish, 1991a,b; Patterson et al., 1993; Thorrold et al., 1997). Conversely, although $\delta^{13}C_{(CaCO_3)}$ values of otoliths occasionally are interpreted solely as recording dissolved inorganic carbon (DIC) $\delta^{13}C$ values (e.g., Degens et al., 1969), other authors report an important metabolic contribution (e.g., Kalish, 1991a,b; McConnaughey et al., 1997; Schwarcz et al., 1998; Weidman and Millner, 2000). Long-term records of variation in metabolic rate can provide valuable information for understanding the evolutionary history of physiological traits of fishes (e.g., Liem, 1980; Calow, 1985). A central problem is the lack of proxies for variation in metabolism on historic and geologic timescales. Moreover, a proxy for metabolic rate through fish ontogeny could help elucidate other questions in bioenergetics, such as fish activity, food consumption, and tissue turnover (e.g., Boisclair and Leggett, 1989; He and Stewart, 1998; Schaeffer et al., 1999).

Otoliths are accretionary structures composed of the metastable calcium carbonate mineral aragonite found within the inner ear of teleost fish. These structures often display yearly and sometimes daily banding patterns providing age and growth data for fish species (e.g., Panella, 1980; Casselman, 1987). Sagittae, usually the largest of three pairs

[2] Wurster, C. M., and W. P. Patterson, 2003. Metabolic rate of late Holocene freshwater fish: evidence from $\delta^{13}C$ values of otoliths. Paleobiology 29(4): 492-505. Reprinted with kind permission of the Paleontological Society.

of otoliths, are often recovered as pristine aragonite from Holocene archaeological sites (Casteel, 1976), and in the geologic record as far back as the Jurassic Period (e.g., Nolf, 1995; Patterson, 1999). Unlike bone, otoliths are chemically stable, acellular, and rarely resorbed in nature (Campana and Neilson, 1985; Campana, 1999).

Variation among $\delta^{13}C_{(CaCO_3)}$ values of otoliths was originally thought to reflect solely $\delta^{13}C_{(DIC)}$ values (Degens et al., 1969). However, $\delta^{13}C_{(CaCO_3)}$ values were considerably lower than those predicted assuming equilibrium with ambient water (e.g., Kalish, 1991a), indicating either a kinetic isotope effect or a significant metabolic contribution of otolith carbon. Kalish (1991b) favored the metabolic hypothesis because $\delta^{18}O_{(CaCO_3)}$ values of otoliths were found to be in equilibrium with the environment. This led to a model in which fish O_2 consumption (metabolic rate) is negatively correlated with the $\delta^{13}C_{(CaCO_3)}$ value (Kalish, 1991b); the higher the metabolic rate of fish, the lower the $\delta^{13}C_{(CaCO_3)}$ value of the otolith. Gauldie (1996) also favored a metabolic source for low $\delta^{13}C$ values in otoliths. A laboratory study using whole otoliths of young Atlantic croaker (*Micropogonias undulates*, Sciaenidae) exhibited a significant positive correlation between somatic growth rate and otolith $\delta^{13}C$ values (Thorrold et al., 1997). This contrasts with what is expected if metabolic rate is controlling the variation in $\delta^{13}C$ values of otoliths; however, early life-history stages often have mass-independent metabolic rates (Post and Lee, 1996).

Schwarcz et al. (1998) and Wiedman and Millner (2000) reported carbon isotope trends within individual otoliths of Atlantic cod (*Gadus morhua*, Gadidae). They interpreted $\delta^{13}C_{(CaCO_3)}$ values as representing equilibrium precipitation with the HCO_3^- of the endolymph, which was derived by a mixture of metabolic carbon and DIC of the seawater. Intra-otolith variation in $\delta^{13}C$ values displayed a pattern of increasing $\delta^{13}C$ values to a maximum at maturity, a pattern that was attributed to ontogenetic variation in metabolic rate and trophic position (Schwarcz et al., 1998; Weidman and Millner, 2000).

We aim to investigate controls of intra-otolith $\delta^{13}C$ variation from sub-fossil freshwater drum (*Aplodinotus grunniens*, Sciaenidae) by comparing observed patterns with a mass balance model previously applied to marine otoliths (Kalish, 1991a,b; Schwarcz et al., 1998). We present the highest resolution intra-otolith $\delta^{13}C$ values to date,

and they are amongst the first for a freshwater fish. Additionally, ontogenetic trends in $\delta^{13}C_{(CaCO_3)}$ values are compared with environmental factors during the late Holocene. $\delta^{18}O_{(CaCO_3)}$ values from some of the otoliths examined herein were previously interpreted as revealing paleoclimatic trends during the late Holocene (Wurster and Patterson, 2001).

3.2 Materials and Methods

3.2.1 Micromilling of Eastman rockshelter sagittae and analysis of stable isotope values

A full description of the study site in northeast Tennessee, the recovery of sub-fossil material, and the construction of the age model is presented by Wurster and Patterson (2001). Using methodology described in Wurster et al. (1999), we micromilled 14 *A. grunniens* sub-fossil sagittae to produce a high-resolution record of $\delta^{13}C_{(CaCO_3)}$ and $\delta^{18}O_{(CaCO_3)}$ values. Specimens were polished to reveal growth annuli, attached to a stage beneath a fixed dental drill, and viewed on a monitor via a color digital video camera. Annuli were digitized in realtime as a series of three-dimensional coordinates, and intermediate coordinates were interpolated by using a cubic spline. An array of intermediate sampling paths was calculated between digitized curves. Sample path arrays served to guide three high-precision actuators, which positioned the sample stage relative to the fixed dental drill. We micromilled 3249 samples (an average of 232 samples/specimen) in order to collect carbonate aliquots with subweekly (~4-6 day) resolution. The smallest sample mass was estimated to be ~20-30 μg. To characterize seasonal variation in $\delta^{18}O_{(CaCO_3)}$ and $\delta^{13}C_{(CaCO_3)}$ values, we analyzed 1673 microsamples (an average of 120 samples/specimen); remaining samples were temporarily archived. A subset of 1,673 microsamples was analyzed. Mineralogy of microsampled otoliths was determined by X-ray diffraction to be pristine aragonite.

Intra-otolith $\delta^{13}C_{(CaCO_3)}$ trends were determined for an additional 30 sub-fossil sagittae by milling a line from the center of the otolith to the edge usually along the longest growth axis. From this low-resolution method, 4–13 samples from each otolith transect were recovered, which approximate average $\delta^{13}C_{(CaCO_3)}$ and $\delta^{18}O_{(CaCO_3)}$ values of micromilled samples (Figure 3.1, 3.2). We plotted $\delta^{13}C_{(CaCO_3)}$ values as a function of age, by assuming that each sample is equidistant along the sampling transect. In most cases,

we determined the increment distance from the core along a sample transect as a function of age by using a von Bertalanffy growth model (von Bertalanffy, 1938) where the set of coefficients was determined with the Levenberg-Marquardt method. Occasionally, when two linear regressions or a log and linear regression provided a better fit, we used these models to describe otolith growth as a function of age. A separate growth model was determined for each otolith.

Once extracted, samples were roasted *in vacuo* for one hour at 200°C to remove volatiles that may interfere with $\delta^{18}O$ and $\delta^{13}C$ values. Samples were reacted in a Kiel III automated carbonate preparation device directly coupled to a Finnigan MAT 252 stable isotope ratio mass spectrometer at Syracuse University. Carbon dioxide was generated by reaction of carbonate with three drops of anhydrous phosphoric acid in individual reaction vessels at 70°C. We analyzed, individual samples by using a micro-inlet, which reduces sample "memory" and permits analysis of ~20 μg of carbonate. Carbonate samples were analyzed with a precision of ±0.08‰ (1σ), determined by analysis of international carbonate standards NBS-18 and NBS-19 and reported relative to the Vienna Pee Dee Belemnite standard (VPDB).

3.2.2 Bioenergetics modeling

Bioenergetic models have been developed and used since the eighteenth century (Elliot, 1979), and today this method has been widely and successfully applied in many studies (e.g., Kitchell et al., 1977; Stewart et al., 1983; Hartman and Brandt, 1995a,b) including a study investigating temporal dynamics of $\delta^{13}C$ and $\delta^{15}N$ values of fish tissues (Harvey et al., 2002). We used already constructed bioenergetics models for weakfish (*Cynoscion regalis*, Sciaenidae), yellow perch (*Perca flavescens*, Percidae), and steelhead (*Oncorhynchus mykiss*, Salmonidae) to investigate patterns of change in total specific respiration rate that are repeatable through species (and families) because of basic energetic equations. Therefore, these ontogenetic and seasonal specific respiration rate patterns are assumed to represent specific respiration rate patterns of freshwater drum. These particular species were chosen because they already have well-parameterized and published models, with site-specific variables, and the specific bioenergetic parameters are already defined in Fish Bioenergetics 3.0 computer program (Hanson et al., 1997).

We used bioenergetic models for weakfish developed by Hartman and Brandt (1995a) with site-specific variables (temperature, growth, predator and prey energy densities, and prey proportions consumed) published by Hartman and Brandt (1995b). For yellow perch and steelhead, we used the bioenergetic models and site-specific variables of Kitchell et al. (1977) and Rand et al. (1993), respectively. To implement bioenergetic models for each fish, we used the computer program Fish Bioenergetics 3.0 (Hanson et al., 1997). We ran the bioenergetic models for specific respiration rate and specific dynamic action (joules/g/day) outputs with growing season temperatures above 10 °C to better represent the time of freshwater drum carbonate accretion. These outputs were summed to determine total specific respiration rate.

3.3 Results

3.3.1 High-resolution $\delta^{13}C$ values

Fourteen otoliths were sampled at high resolution to determine intra-otolith variation in $\delta^{13}C_{(CaCO_3)}$ and $\delta^{18}O_{(CaCO_3)}$ values (Figure 3.1, 3.2). Most otoliths displayed very large intra-otolith variation, both seasonally and ontogenetically. Early $\delta^{13}C$ values were very negative compared with previously reported $\delta^{13}C_{(CaCO_3)}$ values. The specimen sampled from 2.7 Ka recorded both the lowest $\delta^{13}C_{(CaCO_3)}$ value (–23.4‰VPDB) and the largest variation between minimum and maximum $\delta^{13}C_{(CaCO_3)}$ values ($\delta^{13}C_{max–min}$ = 14.2‰; Figure 3.1G). The highest $\delta^{13}C$ value (–7.3‰VPDB) was recorded by a specimen dated ~1.0 Ka (Figure 3.2B). Seasonal variation in $\delta^{13}C$ values often display large variation (over 5‰), and in one specimen we observed a seasonal variation of over 11‰ (Figure 3.1G).

Two otoliths were sampled at high resolution from the core to the edge of the otolith and both of these display similar patterns (Figure 3.2B, F). Note that lowest $\delta^{13}C_{(CaCO_3)}$ values are recorded during the first year of each fish's life, followed by an increase toward relatively constant values as the fish matured. Other specimens display a similar pattern, although the entire ontogeny was not sampled.

Stable isotope values for each year of each otolith were normalized to a mean of 0 and 1 standard deviation to investigate changes in the patterns of covariation between $\delta^{18}O$

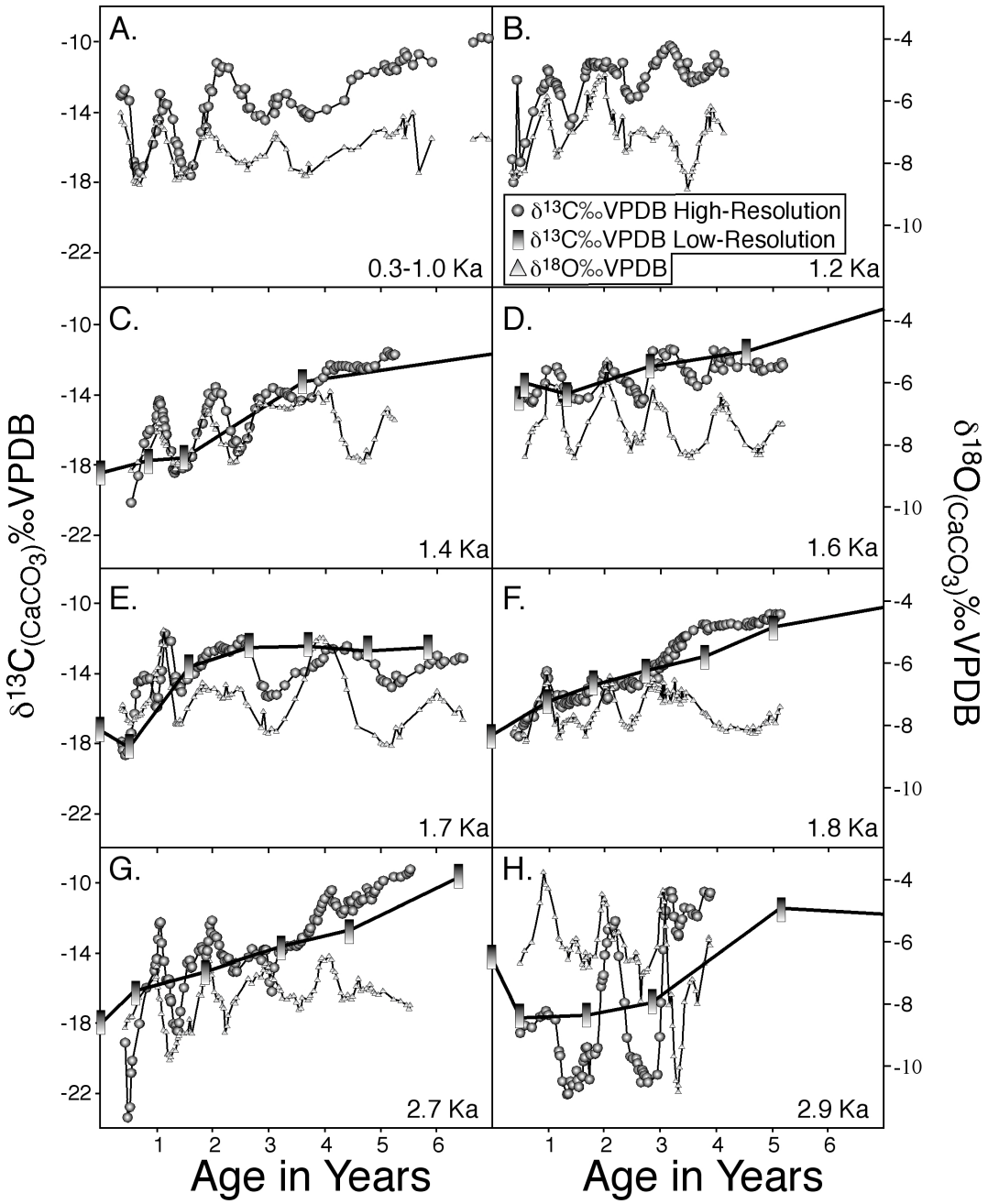

Figure 3.1—Intra-otolith variation in high-resolution $\delta^{13}C$ and $\delta^{18}O$ values of micromilled sagittae recovered from time periods 0.3 to 2.9 Ka.

Samples were taken only from the first eight years or less. Each subplot represents an individual otolith. Each high-resolution sample represents an individual carbonate aliquot removed by micromilling. Low-resolution samples that approximate the average values of micromilled aliquots are plotted for comparison. Represented time periods are 0.3-1.0 Ka, 1.2 Ka, 1.4 Ka, 1.6 Ka, 1.7 Ka, 1.8 Ka, 2.7 Ka, and 2.9 Ka. Specimens from A and B were destroyed before low-resolution sampling could be performed.

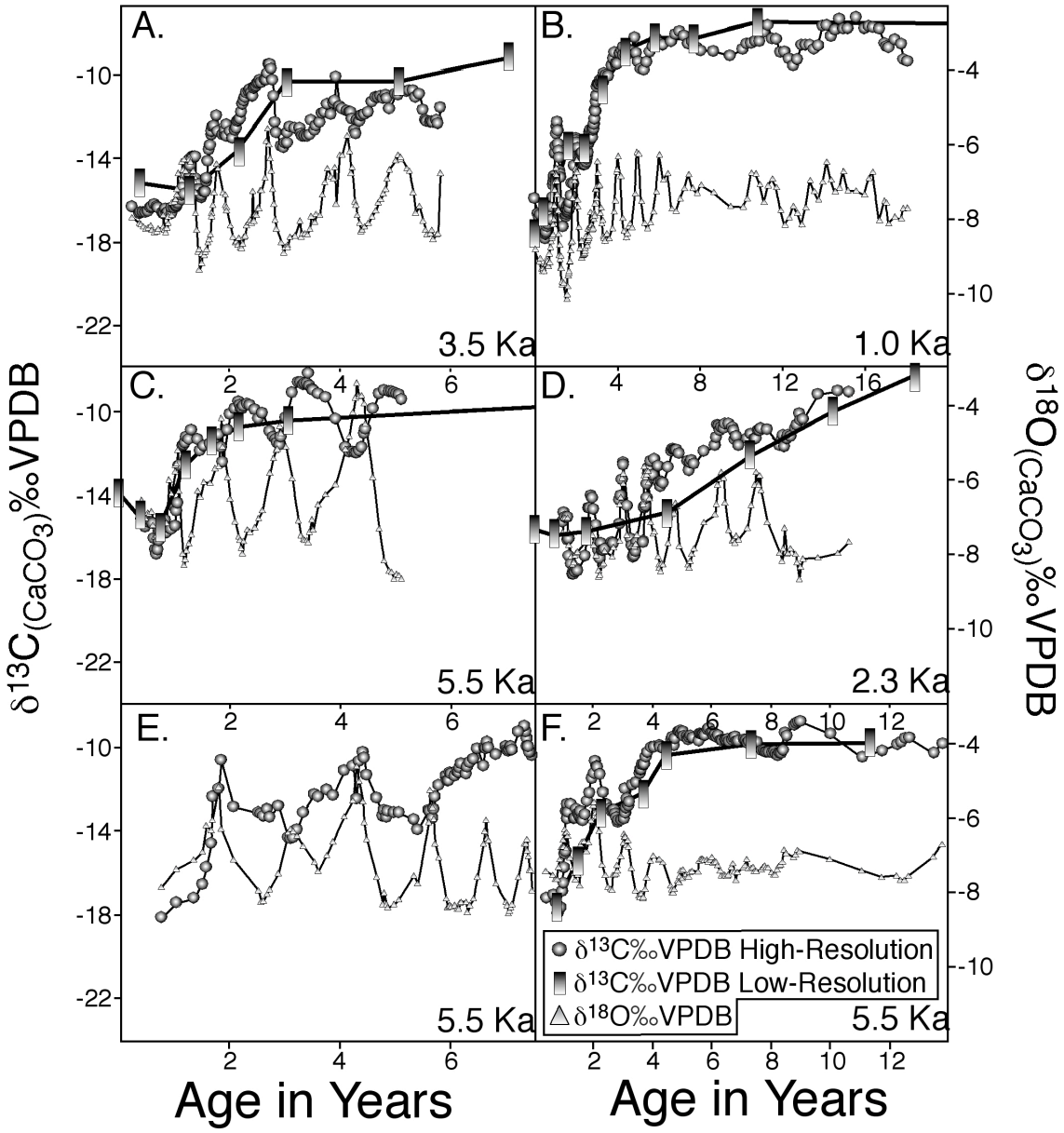

Figure 3.2—Intra-otolith variation in high-resolution $\delta^{13}C$ and $\delta^{18}O$ values of micromilled sagittae from time periods that are 1.0 Ka, 2.3 Ka, 3.5 Ka, and 5.5 Ka.

Each subplot represents an individual otolith. Each high-resolution sample represents an individual carbonate aliquot removed by micromilling. Low-resolution samples that approximate the average values of micromilled aliquots are plotted for comparison. Note different age axes on subplots. Subplots on the left side include sagittae sampled no more than eight years, whereas plots on the right side include sagittae sampled over eight years. The specimen from C was destroyed before low-resolution sampling could be performed.

Table 3.1—Slope and r^2 of least-squares linear regressions on normalized seasonal $\delta^{18}O$ and $\delta^{13}C$ values of freshwater drum fossil otoliths.

Year Class	Slope	r^2
0	0.83	0.70, $p < 0.01$
1	0.61	0.48, $p < 0.01$
2	0.52	0.35, $p < 0.01$
3	0.18	0.06
4	0.32	0.20, $p < 0.01$
5	0.40	0.16, $p < 0.01$
6	0.27	0.07

and $\delta^{13}C$ values among age classes without considering specific values. As the fish ages, both r^2 values and slopes of least-squares linear regressions between $\delta^{18}O_{(CaCO_3)}$ and $\delta^{13}C_{(CaCO_3)}$ values tend to progressively decrease (Table 3.1). In these otoliths, seasonal variation in $\delta^{18}O_{(CaCO_3)}$ values is predominantly controlled by and inversely related to seasonal temperature change (Wurster and Patterson, 2001). Therefore, the seasonal change in $\delta^{13}C$ also inversely covaries with seasonal temperature change, and the magnitude of this change is much greater early in the ontogeny of the fish. However, it should be noted that $\delta^{13}C$ and $\delta^{18}O$ values are negatively correlated for one otolith profile (Figure 3.2C), which is an anomaly to the general patterns (Table 3.1).

3.3.2 Low-resolution $\delta^{13}C$ values

Low-resolution $\delta^{13}C_{(CaCO_3)}$ values ranged from –19.9‰ to –7.5‰VPDB (Figure 3.3). The greatest ontogenetic range in $\delta^{13}C_{(CaCO_3)}$ values in a specimen was 10.3‰ (Figure 3.3C). Note that the lowest $\delta^{13}C_{(CaCO_3)}$ values appear within the first two years, and the highest values are exhibited toward the edge of the otolith (Figure 3.4). All otoliths sampled at low-resolution displayed the same pattern of first-order ontogenetic variability in $\delta^{13}C$ values as otoliths sampled at high resolution, a steep initial increase toward relatively stable $\delta^{13}C$ values as the fish matured (Figure 3.3). Level 1, the Mississippian archaeological cultural period (0.3 to 1.0 Ka) has the greatest variation in $\delta^{13}C_{max–min}$ values (3.9‰) but also encompasses the greatest variability in age constraints (Wurster and Patterson, 2001).

3.3.3 Bioenergetic output

Total specific respiration rate for weakfish, yellow perch, and steelhead display repeatable patterns of ontogenetic and seasonal change (Figure 3.5). The highest modeled total specific respiration rate (1246 joules/g/day) and the greatest total seasonal (1181 joules/g/day) and ontogenetic shifts (1119 joules/g/day) were found for weakfish (Sciaenidae— the same family as freshwater drum). For weakfish and yellow perch, juvenile total specific respiration rate was modeled, and both these species display a distinct first-order pattern where total specific respiration rate decreases less than proportionally to fish age and weight. Note that we did not model juvenile steelhead

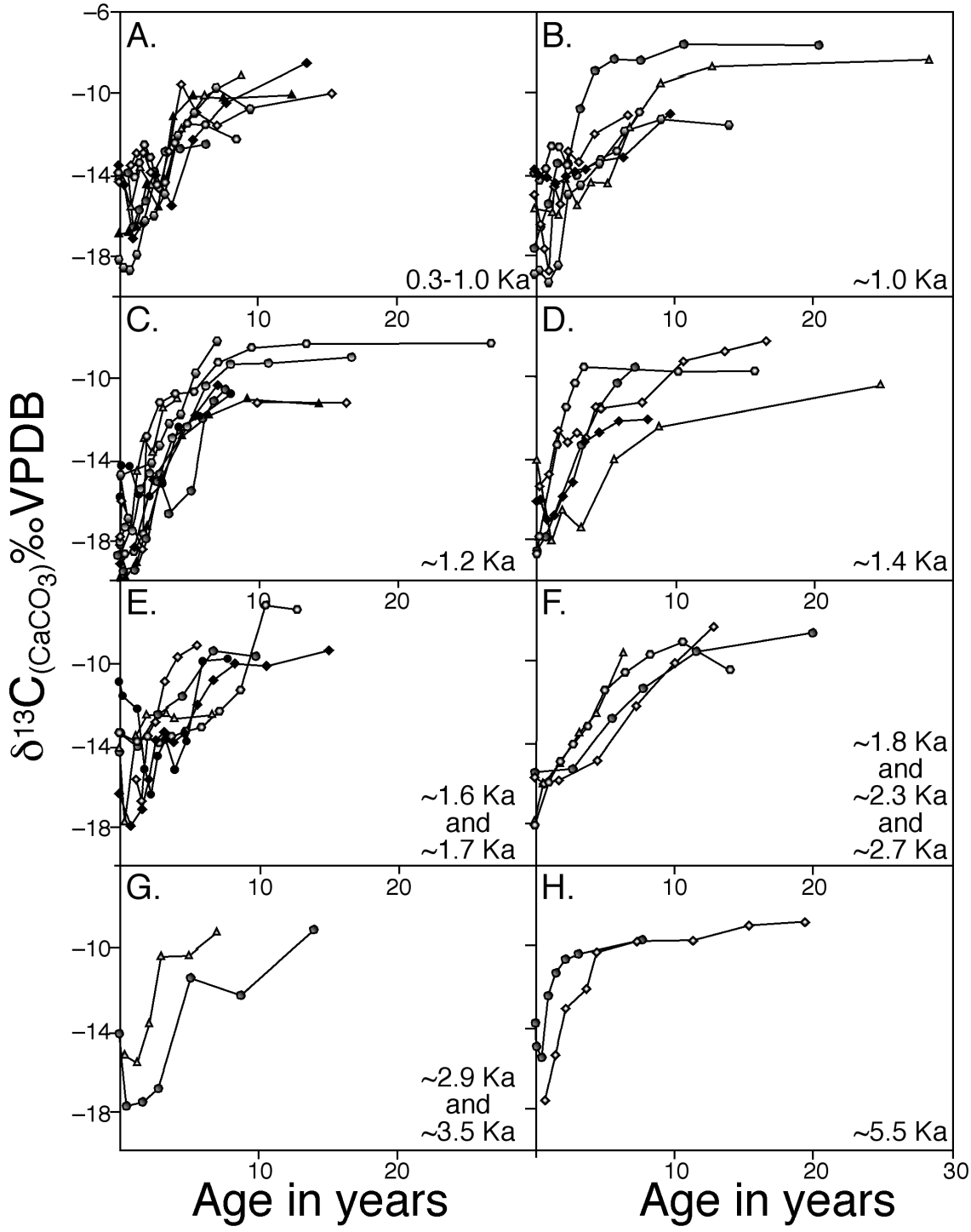

Figure 3.3—Low-resolution ontogenetic variation in $\delta^{13}C$ values of sub-fossil otoliths.

See text for explanation of fish age model. Each subplot represents otoliths recovered from one or more archaeological level/time period(s).

because Rand et al. (1993) did not publish a juvenile model nor give diet proportions for juvenile fish (steelhead reside in tributaries and do not enter the lake until reaching approximately 50 g of weight wet). A seasonal pattern where total specific respiration rate covaries with temperature is present for all modeled species, though a distinct lead is noted for juvenile yellow perch (Figure 3.5). Finally, in all modeled species the amplitude of the seasonal variation in total specific respiration rate declines with age (Figure 3.5).

3.4 Discussion

3.4.1 Modeling $\delta^{13}C$ values of otoliths

Intra-otolith $\delta^{13}C_{(CaCO_3)}$ values display three repetitive patterns irrespective of the geologic age of the specimen, although specific $\delta^{13}C$ values vary. The primary pattern is as follows: $\delta^{13}C_{(CaCO_3)}$ values begin most negative early in the ontogeny of the fish and increase to a plateau of relatively constant values as the fish matures. The secondary pattern, a seasonal covariation between $\delta^{13}C$ and $\delta^{18}O$ values, occurs because both $\delta^{13}C$ and $\delta^{18}O$ values display a distinct seasonal pattern similar to a sinusoid curve. The third is that these seasonal covariations between $\delta^{13}C$ and $\delta^{18}O$ values tend to have progressively lower r^2 values and slopes as the fish ages (Table 3.1). This progressive pattern is a result of $\delta^{13}C$ values displaying greater seasonal range early in the ontogeny of the fish. These patterns are illustrated and compared with "idealized" intra-otolith $\delta^{18}O_{(CaCO_3)}$ values in Figure 3.4. $\delta^{18}O_{(CaCO_3)}$ values of otoliths reflect an equilibrium temperature-fractionation relationship (Kalish, 1991a,b; Patterson et al., 1993; Thorrold et al., 1997). Importantly, $\delta^{18}O_{(CaCO_3)}$ value is controlled by temperature and $\delta^{18}O_{(H_2O)}$ value. In these freshwater drum otoliths we find the seasonal pattern of $\delta^{18}O_{(CaCO_3)}$ values to inversely reflect seasonal temperature change (Wurster and Patterson, 2001), because the seasonal range in temperature is usually much greater than the seasonal oscillation in $\delta^{18}O_{(H_2O)}$ values. However the specific average $\delta^{18}O$ value reflects $\delta^{18}O_{(H_2O)}$ value (see below). Wurster and Patterson (2001) describe controls of $\delta^{18}O_{(CaCO_3)}$ value in greater detail and note seasons in which $\delta^{18}O_{(H_2O)}$ values played more of a role in seasonal variation in $\delta^{18}O_{(CaCO_3)}$ values.

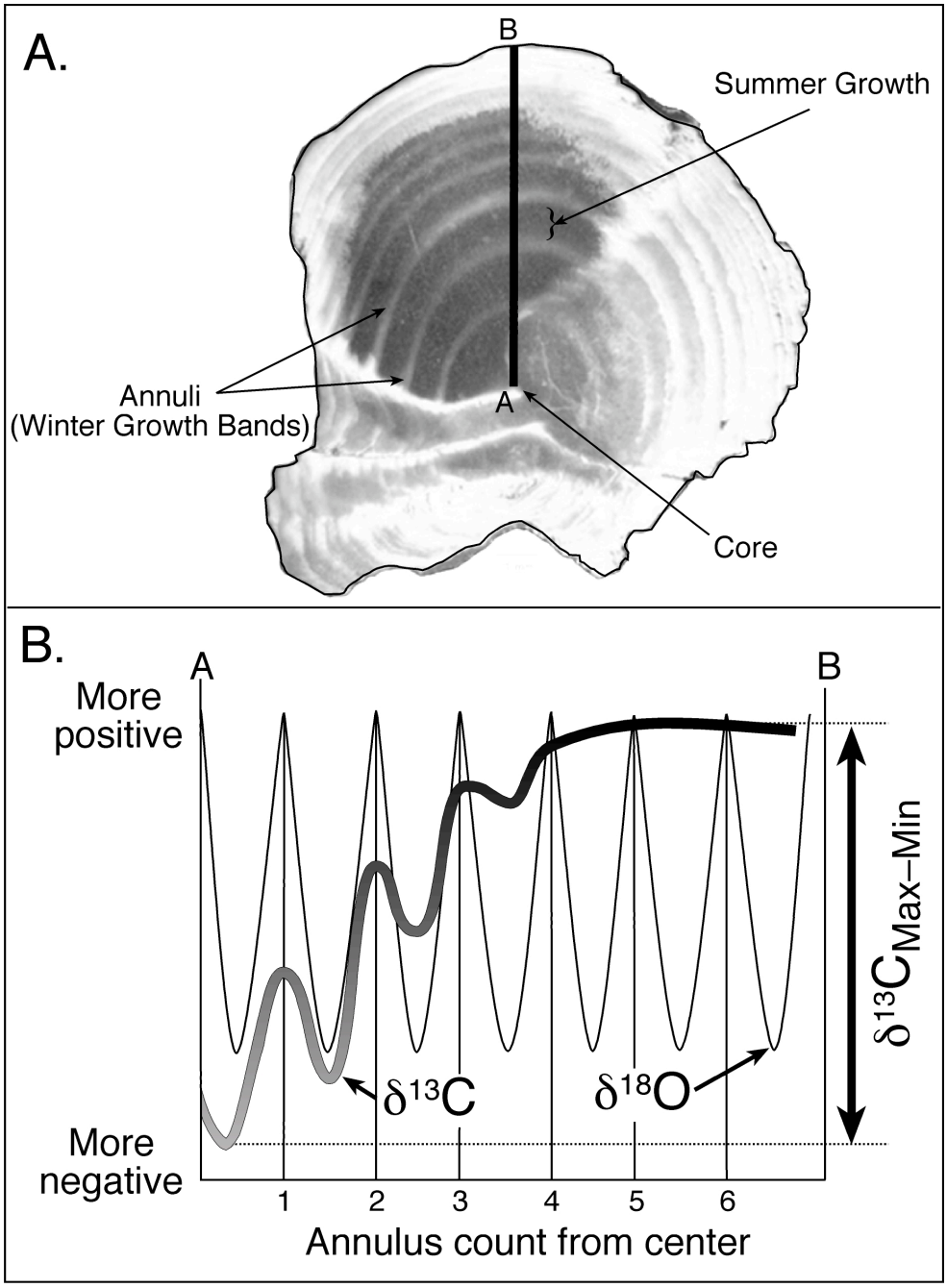

Figure 3.4—Idealized $\delta^{18}O$ and $\delta^{13}C$ profile and digital image of typical prepared teleost otolith.

A. Digital image of sampled specimen from 3.5 Ka illustrates a typical prepared freshwater drum sagittal otolith. B. An idealized transect of $\delta^{18}O$ and $\delta^{13}C$ values across an otolith. $\delta^{13}C$ values begin low and increase to relatively constant values and seasonally decrease with increasing temperature. $\delta^{18}O$ values display a seasonal pattern with lowest seasonal values representing maximum summer temperatures. This illustrates the primary pattern of a differential increase of intra-otolith $\delta^{13}C$ values, and a secondary pattern of an initial covariation between seasonal $\delta^{18}O$ and $\delta^{13}C$ values that decreases as the fish ages. Additionally illustrated is $\delta^{13}C_{max-min}$ for this idealized transect.

We used a mass balance model in which $\delta^{13}C_{(CaCO_3)}$ values of otolith aragonite reflect equilibrium with endolymph HCO_3^-, which is derived primarily from two reservoirs of carbon: the HCO_3^- of ambient water delivered directly to the endolymph through the gills, and blood HCO_3^- derived from metabolic processes. It is assumed that the $\delta^{13}C$ value of blood HCO_3^- derived from metabolic processes (Degens et al., 1969; Kalish, 1991a,b; Schwarcz et al., 1998) is close to the average $\delta^{13}C$ value of the fish's diet (DeNiro and Epstein, 1978; Tieszen et al., 1983; McConnaughey et al., 1997). Therefore, $\delta^{13}C_{(CaCO_3)}$ values of otoliths can be described by the mass balance equation:

$$\delta^{13}C_{(CaCO_3)} = M \bullet \delta^{13}C_{(diet)} + (1-M) \bullet \delta^{13}C_{(DIC)} + (2.7 \pm 0.6‰) \quad (3.1)$$

where M is the metabolic contribution of blood HCO_3^-, $\delta^{13}C_{(diet)}$ is the $\delta^{13}C$ value of the fish's diet, and $\delta^{13}C_{(DIC)}$ is the $\delta^{13}C$ value of ambient water HCO_3^- at the time of carbonate deposition. Equation (3.1) assumes that the $\delta^{13}C_{(CaCO_3)}$ value of the otolith is a product of the same fractionation relationship that characterizes precipitation of inorganic aragonite. Romanek et al. (1992) determined the aragonite-bicarbonate enrichment factor ($2.7 \pm 0.6‰$) to be independent of the temperature and precipitation rate. Likewise, Kalish (1991a,b) and Thorrold et al. (1997) found no evidence that the $\delta^{13}C_{(CaCO_3)}$ value of otoliths is directly influenced by temperature. Therefore, in this mass balance model, $\delta^{13}C_{(CaCO_3)}$ values of otoliths are described by three variables: $\delta^{13}C_{(DIC)}$, $\delta^{13}C_{(diet)}$, and metabolic contribution (M). We discuss each variable and describe how it may influence intra-otolith variation in $\delta^{13}C$ values.

3.4.2 Variable 1: $\delta^{13}C$ value in freshwater DIC

$\delta^{13}C_{(DIC)}$ values of freshwater systems are dominantly controlled by groundwater input, and by the respiration/photosynthesis ratio (e.g., Atekwana and Krishnamurthy, 1998; Veinott and Cornett, 1998; Dettman et al., 1999). Seasonal variation in $\delta^{13}C_{(DIC)}$ values is likely to be annually consistent because the annual variability of groundwater flow and productivity is repetitive (e.g., Quay et al., 1986; LaBaugh et al., 1995; Veinott and Cornett, 1998). Seasonal patterns of $\delta^{13}C_{(DIC)}$ values are documented to increase

during the summer because of increased photosynthesis and preferential sequestering of ^{12}C by plants (e.g., Yoshioka et al., 1994; Veinott and Cornett, 1998; von Grafenstein et al., 1999; Wang and Veizer, 2000).

We suggest that $\delta^{13}C_{(DIC)}$ does not explain the lifelong pattern described for intra-otolith $\delta^{13}C$ values (Figure 3.4). $\delta^{13}C_{(DIC)}$ values are not likely to differentially increase as the fish matures for each otolith analyzed regardless of its geologic age. Moreover, the seasonal patterns are contrary to what has been described for seasonal variation in $\delta^{13}C_{(DIC)}$ values. Seasonal $\delta^{13}C_{(CaCO_3)}$ values positively covary with $\delta^{18}O_{(CaCO_3)}$ values, suggesting that $\delta^{13}C_{(CaCO_3)}$ values decrease with increasing temperature (Figure 3.4). However, $\delta^{13}C_{(DIC)}$ values of aquatic environments typically increase seasonally with temperature (e.g., Veinott and Cornett, 1998; von Grafenstein et al., 1999; Wang and Veizer, 2000). Therefore, we conclude that although $\delta^{13}C_{(DIC)}$ value may be important for determining the baseline $\delta^{13}C$ values in otoliths, it is not a dominant control in intra-otolith variation.

3.4.3 Variable 2: $\delta^{13}C$ value of freshwater drum's diet

The diet of freshwater drum living in large rivers is dominantly composed of detritus-consuming invertebrates, including molluscs, crayfish and insect collector-gatherers—Trichoptera, Ephemeroptera and Diptera (Wahl et al., 1988; Dreves et al., 1996). The primary $\delta^{13}C_{(CaCO_3)}$ value pattern (a less-than-proportional increase with age) may be partially explained by a change in trophic position as a freshwater drum matures. In a food chain progression, consumer $\delta^{13}C$ values of tissues increase approximately 0.5-1‰ per trophic level (DeNiro and Epstein, 1978; McConnaughey et al., 1997). Food web isotope systems can become considerably more complex if consumers derive carbon from sources with entirely different $\delta^{13}C$ values. For example, a mobile predator may switch from a plankton-based diet to a detritus-based diet. Therefore, we cannot rule out significant trophic changes in freshwater drum diet. However, energy pathways in large rivers are largely detritus-based (Vannote et al., 1980; Wahl et al., 1988), suggesting a single dominant carbon source from detritus. Furthermore, available data suggest that riverine freshwater drum diet is largely detritus-based, and to be consistent with intra-otolith $\delta^{13}C$ variation (often over 10‰), freshwater drum would have to proportionally

switch between diets based on significantly different carbon sources, both seasonally and ontogenetically. The secondary pattern is not likely explained by seasonal dietary changes. There is little seasonal variation in $\delta^{13}C$ values of terrestrial detritus, and in the organisms consuming that detritus (Fry and Sherr, 1984; Yoshioka et al., 1994). A seasonal decrease in $\delta^{13}C_{(CaCO_3)}$ values of 5‰ is common in the first year, but seasonal changes in $\delta^{13}C_{(diet)}$ value would be minimal for a fish whose diet is composed primarily of detritivores (Fry and Sherr 1984; Yoshioka et al., 1994). Therefore, intra-otolith $\delta^{13}C_{(CaCO_3)}$ values of freshwater drum are unlikely to be explained by variation in $\delta^{13}C$ values of their diet, although a change in trophic position may be partially responsible for the intra-otolith (lifetime) shift toward more positive $\delta^{13}C_{(CaCO_3)}$ values (Figure 3.4).

3.4.4 Variable 3: Metabolic rate of freshwater drum

Finally we consider variation in the variable *M* from equation (3.1), the ratio of metabolic delivery of carbon to the endolymph. If the rate of DIC supply to the endolymph remains constant, variation in *M* will be controlled by metabolic rate of the fish (Kalish, 1991a,b; Schwarcz et al., 1998). This is likely true, because gill surface area, the method by which environmental DIC enters a fish, remains proportional to body volume once a fish has reached 1 g (Ursin, 1979; Hughes and Al-Kadhomiy, 1988). Metabolic rate cannot be modeled for freshwater drum because sufficient bioenergetic models have not been developed for freshwater drum nor can past site-specific variables be confidently estimated. However, many bioenergetic models have been published and tested for other freshwater species. Certain patterns are comparable for total specific respiration rate because the models rely on similar equations to calculate respiration rate.

Specifically, respiration (R) can be subdivided into three main components such that

$$R = R_s + R_a + R_d \qquad (3.2)$$

where R_s is the energy equivalent to that released in the course of metabolism in an unfed and resting fish (standard metabolism), R_a is the energy cost of activity, and R_d is the energy required for the processes of digestion and assimilation of food materials including specific dynamic action (Elliott, 1979). The term R_s can be defined by the following equation (Kitchell et al., 1977):

$$R_s = RA \bullet W^{RB} \bullet r_R \quad (3.3)$$

where RA and RB are constant and r_R is a temperature-dependent proportional adjustment of respiration, which will be further explained below. R_d can be determined as a constant proportion of consumption (e.g., Kitchell et al., 1977; Hanson et al., 1997). Therefore, as the mass of the fish increases the specific respiration rate decreases less than proportionally to body mass (allometric). This would indicate that term *M* in equation (3.1) would initially be high and relatively more respiratory carbon (with relatively more negative $\delta^{13}C$ values) would ultimately be incorporated into the otolith. *M* would decrease allometrically as the fish matures. This is the primary pattern observed, and idealized in Figure 3.4.

There is also a temperature component to specific respiration rate. Two common equations are used in respiration models and both account for activity (R_a in equation 3.2) (Hanson et al., 1997). In both equations, the basis of the temperature dependence is an exponential relationship with metabolic rate (for example, $e^{T \bullet K}$) (e.g., Kitchell et al., 1977; Stewart et al., 1983; Hanson et al., 1997). Both of these temperature dependent functions result in specific respiration rate increasing with temperature, at least until maximum lethal temperatures are attained. Therefore, if temperatures increase, *M* in equation (3.1) would increase, resulting in more negative otolith $\delta^{13}C$ values. $\delta^{13}C$ values would thus negatively covary with temperature. If the seasonal change noted in intra-otolith $\delta^{18}O$ values represents changing seasonal temperatures, then seasonal $\delta^{13}C$ values would be expected to covary with $\delta^{18}O$ values within the same growing season; this is our observed second pattern (Figure 3.4).

Specific respiration rate can be modeled to demonstrate patterns that would be expected seasonally and through the ontogeny of various fish species (Figure 3.5). Each modeled species (using previously published site-specific variables) demonstrates three patterns of change in specific respiration rate. First, we observe a decrease in specific respiration rate that is less than proportional to age. Second, we observe a seasonal covariation with temperature, although leads can be present as displayed in the yellow perch output (Figure 3.5). Third, we observe a decrease in the magnitude of seasonal change with ontogeny (Figure 3.5). Each pattern is consistent with the notion that *M* in equation (3.1) is driving intra-otolith variation in $\delta^{13}C$ values. The strong similarity

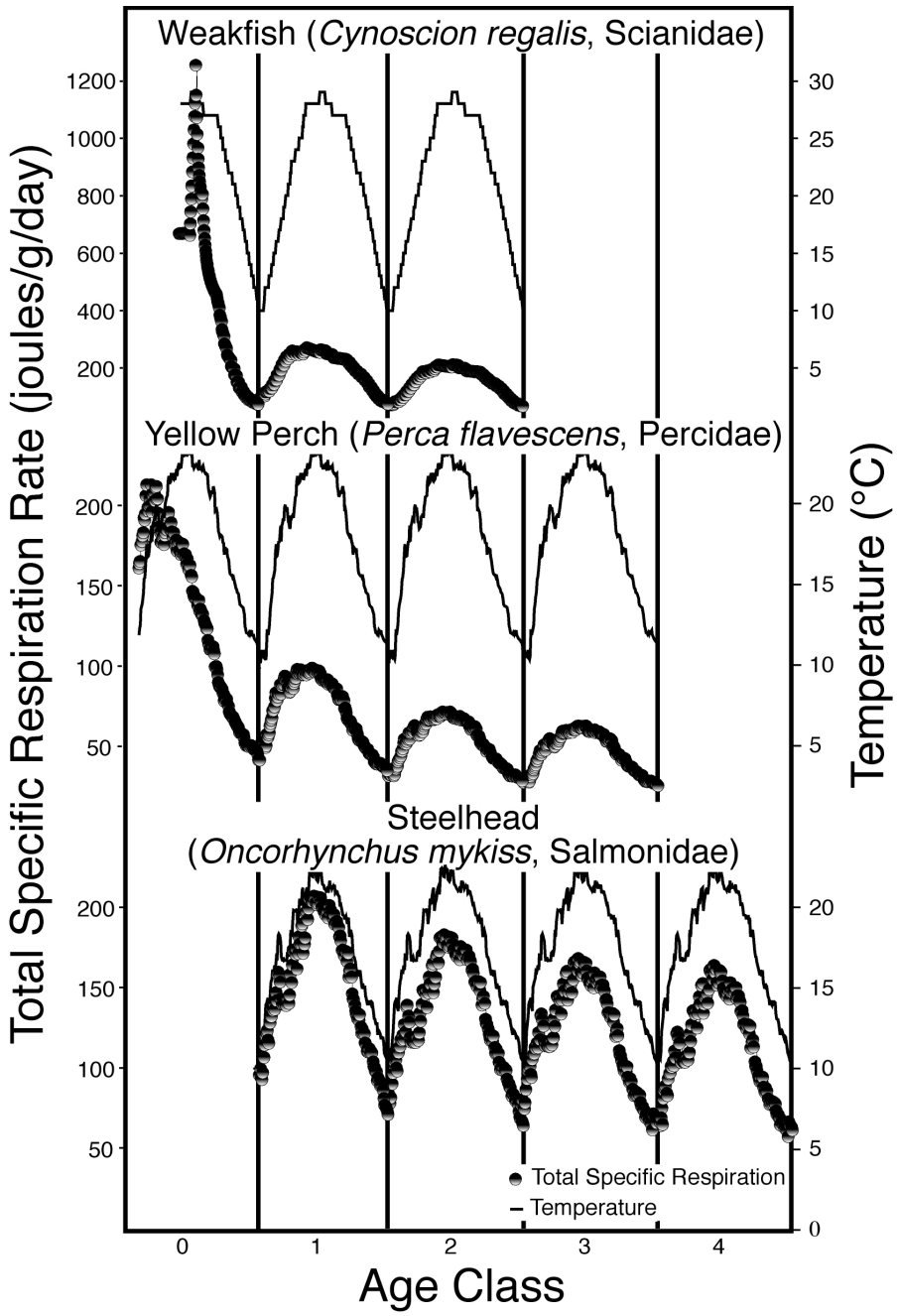

Figure 3.5—Bioenergetically modeled total specific respiration rate for three species of fish with well-parameterized bioenergetic models and published site-specific variables.

Temperatures used in the simulations are also plotted for comparison. Modeled total specific respiration rates (joules/g/day) were determined assuming a growing season above 10°C to better compare with freshwater drum $\delta^{13}C$ values (McInerny and Held, 1995; Patterson, 1998). Specific juvenile models have been parameterized for weakfish and yellow perch, and therefore Age Class 0 is displayed for these two species only. The weakfish bioenergetic model was parameterized by Hartman and Brandt (1995a) and site-specific variables are presented by Hartman and Brandt (1995b). Bioenergetic models and site-specific variables for yellow perch and steelhead were developed by Kitchell et al. (1977) and Rand et al. (1993), respectively. Model output was generated with Fish Bioenergetics 3.0 (Hanson et al., 1997).

between modeled specific respiration rate of various fish species and freshwater drum intra-otolith $\delta^{13}C$ values, coupled with a consistent theoretical basis, provides strong intuitive evidence that metabolism is driving intra-otolith $\delta^{13}C$ values in these freshwater drum otoliths.

Is the magnitude of change in specific respiration rate reasonable to explain a 10‰ decrease in intra-otolith $\delta^{13}C$ values both through ontogeny and through a growing season? For freshwater drum, this cannot be directly answered; however, we do want to note the dramatic change in metabolism, both ontogenetically and seasonally. Weakfish, in the same family as freshwater drum, exhibits a maximum of 1246 joules/g/day in the first year to a minimum of 62 joules/g/day in the last modeled year, accounting for a change of over 95%. Even yellow perch displays a maximum of 210 joules/g/day in the first year to a minimum of 24 joules/g/day in the last year (approximately a 90% change). Similar changes also occur within the first year of growth. If this percent change were directly translated to *M* in equation (3.1), and assuming a constant $\delta^{13}C_{DIC}$ and $\delta^{13}C_{diet}$ value within a season or through the lifetime, calculated $\delta^{13}C$ diet values are not out of the realm of possibility (Table 3.2). For example, Whitledge and Rabeni (1997) found crayfish $\delta^{13}C$ values similar to those of allochthonous detritus, a value of approximately –28‰ VPDB in an Ozark stream. $\delta^{13}C$ values of clams in San Francisco Bay range in the North Bay from –21.5‰ to –26.8‰ and in the South Bay from –17.7‰ to –23.2‰VPDB, varying in concert with $\delta^{13}C_{(DIC)}$ values (Fry, 1999). Additionally, Junger and Planas (1994) measured both $\delta^{13}C_{(DIC)}$ and $\delta^{13}C$ seston samples in boreal streams ranging in different catchment areas and found differences over 13‰ to 20‰. This exercise is merely to show that a 10‰ shift in intra-otolith $\delta^{13}C$ values can be reasonably accounted for from a shift in metabolic rate alone (Table 3.2).

3.4.5 Late Holocene temporal variation in metabolic rate of freshwater drum

If we assume that variation in $\delta^{13}C_{(CaCO_3)}$ values is largely a function of variation in metabolic rate, then we can assume that the total ontogenetic change in $\delta^{13}C_{(CaCO_3)}$ values ($\delta^{13}C_{max–min}$) can serve as a proxy for the change in metabolic rate from a juvenile to mature freshwater drum (Figure 3.4). Because we are limited at this time to observing only variation in intra-otolith $\delta^{13}C$ values (not the value itself), we focus our discussion

Table 3.2—$\delta^{13}C$ diet values calculated by using $\delta^{13}C$ otolith mass balance model (equation 3.1 in text). Inputs include change in intra-otolith $\delta^{13}C$ value, *M*, and $\delta^{13}C_{(DIC)}$. Total change indicates within a season or through the lifetime, assuming a constant $\delta^{13}C_{(DIC)}$ and $\delta^{13}C_{(diet)}$ within a season or through the lifetime.

Change in intra-otolith $\delta^{13}C$ value	Change in *M*	$\delta^{13}C_{(DIC)}$	Calculated $\delta^{13}C_{(diet)}$	$\delta^{13}C_{(DIC)} - \delta^{13}C_{(diet)}$
–10	0.95	0	–10.5	10.5
–10	0.95	–5	–15.5	10.5
–10	0.95	–10	–20.5	10.5
–10	0.95	–15	–25.5	10.5
–5	0.80	0	–6.3	6.3
–5	0.80	–5	–11.3	6.3
–5	0.80	–10	–16.3	6.3
–5	0.80	–15	–21.3	6.3

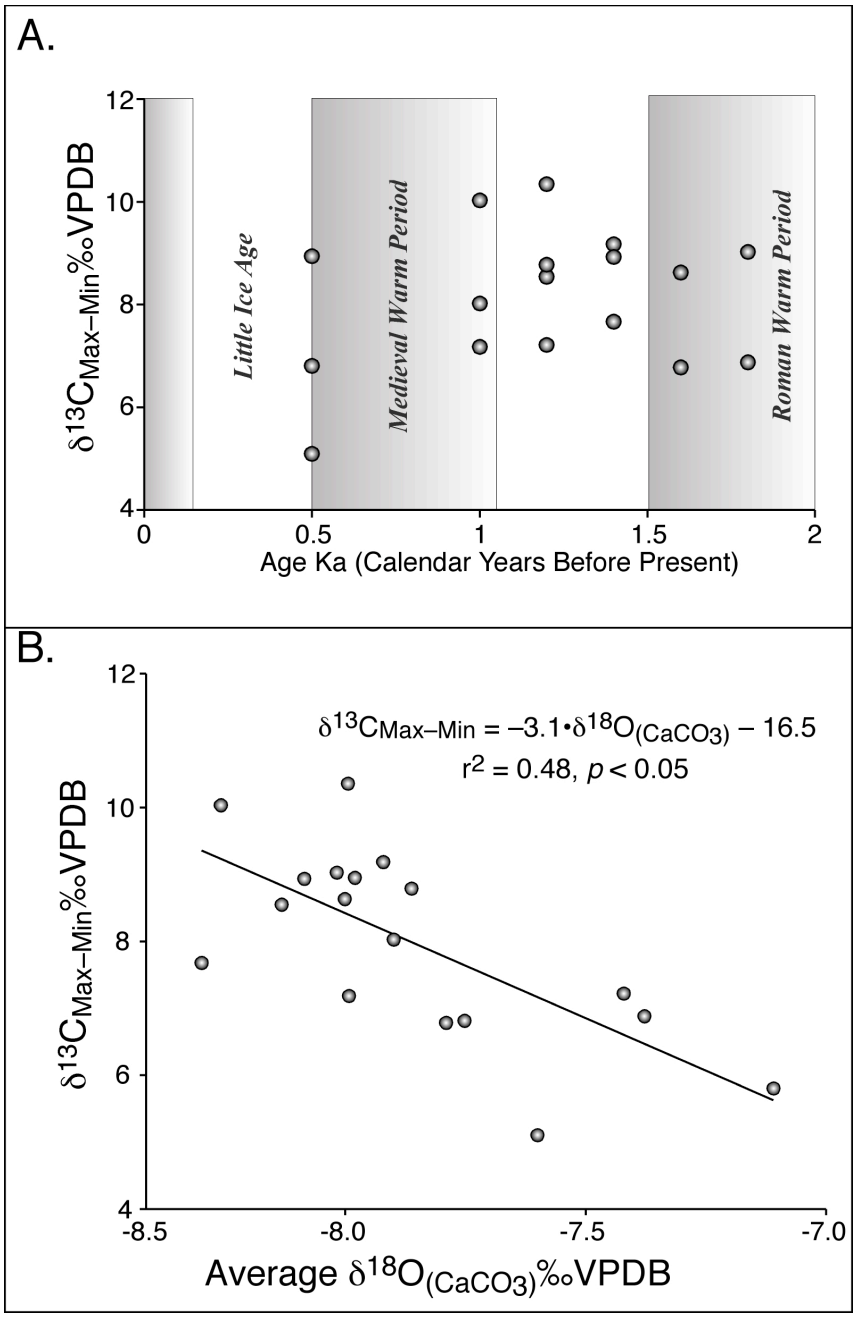

Figure 3.6—Secular variation in $\Delta^{13}C_{max-min}$ value and its relationship to climate.

A. Secular variation in $\Delta^{13}C_{max-min}$ value of low-resolution sub-fossil otoliths over the past 2000 years, possibly representing a change in metabolic history of freshwater drum; see text for explanation. B. $\Delta^{13}C_{max-min}$ values, used as a proxy for the change in metabolic rate from juvenile to mature fish, as a function of average $\Delta^{18}O_{(CaCO_3)}$ value, used as a proxy for climate.

on $\delta^{13}C_{max-min}$ values. We therefore investigated temporal changes and possible climatic controls on $\delta^{13}C_{max-min}$.

To ensure that $\delta^{13}C_{(CaCO_3)}$ values have reached the ontogenetic maximum value, we used otoliths aged at least 12 years that display a distinct $\delta^{13}C_{(CaCO_3)}$ plateau to calculate $\delta^{13}C_{max-min}$. Over the past 2000 years, we observe large variation within time periods and perhaps a weak temporal trend in $\delta^{13}C_{max-min}$ value (Figure 3.6A). Because climate can fluctuate within each age group, we investigated $\delta^{13}C_{max-min}$ values as a function of average $\delta^{18}O_{(CaCO_3)}$ values of individual otoliths. A linear regression between these two variables resulted in a significant negative correlation (r^2=0.48, $p < 0.05$; Figure 3.6B).

We suggest that over a lifetime, freshwater drum undergo greater variation in metabolic rate during periods of time represented by more negative $\delta^{18}O_{(CaCO_3)}$ values. Average $\delta^{18}O_{(CaCO_3)}$ values (driven dominantly by the $\delta^{18}O_{(H_2O)}$ value component in the temperature-fractionation relationship) are significantly related to local average annual temperatures (e.g., Dansgaard, 1964; Rozanski et al., 1993; Patterson, 1998) or to a change in the summer/winter precipitation ratio (Rozanski et al., 1993; Patterson, 1998). Because we find a significant relationship between $\delta^{13}C_{max-min}$ and $\delta^{18}O_{(CaCO_3)}$ value, we suggest metabolism-climate interactions are related to the length of the growing season (perhaps including milder winters). During climates characterized by more positive $\delta^{18}O_{(CaCO_3)}$ value, the metabolic difference between juvenile and mature freshwater drum appears to be smaller. This may result from increased foraging opportunities during warmer climates with longer growing seasons as well as the possibility that more food may be available. Although it may be more relevant to examine the relationship between climate and energetic factors other than the difference between juvenile and adult metabolism, we are constrained at this time by the necessity to observe intra-otolith change in $\delta^{13}C$ values as a proxy for changes in metabolic rate. It is nonetheless interesting to note that juvenile and/or mature freshwater drum do apparently alter their energetic behavior with changing $\delta^{18}O_{(CaCO_3)}$ values. This significant covariation suggests that fish energetic behavior is modified in a specific way, and this may be a working hypothesis for evolutionarily driven studies on energetics.

3.5 Conclusions

We find three dominant and repetitive intra-otolith $\delta^{13}C$ patterns from freshwater drum otoliths recovered from an archaeological site in northeast Tennessee. The first-order pattern of intra-otolith $\delta^{13}C$ values is a lifelong increase from more negative values early in the ontogeny of the fish to more positive and stable values as the fish matures. The second-order pattern is one of strong seasonal linear covariations between $\delta^{13}C_{(CaCO_3)}$ and $\delta^{18}O_{(CaCO_3)}$ values. And third, these covariations have r^2 values and slopes that tend to progressively decrease with age as a result of a lower magnitude of $\delta^{13}C$ seasonal change with age. The total variation in these drum otoliths ($\delta^{13}C_{\ max–min}$) is up to 14.2‰, and total seasonal variations are often greater than 5‰, indicating that a wealth of variability and information is potentially lost if otoliths are analyzed whole rather than subsampled.

We find these patterns similar to modeled specific respiration rates from different fish species and families. Therefore, we propose that intra-otolith $\delta^{13}C$ values are dominantly a result of changing metabolic rate of the fish, yielding the potential of otolith $\delta^{13}C$ value to be used as a proxy for respiration throughout the entire ontogeny of the fish. This would provide information for studies on the energetic studies of fishes, including helping to answer current questions on tissue turnover and activity. Moreover, these energetics studies could be applied to past populations of fish, on both a historic and a geologic time frame, for which we show an example. Further investigation of $\delta^{13}C_{(CaCO_3)}$ values derived from species with well-parameterized bioenergetics models could lead to further insights into factors that determine $\delta^{13}C$ values of otoliths. Those studies could, in turn, facilitate additional investigations in paleoclimatology, evolutionary studies, paleoecology, and bioenergetics.

Chapter 4. Thermal histories, stress, and metabolic rates of chinook salmon (*Oncorhynchus tshawytscha*) in Lake Ontario: evidence from intra-otolith stable isotope analyses[3]

4.1 Introduction

There is considerable concern that Lake Ontario's salmonine sport fishery is reaching the limits of sustainability (e.g., Rand et al., 1994; Rand and Stewart, 1998a; Mills et al., 2003). Chinook salmon (*Oncorhynchus tshawytscha*; hereinafter referred to as chinook) were estimated to generate five times as much lake-wide production than either coho salmon (*Oncorhynchus kisutch*) or lake trout (*Salvelinus namaycush*) in Lake Ontario (Rand and Stewart, 1998b) and, therefore, chinook were the top predators with the highest forage demand of all stocked salmonines (Jones et al., 1993). Because the diet of chinook in Lake Ontario during their pelagic residence is composed almost entirely of alewife (*Alosa pseudoharengus*) (Brandt, 1986; Rand and Stewart, 1998b; Lantry, 2001), chinook energetics are key to understanding ecological stress in this system. Originally introduced in the 1970s to control a burgeoning population of non-native alewife, chinook have subsequently been found by a number of studies to rely dominantly on alewife, despite the latter's decreasing abundance and quality (e.g., Mason et al., 1995; Rand and Stewart, 1998b; Lantry, 2001). The presence of chinook subsequently allowed the development of an important recreational fishery that generates considerable economic activity for many coastal districts (Talhelm, 1988; Mills et al., 2003). This substantial economic resource stimulated the growth of salmonine hatcheries around the lake (Hartig et al., 1991). However, prey fish production may be inhibited by significant

[3] Wurster, C. M., W. P. Patterson, D. J. Stewart, J. N. Bowlby, and T. J. Stewart, 2005. Thermal histories, stress, and metabolic rates of chinook salmon (*Oncorhynchus tshawytscha*) in Lake Ontario: evidence from intra-otolith stable isotope analyses. Canadian Journal of Fisheries and Aquatic Sciences 62(3): 700-713. Reprinted with kind permission of the National Research Council of Canada

reductions in total phosphorous concentrations and nutrient loading in Lake Ontario (Johengen et al., 1994), and subsequent zebra and quagga mussel invasions (e.g., Mills et al., 2003). In addition to the increase in predatory pressure (e.g., O'Gorman and Stewart, 1999), these conditions in Lake Ontario may have contributed to the observed rapid reduction in prey availability and quality (e.g., Mills et al., 2003), and the concern that chinook cannot maintain current growth and survival rates (e.g., Rand and Stewart, 1998a).

Bioenergetic simulations suggest that consumption by chinook is near the maximum rate for the current environment in Lake Ontario (e.g., Rand and Stewart, 1998b), although consumption may be limited more by thermal stress than by production itself. Rand et al. (1994) originally predicted that chinook would have to triple their ingestion of prey fish to make up for decreases in prey size and condition, an inference that was subsequently supported (e.g., Rand and Stewart, 1998a; Lantry, 2001). Chinook in Lake Michigan, undergoing similar stress due to reduction in prey abundance and quality, have already been observed to undergo a reduction in growth and survival, coupled with an increase in disease (Stewart and Ibarra, 1991; Rand and Stewart, 1998a). Bioenergetic simulations were conducted with the assumption that chinook occupy water at 11 °C during the midsummer. However, the highest alewife biomass density in Lake Ontario is in the epilimnion at 21 °C (Mason et al., 1995), and there is some evidence that chinook may move to warmer water to obtain increasingly scarce food resources (e.g., Olson et al., 1988; Goyke and Brandt, 1993). Higher temperatures require higher food intake to compensate for the increased energetic cost of respiration. We can now reconstruct individual thermal history records preserved in sagittal otoliths of chinook to test the hypothesis that chinook in Lake Ontario are now found in warmer water than in the past.

Otoliths are aragonitic biominerals produced in the inner ear of teleost fish and used in hearing and balance (Campana, 1999). This structure grows sequentially, without resorbtion, and often displays yearly and daily banding patterns that provide age and growth information for most fish species (e.g., Panella, 1980). Therefore, high-resolution $\delta^{18}O$ and $\delta^{13}C$ subseasonal records can be acquired from these biominerals. Because $\delta^{18}O$ values of otoliths have been determined to form at or near equilibrium with the ambient

water (e.g., Patterson et al., 1993; Thorrold et al., 1997; Høie et al., 2004a), the temperature experienced by the fish can be tracked throughout its life if the $\delta^{18}O$ value of the ambient water is known, and variations in that value are unlikely (in a large lake with relatively constant $\delta^{18}O$ values, for example). Conversely, widely disparate $\delta^{18}O_{(H_2O)}$ values can be used to track migration patterns (tributary-to-lake migrations, for example).

The $\delta^{13}C$ values of otoliths were originally thought to reflect $\delta^{13}C$ values of dissolved inorganic carbon (DIC) only (Degens et al., 1969). However, otolith $\delta^{13}C$ values are considerably lower than those predicted assuming equilibrium with ambient water, suggesting that there is a metabolic contribution of respiratory carbon to the otolith (e.g., Kalish, 1991a,b). Recent studies clearly indicate a relationship between metabolic rate and incorporation of otolith carbon (Tohse and Mugiya, 2002; Høie et al., 2003) and intra-otolith $\delta^{13}C$ values have been shown to record ontogenetic variations in metabolic rate (Schwarcz et al., 1998; Wurster and Patterson, 2003; Høie et al., 2004b). Although more work is necessary to evaluate intra-otolith $\delta^{13}C$ values given the confounding influences of environment, diet and tissue turnover, $\delta^{13}C$ values may become a powerful proxy for fish physiology and (or) environment once relative controls are quantified. So $\delta^{13}C$ values may provide a unique proxy for individual energetic behavior, such as the cost of activity (Sherwood and Rose, 2003; Wurster and Patterson, 2003), especially in fishes with a relatively stable diet and whose reproduction is reserved for the end of life such as adult chinook. Therefore, intra-otolith $\delta^{18}O$ and $\delta^{13}C$ values may provide both an indirect record of the most fundamental variable, temperature (He and Stewart, 1998), and arguably the most difficult parameter to estimate, respiration of activity in free-ranging fishes (e.g., Rowan and Rasmussen, 1996; Trudel et al., 2004).

The primary goal of this study is to track temperatures that chinook experience during their pelagic residence in Lake Ontario. Temperatures are estimated from an otolith-specific aragonite temperature-fractionation relationship for freshwater fish (Patterson et al., 1993) using intra-otolith $\delta^{18}O$ values, and measured $\delta^{18}O$ values of Lake Ontario water. Intra-otolith $\delta^{18}O$ and $\delta^{13}C$ values are analyzed for a suite of otoliths collected in 1991 (archived group) and in 1997 (Salmon River group) to compare potential changes in temperature of waters occupied as prey fish abundance and quality declined after 1991. We coupled this new information with a chinook bioenergetic model (Stewart and Ibarra,

1991) to evaluate the level of stress within the Lake Ontario pelagic food web using specific growth rate and gross conversion efficiency (GCE; gross production/prey consumption) as a measure of that stress. We examined rates of exploitation of prey fish and compared results to earlier simulations that modeled chinook at preferred temperatures in midsummer (Rand et al., 1994; Rand and Stewart, 1998b). A secondary goal of this study is to evaluate intra-otolith $\delta^{13}C$ values as a potential indicator of metabolic rate.

4.2 Methods

4.2.1 Field collection, micromilling, and analysis of $\delta^{18}O$ and $\delta^{13}C$ values

Archived otoliths were obtained from angler-caught chinook from Ontario waters of Lake Ontario in 1991 (Stewart et al., 2003). Chinook also were taken during their spawning run into the Salmon River, New York, on 7 October 1997. Sex and total length were noted, and both otoliths were removed and stored in an envelope. Six archived otoliths collected in 1991, and a subset of nine otoliths collected in 1997 were chosen for application of micromilling techniques. Chinook otolith lengths were generally 9-10 mm for a sagittal section. The monthly trend in body condition was determined as the mean weight of a 600 mm long chinook after adjusting for differences in length and year using analysis of covariance. Fork length and wet weight of chinook were measured in angler surveys during 1988-1992 (Stewart et al., 2003). Fork lengths ranged from 300 to 780 mm. Body condition was not significantly different between ages 1 and 2, and so these fish were combined for this analysis.

Detailed methodology for micromilling is described by Wurster et al. (1999). Specimens were polished to reveal growth annuli, attached to a stage beneath a fixed dental drill, and viewed on a computer monitor via a color digital video camera. Annuli were subsequently digitized in real-time as a series of three-dimensional coordinates, while intermediate coordinates were interpolated using a cubic spline algorithm. An array of intermediate sampling paths was calculated between digitized curves. Sample path arrays guided three high-precision actuators, which positioned the sample stage relative to the fixed dental drill. Approximately 30 to 50 µg aliquots of sample carbonate were recovered for routine analysis.

Once extracted, samples were roasted *in vacuo* for one hour at 200 °C to remove volatiles that may have interfered with $\delta^{18}O$ and $\delta^{13}C$ measurement. Samples were reacted in a Kiel III automated carbonate preparation device directly coupled to a Finnigan MAT 252 or a MAT 253 stable isotope ratio mass spectrometer. Carbon dioxide was generated by the reaction of carbonate with 3 to 4 drops of anhydrous phosphoric acid in individual reaction vessels at 70 °C. Individual samples were analyzed using a micro-inlet, which reduces sample "memory" and permits analysis of ~20 μg of carbonate. Carbonate samples were analyzed with a precision of ± 0.08‰ (1σ), determined by analysis of international carbonate standards NBS-18 and NBS-19, and reported relative to Vienna Pee Dee Belemnite (VPDB).

Water samples were collected from the surface of Salmon River and Lake Ontario in Nalgene™ containers, which were sealed until analyzed for $\delta^{18}O_{(H_2O)}$. Most samples were measured using a Finnigan HDO-II water equilibration device directly coupled to a Finnigan MAT 252 gas ratio mass spectrometer. For measuring $\delta^{18}O_{(H_2O)}$, standard carbon dioxide gas was equilibrated with water samples for six hours at 25 °C and then analyzed sequentially. Values are reported to ± 0.1‰ for $\delta^{18}O_{(H_2O)}$ relative to Vienna Standard Mean Ocean Water (VSMOW). Replicate analyses of water samples were better than ± 0.1‰. A few additional Lake Ontario $\delta^{18}O_{(H_2O)}$ values were analyzed on a Finnigan High-Temperature Conversion/Elemental Analyzer via high-temperature pyrolysis. Samples analyzed for $\delta^{18}O_{(H_2O)}$ via both high-temperature pyrolysis and water equilibrator methods agreed within ± 0.1‰. Carbonate and water stable isotope analyses were performed at the isotope laboratories of Syracuse University, Syracuse, New York, and the University of Saskatchewan, Saskatoon.

4.2.2 Estimation of chinook temperatures

Temperatures can be calculated from otolith aragonite with a precision and accuracy better than 1 °C (Thorrold et al., 1997; Høie et al., 2004b). Several otolith-specific aragonite temperature-fractionation relationships have been determined from well-constrained environments (e.g., Patterson et al., 1993; Thorrold et al., 1997; Høie et al., 2004a). These relationships have slopes that are statistically indistinguishable from each other and from Kim and O'Neil's (1997) theoretical temperature-fractionation

relationship for inorganic aragonite, although the intercepts may differ significantly (Campana 1999; Thorrold and Hare, 2002). Because of the similar slopes, we calculated chinook temperatures from the aragonite temperature-fractionation relationship of Patterson et al. (1993) (which included freshwater salmonid otoliths) using the measured otolith $\delta^{18}O$ value and the Lake Ontario $\delta^{18}O$ value. We used –6.8‰VSMOW as the $\delta^{18}O$ value of Lake Ontario water (e.g., Hodell et al., 1998; Coplen and Kendall, 2000; this study).

Because of differing growth rates and size of otoliths, not all the specimens were microsampled at the same resolution. In order to compare seasonal values, we assume limited otolith growth for winter months. We matched each calculated minimum temperature to the average Lake Ontario water temperature to estimate both the spring and fall Julian day that the minimum temperature represents. We then assumed equal growth through the growing season to determine the day of the year each temperature estimate represents. Therefore, we are not accounting for seasonal growth changes within and among otoliths; nonetheless, this is a relatively unbiased way to transform data and compare individual years. Lake Ontario water temperature estimates are derived from Hodell et al. (1998) and from the National Oceanic and Atmospheric Administration's Great Lakes Environmental Research Laboratory (http://coastwatch.glerl.noaa.gov).

4.2.3 Chinook energetics

We used the chinook bioenergetics model of Stewart and Ibarra (1991), implemented with the "Fish Bioenergetics 3.0" computer application (Hanson et al., 1997), to evaluate production, predation, and stress of chinook in Lake Ontario. Detailed inputs to the model differ from those used by Rand and Stewart (1998b) in temperature only; therefore, we do not include a detailed description of the energetics model nor the inputs. Energy density of predator and prey, and diet proportions (including invertebrates and prey fish) can be found in other publications (Elrod and O'Gorman, 1991; Stewart and Ibarra, 1991; Rand et al., 1993).

Most chinook in Lake Ontario spawn in their third year or fourth year, and discounting age 0+ and the year of spawning, most chinook have spent 1 or 2 "full" summers as offshore residents (e.g., Rand and Stewart, 1998b). We therefore modeled the

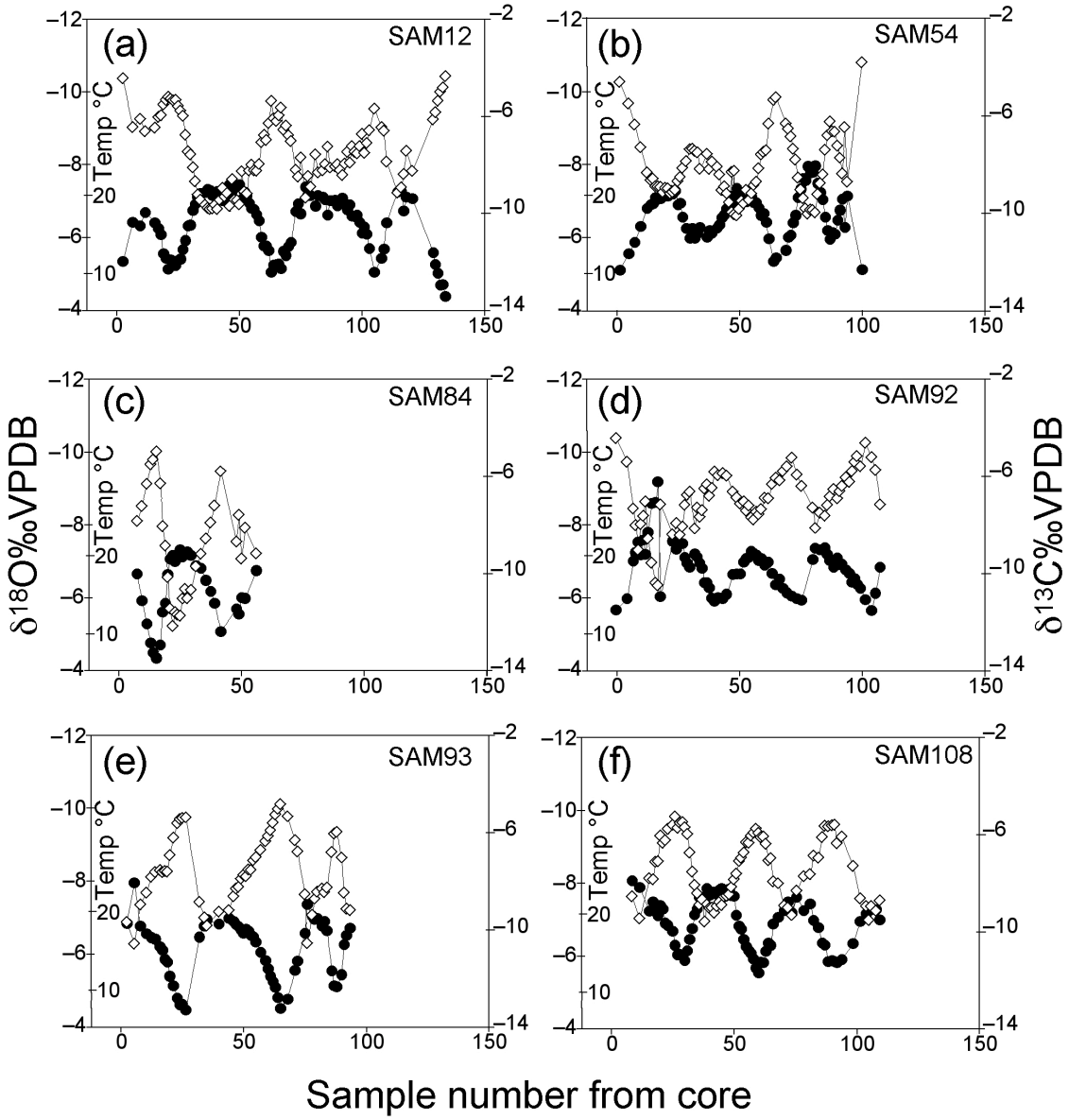

Figure 4.1—Intra-otolith $\delta^{18}O$ values and calculated temperatures (dark circles), and $\delta^{13}C$ values (open diamonds) relative to Vienna Pee Dee Belemnite (VPDB) for the archived group of chinook (*Oncorhynchus tshawytscha*) in Lake Ontario.

Archived specimens were collected in 1991 from offshore waters of Lake Ontario. Each subplot represents one otolith from an individual fish. $\delta^{18}O$ and $\delta^{13}C$ values are plotted according to the number of sample from the core of the otolith; note $\delta^{18}O$ values are plotted with more negative values toward the top. Temperature (°C) scale (inset) is calculated using a Lake Ontario $\delta^{18}O$ value of –6.8‰ Vienna Standard Mean Ocean Water (VSMOW) and Patterson et al.'s (1993) temperature-fractionation relationship for freshwater fish otolith aragonite.

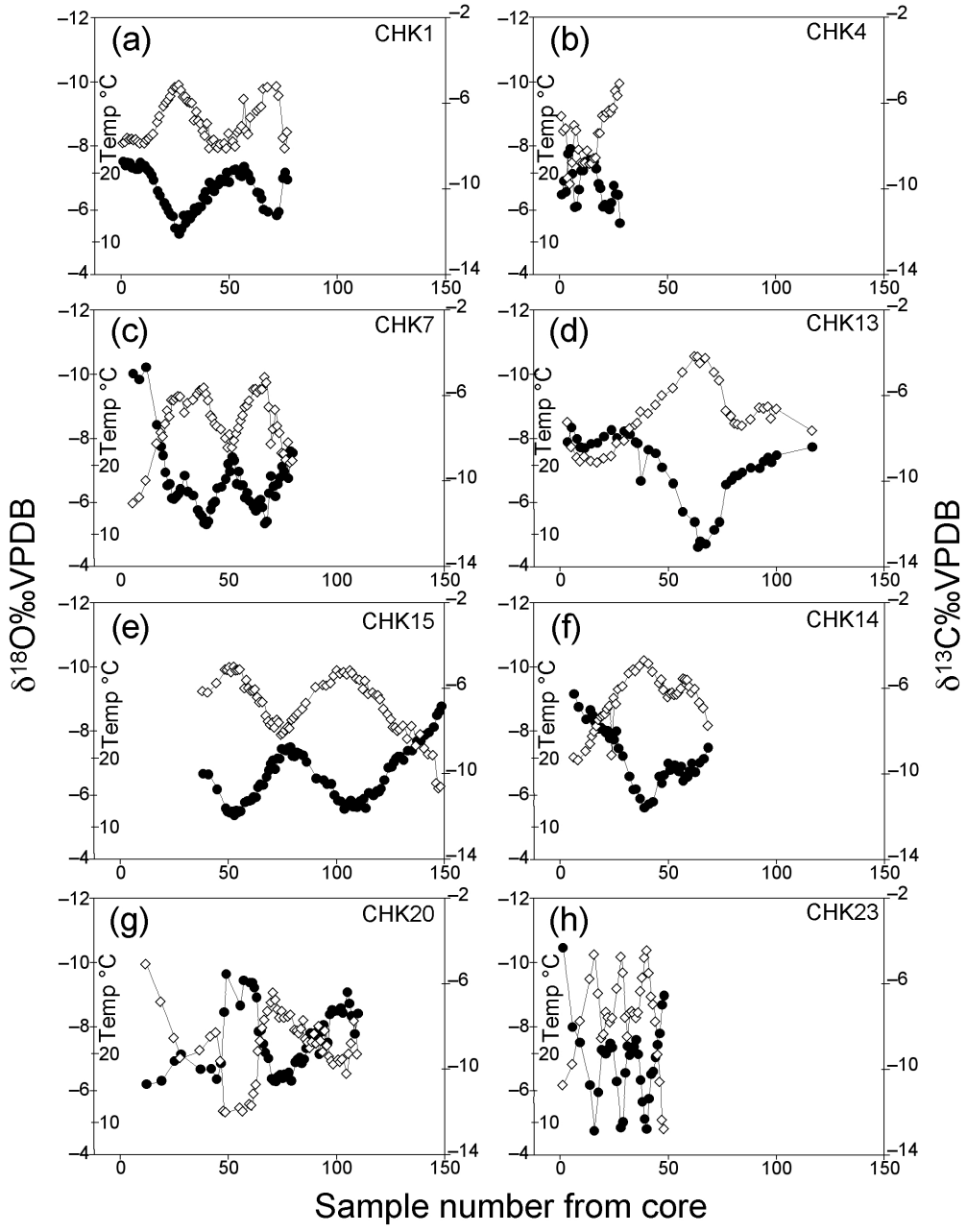

Figure 4.2—Intra-otolith $\delta^{18}O$ values and calculated temperatures (dark circles), and $\delta^{13}C$ values (open diamonds) relative to Vienna Pee Dee Belemnite (VPDB) for chinook (*Oncorhynchus tshawytscha*) from the Salmon River group.

Otoliths were collected on 7 October 1997 during the annual Salmon River, New York, spawning run. Each subplot represents one otolith from an individual fish. $\delta^{18}O$ and $\delta^{13}C$ values are plotted by the number of sample from the core of the otolith; note that $\delta^{18}O$ values are plotted with lower values toward the top. Temperature (°C) scale (inset) is calculated using a Lake Ontario $\delta^{18}O$ value of –6.8‰ Vienna Standard Mean Ocean Water (VSMOW) and Patterson et al.'s (1993) temperature-fractionation relationship for freshwater fish otolith aragonite.

dominant life forms of chinook for an average fish from 1989-1991, and an average fish from 1995-1997 to compare with a nominal simulation by Rand and Stewart (1998b).

From the bioenergetic model outputs, we estimated specific growth rate, GCE, and prey consumption of an average individual chinook in Lake Ontario as a measure of stress. This modeling exercise was repeated using assumed preferred temperatures (nominal simulation) to compare bioenergetic outputs with chinook temperatures found via the otolith thermometry technique.

4.3 Results

4.3.1 Intra-otolith $\delta^{18}O$ and $\delta^{13}C$ values

Specimens from the archived group, collected in 1991 from Lake Ontario, display cyclic patterns in $\delta^{18}O$ values that range from –7.4 ± 0.3‰VPDB to –5.3 ± 0.6‰VPDB. $\delta^{13}C$ values covary with $\delta^{18}O$ values (Table 4.1; Figure 4.1). Specimens collected in 1997 from the Salmon River (Salmon River group) also display cyclicity, however both $\delta^{18}O$ and $\delta^{13}C$ values in the first and last years, are much more negative than the other values (Figure 4.2). We assume that each cycle represents one year of otolith growth, and pelagic residence is assumed to include all cycles except the first, which corresponds to the age 0+, and the last half-year of growth in the Salmon River group, which corresponds to the spawning run. Intra-otolith $\delta^{18}O$ and $\delta^{13}C$ values of specimen CHK20 (CHK is a sample code for chinook from the Salmon River group) are unique relative to the other 14 otoliths sampled (Figure 4.2g). This specimen's $\delta^{18}O$ values are generally more negative and show a much greater seasonal range. Because no distinct pelagic-residence years could be interpreted from CHK20, we did not consider this data set in analyses requiring Lake Ontario residence, but it should be noted as an example of alternate behavior, perhaps this fish spent a year in a river before smolting.

Minimum $\delta^{18}O$ values for all pelagic-residence years were remarkably consistent for both the archived group and the Salmon River group (–7.4 ± 0.3‰VPDB, and –7.5 ± 0.1‰VPDB, respectively), and mean values did not differ significantly between groups (*t* test, $p < 0.05$). However, maximum $\delta^{18}O$ values for individual pelagic-residence years did vary somewhat more among specimens, yet they had the same mean value, –5.3 ± 0.6‰VPDB and –5.3 ± 0.5‰VPDB for the Archived and Salmon River groups,

Table 4.1—Covariation between intra-otolith $\delta^{18}O$ and $\delta^{13}C$ values of individual Lake Ontario chinook (*Oncoryhnchus tshawytscha*).

Specimen	Equation	r^2
Salmon River group		
CHK1	$\delta^{13}C = 1.3 \bullet \delta^{18}O + 1.5$	0.73
CHK4	$\delta^{13}C = 1.3 \bullet \delta^{18}O + 1.7$	0.73
CHK7	$\delta^{13}C = 1.3 \bullet \delta^{18}O + 1.5$	0.73
CHK13	$\delta^{13}C = 1.8 \bullet \delta^{18}O + 4.6$	0.78
CHK14	$\delta^{13}C = 1.3 \bullet \delta^{18}O + 2.6$	0.84
CHK15	$\delta^{13}C = 1.4 \bullet \delta^{18}O + 2.8$	0.90
CHK23	$\delta^{13}C = 1.5 \bullet \delta^{18}O + 2.7$	0.81
Pooled	$\delta^{13}C = 1.2 \bullet \delta^{18}O + 1.5$	0.71
Archived group		
SAM12	$\delta^{13}C = 1.7 \bullet \delta^{18}O + 3.3$	0.87
SAM54	$\delta^{13}C = 1.9 \bullet \delta^{18}O + 4.9$	0.85
SAM84	$\delta^{13}C = 2.2 \bullet \delta^{18}O + 4.6$	0.87
SAM92	$\delta^{13}C = 1.6 \bullet \delta^{18}O + 4.0$	0.84
SAM93	$\delta^{13}C = 1.6 \bullet \delta^{18}O + 2.5$	0.87
SAM108	$\delta^{13}C = 1.6 \bullet \delta^{18}O + 3.4$	0.70
Pooled	$\delta^{13}C = 1.4 \bullet \delta^{18}O + 1.8$	0.57
All data pooled	$\delta^{13}C = 1.3 \bullet \delta^{18}O + 1.1$	0.55

respectively. Mean maximum $\delta^{18}O$ values for pelagic-residence years also did not differ significantly between the groups (*t* test, $p < 0.05$).

In contrast to the remarkable consistency in seasonal minimum $\delta^{18}O$ values among individual chinook otoliths, seasonal minimum $\delta^{13}C$ values are inconsistent despite strong covariations between $\delta^{13}C$ and $\delta^{18}O$ values (Table 4.1; Figure 4.1, 4.2). Both groups have notable covariation between $\delta^{18}O$ and $\delta^{13}C$ values, with CHK15 having the highest correlation coefficient ($r^2 = 0.90$; Table 4.1). Least squared linear regressions are significantly different and cannot be considered as having the same relationship between $\delta^{13}C$ and $\delta^{18}O$ values for any of the populations–archived, Salmon River, or grouped. However, linear regressions for specimens in the archived group except specimen SAM84 (SAM is a sample code for chinook from the archived group) are not significantly different based on analysis of covariance ($\alpha = 0.05$, $F_{[4,375]} = 2.26$).

4.3.2 Chinook thermal histories and energetics

We measured $\delta^{18}O_{(H_2O)}$ values of –6.9 ± 0.05‰VSMOW for Lake Ontario in 1998 and 2000 (n = 4), that are consistent with Hodell et al.'s (1998) $\delta^{18}O_{(H_2O)}$ values of –6.7 ± 0.13‰VSMOW from Rochester basin surface waters and a depth transect during the years 1993-1995 (n = 37). Those authors concluded that Lake Ontario showed relatively little variation with depth, time, or space. Additionally, these values agree well with that of the Niagara River (–6.8‰VSMOW; Gat et al., 1994; Coplen and Kendall, 2000), which is considered characteristic of the eastern portion of the Great Lakes system (Gat et al., 1994). We used a value of –6.8‰VSMOW to calculate chinook temperatures and consider this value stable through space, depth, and time for Lake Ontario's water.

Midsummer temperatures calculated using this $\delta^{18}O_{(H_2O)}$ value (–6.8‰VSMOW) and Patterson et al.'s (1993) temperature-fractionation relationship are consistently near 20 °C (Figure 4.3), and exceed 22 °C in two specimens (Figure 4.1b, 4.1f). The lowest maximum temperature calculated was 18 °C from SAM93 in the archived group (Figure 4.3a). Most specimens appear to reach and stay within a narrow temperature range in midsummer for two or three weeks (Figure 4.3). Several pelagic-residence years show evidence of a two-step temperature change, where the chinook remain at one temperature

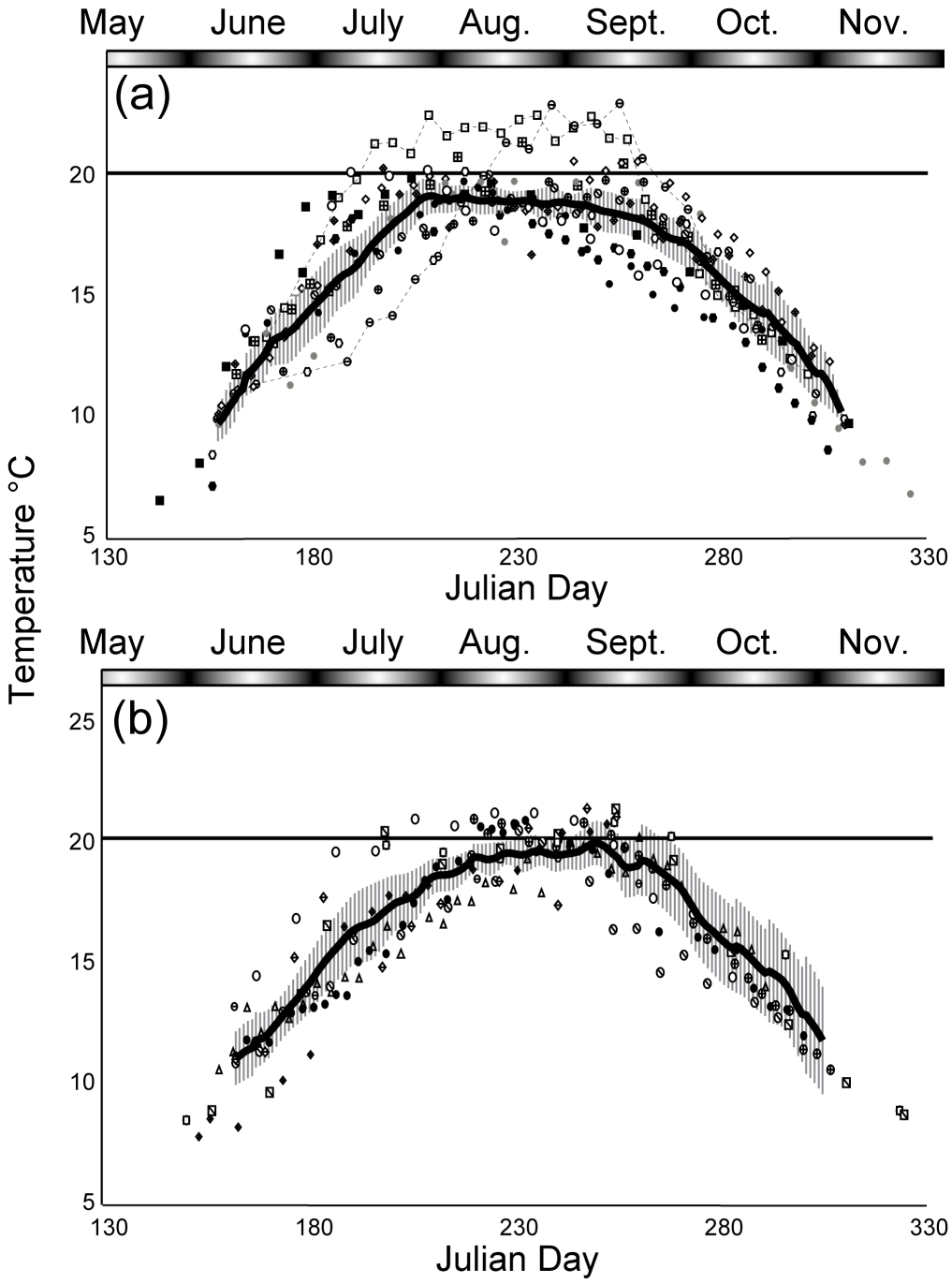

Figure 4.3—Estimated seasonal temperatures during chinook in the archived group (a) and the Salmon River Group (b) in Lake Ontario calculated via otolith thermometry.

Minimum calculated temperature was used to determine the Julian day for the first day of growth (spring) and the last day of growth (fall) for each yearly profile. Invariant growth rates were assumed within one growing season to reconstruct and compare chinook seasonal temperature variation. Average seasonal temperature profiles and confidence intervals were determined from cubic spline interpolations of each specimen's temperature profile to ensure equal representation of each year. Each symbol represents one pelagic-residence year.

for a period of time and then move into water that is 1-2 °C warmer or colder for the remainder of the midsummer period (for examples see Figures 4.1a and 4.2g).We do not know to what extent deviation from this dominant pattern is merely a result of differences in seasonal growth in the otolith or in fish movement in Lake Ontario. We then averaged temperatures for the Salmon River group and for the archived group separately (Figure 4.3). In order to weight each specimen equally, we interpolated daily temperatures for each specimen using a cubic spline. Averages of both groups show a similar pattern, reaching relatively stable temperatures at about 19 °C in midsummer. Despite the similarity, mean temperatures of each group from day 210 to day 250 (midsummer) are significantly different (*t* test, $p < 0.05$), with the Salmon River group mean temperature +0.4 °C higher than that of the archived group. Additionally, we find linear regressions between estimated pelagic temperatures and $\delta^{13}C$ values are homogenous for otoliths within the archived group (except SAM84), the Salmon River group, and between these two groups, suggesting that given the same Lake Ontario environment, the relationship between $\delta^{13}C$ and $\delta^{18}O$ values is the same. SAM84 displays unusually negative $\delta^{13}C$ values during pelagic residence (Figure 4.1c) resulting in a much greater slope (Table 4.1).

Otolith thermometry of the archived and Salmon River groups suggests that chinook are reaching and staying for some time in ~19 °C water. Therefore we re-ran the bioenergetic simulation of Rand and Stewart (1998b) assuming chinook inhabited the warmest available water up to but not exceeding 11 °C (nominal simulation) or 19 °C (otolith thermometry simulation). Energetic comparisons between the nominal and otolith thermometry simulations indicate significant stress imposed upon Lake Ontario chinook in midsummer (Figure 4.4). Specific growth rate declines to near 0 in midsummer for the otolith thermometry simulation and is nearly six times lower than for the comparative nominal simulation in midsummer (Figure 4.4). However, specific growth rate is higher for the otolith thermometry simulation relative to the nominal simulation just prior to and just post the growth depression in midsummer. GCE imitates this pattern, declining in midsummer to less than 0.1 (Figure 4.4). In order to maintain observed growth, chinook in the otolith-based simulation are consuming prey fish near the maximum rate and annually consume 18% more prey by weight relative to the nominal simulation (Table

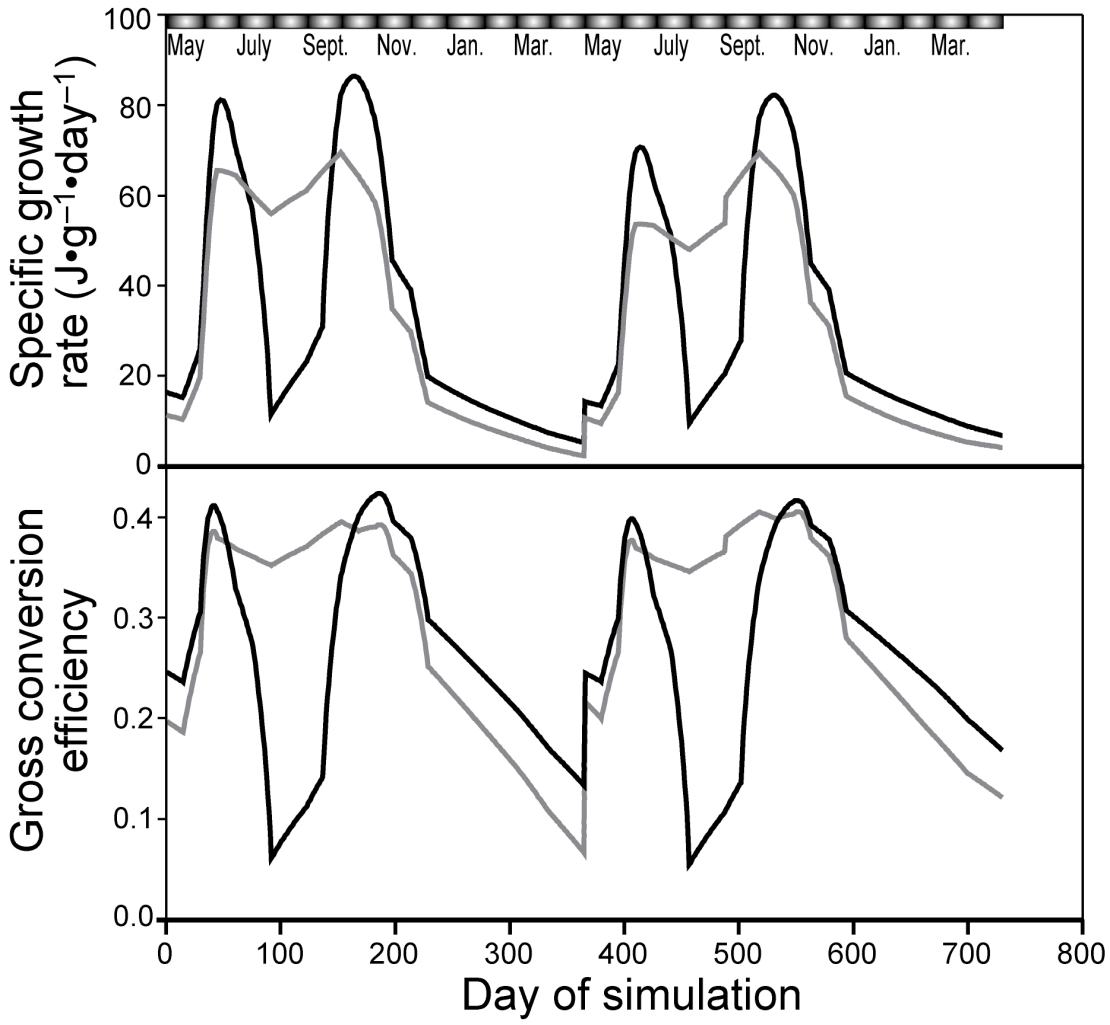

Figure 4.4—Energetic output for pelagic residence of age 3+ chinook comparing nominal (grey line) and otolith thermometry (dark line) bioenergetic simulations.

Model parameters were kept constant, and only temperature and associated *p* value (i.e., proportion of maximum consumption estimated by iterative fit to growth) differed between the two simulations. The nominal simulation assumes chinook stay at 11 °C in midsummer, whereas in otolith-based simulations, temperatures indicate chinook swimming at up to 19 °C during midsummer.

4.2). Since chinook must eat more to attain the same growth at warmer temperatures, annual GCE is estimated to be 18.2% lower than in the nominal simulation (Table 4.2).

4.4 Discussion

4.4.1 Derivation of adult chinook temperature histories

Before further interpreting chinook temperature histories, we must first qualify uncertainties associated with the use of the otolith thermometry technique. This requires discussion of two key elements: 1) the temperature-fractionation relationship, and 2) the appropriate $\delta^{18}O_{(H_2O)}$ value used in the selected temperature-fractionation relationship. We therefore begin our discussion addressing these key issues.

Although it is well established that otoliths produce aragonite at least close to equilibrium with the ambient water (Campana, 1999) with a temperature precision and accuracy better than 1 °C (Thorrold et al., 1997; Høie et al., 2004b), there still may be species-dependant temperature-fractionation relationships (Høie et al., 2004a). Therefore, we must choose the appropriate temperature-fractionation relationship if direct estimation of environmental temperatures is to be done accurately. We chose to calculate temperatures using Patterson et al.'s (1993) equation, because it was specifically developed for freshwater fishes in natural systems and includes freshwater salmonids from the Great Lakes. We consider this equation representative of those calculated using Radtke et al. (1996), Høie et al. (2004a), and Kim and O'Neil's (1997) equations because temperatures calculated are all within 1 °C. Thorrold et al.'s (1997) equation, however, produces temperatures ~4 °C warmer than the other equations. Thorrold et al.'s (1997) equation therefore predicts temperatures beyond lethal limits for chinook and is thus not appropriate.

The slope of the temperature-fractionation relationship is such that an error in $\delta^{18}O_{(H_2O)}$ value of ~0.25‰ results in a temperature error of 1 °C, and it is therefore critical to have accurate $\delta^{18}O$ values of Lake Ontario water. In addition to Hodell et al.'s (1998) values, which are in close agreement with our own measured values for Lake Ontario, we plot seasonal values for Sodus Bay and Lake Ontario (this study), Niagara River and St. Lawrence River (Gat et al., 1994; Yang et al., 1996; Coplen and Kendall,

Table 4.2—Comparison of bioenergetic simulation (otolith thermometry and nominal) output of total consumption and gross conversion efficiency (GCE) of adult chinook during pelagic residence in Lake Ontario.

	Year 1	Year 2	Total	GCE
Consumption (g)				
Otolith, age 3+	5323	24 128	29 451	0.27
Nominal, age 3+	4742	19 400	24 142	0.33
Difference (%)	11	20	18%	18
Consumption (g)				
Nominal, age 2+	7546	*	7546	0.27
Otolith, age 2+	6656	*	6656	0.33
Difference (%)	12	*	12	18

*No estimate.

2000) at Lake Ontario's outflow to address variability in Lake Ontario $\delta^{18}O_{(H_2O)}$ values (Figure 4.5). Also plotted are seasonal $\delta^{18}O$ values for the Salmon (this study) and Genesee Rivers (Coplen and Kendall, 2000) as an example of potential river inputs to the Lake Ontario system. River waters have lower and more seasonally variable $\delta^{18}O$ values than Lake Ontario and the Niagara River and St. Lawrence River systems. Although there is distinct seasonality to the larger Niagara and St. Lawrence river systems, this is modified to a high degree from original precipitation input, as they are dominantly outflow from stable sources (lakes Erie and Ontario). These rivers show variations of –6.7 ± 0.14‰ and –6.9 ± 0.26‰VSMOW, respectively. However, Lake Ontario proper shows no seasonal variation in isotope values. Ignoring the Genesee and Salmon Rivers and focusing on Lake Ontario and Niagara, and St. Lawrence Rivers, $\delta^{18}O$ values are more variable in the fall and early summer, but converge on –6.8 ± 0.19‰VSMOW in July and August, the value used in our calculations. We therefore consider this value appropriate to use in determining at least maximum temperatures in midsummer using our otolith thermometry technique; we estimate the precision to be approximately 1 °C. However, spring and early summer $\delta^{18}O$ values may be more variable possibly due to snow melt especially near river inputs (L. I. Wassenaar, Environment Canada, National Hydrology Research Center, Saskatoon, Saskatchewan, S7N 3H5, Canada, personal communication). Additionally, we will overestimate temperatures for chinook that migrate toward a tributary. It is important to recognize that Lake Ontario's $\delta^{18}O_{(H_2O)}$ value does not vary spatially (including with depth) in August, and is not dependant on temperature changes in the lake.

4.4.2 Chinook pelagic residence: temperature histories and energetics

The interpretive character of chinook intra-otolith $\delta^{18}O$ and $\delta^{13}C$ values is illustrated using two exemplary figures, one specimen from each group, both micromilled from the core to the edge of the otolith (Figure 4.6). SAM92 displays a cyclic (seasonal) pattern ranging from approximately –5.5‰VPDB, to about –7.3‰VPDB after an initial decrease in $\delta^{18}O$ values to as low as –9‰VPDB in the first year of growth (Figure 4.6a). There are just over three seasonal patterns, which is consistent with an independent age count of 3+. Otolith growth is negligible during the winter; therefore, maximum $\delta^{18}O$ values record

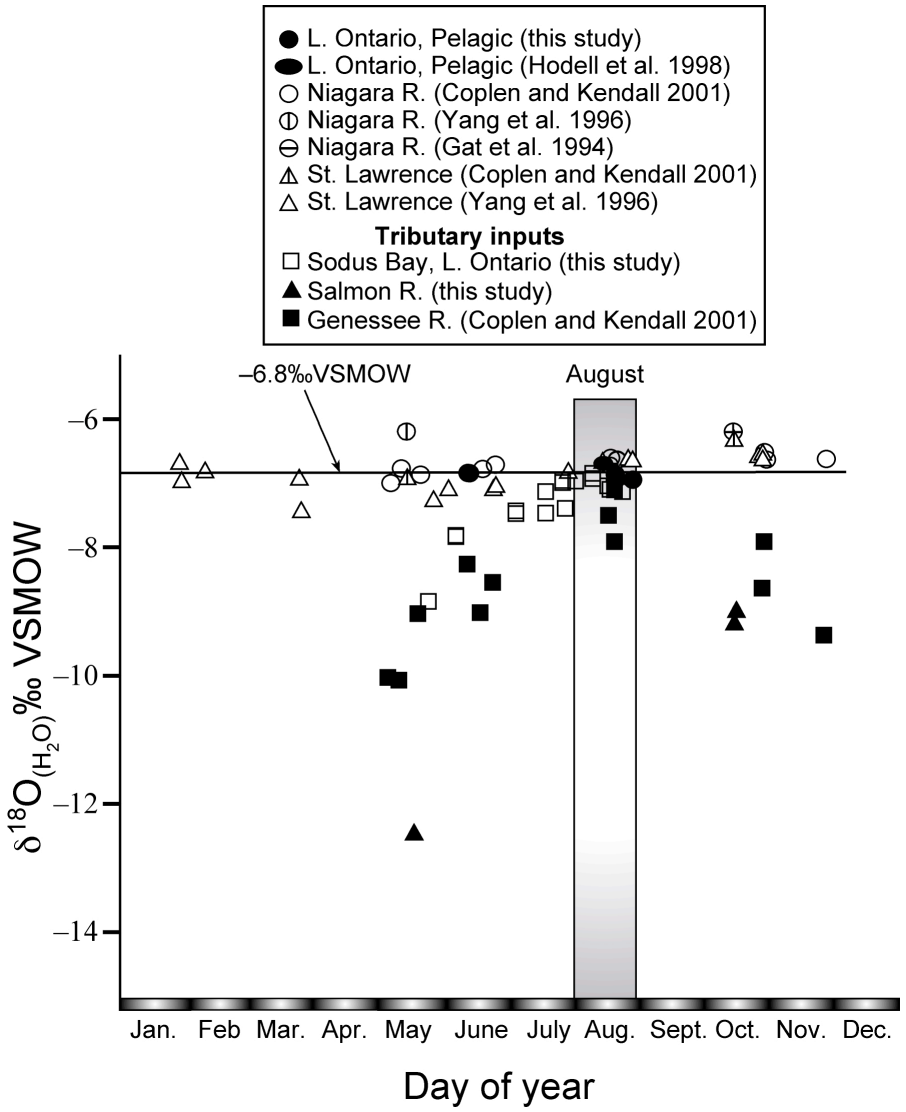

Figure 4.5—Seasonal $\delta^{18}O_{(H_2O)}$ values relative to VSMOW for Lake Ontario, Niagara River, and St. Lawrence River (at Lake Ontario outflow) and smaller tributaries.
The $\delta^{18}O_{(H_2O)}$ values represented are from various years. Data sources are represented on plot.

a spring and (or) fall minimum temperature. This young of the year is interpreted as moving in or near a tributary (recorded as relatively low $\delta^{18}O$ values), permitting inference of juvenile migration to Lake Ontario (Figure 4.6). For example, a temperature of 12 °C is calculated using a Salmon River tributary $\delta^{18}O_{(H_2O)}$ value of –10‰VSMOW (Figure 4.5). Age 1+, 2+, and 3+ represent pelagic residence in Lake Ontario. Converting $\delta^{18}O$ value to temperature using the Lake Ontario $\delta^{18}O_{(H_2O)}$ value, we plot the thermal history of this fish from age 1+ to age 3+, when it was captured offshore on 18 August 1991 (Figure 4.6a). Maximum seasonal temperatures are very near 20 °C, and remain stable just above 20 °C during year 2+ before decreasing. The temperature estimated nearest the time of capture was 18 °C, consistent with the season of capture. We estimate a resolution that averages less than four days per sample for this specimen, typical for specimens in this study.

CHK23 from the Salmon River group displays four seasonal cycles indicating that this fish was also age 3+ at the time of capture (Figure 4.6b). Age 1+ and age 2+ displays a similar pattern to the same age class for SAM92, and calculated mid-summer temperatures appear to remain stable at 20 °C during this fish's pelagic residence. Lower $\delta^{18}O$ values in the first and last year of growth, are representative of the lower $\delta^{18}O$ values of Salmon River water experienced in the hatchery and during the spawning migration, respectively (Figure 4.5). We estimate a resolution of 14 days per sample, which is the lowest sample resolution in this study. Although, intra-otolith $\delta^{18}O$ and $\delta^{13}C$ values agree with known life-history traits of chinook, this technique should be validated by using otoliths from fish fitted with archival tags that provide an independent measure of temperature.

Our otolith thermometry results indicate that adult chinook inhabit water with temperatures considerably warmer than those they prefer (e.g., McCullough, 1999). We estimate that chinook commonly occupied water temperatures near 19 °C in midsummer. We also suggest that chinook are actively seeking water at this temperature through the midsummer, as most pelagic-residence years for nearly all specimens with adequate resolution show evidence of a temperature plateau for at least two weeks. Because Lake Ontario stratifies in the summer and surface temperatures are often above 20 °C, chinook

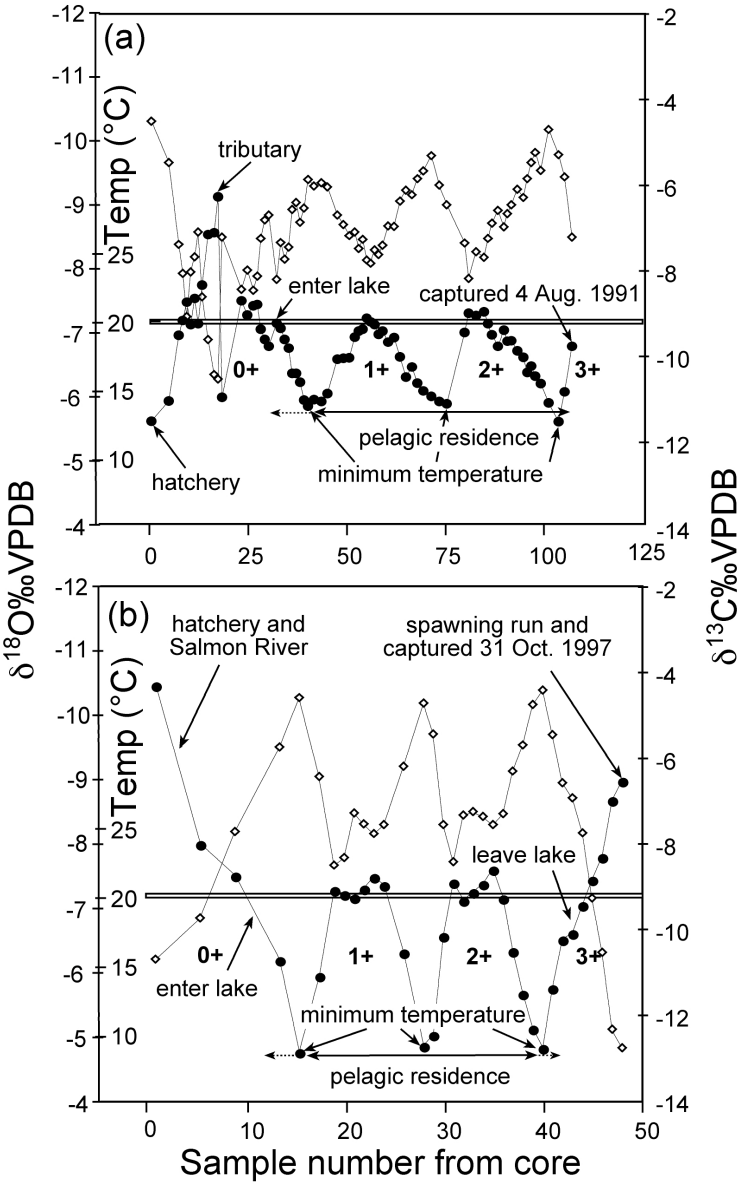

Figure 4.6—Example plots of intra-otolith $\delta^{18}O$ values and calculated temperatures (dark circles) and $\delta^{13}C$ (open diamonds) values relative to VPDB from two chinook otoliths, one from Specimen SAM92 from the archived group (a) and the other from specimen CHK23 from the Salmon River group (b).

Temperature scale (inset) is calculated using a Lake Ontario $\delta^{18}O$ value of –6.8‰ VSMOW and Patterson et al.'s (1993) temperature-fractionation relationship for otolith aragonite of freshwater fish. Pelagic residence indicates the time the chinook spent in Lake Ontario proper. We modeled 2 full years of growth indicated by the solid line. Chinook may also be Lake Ontario residents during the fall of their first year and just prior to spawning, indicated by the dotted lines. Otolith growth decreases or ceases in winter, so winter temperatures are not recorded. Only a minimum temperature just prior to otolith growth cessation can be determined; this is noted on plot. Assuming that otoliths grew during days above the minimum seasonal temperature calculated, the average resolution is 4 days per sample for specimen SAM92 and 14 days per sample for CHK23.

must occupy the epilimnion of Lake Ontario near to but not at the surface, even though the presumed optimal temperature for this species was always available near the thermocline. Highest mean alewife densities are found in the epilimnion (at temperatures above 17 °C), and the highest prey fish biomass is found near 20 °C (Mason et al., 1995). Therefore, it is likely that chinook must search epilimnetic water in Lake Ontario to find prey. It may be that as prey production has become limiting, chinook have had to search the warmer epilimnion more often for food, or it may be that chinook have always foraged here since they were first stocked. Absence of a strong alewife year class from 1992-1997, with year classes in 3 of these years amongst the smallest from 1977-1997, indicates that alewife numbers decreased after 1991 (e.g., Mills et al., 2003). However, we found no corresponding change in chinook thermal orientation over this same period of time.

We find very little difference between chinook maximum temperatures calculated for the archived group and the Salmon River group, in contrast to our hypothesis that thermal orientation of the chinook would change with prey quality and quantity. Interestingly, Haynes and Keleher (1986) found one chinook in 19.7 °C water in the beginning of September as early as 1984. Although it was the only chinook (out of three) found in temperature this high in the summer/fall, they were unable to closely track the other tagged fish during the midsummer due to the methodology used (no fish were found in August). They assumed this was due to chinook moving into deeper waters. However, they were only able to track fish near the shore, and the other chinook may have moved offshore. Our results appear to contradict other reports of these fish being captured closer to the thermocline. Olson et al. (1988) found 82% of chinook above the thermocline and offshore, although they were vertically distributed widely and averaged 14.4 ± 2.9 °C at depths where they were captured using nets set over night for 12-28 hours. Using similar methods, Stewart and Robertson (1991) also found chinook at a similar median temperature, 13.2 °C, and did not capture chinook in 19 °C water. In order to calculate temperatures nearer to these observations, Lake Ontario $\delta^{18}O_{(H_2O)}$ value must be 1.5‰ more negative than those we and others have measured.

A possible interpretation that would allow the results of these capture studies to be correlated with ours is that chinook migrate vertically to warmer water to catch prey, and

then seek thermal refugia nearer the thermocline. In order to be consistent with this interpretation, otolith growth must be highly reduced when chinook are not occupying warmer epilimnetic waters. Otolith growth has been highly correlated with metabolic rate (Wright, 1991; Tohse and Mugiya, 2002) and metabolic rate increases with temperature indicating that there would be a bias toward higher temperature estimates. However, even with this bias, some carbonate accretion should occur while chinook inhabits water near the thermocline. Therefore, our temperature estimates suggest that chinook would experience near lethal temperatures for limited periods if this vertical migration occurred.

Based on a literature review, McCullough (1999) concluded that 21-22 °C was the upper incipient lethal level for adult chinook. Although Bjorn and Reiser, (1991) noted an upper incipient lethal level for adult chinook as high as 26.2 °C, they reported that environmental temperatures from 23-25 °C could be lethal and were actively avoided. Finally, Eaton et al., (1995) reported 23.7 °C as the upper habitat temperature limit for chinook. The remarkable consistency in minimum $\delta^{18}O$ values (maximum temperatures) for pelagic residence regardless of the group (whose members vary both with lake location and time), and the close agreement between maximum calculated temperatures and chinook's upper incipient lethal limit, suggest that chinook in Lake Ontario are seeking alewife prey in water temperatures as high as are tolerable. We found only two years out of a total of 22 where chinook were recorded at temperatures above 22 °C. Such exceedingly high temperature estimates may result if the fish entered waters with more negative $\delta^{18}O_{(H_2O)}$ values than those typical of the open lake indicating that the true temperature experienced is less than that estimated. For example, the fish may have resided in a harbor or near a major tributary input to seek food. Forays into warm littoral habitats are likely to be uncommon because Lake Ontario has very little of such habitat outside the eastern basin and few small embayments (Mason et al., 1995). However, if chinook do migrate to littoral regions, they are still likely to encounter warm water temperatures that are not optimum for growth.

Maximum seasonal $\delta^{18}O$ values (minimum temperatures) are considerably more variable. Interestingly, temperatures are often nearer the preferred temperature of chinook (McCullough, 1999). It is tempting to speculate that chinook are moving to high temperature waters in search of food for as long as can be tolerated, then moving into

water at preferred temperatures, where body and otolith growth are reduced, so these are the minimum temperatures recorded via the otolith thermometry. However, calculated temperatures may be elevated artificially by more negative and more variable $\delta^{18}O_{(H_2O)}$ values measured in the fall and spring (L.I. Wassenaar, Environment Canada, National Hydrology Research Center, Saskatoon, Saskatchewan, S7N 3H5, Canada, personal communication). Finally, we note that mean mid-summer temperatures for the archived and Salmon River groups are significantly different, although mean temperatures differed by just 0.4 °C different. Although this "increased temperature" may be a reflection of ecological adaptation or environmental warming, the observed temperature difference might also be a result of slightly different mean $\delta^{18}O$ values for Lake Ontario. In fact, Hodell et al. (1998) reported a mean Lake Ontario $\delta^{18}O_{(H_2O)}$ value of –6.7‰VSMOW for 1993-1995, while we measured a mean $\delta^{18}O_{(H_2O)}$ value of –6.9‰VSMOW for 1998 and 2001. Mean calculated temperatures would be within 0.2 °C using Hodell et al.'s (1998) value for the archived group and our measured $\delta^{18}O_{(H_2O)}$ value for the Salmon River group. Regardless, such small differences are unlikely to be ecologically significant for chinook.

Adult chinook thermal histories determined from intra-otolith $\delta^{18}O$ values indicate that Lake Ontario's chinook population could be under energetic stress during midsummer. Bioenergetic modeling simulations predict severe growth reductions to near zero in midsummer, and slightly negative growth is predicted for chinook inhabiting water at 20 °C water temperatures (unpublished data). GCE is also reduced during midsummer, providing further evidence of stress. Corresponding to reduced GCE, total annual consumption by chinook is estimated to be up to 20% higher in the otolith thermometry simulation relative to the nominal simulation. This growth stress is corroborated by an observed decrease in condition factor in chinook captured by anglers (Figure 4.7a). Additionally, summer stress marks are often observed in chinook scales and otoliths. Summer stress marks on chinook scales from Lake Ontario preclude accurate aging, and otolith or fish length is used instead (J.N. Bowlby and T. J. Stewart, Ontario Ministry of Natural Resources, Glenora Fisheries Station, Picton, unpublished data). Many otoliths from Lake Ontario chinook show summer growth checks, opaque

regions in the otolith that are less distinct than opaque regions associated with winter growth checks (Figure 4.7b).

There is recent evidence that modeled respiration, a key component of the bioenergetic model, is in error (Trudel et al., 2004). Specifically, the model we used (Stewart and Ibarra, 1991) underestimates respiration at lower ranges and overestimates it at higher ranges with a total mean-squared error of 0.18 (Trudel et al., 2004). However, this bioenergetic model can still be used to compare estimates on a relative basis and to contrast the outcome of various scenarios if the biases are consistent (Trudel et al., 2004). We compare two model outputs changing the temperature input only, thus fulfilling this requirement. In addition, growth and consumption obtained from model output and field studies for Lake Ontario chinook agree (Rand and Stewart, 1998a) and midsummer stress predicted by our bioenergetic analysis is corroborated by observed condition factor and by otolith and scale stress marks (Figure 4.7).

Rand and Stewart (1998b) suggested that the limit to salmonine production in this ecosystem is being approached. GCE has been trending downward in Lake Ontario due to a reduction in prey quality. Rand et al. (1994) and Rand and Stewart (1998b) concluded that the chinook population might not have been sustainable at 1990 stocking rates due to declines in alewife population and quality. These conclusions were based on a bioenergetic analysis using assumptions about thermal orientation of chinook that we determined to be inaccurate. We find adult chinook to be consuming more and growing less in midsummer than was previously modeled.

4.4.3 Intra-otolith $\delta^{13}C$ value and metabolic rate

Biological carbonates appear to derive carbon from two major sources: DIC from environmental water, and blood carbon derived from the diet (e.g., McConnaughey et al., 1997). These two major pools of carbon are therefore reflected in the $\delta^{13}C$ value of the otolith (e.g., Høie et al., 2003). Tohse and Mugiya (2002) demonstrated via radiocarbon labeling both an ambient water and dietary carbon contribution in fish otoliths, the ratio of which was linked to metabolic activity. Although, DIC is often the dominant source of otolith carbon (e.g., McConnaughey et al., 1997), intra-otolith variation in $\delta^{13}C$ value

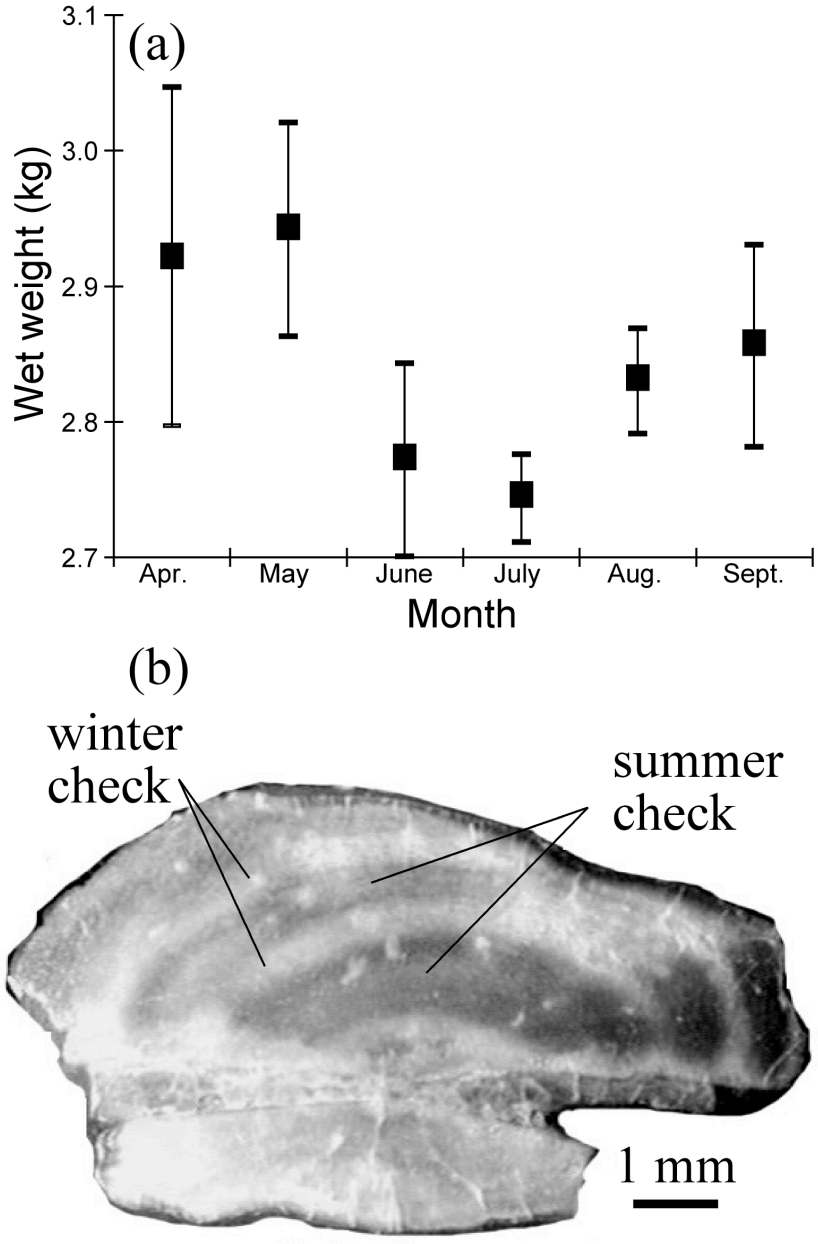

Figure 4.7—Physical evidence of summer growth stress in chinook (*Oncorhynchus tshawytscha*) from Lake Ontario.

(a) Monthly trend in body condition determined as the mean weight of a 600 mm long chinook after adjusting for differences in length and year using analysis of covariance at 95% confidence intervals. Fork length and wet weight of chinook were measured in angler surveys during 1988-1992 (n = 2468). (b) Image of a chinook otolith (specimen SAM12; this study) showing summer and winter check marks. Summer check marks, induced by stress, are opaque regions in the otolith that are less distinct than opaque regions associated with winter growth checks. It should be noted that this section is used for micromilling and not aging.

might reflect changes in contributions between the two sources; this changing ratio is dominantly a result of changing metabolic rate in the individual fish (Wurster and Patterson, 2003; Høie et al., 2004b). This observation should hold true especially for fish such as chinook that do not change their diet greatly during pelagic residence (e.g., Brandt et al., 1986; Rand and Stewart, 1998a; Lantry, 2001).

Chinook otolith $\delta^{13}C$ values display seasonal variability with higher values during spring/fall and lower values occurring in midsummer. This pattern is highlighted by a relatively strong covariation with $\delta^{18}O$ values, and is consistent with the metabolic contribution hypothesis. Higher temperatures (lower $\delta^{18}O$ values) lead to a higher metabolic rate and greater contribution of respiratory carbon to the otolith (and therefore lower $\delta^{13}C$ values relative to DIC). In contrast to intra-otolith $\delta^{18}O$ values, $\delta^{13}C$ values of individual otoliths are quite variable. The highest $\delta^{13}C$ values are approximately –4‰VPDB to –5‰VPDB, whereas lower values are approximately –8‰ to –10‰, with one specimen as low as –12‰VPDB. We estimate a summer metabolic contribution to otolith carbon as high as 50-60% assuming a dietary $\delta^{13}C$ value of –25‰VPDB (Kiriluk et al., 1995) and a $\delta^{13}C_{(DIC)}$ value of 0‰VPDB (Hodell et al., 1998; Leggett et al., 1999; Hélie et al., 2002). Despite the individual variability in intra-otolith $\delta^{13}C$ values, we find least-squares regressions between seasonal pelagic-residence temperatures and $\delta^{13}C$ values not significantly different among archived ($\alpha = 0.05$, $F_{[5,297]} = 1.59$; ignoring SAM84) and Salmon River ($\alpha = 0.05$, $F_{[9, 184]} = 2.14$) specimens and groups ($\alpha = 0.05$, $F_{[1,529} = 2.72$). This suggests that although individual chinook may vary in activity, they respond similarly to temperature changes given a similar environment.

The environmental $\delta^{13}C_{(DIC)}$ value appears to have the largest modifying influence on intra-otolith $\delta^{13}C$ values because it represents the largest proportion of otolith carbon. Tributary $\delta^{13}C_{(DIC)}$ values are much lower than Lake Ontario values (e.g., Leggett et al., 1999; Hélie et al., 2002) and this is recorded by otolith $\delta^{13}C$ values, even during the spawning run, when dietary $\delta^{13}C$ values are derived from reserves stored during pelagic residence. In many cases variation in intra-otolith $\delta^{13}C$ and $\delta^{18}O$ values can be used to infer when chinook migrate between Lake Ontario and tributaries (Figure 4.6), although this should be corroborated using growth models. Therefore seasonal changes in Lake

Table 4.3—Estimates of metabolic contribution to otolith carbon made using a simple mass balance model.

	$\delta^{13}C$ (‰)		$\delta^{13}C_{(DIC)}$		*M*	
Group	Otolith	Diet	epilimnion	hypolimnion	epilimnion	hypolimnion
Salmon River Group						
Summer	–7.9‰	–25.2‰	–0.6‰	–2.5‰	0.41	0.36
Fall/spring	–5.3‰	–25.2‰	*	–2.5‰	***	0.24
Archived group						
Summer	–8.7‰	–25.2‰	–0.6‰	–2.5‰	0.44	0.39
Fall/spring	–6‰	–25.2‰	*	–2.5‰	***	0.27

Note: Metabolic contribution to otolith carbon is calculated using a model described by Wurster and Patterson (2003): $\delta^{13}C_{(otolith)} = M \bullet \delta^{13}C_{(diet)} + (1–M) \bullet \delta^{13}C_{(DIC)} + 2.7$, where *M* is the proportional metabolic contribution. $\delta^{13}C$ value of the dissolved inorganic carbon (DIC) is estimated for the epilimnion and hypolimnion and fall/spring (same as hypolimnion) from Leggett et al. (1999). $\delta^{13}C$ values of alewife and rainbow smelt reported in Kiriluk et al. (1995) were used in conjunction with dietary estimates to determine average $\delta^{13}C$ values of chinook diet (*, no estimate).

Ontario $\delta^{13}C_{(DIC)}$ values and variation in habitat depth (e.g., Legget et al., 1999) may influence $\delta^{13}C$ values of chinook otoliths.

The diet of chinook in Lake Ontario varies little during pelagic residence (Brandt, 1986; Rand and Stewart, 1998b; Lantry, 2001), and during the summer $\delta^{13}C_{(DIC)}$ values increase in the epilimnion because of preferential incorporation of ^{12}C by phytoplankton, whereas values in the hypolimnion remain invariant (e.g., Leggett et al., 1999). However, $\delta^{13}C_{(otolith)}$ values decrease during the summer, suggesting an increasing influence of dietary carbon with lower $\delta^{13}C$ values over more positive $\delta^{13}C_{(DIC)}$ values. We therefore conclude that intra-otolith $\delta^{13}C$ values are primarily influenced by changing metabolic rate as further evidenced by a strong and similar covariation with estimated temperature and corroborated by a covariation with the modeled specific respiration rate. A direct temperature effect on $\delta^{13}C$ values of biogenic carbonates is equivocal (e.g., Thorrold et al., 1997; Schwarcz et al., 1998), and if it exists is small (approximately –1.3‰ VPDB for a temperature increase of 10 °C (Grossman and Ku, 1986).

We estimated various metabolic contributions assuming different depth habitats or varying $\delta^{13}C_{(DIC)}$ values (Table 4.3). It is important to note that $\delta^{13}C$ values vary greatly among individuals; however, on average, summer $\delta^{13}C$ values for the archived group are almost 0.8‰ more negative then those for the Salmon River group. This corresponds to an additional 3% metabolic contribution to the otolith carbon of the archived group otolith carbon. An alternate explanation is that chinook inhabited the hypolimnion more often in the late 1980s and early 1990s than in the mid-1990s (Table 4.3). This however, contrasts with our contention that chinook are feeding in the epilimnion as inferred from $\delta^{18}O$ values.

This study clearly demonstrates the need for detailed laboratory studies that determine the relationship between metabolic rate, diet, and intra-otolith $\delta^{13}C$ values. However, we hope that we have demonstrated that $\delta^{13}C$ can be used to determine metabolic rate “in the field”, and perhaps can be used as an additional proxy with which to infer vertical distributions of fish within a water column. Alternatively, if metabolic rate can be accurately modeled and the environmental $\delta^{13}C_{(DIC)}$ value is known, it may be possible to estimate diet changes in longer-lived fish.

Chapter 5. Abrupt onset of the North American monsoon at the termination of the Younger Dryas event inferred from chitin $\delta^{13}C$ and δD values derived from bat guano

5.1 Introduction

Multi-proxy records from ice cores document abrupt climate changes at high-latitudes during the last deglacial period (Taylor et al., 1997; Alley, 2000). Variation in the production of North Atlantic Deep Water (NADW) formation is usually invoked as the mechanism that toggles the climate system into multiple stable modes punctuated by abrupt transitions (Rahmstorf, 2002; Broecker, 2003). Just such a scenario is thought to have forced the well-documented Younger Dryas (YD) event (Broecker et al., 1989; Broecker, 2003). However, well-dated terrestrial records that document the YD outside the North Atlantic region are rare, and the global extent of this event is equivocal (Peteet, 1995). There is currently no evidence for a Younger Dryas in the low-elevation deserts of the southwestern United States (Anderson et al., 2000), although nearby marine records in the Santa Barbara Basin, and Gulf of California have strong teleconnections with the North Atlantic region (e.g., Kennett and Ingram, 1995). Today, the dominant climatological feature in the southwest United States is the North American monsoon (NAM), a seasonal change in atmospheric circulation expressed as a pronounced increase in summer precipitation after a hyper-arid spring (Adams and Comrie, 1997; Wright et al., 2001; Sheppard et al., 2002). The nature of this NAM dominated climate during the last deglaciation is poorly understood (Ehleringer et al., 1998; Anderson et al., 2000; Metcalfe et al., 2000; Poore et al., 2005). Herein is presented the first high-resolution record of chitin $\delta^{13}C$ and δD values derived from bat guano. This terrestrial archive from a semi-arid ecosystem is used to document the YD in the southwestern United States, and infer an abrupt onset of the NAM at the termination of this event.

Much of what is known about past climate change in the semi-arid regions of the western United States during the last deglaciation is from the study of packrat midden macrofossils (Van Devender and Spaulding, 1979; Betancourt et al., 1990a; Anderson et al., 2000). A spatially and temporally extensive analysis of paleobotanic and paleoclimate records from the Colorado plateau and southwestern United States offers a consistent climate interpretation for the last deglaciation (Betancourt et al., 1990b; Anderson et al., 2000). Temperatures during the latest Pleistocene were at least 5°C cooler than today, while the temperatures during the Last Glacial Maximum where somewhat warmer (Anderson et al., 2000). Noble gas thermometry of paleogroundwaters in the southwestern United States also record ~5°C rise in average temperature from the LGM to the Holocene (Phillips et al., 1986; Stute et al., 1992; Stute et al., 1995) However, the midden vegetation record from the Southwest United States appears relatively monotonous (Van Devender et al., 1987; Betancourt 1990b), and does not appear to be sensitive to rapid climate fluctuations despite ample evidence for global-scale changes during the last glacial period (Anderson et al., 2000). The discontinuous nature of packrat midden archives (essentially climate snapshots) can not provide the type of records during abrupt climate change that can be derived from continuously deposited sediment (Anderson et al., 2000). Unvortuneately, most clastic sediment records in arid and semi-arid regions are by nature of the climate discontinuous.

A continuous sediment record can however be recovered from guano deposits found in *Tadarida brasiliensis* (the Mexican free-tailed bat) maternity roosts. *T. brasiliensis* is one of most widely distributed mammals in the western hemisphere, common from the semi-arid regions of the southwest United States to the humid regions of Brazil (Koopman, 1982; Wilkins, 1989). Mexican free-tailed bats numbering in the millions can produce up to 90 tons of guano annually within individual maternity caves (Constantine, 1970). The Mexican free-tailed bat is a generalist insectivore with a dietary composition strongly correlated with local insect abundance (Lee and McCracken, 2002). Because bats sample insects on a relatively large spatial scale, it is hypothesized that variations in vegetation resulting from climate change will be documented in the isotope profiles of subfossil chitin. This hypothesis is substantiated in arid Baja California where large precipitation anomalies are documented in carbon isotope values of soils (Amundson et

al., 1994), and the island communities of insects, spiders, and predatory scorpions (Stapp et al., 1999; Smith et al., 2002; Stapp and Polis, 2003).

Guano from insectivorous bats is composed predominantly of finely commutated insect exoskeletons (Jeuniaux, 1971; McFarlane et al., 2002). Chitin is a resistant biomacromolecule (Miller et al., 1988), and guano in arid environments is effectively mummified, virtually arresting bacterial degradation (Mizutani et al., 1992a; Shahack-Gross et al., 2004). When chitin diagenesis occurs, bound proteins are the first to degrade, and remaining chitin apparently transforms to aliphatic compounds (Stankiewicz et al., 1998; Briggs, 1999). During early diagenesis, stable isotope values of chitin remain unaffected (Schimmelmann et al., 1986). Stable isotope values of insect chitin can be used to reconstruct trophic and climatic conditions at the time of formation (Schimmelmann and DeNiro, 1986a; Mizutani et al., 1992a,b; Motz, 2000; McFarlane et al., 2002). $\delta^{13}C$ values of insect chitin reflect $\delta^{13}C$ values of plants fed upon by the insects. Plant values are forced by changing precipitation and humidity such that higher values are equated with lower humidity and/or precipitation (Fry, 1978; Webb et al., 1998). δD values of insect chitin are directly related to local environmental water δD values. Higher δD values indicate higher temperature, greater summer/winter precipitation ratio, and (or) lower relative humidity (Miller et al., 1988; Schimmelmann et al., 1993; Motz, 2000). Consequently, chitin $\delta^{13}C$ and δD values derived from bat guano deposits are archives of vegetation and regional climate conditions near the site.

5.2 Study Area and Methods

Methods detailing chemical extraction and evaluation of diagenesis are described more fully in Appendix B. Briefly, a guano core was recovered from Bat Cave, Grand Canyon National Park (Figure 5.1). The core was transferred back to the laboratory, opened, and samples were taken and homogenized in 4 mm sections from 0-260 mm, and then continued in 8 mm sections to the end of the core at 360mm. Samples were placed in a 2.0 specific gravity 2N HCl-$ZnCl_2$ solution for three hours to separate the organic and mineral fractions and remove carbonate. The organic portion was placed on a 12-μm metal sieve and rinsed to neutral using deionized H_2O. Samples were then washed once

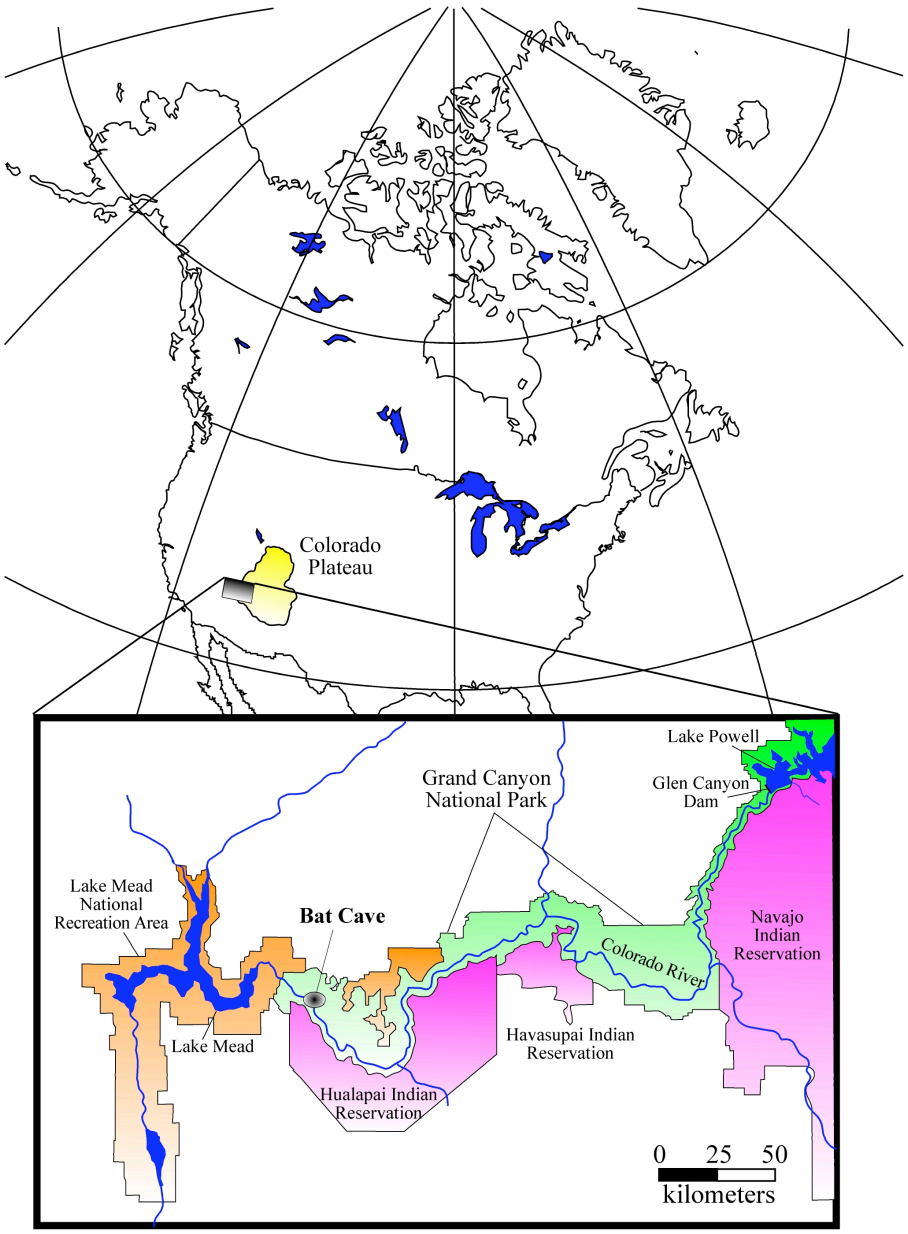

Figure 5.1—Study area and location of *Tadarida brasiliensis* maternity roost, where a guano core was excavated for retrieval of chitin $\delta^{13}C$ and δD values. Inset map after Bowers et al. 1997.

in methanol, followed by three washes in a chloroform:methanol 2:1 (v/v) mix leaving this first wash overnight.

$\delta^{13}C$, $\delta^{15}N$, and weight percent organic carbon (C%) and nitrogen (N%) were determined by continuous flow-isotope ratio mass spectrometry (CF-IRMS) using a ThermoFinnigan Flash 1112 Elemental Analyzer coupled by a ConFlo III to a Delta XL Plus mass spectrometer. Samples were massed in tin foil capsules and loaded in a FlashMAS200 autosampler. Samples were dropped in a combustion chamber and first oxidized at 1000 °C and subsequently reduced at 680 °C to produce CO_2 and N_2 gases, which were at 1000 °C and subsequently reduced at 680 °C to produce CO_2 and N_2 gases, which were then separated in a 5 Å Gas Chromatograph (GC) column kept at 50 °C. The column flow rate was set to 120 ml He/min. All $\delta^{13}C$ and $\delta^{15}N$ values are reported relative to VPDB and AIR standard scales, respectively, standardized using three internal laboratory standards. C% and N% were determined by comparison of gas pulse peak area and mass to that of a known standard. Repeated analyses of internal laboratory standards yielded an external reproducibility of better than ±0.2‰ and 0.3‰ for $\delta^{13}C$ and $\delta^{15}N$ values, respectively.

δD values and weight percent H (H%) were determined by high-temperature flash pyrolysis CF-IRMS using a ThermoFinnigan High-Temperature Conversion Elemental Analyzer (TC/EA) coupled through a ConFlo III to a DeltaPlus XL mass spectrometer. Samples were wrapped in silver foil and admitted into a combustion chamber using a Costech zero blank autosampler where atmosphere is replaced with He. In the combustion chamber, samples were reduced at 1270 °C to H_2 gas (and N_2 and CO) and passed through and separated by a 5 Å GC column held at 90 °C. The column flow rate was set to 110-120 ml He/min. All δD values are reported relative to VSMOW-SLAP standard scale. Repeat analyses of international material IAEA CH-7, NBS-22, and three internal laboratory standards yielded an external reproducibility of better than ±3‰. Because hydrogen in complex organic matter bonded to nitrogen or oxygen can exchange with the atmospheric water vapor, correction for this labile hydrogen exchange is required (e.g., Schimmelmann, 1991). To correct for exchangeable hydrogen, two natural chitin standards were analyzed for δD_n value (non-exchangeable δD value), permitted to air-equilibrate with samples, analyzed together using high-temperature pyrolysis CF-

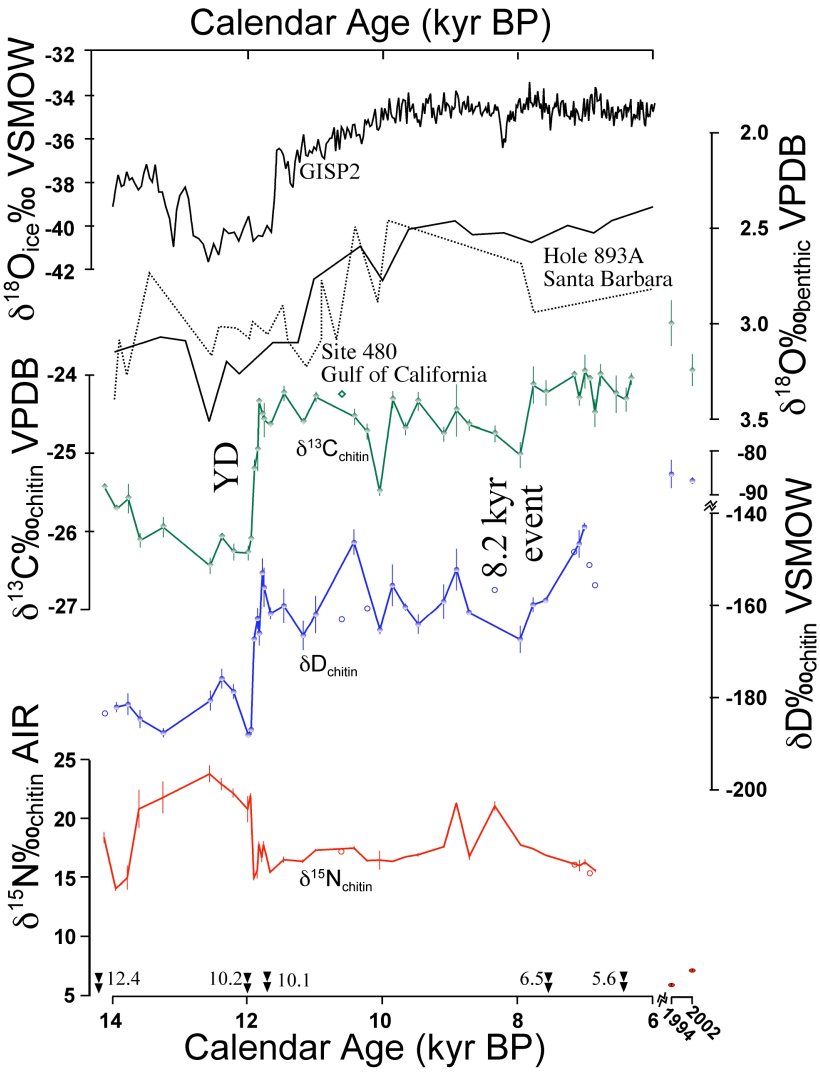

Figure 5.2—Chitin $\delta^{13}C$ (green diamonds), δD (blue circles), and $\delta^{15}N$ values (red, no symbols) from a guano deposit located in a *Tadarida brasiliensis* roost in Grand Canyon, NP.

Two individual analyses are averaged per plotted point with 1 S.D. indicated by the vertical variance bars. Open symbols represent single analyses. δD values are corrected for atmospheric vapor exchange by air-equilibration with standards and correction to non-exchangeable δD values (after Wassenaar and Hobson, 2000, 2003). $\delta^{18}O$ values of ice from GISP 2 (Grootes et al., 1993; Stuiver et al., 1995), and benthic foraminifera from Santa Barbara Basin (Kennett and Ingram, 1995) and Gulf of California (Keigwin and Jones, 1990; calibrated ages after Kennett and Ingram, 1995) are given for comparison. Highlighted are two important events, the Younger Dryas and 8.2 kyr event. Chronology in calendar years is determined from linear interpolation between five radiocarbon dates indicated by double arrows. Calibration was performed using Calib 5.0 (Stuiver and Reimer, 1998; Reimer et al., 2004)..

Table 5.1—Radiocarbon control on guano core 96-04.

Sample Number	Core Location	$\delta^{13}C$ value	Radiocarbon Years BP	Laboratory Number	Laboratory
1.	Surface (0-4mm)	-24.4	5620±70	Beta #95152	Beta Analytic
2.	56-60 mm		6490±50	GdA-494	Gliwice
3.	144-152 mm	-25.9	10130±60	GdA-319	Gliwice
4.	256-264 mm	-27.2	10230±60	GdA-321	Gliwice
5.	End (360-368mm)	-22.5	12400±90	Beta #95153	Beta Analytic

IRMS, and standard δD_n values were used to correct for δD_n values of samples (after Wassenaar and Hobson, 2000, 2003). Ten repeat measurements on selected samples analyzed a year apart confirmed that the air-equilibration technique generated precise measurements. All repeat measurements were within reported analytical precision, and most were within 1‰.

AMS radiocarbon dates were obtained from the Gliwice Radiocarbon Laboratory (three samples) and Beta analytic (two samples and calibrated to calendar years using CALIB 5.0 noted on Figure 5.2 and Table 5.1 (Stuiver et al., 1998; Reimer et al., 2004). The age model was constructed by linear interpolation between consecutive AMS dates. Because it was observed that samples with C:N ratios lower than 6 tended to have higher $\delta^{13}C$ and δD values, only samples with C:N ratios between 6 and 8 are considered, and remaining sample data were removed.

5.3 Results

Elemental ratios (C:N and N:H) of most samples are close to theoretical chitin, indicating that protein was naturally removed and that chitin was isolated by this procedure. Diagenesis is not likely a governing influence on isotope values because C:N and N:H ratios of grouped samples of different ages are not significantly different (α = 0.05, $H_{[2,33]} = 5.45$), and not significantly correlated with $\delta^{13}C$ and δD values either prior to, within, or after a notable abrupt rise in $\delta^{13}C$ and δD values.

Figure 5.2 illustrates $\delta^{13}C$, δD, and $\delta^{15}N$ values of bat guano-derived subfossil, and modern chitin collected in 1994 and 2002. Both $\delta^{13}C$ and δD chitin values display similar trends and covary throughout the record ($r = 0.88$, $p < 0.001$). The Pearson product-moment correlation coefficient is lower over the Holocene ($r = 0.57$, $p < 0.01$), and prior to 12 cal. kyr, $\delta^{13}C$ and δD values diverge and are not significantly correlated ($r = –0.21$). $\delta^{13}C$ values range from –26.5‰ to –24.0‰ VPDB, while δD values range from –188‰ to –143‰ VSMOW. Minimum $\delta^{13}C$ and δD values both occur during the Younger Dryas event. $\delta^{13}C$ values of chitin derived from modern bat guano collected in 1994 and 2002 from the Bat Cave are similar to Holocene values of subfossil guano. However, modern bat guano-derived chitin δD values are much higher. $\delta^{15}N$ values increase about 10‰ prior to the Younger Dryas event, and decrease abruptly to ~16‰ AIR to relatively

constant values at the end of this event. Subfossil chitin $\delta^{15}N$ values are much higher than modern chitin values. The most salient feature of both $\delta^{13}C$ and δD profiles is a rapid increase occurring over a period of rapid deposition rate, and corresponding to the end of the Younger Dryas event (Table 5.1, Figure 5.2). Additionally, $\delta^{13}C$ and δD values initially decrease between ~8.4-7.8 cal. kyr, followed by an abrupt rise in values.

The depositional rate of guano is generally invariant, except at the termination of the YD, where 114 mm was deposited over a period of 100 radiocarbon years. Such a large increase in depositional rate is difficult to interpret, firstly because a radiocarbon plateau occurred at this time. Although recent varved *Tadarida brasiliensis* guano deposits have been used to infer population size (McFarlane 1990), bat movement within the cave that is independent of climate or population size, and/or changes in the influx of inorganic material such as increased silica deposition, complicate an unequivocal interpretation of this variable. Such an analysis requires better radiocarbon control, but it does appear that some major change occurred at the termination of the YD.

5.4 Discussion

5.4.1 $\delta^{13}C$ values of bat guano-derived chitin

$\delta^{13}C$ values of insect chitin are dependent on the animal's diet (Schimmelmann et al., 1986a; Webb et al., 1998). *Tadarida brasiliensis* is an opportunistic feeder, and has been demonstrated to consume insects in proportion to their local diversity (Lee and McCracken, 2002). In the Grand Canyon, bats feed dominantly along river corridors, especially along the Colorado River valley (Mizutani et al., 1992b). Although emergetic aquatic insects can be an important source of energy to riparian predators (Sanzone et al., 2003), it is assumed that the bats feed dominantly on riparian flying herbivorous insects. Therefore, $\delta^{13}C$ values of bat guano-derived chitin are presumed to reflect local vegetation, and any major excursions in sub-fossil chitin $\delta^{13}C$ values will be directly related to changes in average $\delta^{13}C$ values of local vegetation.

All higher plants share the core biophysical and biochemical processes of photosynthesis by fixing inorganic carbon using the enzyme 1,5-biphosphate carboxylase/oxygenase (Rubisco), however different mechanisms have evolved to

transport CO_2 to the site of fixation leading to different isotope discriminations (Collatz et al., 1998). In C_3 plants, CO_2 enters the site of fixation in the chloroplasts by diffusion across stomata where Rubisco strongly discriminates against $^{13}CO_2$, the effective amount of discrimination is determined by the ratio of internal/atmospheric CO_2 concentration (c_i/c_a), quantified as (Farquhar et al., 1982):

$$\delta^{13}C_p = \delta^{13}C_s - (a \bullet (1 - c_i/c_a) + b \bullet (c_i/c_a)) \quad (5.1)$$

where $\delta^{13}C_p$ is the average $\delta^{13}C$ value of the plant, $\delta^{13}C_s$ is the $\delta^{13}C$ value of the source (atmosphere), a is the diffusional fractionation constant (4.4‰), and b is the average enzymatic fractionation (~27‰). This equation is simplified and does not include additional diffusional fractionations that may occur from the atmosphere to the internal leaf, and the internal leaf to the site of fixation in the chloroplast (Farquhar et al., 1982). It has been demonstrated that elevated c_a does not change the c_i/c_a ratio given that all other conditions remain equivalent (e.g., Peñuelas and Azcón-Bieto, 1992; Collatz et al., 1998), and therefore $\delta^{13}C$ values of C_3 plants reflects atmospheric $\delta^{13}C$ values and (or) c_i. Moisture stress and associated stomatal closure will cause a reduction in c_i, and result in relatively higher $\delta^{13}C$ values (e.g., Van de Water et al., 2002; Ehleringer et al., 2002). Plants with high water use efficiency, are generally more abundant as water stress increases, and have higher relative $\delta^{13}C$ values (e.g., Ehleringer, 1989). C_3 vegetation has higher relative $\delta^{13}C$ values in slope (dry) habitats, and lower $\delta^{13}C$ values on wash habitats (Ehleringer and Cooper, 1988). Therefore more arid conditions, and higher temperatures will likely decrease total terrestrial carbon isotope discrimination (increasing $\delta^{13}C$ values) in the riparian zones of the Grand Canyon.

C_4 plants transport and concentrate CO_2 at the site of fixation by hydration of inorganic carbon and PEP carboxylation, leading to a much lower discrimination against ^{13}C, quantified as (Farquhar, 1983):

$$\delta^{13}C_p = \delta^{13}C_s - (a \bullet (1 - c_i/c_a) + b_4 \bullet (c_i/c_a) + (b_3 - s) \bullet (c_i/c_a) \bullet \phi) \quad (5.2)$$

where b_4 is the discrimination associated with PEP carboxylation (–5.7‰ at 30 °C), b_3 is the enzymatic fractionation associated with Rubisco carboxylation, s is fractionation occurring during leakage from the bundle sheath cells, and $ø$ is the fraction of carbon fixed in the mesophyll after leaking from the bundle sheath cells. Plants using Crassulacean Acid Metabolism (CAM) switch from C_3 to C_4 type carboxylation mechanisms and thus have intermediate discrimination values (Farquhar et al., 1982). In the semi-arid regions of the southwest United States, however, $\delta^{13}C$ values of CAM and C_4 plants are similar (Des Marais et al., 1980; Mizutani et al., 1992b; Flemming et al., 1993), because most carbon is fixed first using PEP carboxylase at night during low relative humidity to conserve water. Although, during wet periods CAM plants do switch to C_3 photosynthesis (Ehleringer, 1989)

Therefore, $\delta^{13}C$ values of C_3 plants are lower than those of C_4 or CAM vegetation. Local environmental conditions determine the photosynthetic efficiencies of C_3 vegetation, and competitive success of a particular photosynthetic mechanism (Ehleringer, 1978; Ehleringer et al., 1997). At current atmospheric CO_2 and O_2 partial pressures, the efficiency of Rubisco at carboxylation is limiting. O_2 competes with CO_2 for Rubisco sites, and at higher temperature Rubisco's affinity for O_2 increases, thus reducing photosynthetic capacity and exhibiting higher photorespiration rates (Collatz et al., 1998). At higher temperatures and lower CO_2 partial pressures, photosynthetic efficiency of C_3 plants is reduced, and at a particular threshold temperature for a given atmospheric CO_2 partial pressure, C_4 will have a competitive advantage (Ehleringer et al., 1997). Although effective moisture plays a secondary role in determining competitive advantage, C_4 grasses are able to use summer moisture resources more effectively (Lin et al., 1996; Schwinning et al., 2002, 2003), but in very dry regions, C_3 shrubs that can tap into deep groundwater sources replace C_4 grasses (Paruelo and Lauenroth, 1996; Collatz et al., 1998).

$\delta^{13}C$ values of chitin display a total variation of 2.5‰, which may reflect changing abundance of C_4/CAM vegetation, because the presence or absence of C_4 vegetation is the greatest determinant of total terrestrial ecosystem carbon isotope discrimination (Lloyd and Farquhar, 1994). Because average $\delta^{13}C$ values of C_3 and C_4/CAM differ by ~10‰, even if bats concentrate feeding in riparian systems dominated by C_3 vegetation, a

Table 5.2—Estimated % change in C_3 diet of insects inferred from bat guano deposits.

Past $\delta^{13}C$ values for C_3 and C_4 plants are estimated by adding the difference between modern and past atmospheric CO_2 $\delta^{13}C$ values to modern plant isotope values (Ehleringer and Monson, 1993; after Koch et al., 2004). $\delta^{13}C$ values of atmospheric CO_2 are from Indermühle et al. (1999) and Smith et al. (1999). Atmospheric pCO_2 values are from Collatz et al. (1998) and Monnin et al. (2001).

Time	pCO_2 ppmV (C_a)	Estimated C_3 $\delta^{13}C$	Estimated C_4/CAM $\delta^{13}C$	Average chitin $\delta^{13}C$	Estimated C_3 vegetation
Modern	350	-27.5‰	-12.5‰	***	***
Holocene	280	-26‰	-11‰	-24.4‰	89%
Younger Dryas	235	-26.3‰	-11.3‰	-26.2‰	100%
% Change		***	***	***	11%

small change in C_4/CAM abundance (and insects feeding on these plants) is likely to be reflected in the bat's diet. However, chitin $\delta^{13}C$ values also likely reflect changing $\delta^{13}C$ values of riparian C_3 plants. Both interpretations are discussed below.

Although rising CO_2 partial pressures over the Holocene (Indermühle et al., 1999; Smith et al., 1999) should favor C_3 vegetation (e.g., Ehleringer et al., 1997; Collatz et al., 1998), chitin $\delta^{13}C$ values instead imply a greater proportion of C_4/CAM vegetation. An 11% increase in C_4 or CAM production in the Grand Canyon from the Younger Dryas to the Holocene is estimated after correcting for variation in Pleistocene/Holocene atmospheric $\delta^{13}C$ values (Indermühle et al., 1999; Smith et al., 1999), and this change is relatively insensitive to assumed $\delta^{13}C$ values of C_3 and C_4/CAM vegetation (Table 5.2).Using the modern relationship between mean annual temperature (MAT) and the relative production of C_4 and C_3 grasses, a 1 °C increase in MAT leads to a 4% decrease in the relative production of C_3 grasses (Epstein et al., 1997). Therefore, an 11% increase in C_4 vegetation corresponds to a 2-3 °C increase in MAT. Although this estimate is tentative, it is approximately half the temperature increase inferred from noble gas thermometry in the southwest United States from the Late Glacial Maximum to the Holocene (e.g., Stute et al., 1992) and does not account for increasing atmospheric CO_2 partial pressures (favoring C_3 production) that would serve to increase this estimate.

However, bats feed along riparian systems, whose major vegetative components use C_3 photosynthesis. If chitin $\delta^{13}C$ values indicate a change in average $\delta^{13}C$ values of C_3 plants, increased $\delta^{13}C$ values would reflect overall decreasing c_i/c_a by over 0.1 (e.g., Ehleringer et al., 2002) indicating increased moisture stress (Lloyd and Farquhar, 1994; Ehleringer et al., 2002) and selection for more water-use efficient plants, and a decrease in wash and transitional habitats relative to slope habitats in semi-arid regions (Ehleringer and Cooper, 1988). Therefore, lower $\delta^{13}C$ values of chitin probably reflect more moisture, particularly winter-sourced, and lower temperatures in the Grand Canyon. Regardless of whether $\delta^{13}C$ values increase because C3 plant values increase due to moisture stress, or because C4/CAM plants become more dominant due to moisture stress, the net climate change in unequivocal.

5.4.2 δD values of bat guano-derived chitin

δD values of chitin reflect both metabolic and drinking water sources of insects, both correlated with local precipitation δD values and Mean Annual Temperature (MAT) (Miller et al., 1988; Motz, 2000). In the Grand Canyon, δD values of the Colorado River are lower than regional precipitation (Coplen and Kendell, 2000), reflecting higher latitude and altitude sources along its drainage area. The total variation in δD values of chitin is 45‰, and cannot be accounted for solely by a change in temperature (e.g., Miller et al., 1988). Instead, changing δD values of subfossil insect chitin must indicate a change in source or seasonality of precipitation, or plant water-use preference. Higher δD values of chitin may be forced by increased summer precipitation (monsoonal moisture) relative to winter precipitation, or changing Colorado River water values due to a reduction of high altitude/latitude sources or an increase in δD values of those sources. In all cases, higher δD values indicate higher temperatures, and lower humidity. However, the strong covariation with $\delta^{13}C$ values implies that the local climate affected δD values of guano-derived chitin, at least until prior to 8.0 cal. kyr, when a decoupling may have occurred.

Notably, δD values of chitin derived from the bat guano core are lower than modern collected specimens. De-proteination of modern material could not be completed due to the risk of de-acetylization and resulting isotopic changes (Schimmelmann and DeNiro, 1986b; Schimmelmann et al., 1998). C:N ratios are lower for the modern chitin, than chitin derived from the guano core. However, this is unlikely to result in modern samples with ~75‰ higher δD values. Instead, source region likely changed, possibly due to the reduction in meltwater from the Laurentide and Cordilleran ice sheets or regional glaciers. Additionally, recent damming of the Colorado River may have increased δD values of the Colorado River through increased evaporation.

5.4.3 $\delta^{15}N$ values of bat guano-derived chitin

$\delta^{15}N$ values of chitin do not directly reflect dietary values because a significant portion of nitrogen in chitin is recycled from ^{15}N depleted excretory ammonia (Webb et al., 1998). Nonetheless, $\delta^{15}N$ values of chitin have been linked to arthropod trophic level and diet (Schimmelmann et al., 1998). Therefore, variation in $\delta^{15}N$ values of bat guano-derived chitin through time may indicate changing dietary sources and trophic level. $\delta^{15}N$

values of chitin are relatively constant throughout the record except from 13.6 to 12.0 cal. kyr where $\delta^{15}N$ values of chitin are ~5‰ more positive. $\delta^{15}N$ values are much higher than modern values of chitin, perhaps resulting from recent damming of the Colorado River. Relatively enriched $\delta^{15}N$ values are not uncommon in semi-arid regions. Bat guano $\delta^{15}N$ values are reported to be 14-20‰ (Mizutani et al., 1992b; McFarlane et al., 1995), and $\delta^{15}N$ values of bat muscle tissue are 15-20‰ AIR in arid Venezuela (Nassar et al., 2003). Animals in regions with low annual precipitation amount have higher $\delta^{15}N$ values (e.g., Sealy et al., 1987). However, $\delta^{15}N$ values of chitin are not strongly covariant with either $\delta^{13}C$ or δD values, which represent dietary sources. The offset between ancient and modern $\delta^{15}N$ values may be due to the extensive use of nitrogen fertilizer with $\delta^{15}N$ values that approximate atmospheric values of zero enters the river via runoff and works its way throught the food chain. Considering that chitin $\delta^{15}N$ values are depleted relative to diet (Schimmelmann et al., 1998), and although there are exceptions, most modern measured guano $\delta^{15}N$ are lower than 10‰ (Mizutani et al., 1992a,b), interpreting $\delta^{15}N$ profiles of ancient chitin will require further study.

5.4.4 Climate interpretation inferred from stable isotope profiles of bat guano derived chitin

Coeval δD and $\delta^{13}C$ values indicate that a decrease in temperature and/or an increase in winter-sourced precipitation occurred in the interior semi-arid regions of the United States, synchronous with the YD. $\delta^{13}C$ values decrease from ~14 to 12.6 cal kyr coincident with multi-proxy GRIP and GISP2 ice-core records from the North Atlantic region. Although, the onset of the Younger Dryas is not clearly evident in δD values of chitin, both $\delta^{13}C$ and δD values rise abruptly between 10,230±50 and 10,130±50 radiocarbon years, which is synchronous with termination of the Younger Dryas (~10,150 radiocarbon years BP, Renssen et al., 2001). Comparison of chitin $\delta^{13}C$ and δD profiles with multi-proxy evidence from the Santa Barbara basin (Kennett and Ingram, 1995; Hendy et al., 2001), and benthic foraminifera $\delta^{18}O$ values from the Gulf of California (Keigwin and Jones, 1990) indicate an atmospheric driven teleconnection between the North Atlantic and southwestern United States/northwestern Mexico. The

abrupt change in the Santa Barbara and Gulf of California records and those presented here exhibit a step-like change out of the YD.

Most studies infer climate of the last glacial period to be characterized by greater winter precipitation and lower temperatures due to a more southerly average position of the polar front jet stream, lower sea surface temperatures and lower sea level (Figure 5.3) (Thompson et al., 1993; Bartlein et al., 1998). Continental heating was substantially lower due to increased winter snowpack and cooler summers preventing the strong thermal low-pressure trough that develops today. Additionally, lower ocean temperatures and lower sea level served to reduce summer moisture transport (Guilderson et al., 1994; Gutzler and Preston, 1997; Anderson et al., 2000). Today, atmospheric circulation over the southwestern United States is characterized by a monsoonal system resulting from the seasonal cycle of solar insolation. Large-scale circulation patterns are forced by differential heating of the North American continent in the summer resulting in the development of a thermal low over the southwest United States, and northward displacement of the Pacific and Bermuda highs (Figure 5.4). Moist tropical air is channeled through the Gulf of California as far as the Great Basin (Adams and Comrie, 1997). Therefore, today's climate, characterized by the NAM, has warmer summers, increased summer/winter precipitation ratio, and increased aridity relative to the last glacial period.

The timing for the onset of a NAM featured climate is poorly understood (Ehleringer et al., 1998; Anderson et al., 2000; Metcalfe et al., 2000). Locally, vegetation extinction and immigration rates in the Grand Canyon were largest near 12 cal. kyr BP (Cole, 1990). Additional studies find a rapid expansion of C_4 vegetation in Northern Mexico (Huang et al., 2001) and Texas (Nordt et al., 2002) near the end of the Younger Dryas, and this is also the approximate time of a strengthening of the Indian monsoon (Overpeck et al., 1996). Therefore, the abrupt increase in both $\delta^{13}C$ and δD values of chitin suggests that the onset of the NAM climate was abrupt, possibly due to positive feedbacks between melting snowpack in the southern Rockies and Colorado plateau, decreasing soil moisture, and increased thermal heating of the land surface in the summer. Winter precipitation associated with frontal storms may have already been substantially decreased as the Cordilleran and Laurentide Ice Sheets reduced in size (e.g., Thompson et

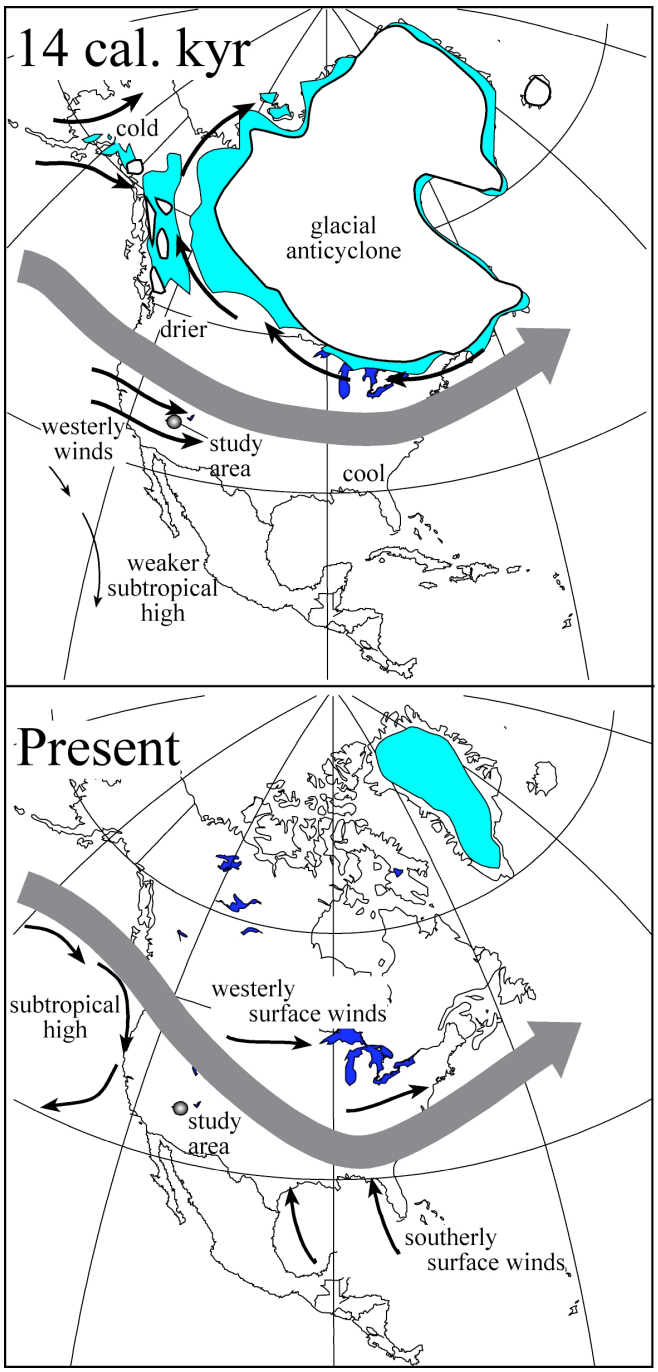

Figure 5.3—Major atmospheric circulation features simulated at 14 cal. kyr BP and today.

Atmospheric circulation features after COHMAP, 1988; Thompson et al., 1993. Ice sheet reconstruction after Dyke et al. (2003), where blue is 14 cal. kyr BP reconstruction and overlaid white reconstruction is 12 cal. kyr BP.

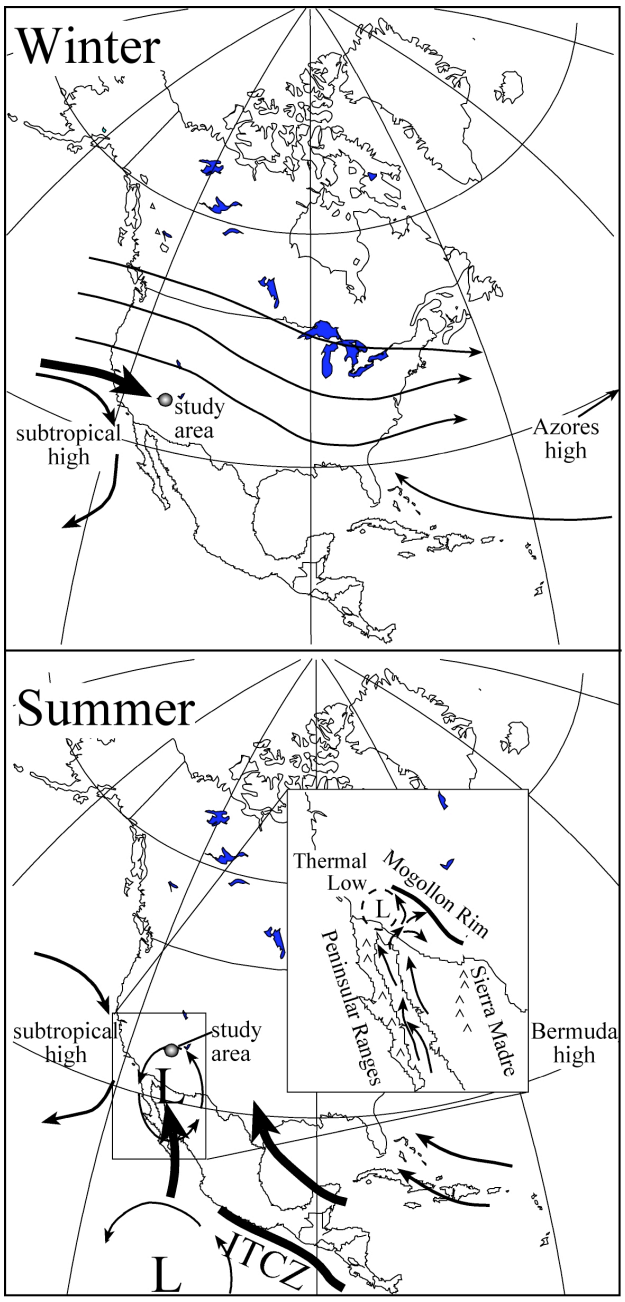

Figure 5.4—Generalized large-scale atmospheric circulation patterns describing the North American Monsoon (NAM) associated with seasonal contrast between summer and winter insolation.

Large arrows show dominant wind directions and moisture sources. Inset illustration shows topographical influences of major low-level moisture advected from the Gulf of California (after Adams and Comrie, 1997; Metcalfe et al., 2000).

al., 1993; Kovanen and Easterbrook, 2002; Licciardi et al., 2004). Increased thermal heating would permit stronger summertime low-pressure over the southwest United States (Thompson et al., 1993; Nordt et al., 2002).

The abrupt increase in chitin $\delta^{13}C$ and δD values at the termination of the YD corresponds to abrupt mid-high latitude warming forced by the resumption of NADW formation (Manabe and Stouffer, 2000; Broecker, 2003; McManus et al., 2004). Climate models show at most a weak response to NADW formation for the southwest United States (Overpeck et al., 1996; Schiller et al., 1997; Mikolajawicz et al., 1997; Renssen et al., 2002). NAM moisture is primarily derived from the Gulf of California (GOC) and Eastern Pacific, and secondarily from the Gulf of Mexico (Adams and Comrie, 1997; Sheppard et al., 2002). Today, sea surface temperature (SST) of the northern GOC must reach 26 °C before the annual onset of the NAM, and 29 °C before heavy rainfall occurs (Mitchell et al., 2002). Therefore, increasing GOC SST associated with increasing global temperature at the end of the YD may have reached a threshold level to induce moisture transport associated with the NAM. This hypothesis is in full agreement with a notable abrupt rise in $\delta^{18}O$ values of benthic foraminfera from the central Gulf of California at the termination of the YD (Keigwin and Jones, 1990).

Additionally, $\delta^{13}C$ and δD values display an initial decrease between 8.4 and 8.0 cal. kyr BP, followed by a stepwise increase in $\delta^{13}C$ values of ~0.5‰. δD values continue to rise after 8.0 cal. kyr BP. Notably, a North Atlantic cold-event associated with the final drainage of Lake Agassiz occurred between ~8.4 and 8.0 cal. kyr BP (Alley et al., 1997; Barber et al., 1999; Teller et al., 2002). In the Northern Great Plains, an abrupt switch in atmospheric circulation also occurred at this time (Dean et al., 2002). This change in atmospheric circulation pattern may have been caused by the reduction in the extent of Hudson Bay and the final stage of the loss of continental glacial ice that may have initiated the Hypsithermal (Dean et al., 2002). A northward movement of the polar front and intensification of the westerlies, would serve to warm summers and intensify the NAM over the southwest United States, although this summer warming was probably also enhanced by increased seasonality due to differences in solar insolation relative to today (e.g., Harrison et al., 2003). The rapid increase in $\delta^{13}C$ and δD values agree with

increased summer temperature and increased monsoon moisture for the mid-Holocene (e.g., Van Devender and Spaulding, 1979).

Bat guano chitin $\delta^{13}C$ and δD values are shown here to be faithful archives of terrestrial semi-arid climate that compliment more traditional investigations that use packrat middens. High-resolution, well-dated records of stable isotopes carry information that can describe abrupt mode changes in the climate system. Data is presented that supports an abrupt switch from a pluvial climate episode to a modern southwestern climate characterized by the NAM. The initiation of the NAM was previously poorly understood. It is hypothesized that at the termination of the Younger Dryas climate event, a sudden warming of the northern Gulf of California above a threshold temperature, today observed to be 26-29 °C, triggered summer moisture influx to the southwest United States and initiated the Holocene climate mode in the southwestern United States.

Chapter 6. General discussion and conclusions

6.1 Introduction

This chapter discusses the contributions this thesis makes to the acquisition of high-resolution stable isotope profiles, and will highlight the major themes and discuss specific contributions presented in the preceding chapters. The main focus of this research, the application of high sample frequency (high-resolution) light stable isotope data at various temporal and spatial scales, is in part, a result of major strides in SIRMS and CF-IRMS technology in sample throughput, precision, and critical size, and innovations in sampling strategies. This research initiated over five years ago, would not have been feasible even a few years earlier and is a direct result of such innovations.

6.2 Theme 1: high-resolution stable isotope chemistry

This thesis consists of four separate investigations using temporally high-resolution light stable isotope profiles applied at various spatio-temporal scales. Such data sets are necessary to capture events occurring at both subseasonal and geologically abrupt time scales, and critical for addressing certain ecological and geological research hypotheses. Within this thesis, temporal scales vary from ~daily to 100's of years, and spatial scales vary from that of individual animals to entire ecosystems. In each specific study, high-resolution light stable isotope profiles were used to investigate problems that ranged from fish energetics to deglacial climate change.

In chapter 2, $\delta^{18}O$ values from two bivalve shells, *Sphaerium simile* and *Dreissena polymorpha*, acquired from lakes with varied drainage areas were found to compare favorably with predicted temperature-fractionation relationships. Intra-shell $\delta^{13}C$ values were consistent with a metabolic rate model. A subseasonal to ~daily temporal resolution was captured, and this resolution enabled a simple field test of the applicability of $\delta^{18}O$ thermometry in freshwater molluscs. The primary goal of this research was to determine the suitability of freshwater mollusc intra-shell $\delta^{18}O$ values for paleoclimate research. It

was found that seasonal local air temperature was accurately recorded. Additionally, *Sphaerium simile* was found to have a shutdown temperature ~12°C, permitting discrete calculation of $\delta^{18}O_{(H_2O)}$ value and de-convolution of this value from seasonal temperature change, which is only possible with high-resolution sampling. Each organism was captured from different sized drainage basins to compare spatial scales. Although both molluscs were found to record, via $\delta^{18}O$ values, their respective local environments, differences in the variation about the seasonal pattern were observed. *Dreissena polymorpha* $\delta^{18}O$ values comparatively displayed lower seasonal variation because it came from a larger lake system.

In chapter 3, the highest-resolution intra-otolith $\delta^{13}C$ values to date from freshwater drum (*Aplodinotus grunniens*) sub-fossil otoliths were determined. Ontogenetic and seasonal patterns in intra-otolith $\delta^{13}C$ values were compared with fish respiration rate determined by bioenergetic models. Such a comparison suggests that the governing influence of intra-otolith $\delta^{13}C$ values for freshwater drum was metabolic rate. Subseasonal and ontogenetic $\delta^{13}C$ values from these otoliths were essential to test this hypothesis, as these patterns would have remained unobserved using a temporally lower-resolution $\delta^{13}C$ values, providing an example of the use of high-, and low-resolution stable isotope chemistry in physiological ecology. The spatial scale employed here is essentially that of the individual organism.

In chapter 4, high-resolution intra-otolith $\delta^{18}O$ and $\delta^{13}C$ values were used to investigate seasonal and ontogenetic migrations of chinook (*Oncorhynchus tshawytscha*) in Lake Ontario. This data set was used to infer thermal histories from two chinook temporal "populations" to investigate migratory and energetic changes that might have occurred with decreasing prey fish population and quality. Surprisingly, chinook were found in the warm epilimnetic water of Lake Ontario in midsummer even though temperatures were near the lethal temperature limit of chinook. Chinook were observed to inhabit these high temperatures in mid-summer regardless of prey fish quality and quantity. Therefore, the temporal scale of this ecological study was at multiple levels: subseasonal, over the lifetime of chinook, and at two discrete time slices a decade apart. Spatially, $\delta^{18}O$ values signify the thermal histories of each individual, while $\delta^{13}C$ values recorded individual energetic behavior.

In chapter 5, a high-resolution record of $\delta^{13}C$ and δD values of chitin derived from bat guano revealed an abrupt change at the end of the Younger Dryas. From these profiles, the onset of a climate featured by the North American monsoon is inferred. This chapter has contrasting temporal resolution relative to those described above. However, it is only through such high-resolution data acquisition, that this abrupt climate change can be recognized. Previous studies lacked such high-resolution data and were unable to determine the exact timing of the monsoon and to link it with variation in North Atlantic Deep Water Formation (e.g., Stute et al., 1992; Thompson et al., 1993; Metcalfe et al., 2000).

Thus, contrasting spatio-temporal scales were examined. Stable oxygen isotope profiles from both bivalves and fish otoliths are invariably local in spatial scale, and represent the environment of the organism secreting the carbonate structure. The sampled sedentary molluscs recorded the local lake environment, and to some extent regional air mass controls to lake temperature. Chinook $\delta^{18}O$ profiles, recorded fish location in Lake Ontario during the summer. $\delta^{13}C$ profiles are likely governed by individual energetics. Chitin δD and $\delta^{13}C$ values derived from the guano of a large population of bats are used to infer changes in the riparian ecosystem. The bats consumed insects over a large landscape area, and homogenized insect diet and environment is recorded via stable isotope values.

6.3 Theme 2: development of proxies

Chapter 2 demonstrates that carbonate of freshwater bivalves with small accretionary rates precipitates $\delta^{18}O$ values predictably with the environment of growth and can be used as a climate proxy. This is a subject of debate, as many authors find so-called "vital" effects where there are departures from equilibrium precipitation of carbonate for causes unknown (Wefer and Berger, 1991). This is a key issue in paleoclimate reconstruction, and proper sampling strategies are required to appropriately gauge questions regarding equilibrium. This study will further open the door for seasonality studies, especially as shutdown temperatures were described for *Sphaerium simile* that could permit a discrete calculation of $\delta^{18}O_{(H_2O)}$ value, and thus temperature for the rest of the growing season. This type of sampling strategy has great promise as

already demonstrated by a few others (Patterson et al., 1993; Smith et al., 1994; Patterson, 1998). Furthermore, variation about the mean is suggested as a proxy for paleostorminess. Finally, briefly discussed are intra-shell $\delta^{13}C_{(CaCO_3)}$ values that suggest a large incorporation of metabolic sourced carbon, and might be a proxy for this variable.

$\delta^{13}C$ as a proxy for metabolic rate is discussed as the main hypothesis in chapter 3, and further investigated in chapter 4 using intra-otolith $\delta^{13}C$ and $\delta^{18}O$ values. It was hypothesized that intra-otolith $\delta^{13}C$ values are governed by variation in metabolic rates both seasonally and over the lifetime of the fish, and this could be used to investigate metabolic behavior of fish through geologic time. Although previous work already suggested a contribution of metabolic carbon to otoliths (Kalish, 1991a,b; Tohse and Mugiya, 2002), and some have even looked at intra-otolith $\delta^{13}C$ values (Schwarcz et al., 1998; Weidman and Millner, 2000; Høie et al., 2004a,b), no other study has utilized such high-resolution isotope profiles, and for freshwater fish. Such high-resolution data provide additional evidence that the intra-otolith $\delta^{13}C$ values are dominantly influenced by metabolic rate in fishes. In addition, the innovative combination of bioenergetic models with this type of analysis suggests that intra-otolith $\delta^{13}C$ values may be used as a proxy of activity in free-ranging fishes, a major point of contention in current fish bioenergetic models (Rowan and Rasmussen, 1996; Trudel et al., 2004). Intra-otolith $\delta^{13}C$ values and bioenergetic models in chinook, described in detail in chapter 4, further substantiate this hypothesis. In addition, subseasonal $\delta^{18}O$ and $\delta^{13}C$ values are combined for the first time to track thermal orientation and energetics of a freshwater fish.

Chapter 5 develops a proxy for climate in semi-arid regions. The use of bat guano isotope values as a paleoclimate proxy has been limited despite its ubiquity (Mizutani et al., 1992b; McFarlane et al., 2002), and never before has a high-resolution profile of chitin isotope values been acquired. Importantly, $\delta^{13}C$ is combined with δD from the same sample. This is a particularly exciting proxy, especially for semi-arid regions where few other "continuous" proxies exist (Des Marais et al., 1980). Bat guano has several advantages as a climate archive. First, it can be varved (Altenbach and Petit, 1972; Mizutani et al., 1992a) and may provide very high-resolution data. Second, it can be dated via radiocarbon methods. Third, deposits as old as 40,000 years have been located (Mizutani et al., 1992b), and thus extended records can be generated. Fourth, up to four

light stable isotope ratios can be derived (δD, $\delta^{18}O$, $\delta^{15}N$, $\delta^{13}C$) (Schimmelmann and DeNiro, 1986a,b). Three of these isotope ratios (δD, $\delta^{13}C$, and $\delta^{15}N$) were investigated in this study, but the door is opening, for example, for the combination of δD and $\delta^{18}O$ in the quantification of relative humidity and temperature (Roden et al., 2000; Motz, 2000).

6.4 Theme 3: using sampling innovations and advances in SIRMS/CF-IRMS technology

Two broad areas of innovative sampling strategy using light stable isotope profiles are employed: First, robotic microsampling for subseasonal recovery of $\delta^{18}O$ and $\delta^{13}C$ profiles from accretionary carbonates (Dettman and Lohmann, 1995; Wurster et al., 1999), and second, sample-standard equilibration for rapid analysis of organic matter using CF-IRMS (Wassenaar and Hobson, 2003).

Interest in the recovery of subseasonal temporal resolution in accretionary carbonates has been around since the conception of fossil isotopic study (Wefer and Berger, 1991). Urey et al. (1951) pioneered subseasonal $\delta^{18}O$ values by determining that a belemnite experienced three summers and four winters during its life and moved into colder water with age. Subsequent studies focused on isotope profiles of much smaller organisms to look at seasonality, both because these organisms are much more common in the record, and because isotope profiles may be less dependent on growth rate (Wefer and Berger, 1991). A robotic micromilling apparatus was developed at the University of Michigan (Dettman and Lohmann, 1995) and used on bivalves (Dettman and Lohmann, 1993; Klein et al., 1996a,b) and teleost fish otoliths (Patterson et al., 1993; Smith and Patterson, 1994; Patterson, 1998). Chapter 2 expands on previous work by sampling modern lacustrine bivalve accretionary carbonate using a further development in robotic micromilling (Wurster et al., 1999) that adds three-dimensional sampling capability. This increased functionality is used to sample whole valves (not sectioned), thus preserving carbonate for higher-resolution capabilities. Using the same technology in chapters 3 and 4, the highest resolutions in subseasonal intra-otolith carbonate $\delta^{18}O$ and $\delta^{13}C$ values to date are obtained.

The success of δD values as a climate proxy from ice-cores have prompted investigations as to its utility in organic compounds (Ehleringer and Rundel, 1989;

Hobson et al., 1999). However, a considerable problem for many organic compounds is that hydrogen not bonded to carbon is available to exchange with hydrogen in atmospheric water vapor (Schimmelmann, 1991). This problem can be overcome in some compounds by chemical nitrification, as is commonly applied in cellulose study (Epstein et al., 1979). However, nitrification is relatively difficult and time-consuming, compromising the ability to do high-resolution work, and suffers from the inability to replace all exchangeable hydrogen in some compounds such as chitin (Schimmelmann , 1991; Schimmelmann and Miller, 2002). The idea of equilibrating hydrogen with waters of known δD value to calculate δD values of the non-exchangeable portion of the organic material in question (δD_n) has been around at least since the 1970s (Grinsted and Wilson, 1979). However, recently high-temperature equilibration has greatly increased the precision of this technique (Schimmelmann, 1991; Wassenaar and Hobson, 2000). Finally, Wassenaar and Hobson (2003) developed a means to combine this method with online high-temperature pyrolysis CF-IRMS by simply determining standard δD_n values offline and permitting atmospheric equilibration of these standards set alongside samples. Both are run online and the samples are then corrected using standard δD_n values. In chapter 5, this technique is used to develop a new climate proxy for semi-arid regions using high-resolution δD_n and $\delta^{13}C$ values of chitin derived from bat guano.

6.5 General conclusions and future research

In chapter 2, a high-resolution record was recovered from two species of temperate modern lacustrine molluscs to investigate their suitability for recovering paleoenvironmental records on daily to weekly time scales. *Sphaerium simile* and *Dreissena polymorpha* yield $\delta^{18}O$ values predicted from environmental parameters, although evidence is found for familial differences in the temperature-fractionation equation. Further study is needed to better delineate subtle differences and mechanisms in freshwater molluscan fractionation of stable oxygen isotopes. Additionally, the seasonal pattern of $\delta^{18}O_{(CaCO_3)}$ value is significantly influenced by the organism's environment. For example, a greater variability is found in the mollusc from a small watershed. This is probably due to increased sensitivity of the watershed to day-to-day variation in temperature, in addition to $\delta^{18}O_{(H_2O)}$ variability resulting from input of storm water.

Selection of an appropriate watershed makes it possible to evaluate secular changes in storminess, an important characteristic of climate. Conversely, interpretation of temperature seasonality is best accomplished using a large watershed that provides a relatively predictable seasonal variation in $\delta^{18}O_{(H_2O)}$ value.

Future research should raise *Sphaeridae* and other bivalves under controlled conditions in the laboratory, while manipulating temperature, $\delta^{18}O$ value of the ambient water, and physiological parameters such as growth rate. Monitoring chemistry in the Extra Pallial Fluid (EPF) would enable direct evidence for possible familial differences in accretion of shell carbonate and physico-chemical properties. Measurement of intra-shell $\delta^{18}O$ and $\delta^{13}C$ values was not matched by measurements of environmental variables. It was presumed that the isotopic variability witnessed in the $\delta^{18}O$ carbonate values was due to changing storm input ($\delta^{18}O_{(H_2O)}$ value), but this should be measured.

Chapter 3 documents three dominant intra-otolith $\delta^{13}C$ patterns from fossil freshwater drum otoliths. The first order pattern is one of a lifelong increase from more negative $\delta^{13}C$ values early in the ontogeny of the fish to more positive and stable values as the fish matures. The second order pattern reveals strong seasonal linear covariations between $\delta^{13}C_{(CaCO_3)}$ and $\delta^{18}O_{(CaCO_3)}$ values. And third, lower magnitudes of seasonal change in $\delta^{13}C$ values occur with age. The total variation in these drum otoliths ($\delta^{13}C_{max-min}$) is up to 14.2‰, and total seasonal variations are often greater than 5‰, indicating that a wealth of variability and information is potentially lost if otoliths are analyzed whole rather than subsampled. Each of these documented patterns strongly infers that specific respiration rate (metabolic activity) governs intra-otolith $\delta^{13}C$ values.

In chapter 4, chinook thermal behavior in Lake Ontario is documented using $\delta^{18}O$ carbonate thermometry coupled with a bioenergetic model to infer energetic conditions and sustainability in this ecosystem. Chinook are found to inhabit much higher temperatures in midsummer then previously thought, showing that novel techniques can provide a unique perspective on ecological problems that are difficult or expensive to determine using traditional methods. As in chapter 3, but with greater constraint on variables, $\delta^{13}C$ values show promise as a means to determine fish activity "in the field", and perhaps can be used as an additional proxy with which to infer vertical distributions

of fish within a water column. Alternatively, if metabolic rate can be accurately modeled and the environmental $\delta^{13}C_{(DIC)}$ value known, it may be possible to estimate diet changes in longer-lived fish.

Future research of otolith $\delta^{13}C$ values should incorporate direct laboratory measurement and manipulation of oxygen consumption. It is highly desirable to investigate changing $\delta^{13}C$ value of otoliths as a function of fish mass, fish activity, and temperature. These treatments should occur on fish with varying $\delta^{13}C$ value of diets and under tanks with different $\delta^{13}C_{DIC}$ values. Additionally, cataloging patterns in intra-otolith $\delta^{13}C$ values of a suite of fish from varying habitats (i.e., river, lake) and trophic niche (i.e., piscovore, detritivore) may be directly applicable to investigation of extinct fish energetics and behavior.

Finally, in chapter 5, an abrupt change in both $\delta^{13}C$ and δD values from guano-derived terrestrial insect chitin at the Pleistocene-Holocene transition is documented and demonstrated to represent the onset of a climate featured by the North American Monsoon, which is characterized by greater temperatures and lower relative humidity from that of the "pluvial" climate during the last glacial period.

Future investigations of bat guano as a paleoclimate archive should begin by concentrating on quantification of isotope variables. Guano should be taken from a host of sites, from various species throughout North America and compared to local temperature, environmental $\delta^{18}O$ and δD value of the local water, trophic level, and local vegetation. More detailed laboratory studies should be investigated by raising insects and bats on controlled δD (and $\delta^{18}O$) value of diet and water to determine metabolic effects, particularly the routing of drinking water and diet. Additionally, these local studies need to be scaled to the regional landscape level. Guano derived insect chitin isotope values need to be compared to terrestrial carbon isotope discrimination and partitioning as a function of changing abiotic properties (i.e., precipitation, temperature). Semi-arid environments are particularly suited to this type of investigation.

Isotope chemistry is an exciting and rapidly changing field of study that depends on advances in technology. There are ~ 30,000 species of teleost fishes in the world, and only a handful of these have been subseasonally analyzed. Yet, as demonstrated in this thesis, there is tremendous application for study in behavioral, environmental, trophic,

paleoclimatalogical, archaeological, and physiological sciences. As fish are extraordinarily important economically in commercial, sport, and farming fisheries (e.g., Naylor et al., 2000), this kind of study has applied potential. A key to successful applications will be the combination of bioenergetic models with intra-otolith $\delta^{13}C$ and $\delta^{18}O$ values. Clearly, there is still much future research to be done. There is still the need for detailed laboratory studies that determine the quantitative relationship between metabolic rate, diet, and intra-otolith $\delta^{13}C$ values, followed by field corroboration, and only then might many applications be realized.

It is also clear that there is much work still possible using bat guano as an environmental and ecological proxy in both past and modern study. Modern ecological and species relationships need to be developed for more quantitative contributions. The varved nature of some guano deposits, the fact that they can date back farther than 40,000 ^{14}C years, and the ubiquity nature of bats (found on all continents but Antarctica) testify to the great potential applicability of the technique described in chapter 5.

Literature cited

Adams, D. K., and A. C. Comrie, 1997. The North American Monsoon. Bulletin of the American Meteorological Society 78: 2197-2212.

Alley, R. B., 2000. The Younger Dryas cold interval as viewed from central Greenland. Quaternary Science Reviews 19: 213-226.

Alley, R. B., P. A. Mayewski, T. Sowers, M. Stuiver, K. C. Taylor, P. U. Clark, 1997. Holocene climatic instability: A prominent, widespread event 8200 yr ago. Geology 25: 483-486.

Altenbach, J. S., and M. G. Petit, 1972. Stratification of guano deposits of the free-tailed bat *Tadarida brasiliensis*. Journal of Mammalogy 53: 890-893.

Amundson, R., E. Franco-Vizcaíno, R. C. Graham and M. DeNiro, 1994. The relationship of precipitation seasonality to the flora and stable isotope chemistry of soils in the Vizcaíno desert, Baja California, México. Journal of Arid Environments 28: 265-279.

Anderson, R. S., J. L. Betancourt, J. I. Mead, R. H. Hevly, D. P. Adam, 2000. Middle- and late-Wisconsin paleobotanic and paleoclimatic records from the southern Colorado Plateau, USA. Palaeogeography Palaeoclimatology Palaeoecology 155: 31-57.

Atekwana, E. A., and R. V. Krishnamurthy, 1998. Seasonal variations of dissolved inorganic carbon and $\delta^{13}C$ of surface waters: application of a modified gas evolution technique. Journal of Hydrology 205:265-278.

Axelrod, D. I., 1992. What is an equable climate? Palaeogeography Palaeoclimatology Palaeoecology 91: 1-12.

Barber, D. C., A. Dyke, C. Hillaire-Marcel, A. E. Jennings, J. T. Andrews, M.W. Kerwin, G. Bilodeau, R. McNeely, J. Southon, M. D. Moreheand, and J.-M.Gagnon, 1991. Forcing of the cold event of 8,200 years ago by catastrophic drainage of Laurentide lakes. Nature 400: 344-348.

Bartlein, P. J., K. H. Anderson, P. M. Anderson, M. E. Edwards, C. J. Mock, R. S. Thompson, R. S. Webb, T. W. Webb III, and C. Whitlock, 1998. Paleoclimate simulations for North America over the past 21,000 years: Features of the simulated climate and comparisons with paleoenvironmental data. Quaternary Science Reviews 17: 549-585.

Beck, W. J., J. Récy, F. Taylor, R. L. Edwards and G. Cabioch, 1997. Abrupt changes in early Holocene tropical sea surface temperature derived from coral records. Science 385: 705-707.

Betancourt, J. L., T. R. Van Devender, P. S. Martin (Eds.) 1990b. Packrat Middens: the last 40,000 years of biotic change. The University of Arizona Press, Tuscon, 467 pp.

Betancourt, J. L., T. R. Van Devender, P. S. Martin, 1990a. Introduction. Pp. 2-11 *In* Packrat Middens: the last 40,000 years of biotic change, *edited by* J. L. Betancourt, T. R. Van Devender, and P. S. Martin. The University of Arizona Press, Tuscon.

Bjorn, T. C., and D. W. Reiser, 1991. Influences of forest and rangeland management on salmonid fishes and their habitats. American Fisheries Society Special Publication 19: 83 –138.

Boisclair, D., and W. C. Leggett, 1989. The importance of activity in bioenergetics model applied to actively foraging fishes. Canadian Journal of Fisheries and Aquatic Sciences 46: 1859-1867.

Bowers, J. E., R. H. Webb, and E. A. Pierson, 1997. Succession of desert plants on debris flow terraces, Grand Canyon, Arizona, U.S.A. Journal of Arid Environments 36: 67-86.

Brandt, S. B., 1986. Food of salmon and trout in Lake Ontario. Journal of Great Lakes Research 12: 200-205.

Briggs, D. E. G., 1999. Molecular taphonomy of animal and plant cuticles: selective preservation and diagenesis. Philosophical Transactions of the Royal Society of London B 354: 7-17.

Broecker, W. S., 2003. Does the trigger for abrupt climate change reside in the ocean or in the atmosphere? Science 300: 1519-1522.

Broecker, W. S., J. P. Kennett, B. P. Flower, J. T. Teller, S. Trumbore, G. Bonani, and W. Wolfli, 1989. Routing of meltwater from the Laurentide Ice Sheet during the Younger Dryas cold episode. Nature 341: 318-321.

Burgoyne, T. W., and J. M. Hayes, 1998. Quantitative production of H_2 by pyrolysis of gas chromatographic effluents. Analytical Chemistry 70: 5136-5141.

Calow, P., 1985. Adaptive aspects of energy allocation. Pp. 13-31 *In* Fish Energetics: New Perspectives, *edited by* P. Tytler and P. Calow, Johns Hopkins University Press, Baltimore.

Campana, S. E., 1999. Chemistry and composition of fish otoliths: pathways, mechanisms and applications. Marine Ecology Progress Series 188: 263-297.

Campana, S. E., and J. D. Neilson, 1985. Microstructure of fish otoliths. Canadian Journal of Fisheries and Aquatic Sciences 39: 1014-1032.

Casselman, J. M., 1987. Determination of age and growth. Pp. 209-242 *In* The Biology of Fish Growth, *edited by* A. H. Weatherley and H. S. Gill. Academic Press, London.

Casteel, R. W., 1976. Fish Remains in Archeology and Paleoenvironmental Studies. Academic Press, New York.

Clark, P. U., N. G. Pisias, T. F. Stocker, and A. J. Weaver, 2002. The role of the thermohaline circulation in abrupt climate change. Nature 415: 863-869.

Cole, K. L., 1990. Late Quaternary vegetation gradients through the Grand Canyon. Pp. 240-258 *In* Packrat Middens: the last 40,000 years of biotic change, *edited by* J. L. Betancourt, T. R. Van Devender, and P. S. Martin. The University of Arizona Press, Tuscon.

Collatz, G. J., J. A. Berry, and J. S. Clark, 1998. Effects of climate and atmospheric CO_2 partial pressure on the global distribution of C_4 grasses: present, past, and future. Oecologia 114: 441-454.

COMAP project members, 1988. Climatic changes of the last 18,000 years: Observations and model simulations. Science 241: 1043-1052.

Constantine, D. G., 1970. Bats in relation to the health, welfare, and economy of Man. Pp. 319-449 *In* Biology of Bats, *edited by* W. A. Wimsatt. Academic Press, New York.

Coplen, T. B., and C. Kendall, 2000. Stable hydrogen and oxygen isotope ratios for selected sites of the U.S. Geological Survey's NASQAN and Benchmark Surface-water networks. U.S. Geological Survey Open-File Report 00-160.

Dansgaard, W., 1964. Stable isotopes in precipitation. Tellus 16:436-468.

Dean, W. E., R. M. Forester, and J. P. Bradbury, 2002. Early Holocene change in atmospheric circulation in the Northern Great Plains: an upstream view of the 8.2 ka cold event. Quaternary Science Reviews 21: 1763-1775.

Degens, E. T., 1978. Why do organisms calcify? Chemical Geology 25: 257-269.

Degens, E. T., W. G. Deuser, and R. L. Haedrich, 1969. Molecular structure and composition of fish otoliths. Marine Biology 2: 105-113.

DeNiro, M. J., and S. Epstein, 1978. Influence of diet on the distribution of carbon isotopes in animals. Geochimica et Cosmochimica Acta 42: 495-506.

Des Marais, D. J., J. M. Mitchell, W. G. Meinschein, and J. M. Hayes, 1980. The carbon isotope biogeochemistry of the individual hydrocarbons in bat guano and the ecology of the insectivorous bats in the region of Carlsbad, New Mexico. Geochimica et Cosmochimica Acta 44: 2075-2086.

Dettman, D. L., A. K. Reische, and K. C. Lohmann, 1999. Controls on the stable isotope composition of seasonal growth bands in aragonitic fresh-water bivalves (Unionidae). Geochimica et Cosmochimica Acta 63: 1049-1057.

Dettman, D. L., and K. C. Lohmann, 1993. Seasonal change in Paleogene surface water $\delta^{18}O$: Fresh-water bivalves of western North America. Pp. 153-163 *In* Continental Climate Change from Isotopic Records, *edited by* P. Swart, K. C. Lohmann, J. McKenzie, and S. Savin . American Geophysical Union Monograph 78.

Dettman, D. L., and K. C. Lohmann, 1995. Microsampling carbonates for stable isotope and minor element analysis; physical separation of samples on a 20 micrometer scale. Journal of Sedimentary Research A 65: 566-569.

Dial, K. P., and N. J. Czaplewski, 1990. Pp. 43-59 *In* Packrat Middens: the last 40,000 years of biotic change, *edited by* J. L. Betancourt, T. R. Van Devender, and P. S. Martin. The University of Arizona Press, Tuscon.

Dingman, S. L., 1972. Equilibrium temperatures of water surfaces as related to air temperature and solar radiation. Water Resources Research 8: 42-49.

Dreves, D. P., T. J. Timmons, and J. Henson, 1996. Age, growth, and food of freshwater drum, *Aplodinotus grunniens* (Sciaenidae), in Kentucky Lake, Kentucky/Tennessee. Transactions of the Kentucky Academy of Science 57: 22-26.

Dyke, A. S., 2003. An outline of North American deglaciation with emphasis on central and northern Canada. *In* Extent and Chronology of Quaternary Glaciation, *edited by* J. Ehlers. Elsevier.

Eaton, J. G., J. H. McCormick, B. E.Goodno, D. G. O'Brien, H. G. Stefan, M. Hondzo, and R. M. Scheller, 1995. A field information-based system for estimating fish temperature tolerances. Fisheries 20: 10-18.

Edinger, J. E., D. W. Duttweiler, and J. C. Geyer, 1968. The response of water temperatures to meteorological conditions. Water Resources Research 4: 1137-1143.

Ehleringer, J. R., 1978. Implications of quantum yield differences on the distributions of C_3 and C_4 grasses. Oecologia 31: 255-267.

Ehleringer, J. R., 1989. Carbon isotope ratios and physiological processes in aridland plants. Pp. 41-54 *In* Stable isotopes in ecological research, *edited by* P. W.Rundel, J. R. Ehleringer and K. A. Nagy, Springer-Verlag: New York.

Ehleringer, J. R., and P. W. Rundel, 1989. Stable isotopes: history, units, and instrumentation. Pp. 1-15 *In* Stable Isotopes in Ecological Research *edited by* P.W. Rundel, J. R. Ehleringer, and K. A. Nagy. Springer-Verlag, New York.

Ehleringer, J. R., and R. K. Monson, 1993. Evolutionary and ecological aspects of photosynthetic pathway variation. Annual Review of Ecology and Systematics 24: 411-439.

Ehleringer, J. R., and T. A. Cooper, 1988. Correlations between carbon isotope ratio and microhabitat. Oecologia: 76: 562-566.

Ehleringer, J. R., R. D. Evans, and D. Williams, 1998. Assessing sensitivity to change in desert ecosystems—a stable isotope approach. Pp. 223-237 *In* Stable Isotopes, *edited by* J. Griffiths, BIOS Scientific, Oxford.

Ehleringer, J. R., T. E. Cerling, B. R. Helliker, 1997. C_4 photosynthesis, atmospheric CO_2, and climate. Oecologia 112: 285-299.

Elliott, J. M., 1976. Energy losses in the waste products of brown trout (Salmo trutta L.). Journal of Animal Ecology 45: 561-580.

Elliott, J. M., 1979. Energetics of freshwater teleosts. Symposia of the Zoological Society of London 44: 29-61.

Elrod, J. H., and R. O'Gorman, 1991. Diet of juvenile lake trout in southern Lake Ontario in relation to abundance and size of prey fishes, 1979-1987. Transactions of the American Fisheries Society 120: 290-302.

Elsdon, T. S. and B. M. Gillanders, 2003. Reconstructing migratory patterns of fish based on environmental influences on otolith chemistry. Reviews in Fish Biology and Fisheries 13: 219-235.

Epstein, H. E., W. K. Lauenroth, I. C. Burke, and D. P. Coffin, 1997. Productivity patterns of C_3 and C_4 functional types in the U.S. Great Plains. Ecology 78: 722-731.

Epstein, S., C. J. Yapp, and J. H. Hall, 1979. The determination of the D/H ratio of non-exchangeable hydrogen in cellulose extracted from aquatic and land plants. Earth and Planetary Science Letters 30: 241-251.

Farquhar, G. D., 1983. On the nature of carbon isotope discrimination in C_4 species. Australian Journal of Plant Physiology 10: 205-226.

Farquhar, G. D., M. H. O'Leary, and J. A. Berry, 1982. On the relationship between carbon isotope discrimination and the intercellular carbon dioxide concentration in leaves. Australian Journal of Plant Physiology 9: 121-137.

Fastovsky, D. E., M. E. Arthur, N. H. Strater and A. Foss, 1993. Freshwater bivalves (Unionidae), disequilibrium isotopic fractionation, and temperatures. Palaios 8: 602-608.

Flemming, T. H., R. A. Nunez, L. and L. d S. L. Sternberg, 1992. Seasonal changes in the diets of migrant and non-migrant nectarivorous bats as revealed by carbon stable isotope analysis. Oecologia 94: 72-75.

Friedman, I. and J. R. O'Neil, 1977. Compilation of stable isotope fractionation factors of geochemical interest. *In* Data of Geochemistry, *edited by* Fleischer F. U.S. Geological Survey Professional Paper 440-KK, 6th Ed., Reston, VA.

Fry, B. 1999. Using stable isotopes to monitor watershed influences on aquatic trophodynamics. Canadian Journal of Fisheries and Aquatic Sciences 56: 2167-2171.

Fry, B., A. Joern, and P. L. Parker, 1978. Grasshopper food web analysis: use of carbon isotope ratios to examine feeding relationships among terrestrial herbivores. Ecology 59: 498-506.

Fry, B., and E. B. Sherr, 1984. $\delta^{13}C$ measurements as indicators of carbon flow in marine and freshwater ecosystems. Contributions in Marine Science 27:13-47.

Gat, J. R., C. J. Bowser, and C. Kendall, 1994. The contribution of evaporation from the Great Lakes to the continental atmosphere: estimate based on stable isotope data. Geophysical Research Letters 21: 557-560.

Gauldie, R. W., 1996. Biological factors controlling the carbon isotope record in fish otoliths: principles and evidence. Comparative Biochemistry and Physiology B 115B: 201-208.

Goslar, T., J. Czernik and E. Goslar, 2004. Low-energy ^{14}C AMS in Poznan radiocarbon Laboratory, Poland. Nuclear Instruments and Methods in Physics Research B 223-224: 5-11.

Goyke, A. P., and S. B. Brandt, 1993. Spatial models of salmonine growth rates in Lake Ontario. Transactions of the American Fisheries Society 122: 870-883.

Grimm, N. B., A. Chacón, C. N. Dahm, S. W. Hostetler, O. T. Lind, P. L. Starkweather, and W. W. Wurtsbaugh, 1997. Sensitivity of aquatic ecosystems to climatic and anthropogenic changes: the Basin and Range, American southwest and Mexico. Hydrological Processes 11: 1023-1041.

Grinsted, M. J., and A. T. Wilson, 1979. Hydrogen isotopic chemistry of cellulose and other organic material of geochemical interest. New Zealand Journal of Science 22: 281-287.

Grootes, P. M., M. Stuiver, J. W. C. White, S. J. Johnsen, and J. Jouzel, 1993. Comparison of oxygen isotope records from the GISP2 and GRIP Greenland ice cores. Nature 366: 552-554.

Grossman, E. L. and T-L Ku, 1986. Oxygen and carbon isotope fractionation in biogenic aragonite: temperature effects. Chemical Geology 59: 59-74.

Guilderson, T. P., R. G. Fairbanks, and J. L. Rubenstone, 1994. Tropical temperature variations 0-20,000 years: modulating interhemispheric climatic changes. Science 263: 663-665.

Gutzler, D. S. and J. W. Preston, 1997. Evidence for a relationship between spring snow cover in North America and summer rainfall in New Mexico. Geophysical Research Letters 24: 2207-2210.

Hanson, P. C., T. B. Johnson, D. E. Schindler, and J. F. Kitchell, 1997. Fish bioenergetics 3.0. University of Wisconsin, Sea Grant Institute, Technical Report WISCU-T-97-001, Madison, WI.

Harrison, S. P., J. E. Kutzbach, Z. Liu, P. J. Bartlein, B. Otto-Bliesner, D. Muhs, I. C. Prentice, and R. S. Thompson, 2003. Mid-Holocene climates of the Americas: a dynamical response to changed seasonality. Climate Dynamics 20: 663-688.

Hartig, J. H., J. F. Kitchell, D. Scavia, and S. B. Brandt, 1991. Rehabilitation of Lake Ontario: the role of nutrient reduction and food web dynamics. Canadian Journal of Fisheries and Aquatic Sciences 48: 1574-1580.

Hartman, K. J., and S. B. Brandt, 1995a. Comparative energetics and the development of bioenergetics models for sympatric estuarine piscivores. Canadian Journal of Fisheries and Aquatic Sciences 52: 1647-1666.

Hartman, K. J., and S. B. Brandt, 1995b. Predatory demand and impact of striped bass, bluefish, and weakfish in the Chesapeake Bay: applications of bioenergetics models. Canadian Journal of Fisheries and Aquatic Sciences 52: 1667-1687.

Harvey, C. J., P. C. Hanson, T. E. Essington, P. B. Brown, and J. F. Kitchell, 2002. Using bioenergetics models to predict stable isotope ratios in fishes. Canadian Journal of Fisheries and Aquatic Sciences 59: 115-124.

Hass, H.C., 1996. Northern Europe climate variations during late Holocene: evidence from marine Skagerrak. Palaeogeography Palaeoclimatology Palaeoecology 123: 121-145.

Haynes, J. M., and C. J. Keleher, 1986. Movements of Pacific salmon in Lake Ontario in spring and summer: evidence for wide dispersal. Journal of Freshwater Ecology 3: 289-297.

He, J. and D. J. Stewart, 1998. Ontogeny of energetic relationships and potential effects of tissue turnover: a comparative modeling study on lake trout. Canadian Journal of Fisheries and Aquatic Sciences 55: 2518-2532.

Hélie, J-F., C. Hillaire-Marcel, B. Rondeau, 2002. Seasonal changes in the sources and fluxes of dissolved inorganic carbon through the St. Lawrence River—isotopic and chemical constraint. Chemical Geology 186: 117-138.

Hendy, I. L., J. P. Kennet, E. B. Roark, and B. L. Ingram, 2002. Apparent synchroneity of submillennial scale climate events between Greenland and Santa Barbara Basin, California from 30-10 ka. Quaternary Science Reviews 21: 1167-1184.

Hobson, K. A., L. Atwell, and L. I. Wassenaar, 1999. Influence of drinking water and diet on the stable-hydrogen isotope ratios of animal tissues. Proceedings of the National Academy of Sciences 96: 8003-8006.

Hodell, D. A., C. L. Schelske, G. L. Fahnensteil, and L. L. Robbins, 1998. Biologically induced calcite and its isotopic composition in Lake Ontario. Limnology and Oceanography 43: 187-199.

Hodgins, G. W. L., J. L. Thorpe, G. R. Coope, and R. E. M. Hedges, 2001. Protocol development for purification and characterization of sub-fossil insect chitin for stable isotopic analysis and radiocarbon dating. Radiocarbon 43: 199-208.

Høie, H., A. Folkvord, and E. Otterlei, 2003. Effect of somatic and otolith growth rate on stable isotopic composition of early juvenile cod (*Gadus morhua* L) otoliths. Journal of Experimental Marine Biology and Ecology 289: 41-58.

Høie, H., C. Andersson, A. Folkvord, and Ø Karlse, 2004b. Precision and accuracy of stable isotope signals in otoliths of pen-reared cod (*Gadus morhua*) when sampled with a high-resolution micromill. Marine Biology 144: 1039-1049.

Høie, H., E. Otterlei, and A. Folkvord, 2004a. Temperature-dependant fractionation of stable oxygen isotopes in otoliths of juvenile cod (*Gadus morhua* L.). ICES Journal of Marine Science 61: 243-251.

Huang, G. H., K. A. Hughen, D. M. Sigman, L. C. Peterson, and U. Röhl, 2001. Southward migration of the Intertropical Convergence Zone through the Holocene. Science 293: 1304-1308.

Hughes, G. M., and N. K. Al-Kadhomiy, 1988. Changes in scaling of respiratory systems during the development of fishes. Journal of the Marine Biological Association U. K. 68:489-498.

Indermühle, A., T. F. Stocker, F. Joos, H. Fischer, J. J. Smith, M. Wahlen, B. Deck, D. Mastroianni, J. Tschumi, T. Blunier, R. Meyer, and B. Stauffer, 1999. Holocene carbon-cycle dynamics based on CO_2 trapped in ice at Taylor Dome, Antarctica. Nature 398: 121-126.

Jeuniaux, C., 1971. Chitinous structures. Pp. 595-632 *In* Comprehensive Biochemistry, *edited by* M.S. Florkin and E.H. Stotz. Elsevier, Amsterdam.

Johengen, T. H., O. E. Johannsson, G. L. Pernie, and E. S. Millard, 1994. Temporal and seasonal trends in nutrient dynamics and biomass measures in Lakes Michigan and Ontario in response to phosphorus control. Canadian Journal of Fisheries and Aquatic Sciences 51: 2570-2578.

Jones, D. S., and I. R. Quitmyer, 1996. Marking time with bivalve shells: Oxygen isotopes and season of annual increment formation. Palaios 11: 340-346.

Jones, D. S., M. A. Arthur, and D. J. Allard, 1989. Sclerochronological records of temperature and growth from shells of *Mercenaria mercenaria* from Narragansett Bay, Rhode Island. Marine Biology 102: 225-234.

Jones, M. L., J. F. Koonce, and R. O'Gorman, 1993. Sustainability of hatchery-dependent salmonine fisheries in lake Ontario: the conflict between predator demand and prey supply. Transactions of the American Fisheries Society 122: 1002-1018.

Junger, M., and D. Planas, 1994. Quantitative use of stable carbon isotope analysis to determine the trophic base of invertebrate communities in a boreal forest lotic system. Canadian Journal of Fisheries and Aquatic Sciences 51: 52-61.

Kalish, J. M., 1991a. ^{13}C and ^{18}O isotopic disequilibria in fish otoliths: metabolic and kinetic effects. Marine Ecology Progress Series 75: 191-203.

Kalish, J. M., 1991b. Oxygen and carbon stable isotopes in the otoliths of wild and laboratory-reared Australian salmon *Arripis trutta*. Marine Biology 110: 37-47.

Keigwin, L. D., and G. A. Jones, 1990. Deglacial climatic oscillations in the Gulf of California. Paleoceanography 5: 1009-1023.

Kennett, J. P., and B. L. Ingram, 1995. A 20,000-year record of ocean circulation and climate change from the Santa Barbara basin. Nature 377: 510-514.

Kim, S. T., and J. R. O'Neil, 1997. Equilibrium and nonequilibrium oxygen isotope effects in synthetic carbonates. Geochimica et Cosmochimica Acta 61: 3461-3475.

Kiriluk, R. M., M. R. Servos, D. M. Whittle, G. Cabana, and J. B. Rasmussen, 1995. Using ratios of stable nitrogen and carbon isotopes to characterize the biomagnification of DDE, mirex, and PCB in a Lake Ontario pelagic food web. Canadian Journal of Fisheries and Aquatic Sciences 52: 2660-2674.

Kitchell, J. F., D. J. Stewart, and D. Weininger, 1977. Applications of a bioenergetics model to yellow perch (*Perca flavescens*) and walleye (*Stizostedion vitreum vitreum*). Journal of the Fisheries Research Board of Canada 34: 1922-1935.

Klein, R. T., K. C. Lohmann and C. W. Thayer, 1996a. Bivalve skeletons record sea-surface temperature and $\delta^{18}O$ via Mg/Ca and $^{18}O/^{16}O$ ratios. Geology 24: 415-418.

Klein, R. T., K. C. Lohmann and C. W. Thayer, 1996b. Sr/Ca and $^{13}C/^{12}C$ ratios in skeletal calcite of *Mytilus trossulus*: Covariation with metabolic rate, salinity, and carbon isotopic composition of seawater. Geochimica et Cosmochimica Acta 60: 4207-4221.

Koch, P. L., N. S. Diffenbaugh, and K. A. Hoppe, 2004. The effects of late Quaternary climate and pCO_2 change on C_4 plant abundance in the south-central United States. Palaeogeography Palaeoclimatology Palaeoecology 207: 331-357.

Koopman, K. F., 1982. Biogeography of the Bats of South America. Pp. 273-302 *In* Mammalian Biology in South America, *edited by* M. A. Mares and H. H. Genoways. Special Publication Series, vol. 6, Pymatuning Laboratory of Ecology, University of Pittsburgh, Linesville, PA.

Kovanen, D. J., and D. J. Easterbrook, 2002. Timing and extent of Allerød and Younger Dryas age (ca. 12,500-10,000 ^{14}C yr B.P.) oscillations of the Cordilleran Ice Sheet in the Fraser Lowland, western North America. Quaternary Research 57: 208-224.

Krantz, D. E., D. F. Williams, and D. S. Jones, 1987. Ecological and paleoenvironmental information using stable isotope profiles from living and fossil molluscs. Palaeogeography Palaeoclimatology Palaeoecology 58: 249-266.

LaBaugh, J. W., D. O. Rosenberry, and T. C. Winter, 1995. Groundwater contribution to the water and chemical budgets of Williams Lake, Minnesota, 1980-1991. Canadian Journal of Fisheries and Aquatic Sciences 52: 754-767.

Lamb, H. H., 1995. Climate history and the modern world, 2nd ed., London, Methuen, 433 Pp.

Lantry, J. R., 2001. Spatial and temporal dynamics of predation by Lake Ontario trout and salmon. M.S. thesis, State University of New York, College of Environmental Science and Forestry, Syracuse, NY.

Leder, J. J., P. K. Swart, A. M. Szmant, and R. E. Dodge, 1996. The origin of variations in the isotopic record of scleractinian corals: I. Oxygen. Geochimica et Cosmochimica Acta 15: 2857-2870.

Lee, Y.–F., and G. F. McCracken, 2002. Foraging and food resource use of Brazilian free-tailed bats, *Tadarida brasiliensis* (Molossidae). Ecoscience 9: 306-313.

Leggett, M. F., M. R. Servos, R. Hesslein, O. Johannsson, E. S. Millard, and D. G. Dixon, 1999. Biogeochemical influences on the carbon isotope signatures of Lake Ontario biota. Canadian Journal of Fisheries and Aquatic Sciences 56: 2211-2218.

Licciardi, J. M., P. U. Clark, E. J. Brook, D. Elsmore, and P. Sharma, 2004. Variable responses of western U.S. glaciers during the last deglaciation. Geology 32: 81-84.

Liem, K. F., 1980. Acquisition of energy by teleosts: adaptive mechanisms and evolutionary patterns. Pp. 299-334 *In* Environmental Physiology of Fishes, *edited by* M. A. Ali. Plenum, New York.

Lin G. H., S. L. Phillips, and J. R. Ehleringer, 1996. Monsoonal precipitation responses of shrubs in a cold desert community on the Colorado Plateau. Oecologia 106: 8-17.

Linsley, B. K., R. B. Dunbar, G. M. Wellington , and D. A. Mucciarone, 1994. A coral-based reconstruction of Intertropical Convergence Zone over Central America since 1707. Journal of Geophysical Research 99: 9977-9994.

Livingstone, D. M. and A. F. Lotter, 1998. The relationship between air and water temperatures in lakes of the Swiss Plateau: A case study with palaeolimnological implications. Journal of Paleolimnology 19: 181-198.

Lloyd, J., and G. D. Farquhar, 1994. ^{13}C discrimination during CO_2 assimilation by the terrestrial biosphere. Oecologia 99: 201-215.

Manabe, S., and R. J. Stouffer, 2000. Study of abrupt climate change by a coupled ocean-atmosphere model. Quaternary Science Reviews 19: 285-299.

Mason, D. M., A. Goyke, and S. B. Brandt, 1995. A spatially explicit bioenergetics measure of habitat quality for adult salmonines: comparison between Lakes Michigan and Ontario. Canadian Journal of Fisheries and Aquatic Sciences 52: 1572-1583.

McCombie, A. M., 1959. Some relations between air temperatures and the surface water temperature of lakes. Limnology and Oceanography 41: 252-258.

McConnaughey, T. A., J. Burdett, J. F. Whelan, and C. K. Paull, 1997. Carbon isotopes in biological carbonates: respiration and photosynthesis. Geochimica et Cosmochimica Acta 61: 611-622.

McConnaughey, T. A., J. Burdett, J. F. Whelan, and C. K. Paull, 1997. Carbon isotopes in biological carbonates: respiration and photosynthesis. Geochimica et Cosmochimica Acta 61: 611-622.

McConnaughey, T., 1989a. ^{13}C and ^{18}O isotopic disequilibrium in biological carbonates: I. Patterns. Geochimica et Cosmochimica Acta 53: 151-162.

McConnaughey, T., 1989b. ^{13}C and ^{18}O isotopic disequilibrium in biological carbonates: II. *In vitro* simulation of kinetic isotope effects. Geochimica et Cosmochimica Acta 53: 163-171.

McCullough, D. A., 1999. A review and synthesis of effects of alterations to the water temperature regime on freshwater life stages of salmonids, with special reference to chinook salmon. USEPA Report 910-R-00-010. Seattle, Washington. 279 pp.

McFarlane, D. A., and R. C. Keeler, 1990. A proxy population record for the Mexican free-tailed bat at Eagle Creek cave, Arizona. Proceedings, Symposium on Managing Wildlife in the Southwest, Wildlife Society, Tuscon, Arizona: 100-106.

McFarlane, D. A., J. Lundberg, and A. G. Fincham, 2002. A Late Quaternary paleoecological record from caves of southern Jamaica, West Indies. Journal of Cave and Karst Studies 64: 117-125.

McFarlane, D. A., R. C. Keeler, and H. Mizutani,, 1995. Ammonia volatilization in a Mexican bat cave ecosystem. Biogeochemistry 30: 1-8.

McInerny, M. C., and J. W. Held, 1995. First-year growth of seven co-occurring fish species of navigation pool 9 of the Mississippi River. Journal of Freshwater Ecology 10: 33-41.

McManus, J. F., R. Francois, J.-M. Gherardi, L. D. Keigwin, and S. Brown-Leger, 2004. Collapse and rapid resumption of Atlantic meridional circulation linked to deglacial climate changes. Nature 428: 834-837.

Merritt, D. A., and J. M. Hayes, 1994. Factors controlling precision and accuracy in isotope-ratio-monitoring mass spectrometry. Analytical Chemistry 66: 2336-2347.

Metcalfe, S. E., S. L. O'Hara, M. Caballero, and S. J. Davies, 2000. Records of late Pleistocene-Holocene climatic change in Mexico – a review. Quaternary Science Reviews 19: 699-721.

Michel, R. L. and T. F. Kraemer, 1995. Use of isotopic data to estimate water residence times of the Finger Lakes, New York. Journal of Hydrology 164: 1-18.

Mikolajawicz, U., T. J. Crowley, A. Schiller, and R. Voss, 1997. Modelling teleconnections between the North Atlantic and North Pacific during the Younger Dryas. Nature 387: 384-387.

Miller, R. F., 1991. Chitin paleoecology. Biochemical Systematics and Ecology 19: 401-411.

Miller, R. F., P. Fritz, and A. V. Morgan, 1988. Climatic implications of D/H ratios in beetle chitin. Palaeogeography Palaeoclimatology Palaeoecology 66: 277-288.

Mills, E. L., J. M. Casselman, R. Dermott, J. D. Fitzsimons, G. Gal, , K. T. Holeck, J. A. Hoyle, O. E. Johannsson, B. F. Lantry, J. C. Makarewicx, E. S. Millard, I. F. Munawar, M. Munawar, R. O'Gorman, R. W. Owens, L. G. Rudstam, T. Schaner, and T. J. Stewart, 2003. Lake Ontario: food web dynamics in a changing ecosystem (1970-2000). Canadian Journal of Fisheries and Aquatic Sciences 60: 471-490.

Mitchell D. L., D. C. Ivanova, R. Rabin, T. J. Brown, and K. Redmond, 2002. Gulf of California sea surface temperatures: mechanistic implications from observations. Journal of Climate 15: 2261-2281.

Mizutani, H., and E. Wada, 1988. Nitrogen and carbon isotope ratios in seabird rookeries and their ecological implications. Ecology 69: 340-349.

Mizutani, H., D. A. McFarlane, and Y. Kabaya, 1992a. Nitrogen and carbon isotope study of a bat guano core from Eagle Creek Cave, Arizona, USA. Mass Spectroscopy 40: 57-65.

Mizutani, H., D. A. McFarlane, and Y. Kabaya, 1992b. Carbon and nitrogen isotopic signatures of bat guanos as a record of past environments. Mass Spectroscopy 40: 67-82.

Monnin, E., A. Indermühle, J. Fluckiger, B. Stauffer, T. F. Stocker, D. Raynaud, J.-M. Barnola, 2001. Atmospheric CO_2 concentrations over the last glacial termination. Science 291: 112-114.

Motz, J. E., 2000. Oxygen and hydrogen isotopes in fossil insect chitin as paleoenvironmental indicators. Ph.D. Thesis, Waterloo, Ontario, Canada.

Nason, E. S., 1948. Morphology of hair of eastern North American bats. The American Midland Naturalist. 39: 345-361.

Nassar, J. M., H. Beck, L. Da S. L. Sternberg, and T. H. Flemming, 2003. Dependence on cacti and agaves in nectar-feeding bats from Venezuelan arid zones. Journal of Mammalogy 84: 106-116.

Naylor, R. L., R. J. Goldburg, J. H. Primavera, N. Kautsky, M. C. M. Beveridge, J. Clay, C. Folke, J. Lubchenco, H. Mooney, and M. Troell, 2000. Effect of aquaculture on world fish supplies. Nature 405: 1017-1024.

Neff, U., S. J. Burns, A. Mangini, M. Mudelsee, D. Fleitmann, and A. Matter, 2001. Strong coherence between solar variability and the monsoon in Oman between 9 and 6 kyr ago. Nature: 411: 290-293.

Neumann D., J. Borcherding and B. Jantz, 1993. Growth and seasonal reproduction of *Dreissena polymorpha* in the Rhine River and adjacent waters. Pp. 95-110 *In* Zebra Mussels: Biology, Impacts, and Control, *edited by* T.F. Nalepa and D.W. Schloesser. Lewis Publishers.

Nolf, D., 1995. Studies on fossil otoliths—the state of the art. Pp. 513-544 *In* Recent Developments in Fish Otolith Research, *edited by* D. H. Secor, J. M. Dean, and S. E. Campana. University of South Carolina, SC.

Nordt, L. C., T. W. Boutton, J. S. Jacob, and R. D. Mandel, 2002. Plant productivity and climate-CO_2 variations in South-Central Texas during the late Quaternary. Quaternary Research 58: 182-188.

O'Gorman, R., and T. J. Stewart, 1999. Ascent, dominance, and decline of the alewife in the Great Lakes: food web interactions and management strategies. Pp. 489-514 *In* Great Lakes Fisheries Policy and Management: A Binational Perspective, *edited by* W.W. Taylor and C.P. Ferreri. Michigan State University Press, East Lansing, MI.

Olson, R. A., J. D. Winter, D. C. Nettles, and J. M. Haynes, 1988. Resource partitioning in summer by salmonids in south-central Lake Ontario. Transactions of the American Fisheries Society 117: 552-559.

Overpeck, J., D. Anderson, S. Trumbore, and W. Prell, 1996. The southwest Indian Monsoon over the last 18,000 years. Climate Dynamics 12: 213-225.

Panella, G., 1980. Growth patterns in fish sagittae. Pp. 519-560 *In* Skeletal Growth of Aquatic Organisms, *edited by* D.C. Rhodes and R.A. Lutz. Plenum Press, New York, NY.

Paruelo, J. M., and W. K. Lauenroth, 1996. Relative abundance of plant functional types in grasslands and shrublands of North America. Ecological Applications 6: 1212-1224.

Patterson, W. P., 1998. North American continental seasonality during the last millennium: high-resolution analysis of sagittal otoliths. Palaeogeography Palaeoclimatology Palaeoecology 138: 271-303.

Patterson, W. P., 1999. Oldest isotopically characterized fish otoliths provide insight to Jurassic continental climate of Europe. Geology 27: 199-202.

Patterson, W. P., and G. R. Smith, 2002. Uses of fishes in analysis of paleolimnology. Pp. 173-187 *In* Tracking Environmental Change Using Lake Sediments Volume 4: Zoological Indicators, *edited by* J. P. Smol, J. J. B. Birks, and W. M. Last. Kluwer.

Patterson, W. P., G. R. Smith, and K. C. Lohmann, 1993. Continental paleothermometry and seasonality using the isotopic composition of aragonitic otoliths of freshwater fishes. Pp. 191-202 *In* Continental Climate Change from Isotopic Records, *edited by* P. Swart, K. C. Lohmann, J. McKenzie and S. Savin. American Geophysical Union Monograph 78.

Peñuelas, J., and J. Azcón-Bieto, 1992. Changes in leaf $\Delta^{13}C$ of herbarium plant species during the past 3 centuries of CO_2 increase. Plant, Cell and Environment 15: 485-489.

Peteet, D., 1995. Global Younger Dryas? Quaternary International 28: 93-104.

Peteet, D., 1995. Global Younger Dryas? Quaternary International 28: 93-104.

Phillips, F. M., L. A. Peeters, M. K. Tansey, and S. N. Davis, 1986. Paleoclimatic inferences from an isotopic investigation of groundwater in the central San Juan basin, New Mexico. Quaternary Research 26: 179-193.

Poore, R. Z., M. J. Pavich, and H. D. Grissino-Mayer, 2005. Record of the North American southwest monsoon from Gulf of Mexico sediment cores. Geology 33: 209-212.

Post, J. R., and J. A. Lee. Metabolic ontogeny of teleost fishes. Canadian Journal of Fisheries and Aquatic Sciences 53: 910-923.

Poulick, M., G. Goffinet, M. F. Voss-Foucart, J. C. Bussers, M. F. Jaspar-Versali, and C. Toussaint. Chitin degradation in natural environments (mollusk shells and crab carapaces). Pp. 547-550 *In* Chitin in Nature and Technology, *edited by* R. A. A. Muzzarelli, C. Jeuniauz and G. W. Gooday. Plenum Press, New York.

Quay, P. D., S. R. Emerson, B. M. Quay, and A. H. Devol, 1986. The carbon cycle for Lake Washington—A stable isotope study. Limnology and Oceanography 31: 596-611.

Radtke, R. L., W. Showers, E. Moksness, and P. Lenz, 1996. Environmental information stored in otoliths: insights from stable isotopes. Marine Biology 127: 161-170.

Rahimpour-Bonab, H., Y. Bone and R. Moussavi-Harami, 1997. Stable isotope aspects of modern molluscs, brachiopods, and marine cements from cool-water carbonates, Lacepede Shelf, South Australia. Geochimica et Cosmochimica Acta 61: 207-218.

Rahmstorf, S., 2002. Ocean circulation and climate during the past 120,000 years. Nature 419: 207-213.

Rand, P. S., and D. J. Stewart, 1998a. Dynamics of salmonine diets and foraging in Lake Ontario, 1983-1993: a test of a bioenergetic model prediction. Canadian Journal of Fisheries and Aquatic Sciences 55: 307-317.

Rand, P. S., and D. J. Stewart, 1998b. Prey fish exploitation, salmonine production, and pelagic food web efficiency in Lake Ontario. Canadian Journal of Fisheries and Aquatic Sciences 55: 318-327.

Rand, P. S., B. F. Lantry, R. O'Gorman, R. W. Owens, and D. J. Stewart, 1994. Energy density and size of pelagic prey fishes in Lake Ontario: implications for salmonine energetics. Transactions of the American Fisheries Society 123: 519-534.

Rand, P. S., D. J. Stewart, P. W. Seelbach, M. L. Jones, and L. R. Wedge, 1993. Modeling steelhead population energetics in Lakes Michigan and Ontario. Transactions of the American Fisheries Society 122: 977-1001.

Reimer, P. J., M. G. L Baillie, E. Bard, A. Bayliss, J. W. Beck, C. Bertrand, P. G. Blackwell, C. E. Buck, G. Burr, K. B. Cutler, P. E. Damon, R. L. Edwards, R. G. Fairbanks, M. Friedrich, T. P. Guilderson, K. A. Hughen, B. Kromer, F. G. McCormac, S. Manning, C. Bronk Ramsey, R.W. Reimer, S. Remmele, J. R. Southon, M. Stuiver, S. Talamo, F. W. Taylor, J. van der Plicht, and C. E. Weyhenmeyer, 2004. IntCal04 Terrestrial radiocarbon age calibration, 26 - 0 ka BP. Radiocarbon 46, 1029-1058.

Renssen, H., B. van Geel, J. van der Plicht, and M. Magny, 2000. Reduced solar activity as a trigger for the start of the Younger Dryas? Quaternary International 68-71: 373-383.

Renssen, J., R. F. B. Isarin, J. Vandenberghe, Workshop participants, 2001. Global and Planetary Change 30: 155-165.

Rhode, D., 2001. Packrat middens as a tool for reconstructing historic ecosystems. Pp. 257-294 *In* The Historical Ecology Handbook : A Restorationist's Guide to Reference Ecosystems, *edited by* D. Egan and E. A. Howell. Island Press, Washington, D.C.

Roden, J. S., G. Lin, and J. R. Ehleringer, 2000. A mechanistic model for interpretation of hydrogen and oxygen ratios in tree-ring cellulose. Geochimica et Cosmochimica Acta 64: 21-35.

Romaneck, C. S., E. L. Grossman and J. W. Morse, 1992. Carbon isotopic fractionation in synthetic aragonite and calcite: Effects of temperature and precipitation rate. Geochimica et Cosmochimica Acta 56: 419-430.

Rowan, D. J., and J. B. Rasmussen, 1996. Measuring the bioenergetic cost of fish activity *in situ* using a globally dispersed radiotracer (^{137}Cs). Canadian Journal of Fisheries and Aquatic Sciences 54: 734-745.

Rozanski, K., L. Araguas-Araguas, and R. Gonfiantini, 1993. Isotopic patterns in modern global precipitation. Pp. 1-36 *In* Continental Climate Change from Isotopic Records, *edited by* P. Swart, K.C Lohmann, J. McKenzie, and S. Savin. American Geophysical Union Monograph 78.

Rundel, P. W., J. R. Ehleringer, and K. A. Nagy, 1989. Stable isotopes in ecological research; Springer-Verlag: New York.

Sanzone, D. M., J. L. Meyer, E. Marti, E. P. Gardiner, J. L. Tank, and N. B. Grimm, 2003. Carbon and nitrogen transfer from a desert stream to riparian predators. Oecologia 134: 238-250.

Schaeffer, J. S., R. C. Haas, J. S. Diana, and J. E. Breck, 1999. Field test of two energetic models for yellow perch. Transactions of the American Fisheries Society 128: 414-435.

Schiller, A., U. Mikolajewicz, and R. Voss, 1997. The stability of the North Atlantic thermohaline circulation in a couple ocean-atmosphere general circulation model. Climate Dynamics 13: 325-347.

Schimmelmann , A., and R. F. Miller, 2002. Review of methods for the determination of deuterium/hydrogen stable isotope ratios in chitin. Pp. 469-474 *In* Chitosan in Pharmacy and Chemistry, *edited by* R. A. A. Muzzarelli and C. Muzzarelli. Atec Edizioni, Italy.

Schimmelmann, A., 1991. Determination of the concentration and stable isotopic composition of nonexchangeable hydrogen in organic matter. Analytical Chemistry 63: 2456-2459.

Schimmelmann, A., and M. J. DeNiro, 1986a. Stable isotopic studies on chitin. Measurements on chitin/chitosan isolates and D-glucosamine hydrochloride from chitin. Pp. 357-364 *In* Chitin in Nature and Technology, *edited by* R. A. A. Muzzarelli, C. Jeuniauz and G. W. Gooday. Plenum Press, New York.

Schimmelmann, A., and M. J. DeNiro, 1986b. Stable isotopic studies on chitin III. The $^{18}O/^{16}O$ and D/H ratios in arthropod chitin. Geochimica et Cosmochimica Acta 50: 1485-1496.

Schimmelmann, A., M. J. DeNiro, M. Poulicek, M.-F. Voss-Foucart, G. Goffinet, and C. Jeuniaux, 1986. Isotopic composition of chitin from arthropods recovered in archaeological contexts as palaeoenvironmental indicators. Journal of Archaeological Science 13: 553-566.

Schimmelmann, A., R. Miller, and S. Leavitt, 1993. Hydrogen isotopic exchange and stable isotope ratios in cellulose, wood, chitin, and amino compounds. Pp. 367-374 *In* Continental Climate Change from Isotopic Records, *edited by* P. Swart, K. C. Lohmann, J. McKenzie, and S. Savin . American Geophysical Union Monograph 78.

Schimmelmann, A., R. P. Wintsch, M. D. Lewan, and M. J. DeNiro, 1998. Chitin: 'Forgotten' Source of Nitrogen—From modern chitin to thermally mature kerogen: lessons from nitrogen isotope ratios. Nitrogen-containing macromolecules in the biosphere-geosphere ACS Symposium series 707: 226-242.

Schwarcz, H. P., Y. Gao, S. Campana, D. Browne, M. Knyf, and U. Brand, 1998. Stable carbon isotope variations in otoliths of Atlantic cod (*Gadus morhua*). Canadian Journal of Fisheries and Aquatic Sciences 55: 1798-1806.

Schwinning, S., B. I. Starr, and J. R. Ehleringer, 2003. Dominant cold desert plants do not partition warm season precipitation by event size. Oecologia 136: 252-260.

Schwinning, S., K. Davis, L. Richardson, and J. R. Ehleringer, 2002. Dueterium enriched irrigation indicates different forms of rain use in shrub/grass species of the Colorado Plateau. Oeocologia 130: 345-355.

Sealy, J. C., N. J. van der Merwe, J. A., Lee Thorp, and J. L. Lanham, 1987. Nitrogen isotopic ecology in southern Africa: Implications for environmental and dietary tracing. Geochimica et Cosmochimica Acta 51: 2707-2717.

Shahack-Gross, R., F. Berna, P. Karkanas, S. Weiner, 2004. Bat guano and preservation of archaeological remains in cave sites. Journal of Archaeological Sciences 31: 1259-1272.

Sheppard P. R., A. C. Comrie, G. D. Packin, K. Angersbach, M. K. Hughes, 2002. The climate of the US southwest. Climate Research 21: 219-238.

Sherwood, G. D., and G. A. Rose, 2003. Influence of swimming form on otolith $\delta^{13}C$ in marine fish. Marine Ecology Progress Series 258: 283-289.

Smith, G. R. and W. P. Patterson, 1994. Mio-Pliocene seasonality on the Snake River plain: comparison of faunal and oxygen isotopic evidence. Palaeogeography Palaeoclimatology Palaeoecology 107: 291-302.

Smith, H. J., H. Fischer, M. Wahlen, D. Mastroianni, and B. Deck, 1999. Dual Modes of the carbon cycle since the Last Glacial Maximum. Nature 400: 248-250.

Smith, K. F., Z. D. Sharp, and J. H. Brown, 2002. Isotopic composition of carbon and oxygen in desert fauna: investigations into the effects of diet, physiology, and seasonality. Journal of Arid Environments 52: 419-430.

Sponheimer, M., T. Robinson, L. Ayliffe, B. Passey, B. Roeder, L. Shipley, E. Lopez, T. Cerling, D. Dearing, and J. Ehleringer, 2003. An experimental study of carbon-isotope fractionation between diet, hair, and feces of mammalian herbivores. Canadian Journal of Zoology 81: 871-876.

Stankiewicz, B. A., D. E. G. Briggs, R. P. Evershed, M. B. Flannery, and M. Wuttke, 1997. Preservation of chitin in 25 million-year-old fossils. Science 276: 1541-1543.

Stankiewicz, B. A., M. Masterlerz, C. H. J. Hof, A. Bierstedt, M. B. Flannery, D. E. G. Briggs, and R. P. Evershed, 1998. Biodegradation of the chitin-protein complex in crustacean cuticles. Organic Geochemistry 28: 67-76.

Stapp, P., and G. A. Polis, 2003. Marine resources subsidize insular rodent populations in the Gulf of California, Mexico. Oecologia 134: 496-504.

Stapp, P., G. A. Polis, and F. Sánchez Piñero, 1999. Stable isotopes reveal strong marine and El Niño effects on island food webs. Nature 401: 467-469.

Steuber, T., 1996. Stable isotope sclerochronology of rudist bivalves: Growth rates and late Cretaceous seasonality. Geology 24: 315-318.

Stewart, D. J., and M. Ibarra, 1991. Predation and production by salmonine fishes in Lake Michigan, 1978-1988. Canadian Journal of Fisheries and Aquatic Sciences 48: 909-922.

Stewart, D. J., D. Weininger, D. V. Rottiers, and T. A. Edsall, 1983. An energetics model for lake trout, *Salvelinus namaycusch*: application to the Lake Michigan population. Canadian Journal of Fisheries and Aquatic Sciences 40: 1647-1666.

Stewart, T. J., D. G. Robertson, 1991. Lake Ontario temperature studies. Ontario Ministry of Natural Resources, Lake Ontario Fisheries Unit 1990 Annual Report, LOA 91.1 20: 1-5.

Stewart, T. J., J. N. Bowlby, M. Rawson, and T. H. Eckert, 2003. The recreational boat fishery for salmonids in Lake Ontario 1985-1995. Pp. 517-537 *In* State of Lake Ontario: Past, Present and Future, *edited by* M. Munawar. Aquatic Ecosystem Health and Management Society. Goodword Books Pvt. Ltd., New Delhi.

Stuiver, M., and P. J. Reimer, 1993. Extended ^{14}C data-base and revised Calib 3.0 ^{14}C age calibration program. Radiocarbon 35: 215-230.

Stuiver, M., P. J. Reimer, E. Bard, J. W. Beck, G. S. Burr, K. A. Hughen, B. Kromer, F. G. McCormac, J. van der Plicht, and M. Spurk, 1998. INTCAL98 Radiocarbon age calibration 24,000 - 0 cal BP. Radiocarbon 40: 1041-1083.

Stuiver, M., P. M. Grootes, and T. F. Braziunas, 1995. The GISP2 ^{18}O climate record of the past 16,500 years and the role of the sun, ocean and volcanoes. Quaternary Research 44: 341-354.

Stute, M., J. F. Clark, P. Schlosser, W. S. Broecker, and G. Bonani, 1995. A 30,000 yr continental paleotemperature record derived from noble gases dissolved in groundwater from the San Juan Basin, New Mexico. Quaternary Research 43: 209-220.

Stute, M., P. Schlosser, J. F. Clark, W. S. Broecker, 1992. Paleotemperatures in the southwestern United States derived from noble gasses in ground water. Science 256: 1000-1003.

Talhelm, D. R., 1988. Economics of Great Lakes fisheries: a 1985 assessment. Great Lakes Fish. Comm. Tech. Rep. No. 54, Ann Arbor, MI.

Tanaka, N., M. C. Monaghan and D. M. Rye, 1986. Contribution of metabolic carbon to mollusc and barnacle shell carbonate. Nature 320: 520-523.

Tarutani, T., R. N. Clayton and T. K. Mayeda, 1969. The effect of polymorphism and magnesium on oxygen isotope fractionation between calcium carbonate and water. Geochimica et Cosmochimica Acta 33: 987-996.

Taylor, K. C., P. A. Mayewski, R. B. Alley, E. J. Brook, A. J. Gow, P. M. Grootes, D. A. Meese, E. S. Saltzman, J. P. Severinghaus, M. S. Twickler, J. W. C. White, S. Whitlow, and G. A. Zielinski, 1997. The Holocene-Younger Dryas transition recorded at Summit, Greenland. Science: 825-827.

Teller, J. T., D. W. Leverington, and J. D. Mann, 2002. Freshwater outbursts to the oceans from glacial Lake Agassiz and their role in climate change during the last deglaciation. Quaternary Science Reviews 21: 879-887.

Tevesz, M. J. S., E. Barrera and S. F. Schwelgien, 1996. Seasonal variation in oxygen isotope composition of two freshwater bivalves: *Sphaerium striatinum* and *Anodonta grandis*. Journal of Great Lakes Research 22: 906-916.

Thompson, R. S., C. Whitlock, P. J. Bartlein, S. P. Harrison, and W. G. Spaulding, 1993. Climatic Changes in the Western United States since 18,000 yr B. P. Pp. 468-513 *In* Global Climates Since the Last Glacial Maximum, *edited by* H. E. Wright, J. E. Kutzbach, T. Webb III, W. F. Ruddiman, F. A. Street-Perrott, and P. J. Bartlein. University of Minnesota Press, Minneapolis.

Thornton, K. W., and A. S. Lessem. 1978. A temperature algorithm for modifying biological rates. Transactions of the American Fisheries Society 107: 284-287.

Thorrold, S. R., and J. A. Hare, 2002. Otolith applications in reef fish ecology. Pp. 243-264 *In* Coral Reef Fishes. Dynamics and Diversity in a Complex Ecosystem, *edited by* P.F. Sale. Academic Press, London, U.K.

Thorrold, S. R., S. E. Campana, C. M. Jones, and P. K. Swart, 1997. Factors determining ^{13}C and ^{18}O fractionation in aragonitic otoliths of marine fish. Geochimica et Cosmochimica Acta 61: 2909-2919.

Tieszen, L. L., B. C. Reed, N. B. Bliss, B. K. Wylie, and D. D. DeJong, 1997. NDVI, C_3 and C_4 production, and distributions in Great Plains grassland land cover classes. Ecological Applications 7: 59-78.

Tieszen, L. L., T. W. Boutton, K. G. Tesdahl, and N. A. Slade, 1983. Fractionation and turnover of stable carbon isotopes in animal tissues: implications for $\delta^{13}C$ analysis of diet. Oecologia 57: 32-37.

Tohse, H., and Y. Mugiya, 2002. Diel variations in carbonate incorporation into otoliths in goldfish. Journal of Fish Biology 61: 199-206.

Tolimieri, N., and P. Levin, 2004. Differences in responses of chinook salmon to climate shifts: implications for conservation. Environmental Biology of Fishes 70: 155-167.

Tripp, J. A., T. F. G. Higham, and R. E. M. Hedges, 2004. A pretreatment procedure for the AMS radiocarbon dating of sub-fossil insect remains. Radiocarbon 46: 147-154.

Trudel, M., D. R. Geist, and D. W. Welch, 2004. Modeling the oxygen consumption rates in Pacific salmon and steelhead: an assessment of current models and practices. Transactions of the American Fisheries Society 133: 326-348.

Urey, H. C., 1947. The thermodynamic properties of isotopic substances. Journal of the Chemical Society: 562-581.

Urey, H. C., H. A. Lowenstam, S. Epstein, and C. R. McKinney, 1951. Measurement of paleotemperatures and temperatures of the Upper Cretaceous of England, Denmark, and the southeastern United States. Bulletin of the Geological Society of America 62: 399-416.

Ursin, E., 1979. Principles of growth in fishes. Symposia of the Zoological Society of London 44: 63-87.

Van de Water, P. K., S. W. Leavitt, and J. L. Betancourt, 2002. Leaf $\delta^{13}C$ variability with elevation, slope aspect, and precipitation in the southwest United States. Oecologia: 132: 332-343.

Van Devender, T. R., and W. G. Spaulding, 1979. Development of vegetation and climate in the southwestern United States. Science 204: 701-710.

Vannote, R. L., G. W. Minshall, K. W. Cummins, J. R. Sedell, and C. E. Cushing, 1980. The river continuum concept. Canadian Journal of Fisheries and Aquatic Sciences 37: 130-137.

Veinott, G. I. and R. J. Cornett, 1996. Identification of annually produced opaque bands in the shell of the freshwater mussel *Elliptio complananta* using the seasonal cycle of $\delta^{18}O$. Canadian Journal of Fisheries and Aquatic Sciences 53: 372-379.

Veinott, G. I., and R. J. Cornett. 1998. Carbon isotopic disequilibrium in the shell of the freshwater mussel *Elliptio complanata*. Applied Geochemistry 13: 49-57.

von Bertalanffy, L., 1938. A quantitative theory of organic growth (inquiries on growth laws, II). Human Biology 10: 181-213.

von Grafenstein, U., H. Erlernkeuser, and P. Trimborn, 1999. Oxygen and carbon isotopes in modern fresh-water ostracod valves: assessing vital offsets and autecological effects of interest for palaeoclimate studies. Palaeogeography Palaeoclimatology Palaeoecology 148: 133-152.

Wahl, D. H., K. Bruner, and L. A. Nielson, 1988. Trophic ecology of freshwater drum in large rivers. Journal of Freshwater Ecology 4: 483-491.

Wang, G., and D. Schimel, 2003. Climate change, climate modes, and climate impacts. Annual Review of Environment and Resources 28: 1-28.

Wang, X., and J. Veizer, 2000. Respiration/photosynthesis balance of terrestrial aquatic ecosystems, Ottawa area, Canada. Geochimica et Cosmochimica Acta 64: 3777-3786.

Wassenaar, L. I., and K. A. Hobson, 2000. Improved method for determining the stable-hydrogen isotopic composition (δD) of complex organic materials of environmental interest. Environmental Science and Technology 34: 2354-2360.

Wassenaar, L. I., and K. A. Hobson, 2003. Comparative equilibration and online technique for determination of non-exchangeable hydrogen of keratins for use in animal migration studies. Isotopes in Environmental and Health Studies 39: 211-217.

Webb, M. S., 1974. Surface temperatures of Lake Erie. Water Resources Research 10: 199-210.

Webb, S. C., R. E. M. Hedges, and S. J. Simpson, 1998. Diet quality influences the $\delta^{13}C$ and $\delta^{15}N$ of locusts and their biochemical components. The Journal of Experimental Biology 201: 2903-2911.

Wefer, G. and W. H. Berger, 1991. Isotope paleontology: growth and composition of extant calcareous species. Marine Geology 100: 207-248.

Weidman, C. R., and R. Millner, 2000. High-resolution stable isotope records from North Atlantic cod. Fisheries Research 46: 327-342.

Whitledge, G. W., and C. F. Rabeni, 1997. Energy sources and ecological role of crayfishes in an Ozark stream: insights from stable isotopes and gut analysis. Canadian Journal of Fisheries and Aquatic Sciences 54: 2555-2563.

Wilkins, K. T., 1989. *Tadarida brasiliensis*. Mammalian Species 331: 1-10.

Wright, P. J., 1991. The influence of metabolic rate on otolith increment width in Atlantic salmon parr, *Salmo salar* L. Journal of Fish Biology 38: 929-933.

Wright, W. E., A. Long, A. C. Comrie, S. W. Leavitt, T. Cavazos, and C. Eastoe, 2001. Monsoonal moisture sources revealed using temperature, precipitation, and precipitation stable isotope timeseries. Geophysical research letters 28: 787-790.

Wurster, C. M., and W. P. Patterson, 2001. Late Holocene climate change for the eastern interior United States: evidence from high-resolution sagittal otolith stable isotope ratios of oxygen. Palaeogeography Palaeoclimatology Palaeoecology 170: 81-100.

Wurster, C. M., and W. P. Patterson, 2003. Metabolic rate of late Holocene freshwater fish: evidence from $\delta^{13}C$ values of otoliths. Paleobiology 29: 492-505.

Wurster, C. M., W. P. Patterson, and M. M. Cheatham, 1999. Advances in micromilling techniques: A new apparatus for acquiring high-resolution oxygen and carbon stable

isotope values and major/minor elemental ratios from accretionary carbonate. Computers and Geosciences 25: 1155-1162.

Xia, J., B. J. Haskell, D. R. Engstrom and E. Ito, 1997. Holocene climate reconstructions from tandem trace-element and stable-isotope composition of ostracodes from Coldwater Lake, North Dakota, USA. Journal of Paleolimnology 17: 85-100.

Yang, C., K. Telmer, and J. Viezer, 1996. Chemical dynamics of the St. Lawrence riverine system: $\delta D_{(H_2O)}$, $\delta^{18}O_{(H_2O)}$, $\delta^{13}C_{(DIC)}$, $\delta^{34}S_{(sulfate)}$, and dissolved $^{87}Sr/^{86}Sr$. Geochimica et Cosmochimica Acta 59: 1107-1146.

Yaun, D., H. Cheng, R. L. Edwards, C. A. Dykoski, M. J. Kelly, M. Zhang, J. Qing, Y. Lin, Y. Wang, J. Wu, J. A. Dorale, Z. An, and Y. Cai, 2004. Timing, duration, and transitions of the last interglacial Asian monsoon. Science 304: 575-578.

Yoshioka, T., E. Wada, and H. Hayashi, 1994. A stable isotope study on seasonal food web dynamics in a eutrophic lake. Ecology 75: 835-846.

Appendix A. Tabulated data incorporated in chapters

Table A1—Tabulated data utilized in chapter 2.
$\delta^{13}C$ and $\delta^{18}O$ values of shell carbonate from *Sphaerium simile* captured in Science Lake and *Dreissena polymorpha* captured in Keuka Lake. SN indicates Sample Number. Calculated distance from umbo is determined from digital coordinates used for sampling.

Calculated Distance from Umbo	SN	Species	Location	$\delta^{13}C$ ‰ VPDB	±	$\delta^{18}O$ ‰ VPDB	±
13.133	1	*S. simile*	SCIENCE L.	-8.2	0.01	-9.4	0.04
13.109	2	*S. simile*	SCIENCE L.	-8.2	0.02	-9.0	0.08
13.085	3	*S. simile*	SCIENCE L.	-8.1	0.03	-9.3	0.03
13.061	4	*S. simile*	SCIENCE L.	-8.1	0.00	-9.5	0.02
13.037	5	*S. simile*	SCIENCE L.	-8.0	0.02	-9.9	0.02
13.013	6	*S. simile*	SCIENCE L.	-8.2	0.01	-9.7	0.03
12.989	7	*S. simile*	SCIENCE L.	-8.1	0.01	-9.8	0.02
12.965	8	*S. simile*	SCIENCE L.	-8.2	0.02	-10.0	0.02
12.941	9	*S. simile*	SCIENCE L.	-7.9	0.01	-9.3	0.02
12.917	10	*S. simile*	SCIENCE L.	-8.1	0.01	-9.9	0.03
12.893	11	*S. simile*	SCIENCE L.	-8.1	0.02	-9.7	0.06
12.869	12	*S. simile*	SCIENCE L.	-8.1	0.03	-9.8	0.03
12.845	13	*S. simile*	SCIENCE L.	-8.1	0.02	-9.8	0.03
12.821	14	*S. simile*	SCIENCE L.	-8.4	0.02	-10.0	0.03
12.797	15	*S. simile*	SCIENCE L.	-8.2	0.02	-9.7	0.03
12.773	16	*S. simile*	SCIENCE L.	-8.2	0.03	-9.8	0.04
12.749	17	*S. simile*	SCIENCE L.	-8.4	0.01	-9.8	0.03
12.725	18	*S. simile*	SCIENCE L.	-8.4	0.01	-10.1	0.03
12.701	19	*S. simile*	SCIENCE L.	-8.2	0.01	-9.9	0.03
12.677	20	*S. simile*	SCIENCE L.	-8.1	0.01	-10.0	0.03
12.653	21	*S. simile*	SCIENCE L.	-8.2	0.02	-9.8	0.03
12.629	22	*S. simile*	SCIENCE L.	-8.3	0.01	-9.9	0.01
12.605	23	*S. simile*	SCIENCE L.	-8.1	0.01	-9.8	0.01
12.581	24	*S. simile*	SCIENCE L.	-8.1	0.01	-9.9	0.01
12.533	26	*S. simile*	SCIENCE L.	-8.2	0.01	-9.6	0.02
12.509	27	*S. simile*	SCIENCE L.	-7.5	0.01	-9.3	0.02
12.485	28	*S. simile*	SCIENCE L.	-8.3	0.01	-9.7	0.02
12.461	29	*S. simile*	SCIENCE L.	-8.0	0.01	-9.6	0.04

Calculated Distance from Umbo	SN	Species	Location	δ^{13}C ‰ VPDB	±	δ^{18}O ‰ VPDB	±
12.437	30	*S. simile*	SCIENCE L.	-8.0	0.01	-9.4	0.02
12.413	31	*S. simile*	SCIENCE L.	-8.1	0.01	-9.6	0.04
12.389	32	*S. simile*	SCIENCE L.	-8.3	0.01	-9.8	0.03
12.365	33	*S. simile*	SCIENCE L.	-8.0	0.01	-9.5	0.02
12.341	34	*S. simile*	SCIENCE L.	-8.2	0.01	-9.7	0.02
12.317	35	*S. simile*	SCIENCE L.	-8.0	0.01	-8.8	0.04
12.293	36	*S. simile*	SCIENCE L.	-8.2	0.02	-9.9	0.03
12.269	37	*S. simile*	SCIENCE L.	-8.3	0.02	-9.9	0.02
12.245	38	*S. simile*	SCIENCE L.	-8.4	0.01	-9.9	0.02
12.221	39	*S. simile*	SCIENCE L.	-8.1	0.01	-9.4	0.05
12.197	40	*S. simile*	SCIENCE L.	-8.5	0.02	-10.1	0.07
12.173	41	*S. simile*	SCIENCE L.	-8.3	0.01	-10.0	0.03
12.149	42	*S. simile*	SCIENCE L.	-8.4	0.00	-9.9	0.03
12.125	43	*S. simile*	SCIENCE L.	-8.4	0.02	-9.5	0.04
12.101	44	*S. simile*	SCIENCE L.	-8.6	0.01	-10.1	0.05
12.053	46	*S. simile*	SCIENCE L.	-8.4	0.01	-9.7	0.03
12.029	47	*S. simile*	SCIENCE L.	-8.7	0.02	-10.2	0.01
12.005	48	*S. simile*	SCIENCE L.	-8.6	0.00	-10.1	0.02
11.981	49	*S. simile*	SCIENCE L.	-8.6	0.01	-9.9	0.01
11.957	50	*S. simile*	SCIENCE L.	-8.5	0.02	-10.0	0.04
11.933	51	*S. simile*	SCIENCE L.	-8.9	0.01	-10.2	0.03
11.909	52	*S. simile*	SCIENCE L.	-8.7	0.01	-10.0	0.01
11.885	53	*S. simile*	SCIENCE L.	-8.8	0.02	-10.2	0.03
11.861	54	*S. simile*	SCIENCE L.	-8.8	0.01	-10.3	0.03
11.837	55	*S. simile*	SCIENCE L.	-9.4	0.01	-10.5	0.03
11.813	56	*S. simile*	SCIENCE L.	-8.9	0.02	-10.2	0.06
11.789	57	*S. simile*	SCIENCE L.	-9.5	0.03	-10.6	0.03
11.765	58	*S. simile*	SCIENCE L.	-8.9	0.01	-10.2	0.01
11.741	59	*S. simile*	SCIENCE L.	-9.1	0.02	-10.2	0.04
11.717	60	*S. simile*	SCIENCE L.	-9.4	0.02	-10.5	0.02
11.693	61	*S. simile*	SCIENCE L.	-9.6	0.02	-10.6	0.05
11.669	62	*S. simile*	SCIENCE L.	-9.5	0.02	-10.5	0.02
11.645	63	*S. simile*	SCIENCE L.	-9.4	0.01	-10.2	0.03
11.621	64	*S. simile*	SCIENCE L.	-9.5	0.01	-10.4	0.02
11.597	65	*S. simile*	SCIENCE L.	-9.8	0.01	-10.7	0.01
11.573	66	*S. simile*	SCIENCE L.	-9.3	0.01	-10.5	0.02
11.549	67	*S. simile*	SCIENCE L.	-9.8	0.01	-10.7	0.03
11.501	69	*S. simile*	SCIENCE L.	-9.8	0.01	-10.8	0.01

Calculated Distance from Umbo	SN	Species	Location	δ^{13}C ‰ VPDB	±	δ^{18}O ‰ VPDB	±
11.477	70	*S. simile*	SCIENCE L.	-9.5	0.03	-10.6	0.06
11.429	72	*S. simile*	SCIENCE L.	-9.8	0.00	-10.3	0.02
11.405	73	*S. simile*	SCIENCE L.	-9.7	0.01	-10.8	0.02
11.357	75	*S. simile*	SCIENCE L.	-9.8	0.01	-10.4	0.02
11.309	77	*S. simile*	SCIENCE L.	-9.9	0.01	-11.0	0.04
11.213	81	*S. simile*	SCIENCE L.	-9.8	0.01	-10.9	0.04
11.189	82	*S. simile*	SCIENCE L.	-9.7	0.01	-10.1	0.01
11.093	86	*S. simile*	SCIENCE L.	-9.7	0.01	-10.8	0.02
11.021	89	*S. simile*	SCIENCE L.	-9.8	0.03	-10.4	0.04
10.997	90	*S. simile*	SCIENCE L.	-9.8	0.03	-10.9	0.03
10.973	91	*S. simile*	SCIENCE L.	-10.4	0.01	-10.7	0.06
10.949	92	*S. simile*	SCIENCE L.	-9.9	0.02	-10.8	0.05
10.925	93	*S. simile*	SCIENCE L.	-10.3	0.02	-11.2	0.02
10.901	94	*S. simile*	SCIENCE L.	-10.3	0.02	-11.2	0.05
10.877	95	*S. simile*	SCIENCE L.	-10.3	0.01	-11.1	0.02
10.853	96	*S. simile*	SCIENCE L.	-10.3	0.02	-10.7	0.03
10.829	97	*S. simile*	SCIENCE L.	-10.7	0.01	-10.8	0.05
10.805	98	*S. simile*	SCIENCE L.	-11.0	0.01	-10.8	0.04
10.781	99	*S. simile*	SCIENCE L.	-10.9	0.01	-10.8	0.02
10.658	103	*S. simile*	SCIENCE L.	-10.8	0.01	-10.3	0.02
10.625	104	*S. simile*	SCIENCE L.	-10.5	0.02	-9.9	0.04
10.592	105	*S. simile*	SCIENCE L.	-10.1	0.01	-9.4	0.01
10.526	107	*S. simile*	SCIENCE L.	-11.1	0.01	-10.3	0.02
10.493	108	*S. simile*	SCIENCE L.	-10.7	0.01	-9.9	0.04
10.427	110	*S. simile*	SCIENCE L.	-10.4	0.01	-9.8	0.03
10.394	111	*S. simile*	SCIENCE L.	-10.1	0.03	-9.6	0.01
10.361	112	*S. simile*	SCIENCE L.	-10.2	0.02	-9.2	0.02
10.328	113	*S. simile*	SCIENCE L.	-10.2	0.02	-9.6	0.03
10.295	114	*S. simile*	SCIENCE L.	-10.1	0.01	-9.1	0.03
10.262	115	*S. simile*	SCIENCE L.	-10.0	0.01	-9.5	0.03
10.229	116	*S. simile*	SCIENCE L.	-10.1	0.02	-9.7	0.02
10.196	117	*S. simile*	SCIENCE L.	-9.6	0.02	-8.6	0.06
10.163	118	*S. simile*	SCIENCE L.	-9.8	0.01	-9.2	0.01
10.130	119	*S. simile*	SCIENCE L.	-9.7	0.02	-9.3	0.03
10.097	120	*S. simile*	SCIENCE L.	-9.7	0.02	-9.2	0.03
10.064	121	*S. simile*	SCIENCE L.	-9.2	0.01	-9.0	0.02
10.031	122	*S. simile*	SCIENCE L.	-9.6	0.01	-8.8	0.02
9.998	123	*S. simile*	SCIENCE L.	-9.2	0.02	-8.9	0.02

Calculated Distance from Umbo	SN	Species	Location	$\delta^{13}C$ ‰ VPDB	±	$\delta^{18}O$ ‰ VPDB	±
9.965	124	*S. simile*	SCIENCE L.	-9.2	0.03	-8.8	0.03
9.932	125	*S. simile*	SCIENCE L.	-9.0	0.02	-9.1	0.02
9.899	126	*S. simile*	SCIENCE L.	-8.7	0.02	-9.0	0.00
9.866	127	*S. simile*	SCIENCE L.	-8.8	0.01	-8.8	0.02
9.833	128	*S. simile*	SCIENCE L.	-8.8	0.01	-8.8	0.04
9.800	129	*S. simile*	SCIENCE L.	-8.8	0.03	-8.8	0.02
9.767	130	*S. simile*	SCIENCE L.	-8.7	0.02	-9.0	0.03
9.734	131	*S. simile*	SCIENCE L.	-8.6	0.01	-8.9	0.03
9.701	132	*S. simile*	SCIENCE L.	-8.6	0.02	-8.7	0.02
9.668	133	*S. simile*	SCIENCE L.	-8.8	0.03	-8.9	0.04
9.635	134	*S. simile*	SCIENCE L.	-8.4	0.02	-9.0	0.04
9.602	135	*S. simile*	SCIENCE L.	-8.4	0.01	-9.0	0.02
9.569	136	*S. simile*	SCIENCE L.	-8.4	0.01	-8.9	0.01
9.536	137	*S. simile*	SCIENCE L.	-8.4	0.01	-8.7	0.05
9.503	138	*S. simile*	SCIENCE L.	-8.3	0.02	-8.9	0.02
9.470	139	*S. simile*	SCIENCE L.	-8.4	0.01	-9.0	0.03
9.437	140	*S. simile*	SCIENCE L.	-8.2	0.01	-8.9	0.03
9.404	141	*S. simile*	SCIENCE L.	-8.2	0.02	-8.9	0.04
9.371	142	*S. simile*	SCIENCE L.	-8.1	0.02	-8.8	0.02
9.338	143	*S. simile*	SCIENCE L.	-8.0	0.02	-9.2	0.01
9.305	144	*S. simile*	SCIENCE L.	-8.1	0.03	-9.2	0.03
9.272	145	*S. simile*	SCIENCE L.	-7.9	0.01	-9.0	0.04
9.239	146	*S. simile*	SCIENCE L.	-7.5	0.01	-8.8	0.04
9.206	147	*S. simile*	SCIENCE L.	-7.9	0.02	-8.8	0.03
9.173	148	*S. simile*	SCIENCE L.	-7.8	0.01	-9.4	0.04
9.140	149	*S. simile*	SCIENCE L.	-7.8	0.02	-9.5	0.02
9.107	150	*S. simile*	SCIENCE L.	-7.7	0.02	-9.3	0.01
9.074	151	*S. simile*	SCIENCE L.	-7.4	0.02	-9.3	0.02
9.041	152	*S. simile*	SCIENCE L.	-7.5	0.01	-9.0	0.01
9.008	153	*S. simile*	SCIENCE L.	-7.7	0.02	-9.3	0.01
8.975	154	*S. simile*	SCIENCE L.	-7.5	0.01	-9.3	0.03
8.909	156	*S. simile*	SCIENCE L.	-7.4	0.01	-9.6	0.03
8.876	157	*S. simile*	SCIENCE L.	-7.3	0.02	-9.5	0.03
8.843	158	*S. simile*	SCIENCE L.	-7.5	0.02	-9.4	0.05
8.810	159	*S. simile*	SCIENCE L.	-7.2	0.01	-9.5	0.01
8.777	160	*S. simile*	SCIENCE L.	-6.9	0.01	-8.9	0.02
8.744	161	*S. simile*	SCIENCE L.	-7.1	0.01	-9.7	0.03
8.711	162	*S. simile*	SCIENCE L.	-6.5	0.01	-9.6	0.07

Calculated Distance from Umbo	SN	Species	Location	δ^{13}C ‰ VPDB	±	δ^{18}O ‰ VPDB	±
8.678	163	*S. simile*	SCIENCE L.	-6.9	0.02	-9.8	0.05
8.645	164	*S. simile*	SCIENCE L.	-7.0	0.00	-9.9	0.05
8.612	165	*S. simile*	SCIENCE L.	-7.0	0.00	-9.7	0.03
8.579	166	*S. simile*	SCIENCE L.	-7.1	0.02	-9.8	0.01
8.546	167	*S. simile*	SCIENCE L.	-7.1	0.02	-9.9	0.02
8.513	168	*S. simile*	SCIENCE L.	-7.0	0.03	-9.8	0.02
8.480	169	*S. simile*	SCIENCE L.	-7.0	0.02	-9.9	0.03
8.447	170	*S. simile*	SCIENCE L.	-7.0	0.01	-9.9	0.07
8.414	171	*S. simile*	SCIENCE L.	-7.0	0.03	-9.9	0.03
8.381	172	*S. simile*	SCIENCE L.	-7.2	0.01	-10.0	0.03
8.315	174	*S. simile*	SCIENCE L.	-6.9	0.02	-9.8	0.02
8.249	176	*S. simile*	SCIENCE L.	-7.2	0.01	-10.0	0.03
8.150	179	*S. simile*	SCIENCE L.	-7.6	0.02	-10.3	0.06
0.000	276.5	*D. polymorpha*	Keuka L.	-4.8	0.04	-8.1	0.04
0.120	274.5	*D. polymorpha*	Keuka L.	-4.3	0.00	-7.9	0.06
0.330	271	*D. polymorpha*	Keuka L.	-4.7	0.02	-8.0	0.02
0.450	269	*D. polymorpha*	Keuka L.	-4.9	0.00	-7.9	0.06
0.690	265	*D. polymorpha*	Keuka L.	-5.1	0.05	-7.4	0.03
0.750	264	*D. polymorpha*	Keuka L.	-5.0	0.01	-7.3	0.07
0.810	263	*D. polymorpha*	Keuka L.	-5.0	0.00	-7.4	0.02
0.870	262	*D. polymorpha*	Keuka L.	-5.0	0.01	-7.4	0.02
0.930	261	*D. polymorpha*	Keuka L.	-5.1	0.01	-7.2	0.06
0.990	260	*D. polymorpha*	Keuka L.	-5.2	0.01	-7.4	0.02
1.050	259	*D. polymorpha*	Keuka L.	-5.2	0.02	-7.3	0.02
1.110	258	*D. polymorpha*	Keuka L.	-5.2	0.02	-7.4	0.02
1.170	257	*D. polymorpha*	Keuka L.	-5.3	0.01	-7.3	0.03
1.290	255	*D. polymorpha*	Keuka L.	-5.1	0.02	-7.1	0.03
1.350	254	*D. polymorpha*	Keuka L.	-5.3	0.01	-7.0	0.03
1.410	253	*D. polymorpha*	Keuka L.	-5.4	0.02	-7.2	0.04
1.470	252	*D. polymorpha*	Keuka L.	-5.4	0.01	-7.2	0.03
1.530	251	*D. polymorpha*	Keuka L.	-5.4	0.00	-7.0	0.03
1.590	250	*D. polymorpha*	Keuka L.	-5.5	0.03	-6.9	0.06
1.710	248	*D. polymorpha*	Keuka L.	-5.5	0.02	-6.8	0.02
1.770	247	*D. polymorpha*	Keuka L.	-5.6	0.01	-7.0	0.02
1.830	246	*D. polymorpha*	Keuka L.	-5.3	0.02	-6.7	0.05
1.890	245	*D. polymorpha*	Keuka L.	-5.4	0.03	-6.8	0.04
2.070	242	*D. polymorpha*	Keuka L.	-5.4	0.01	-6.8	0.04
2.250	239	*D. polymorpha*	Keuka L.	-5.3	0.01	-6.7	0.05

Calculated Distance from Umbo	SN	Species	Location	$\delta^{13}C$ ‰ VPDB	±	$\delta^{18}O$ ‰ VPDB	±
2.430	236	*D. polymorpha*	Keuka L.	-4.9	0.03	-6.8	0.02
2.610	233	*D. polymorpha*	Keuka L.	-4.8	0.02	-6.9	0.03
2.670	232	*D. polymorpha*	Keuka L.	-4.9	0.01	-6.8	0.06
2.730	231	*D. polymorpha*	Keuka L.	-4.9	0.02	-6.8	0.02
2.790	230	*D. polymorpha*	Keuka L.	-4.9	0.03	-6.9	0.02
2.910	228	*D. polymorpha*	Keuka L.	-4.9	0.01	-6.8	0.03
2.970	227	*D. polymorpha*	Keuka L.	-4.9	0.02	-6.7	0.03
3.030	226	*D. polymorpha*	Keuka L.	-4.8	0.02	-6.6	0.04
3.090	225	*D. polymorpha*	Keuka L.	-4.8	0.05	-6.5	0.02
3.390	220	*D. polymorpha*	Keuka L.	-4.6	0.01	-6.4	0.06
3.450	219	*D. polymorpha*	Keuka L.	-4.5	0.02	-6.3	0.03
3.510	218	*D. polymorpha*	Keuka L.	-4.6	0.01	-6.2	0.05
3.570	217	*D. polymorpha*	Keuka L.	-4.5	0.01	-6.1	0.01
3.630	216	*D. polymorpha*	Keuka L.	-4.5	0.01	-6.2	0.04
3.690	215	*D. polymorpha*	Keuka L.	-4.5	0.02	-6.2	0.02
3.690	215	*D. polymorpha*	Keuka L.	-4.6	0.01	-6.2	0.03
3.840	212.5	*D. polymorpha*	Keuka L.	-4.6	0.01	-6.1	0.02
3.930	211	*D. polymorpha*	Keuka L.	-4.4	0.02	-5.8	0.02
3.990	210	*D. polymorpha*	Keuka L.	-4.5	0.01	-5.9	0.04
4.050	209	*D. polymorpha*	Keuka L.	-4.5	0.01	-6.0	0.02
4.110	208	*D. polymorpha*	Keuka L.	-4.5	0.01	-5.8	0.02
4.170	207	*D. polymorpha*	Keuka L.	-4.5	0.01	-5.4	0.04
4.230	206	*D. polymorpha*	Keuka L.	-4.5	0.02	-5.5	0.04
4.290	205	*D. polymorpha*	Keuka L.	-4.5	0.01	-5.5	0.04
4.350	204	*D. polymorpha*	Keuka L.	-4.5	0.01	-5.4	0.06
4.410	203	*D. polymorpha*	Keuka L.	-4.5	0.02	-5.5	0.03
4.470	202	*D. polymorpha*	Keuka L.	-4.5	0.01	-5.5	0.03
4.530	201	*D. polymorpha*	Keuka L.	-4.5	0.01	-5.4	0.03
4.590	200	*D. polymorpha*	Keuka L.	-4.6	0.03	-5.5	0.05
4.650	199	*D. polymorpha*	Keuka L.	-4.5	0.01	-5.4	0.02
4.710	198	*D. polymorpha*	Keuka L.	-4.5	0.03	-5.3	0.01
4.770	197	*D. polymorpha*	Keuka L.	-4.5	0.01	-5.3	0.05
4.830	196	*D. polymorpha*	Keuka L.	-4.6	0.02	-5.2	0.02
4.890	195	*D. polymorpha*	Keuka L.	-4.5	0.02	-5.3	0.07
4.950	194	*D. polymorpha*	Keuka L.	-4.6	0.02	-5.2	0.03
5.010	193	*D. polymorpha*	Keuka L.	-4.6	0.03	-5.1	0.03
5.070	192	*D. polymorpha*	Keuka L.	-4.6	0.03	-5.2	0.06
5.130	191	*D. polymorpha*	Keuka L.	-4.5	0.02	-5.1	0.04

Calculated Distance from Umbo	SN	Species	Location	δ^{13}C ‰ VPDB	±	δ^{18}O ‰ VPDB	±
5.250	189	*D. polymorpha*	Keuka L.	-4.6	0.01	-5.0	0.03
5.250	189	*D. polymorpha*	Keuka L.	-4.6	0.01	-5.0	0.03
5.310	188	*D. polymorpha*	Keuka L.	-4.5	0.02	-4.8	0.03
5.310	188	*D. polymorpha*	Keuka L.	-4.5	0.02	-4.8	0.03
5.430	186	*D. polymorpha*	Keuka L.	-4.5	0.00	-4.8	0.03
5.490	185	*D. polymorpha*	Keuka L.	-4.5	0.03	-4.7	0.04
5.550	184	*D. polymorpha*	Keuka L.	-4.4	0.03	-4.7	0.05
5.610	183	*D. polymorpha*	Keuka L.	-4.3	0.03	-4.5	0.03
5.670	182	*D. polymorpha*	Keuka L.	-4.1	0.03	-4.4	0.03
5.716	181	*D. polymorpha*	Keuka L.	-4.1	0.04	-4.3	0.07
5.762	180	*D. polymorpha*	Keuka L.	-4.1	0.03	-4.4	0.05
5.854	178	*D. polymorpha*	Keuka L.	-4.1	0.02	-4.3	0.08
5.946	176	*D. polymorpha*	Keuka L.	-4.1	0.02	-4.2	0.03
5.992	175	*D. polymorpha*	Keuka L.	-4.1	0.03	-4.2	0.04
6.038	174	*D. polymorpha*	Keuka L.	-4.1	0.03	-4.2	0.02
6.084	173	*D. polymorpha*	Keuka L.	-4.2	0.03	-4.3	0.05
6.130	172	*D. polymorpha*	Keuka L.	-4.1	0.02	-4.2	0.03
6.176	171	*D. polymorpha*	Keuka L.	-4.2	0.03	-4.1	0.02
6.222	170	*D. polymorpha*	Keuka L.	-4.0	0.01	-4.2	0.04
6.268	169	*D. polymorpha*	Keuka L.	-4.1	0.03	-4.2	0.06
6.314	168	*D. polymorpha*	Keuka L.	-4.3	0.04	-4.3	0.04
6.406	166	*D. polymorpha*	Keuka L.	-4.3	0.01	-4.4	0.04
6.498	164	*D. polymorpha*	Keuka L.	-4.3	0.02	-4.5	0.02
6.544	163	*D. polymorpha*	Keuka L.	-4.5	0.01	-4.9	0.02
6.590	162	*D. polymorpha*	Keuka L.	-4.5	0.02	-4.8	0.03
6.636	161	*D. polymorpha*	Keuka L.	-4.5	0.02	-4.9	0.01
6.682	160	*D. polymorpha*	Keuka L.	-4.5	0.02	-4.8	0.04
6.728	159	*D. polymorpha*	Keuka L.	-4.5	0.03	-5.1	0.05
6.843	156.5	*D. polymorpha*	Keuka L.	-4.5	0.01	-5.2	0.06
6.912	155	*D. polymorpha*	Keuka L.	-4.5	0.03	-5.2	0.05
7.004	153	*D. polymorpha*	Keuka L.	-5.0	0.02	-5.5	0.02
7.146	152	*D. polymorpha*	Keuka L.	-4.8	0.01	-5.9	0.04
7.226	150	*D. polymorpha*	Keuka L.	-4.8	0.01	-6.1	0.05
7.266	149	*D. polymorpha*	Keuka L.	-4.8	0.02	-6.1	0.04
7.266	149	*D. polymorpha*	Keuka L.	-4.8	0.02	-6.1	0.02
7.346	147	*D. polymorpha*	Keuka L.	-4.9	0.02	-6.3	0.03
7.386	146	*D. polymorpha*	Keuka L.	-5.0	0.02	-6.3	0.01
7.426	145	*D. polymorpha*	Keuka L.	-4.9	0.02	-6.2	0.04

Calculated Distance from Umbo	SN	Species	Location	δ^{13}C ‰ VPDB	±	δ^{18}O ‰ VPDB	±
7.466	144	*D. polymorpha*	Keuka L.	-5.2	0.02	-6.5	0.05
7.506	143	*D. polymorpha*	Keuka L.	-5.1	0.01	-6.4	0.04
7.546	142	*D. polymorpha*	Keuka L.	-5.1	0.02	-6.4	0.02
7.586	141	*D. polymorpha*	Keuka L.	-5.1	0.01	-6.5	0.02
7.626	140	*D. polymorpha*	Keuka L.	-5.1	0.01	-6.4	0.01
7.666	139	*D. polymorpha*	Keuka L.	-5.2	0.02	-6.5	0.03
7.706	138	*D. polymorpha*	Keuka L.	-5.2	0.01	-6.6	0.04
7.746	137	*D. polymorpha*	Keuka L.	-5.2	0.01	-6.6	0.05
7.786	136	*D. polymorpha*	Keuka L.	-5.2	0.01	-6.3	0.03
7.879	134	*D. polymorpha*	Keuka L.	-5.3	0.02	-6.7	0.04
7.930	133	*D. polymorpha*	Keuka L.	-5.4	0.01	-6.7	0.03
7.981	132	*D. polymorpha*	Keuka L.	-5.4	0.01	-6.6	0.03
8.032	131	*D. polymorpha*	Keuka L.	-5.6	0.01	-6.9	0.05
8.083	130	*D. polymorpha*	Keuka L.	-5.4	0.04	-6.5	0.02
8.134	129	*D. polymorpha*	Keuka L.	-5.4	0.02	-6.8	0.06
8.185	128	*D. polymorpha*	Keuka L.	-5.4	0.02	-7.0	0.02
8.287	126	*D. polymorpha*	Keuka L.	-5.6	0.01	-7.1	0.01
8.338	125	*D. polymorpha*	Keuka L.	-5.6	0.04	-6.9	0.04
8.389	124	*D. polymorpha*	Keuka L.	-5.7	0.01	-7.1	0.03
8.440	123	*D. polymorpha*	Keuka L.	-5.6	0.03	-7.1	0.03
8.491	122	*D. polymorpha*	Keuka L.	-5.7	0.02	-7.2	0.02
8.593	120	*D. polymorpha*	Keuka L.	-5.8	0.03	-7.2	0.04
8.644	119	*D. polymorpha*	Keuka L.	-5.9	0.02	-7.3	0.02
8.695	118	*D. polymorpha*	Keuka L.	-5.9	0.02	-7.3	0.06
8.746	117	*D. polymorpha*	Keuka L.	-6.0	0.02	-7.4	0.03
8.746	117	*D. polymorpha*	Keuka L.	-6.0	0.01	-7.4	0.05
8.848	115	*D. polymorpha*	Keuka L.	-6.1	0.01	-7.5	0.03
8.899	114	*D. polymorpha*	Keuka L.	-6.1	0.01	-7.5	0.02
9.052	111	*D. polymorpha*	Keuka L.	-6.2	0.07	-7.2	0.05
9.103	110	*D. polymorpha*	Keuka L.	-6.3	0.01	-7.7	0.03
9.154	109	*D. polymorpha*	Keuka L.	-6.3	0.02	-7.7	0.05
9.205	108	*D. polymorpha*	Keuka L.	-6.3	0.01	-7.6	0.03
9.256	107	*D. polymorpha*	Keuka L.	-6.4	0.01	-7.7	0.04
9.307	106	*D. polymorpha*	Keuka L.	-6.6	0.03	-7.7	0.04
9.409	104	*D. polymorpha*	Keuka L.	-6.8	0.01	-7.8	0.03
9.460	103	*D. polymorpha*	Keuka L.	-6.8	0.03	-7.6	0.07
9.511	102	*D. polymorpha*	Keuka L.	-7.0	0.01	-8.0	0.04
9.562	101	*D. polymorpha*	Keuka L.	-7.1	0.02	-8.0	0.04

Calculated Distance from Umbo	SN	Species	Location	δ^{13}C ‰ VPDB	±	δ^{18}O ‰ VPDB	±
9.613	100	*D. polymorpha*	Keuka L.	-7.4	0.02	-8.0	0.04
9.656	99	*D. polymorpha*	Keuka L.	-7.5	0.01	-7.7	0.05
9.742	97	*D. polymorpha*	Keuka L.	-7.3	0.01	-7.8	0.03
9.828	95	*D. polymorpha*	Keuka L.	-6.4	0.02	-7.8	0.05
9.871	94	*D. polymorpha*	Keuka L.	-6.3	0.02	-7.6	0.04
9.957	92	*D. polymorpha*	Keuka L.	-6.8	0.01	-7.8	0.05
10.000	91	*D. polymorpha*	Keuka L.	-6.6	0.02	-7.6	0.04
10.086	89	*D. polymorpha*	Keuka L.	-6.7	0.02	-7.7	0.06
10.215	86	*D. polymorpha*	Keuka L.	-6.9	0.04	-7.7	0.04
10.258	85	*D. polymorpha*	Keuka L.	-6.9	0.03	-7.9	0.06
10.301	84	*D. polymorpha*	Keuka L.	-7.1	0.04	-7.7	0.07
10.430	81	*D. polymorpha*	Keuka L.	-7.4	0.04	-7.9	0.03
10.731	74	*D. polymorpha*	Keuka L.	-8.4	0.02	-8.1	0.04
10.817	72	*D. polymorpha*	Keuka L.	-8.0	0.01	-8.2	0.06
10.946	69	*D. polymorpha*	Keuka L.	-7.6	0.01	-8.0	0.02
11.075	66	*D. polymorpha*	Keuka L.	-8.0	0.03	-8.1	0.02
11.333	60	*D. polymorpha*	Keuka L.	-8.3	0.04	-8.3	0.03
11.591	54	*D. polymorpha*	Keuka L.	-8.9	0.02	-8.4	0.02
11.634	53	*D. polymorpha*	Keuka L.	-8.9	0.01	-8.5	0.06
11.677	52	*D. polymorpha*	Keuka L.	-9.0	0.01	-8.4	0.03
11.720	51	*D. polymorpha*	Keuka L.	-9.1	0.02	-8.5	0.04
11.763	50	*D. polymorpha*	Keuka L.	-9.1	0.01	-8.6	0.02
11.806	49	*D. polymorpha*	Keuka L.	-9.1	0.01	-8.4	0.02
11.849	48	*D. polymorpha*	Keuka L.	-9.0	0.01	-8.5	0.03
11.892	47	*D. polymorpha*	Keuka L.	-8.8	0.01	-8.3	0.02
11.935	46	*D. polymorpha*	Keuka L.	-8.4	0.02	-8.1	0.04
11.935	46	*D. polymorpha*	Keuka L.	-8.4	0.02	-8.1	0.04
11.978	45	*D. polymorpha*	Keuka L.	-8.4	0.01	-8.1	0.05
12.021	44	*D. polymorpha*	Keuka L.	-8.3	0.03	-8.1	0.02
12.064	43	*D. polymorpha*	Keuka L.	-8.3	0.01	-8.0	0.03
12.107	42	*D. polymorpha*	Keuka L.	-8.2	0.01	-8.0	0.04
12.150	41	*D. polymorpha*	Keuka L.	-8.2	0.02	-8.0	0.02
12.215	39.5	*D. polymorpha*	Keuka L.	-7.9	0.01	-7.8	0.03
12.322	37	*D. polymorpha*	Keuka L.	-7.9	0.00	-8.0	0.02
12.365	36	*D. polymorpha*	Keuka L.	-7.9	0.02	-7.8	0.06
12.408	35	*D. polymorpha*	Keuka L.	-7.8	0.01	-7.9	0.06
12.451	34	*D. polymorpha*	Keuka L.	-7.5	0.02	-7.8	0.02
12.494	33	*D. polymorpha*	Keuka L.	-7.7	0.01	-7.8	0.05

Calculated Distance from Umbo	SN	Species	Location	$\delta^{13}C$ ‰ VPDB	±	$\delta^{18}O$ ‰ VPDB	±
12.537	32	*D. polymorpha*	Keuka L.	-7.8	0.01	-7.9	0.04
12.580	31	*D. polymorpha*	Keuka L.	-7.6	0.01	-7.9	0.05
12.623	30	*D. polymorpha*	Keuka L.	-7.6	0.02	-7.9	0.04
12.666	29	*D. polymorpha*	Keuka L.	-7.4	0.02	-7.8	0.05
12.752	27	*D. polymorpha*	Keuka L.	-7.3	0.02	-7.6	0.04
12.795	26	*D. polymorpha*	Keuka L.	-7.2	0.02	-7.8	0.01
12.838	25	*D. polymorpha*	Keuka L.	-6.9	0.02	-7.6	0.03
12.881	24	*D. polymorpha*	Keuka L.	-6.8	0.01	-7.3	0.01
12.924	23	*D. polymorpha*	Keuka L.	-6.8	0.03	-7.4	0.04
12.967	22	*D. polymorpha*	Keuka L.	-6.7	0.02	-7.3	0.03
13.010	21	*D. polymorpha*	Keuka L.	-6.4	0.02	-6.9	0.02
13.053	20	*D. polymorpha*	Keuka L.	-6.3	0.01	-7.1	0.05
13.096	19	*D. polymorpha*	Keuka L.	-6.4	0.01	-7.0	0.01
13.139	18	*D. polymorpha*	Keuka L.	-6.4	0.02	-7.2	0.05
13.182	17	*D. polymorpha*	Keuka L.	-6.1	0.02	-6.8	0.03
13.225	16	*D. polymorpha*	Keuka L.	-5.9	0.02	-6.7	0.04
13.268	15	*D. polymorpha*	Keuka L.	-6.0	0.01	-6.8	0.03
13.311	14	*D. polymorpha*	Keuka L.	-6.0	0.02	-6.8	0.03
13.354	13	*D. polymorpha*	Keuka L.	-6.0	0.01	-6.7	0.04
13.483	10	*D. polymorpha*	Keuka L.	-5.6	0.02	-6.7	0.02
13.526	9	*D. polymorpha*	Keuka L.	-5.3	0.01	-6.5	0.04
13.569	8	*D. polymorpha*	Keuka L.	-5.5	0.01	-6.7	0.04
13.612	7	*D. polymorpha*	Keuka L.	-5.2	0.00	-6.5	0.02
13.655	6	*D. polymorpha*	Keuka L.	-5.0	0.01	-6.5	0.03
13.720	4.5	*D. polymorpha*	Keuka L.	-4.9	0.03	-6.4	0.03
13.806	2.5	*D. polymorpha*	Keuka L.	-5.2	0.02	-6.8	0.02

Table A2—Tabulated $\delta^{18}O_{(H_2O)}$ values for Science Lake.

Collection Date	$\delta^{18}O_{(H_2O)}$ ‰ VPDB
3/28/98	-12.4
4/25/98	-12.0
6/27/98	-10.8
7/20/98	-10.7
8/22/98	-9.6
9/12/98	-9.7
10/17/98	-10.1
11/15/98	-10.2

Collection Date	$\delta^{18}O_{(H_2O)}$ ‰ VPDB
12/26/98	-11.1
1/31/99	-11.7
2/27/99	-11.7
3/28/99	-12.1
7/29/99	-9.4
9/5/99	-9.6
10/3/99	-10.1

Table A3—Tabulated data of low-resolution intra-otolith $\delta^{13}C$ and $\delta^{18}O$ values utilized in chapter 3. Also shown are calculated increment distance, calculated age, and equation parameters for *Aplodinotus grunniens*. * denotes same specimen was sampled for high-resolution intra-otolith $\delta^{13}C$ and $\delta^{18}O$ values.

Specimen	Sample Number	Calculated Increment Distance	Calculated Age	$\delta^{13}C$‰ VPDB	±	$\delta^{18}O$‰ VPDB	±	Equation parameters	
C3-1	0	0.000	0.0	-13.5	0.01	-7.2	0.02		
C3-1	1	0.568	0.4	-14.5	0.02	-7.7	0.02	C3-1	
C3-1	2	1.703	1.0	-17.1	0.00	-8.5	0.02	Linf	8.92
C3-1	3	2.838	1.8	-16.4	0.01	-8.1	0.01	K	0.23
C3-1	4	3.973	2.7	-14.0	0.01	-7.5	0.02	t0	0.11
C3-1	5	5.108	3.8	-15.5	0.01	-8.1	0.02	TL	9.08
C3-1	6	6.243	5.3	-12.3	0.01	-7.3	0.01		
C3-1	7	7.378	7.7	-10.5	0.02	-7.4	0.02		
C3-1	8	8.513	13.5	-8.5	0.00	-8.1	0.02		
B2-1B	0	0.000	0.0	-18.2	0.01	-7.8	0.01		
B2-1B	1	0.493	0.3	-18.6	0.01	-9.7	0.02	B2-1b	
B2-1B	2	1.478	0.8	-18.7	0.00	-8.3	0.01	Linf	10.74
B2-1B	3	2.464	1.3	-17.9	0.00	-7.6	0.01	K	0.22
B2-1B	4	3.449	1.9	-16.3	0.01	-7.9	0.01	t0	0.12
B2-1B	5	4.435	2.5	-16.0	0.01	-7.5	0.01	TL	9.86
B2-1B	6	5.420	3.3	-15.0	0.01	-7.5	0.01		
B2-1B	7	6.406	4.2	-12.1	0.01	-7.8	0.01		
B2-1B	8	7.392	5.4	-11.0	0.00	-8.1	0.01		
B2-1B	9	8.377	7.0	-9.7	0.01	-7.8	0.02		
B2-1B	10	9.363	9.5	-10.8	0.01	-7.2	0.01		
B2-1A	0	0.000	0.0	-13.9	0.00	-7.6	0.01		
B2-1A	1	0.480	1.2	-14.1	0.01	-8.2	0.03	B2-1a	
B2-1A	2	1.439	1.5	-13.4	0.02	-7.9	0.01	Linf	10.03
B2-1A	3	2.398	1.9	-12.5	0.01	-7.0	0.01	K	0.32

Specimen	Sample Number	Calculated Increment Distance	Calculated Age	$\delta^{13}C$‰ VPDB	±	$\delta^{18}O$‰ VPDB	±	Equation parameters	
B2-1A	4	3.357	2.3	-13.2	0.01	-7.7	0.01	t0	1.02
B2-1A	5	4.316	2.8	-14.5	0.00	-7.5	0.01	TL	9.59
B2-1A	6	5.275	3.4	-14.4	0.01	-7.4	0.01		
B2-1A	7	6.234	4.1	-12.5	0.00	-7.6	0.01		
B2-1A	8	7.193	5.0	-11.5	0.00	-8.0	0.02		
B2-1A	9	8.152	6.3	-11.6	0.01	-7.7	0.00		
B2-1A	10	9.111	8.5	-12.3	0.00	-8.3	0.01		
D3-1	0	0.000	0.0	-14.3	0.01	-7.5	0.01		
D3-1	1	0.504	0.9	-13.5	0.01	-7.5	0.03	D3-1	
D3-1	2	1.511	1.3	-12.9	0.01	-7.5	0.02	Linf	10.90
D3-1	3	2.518	1.8	-12.9	0.01	-7.6	0.02	K	0.24
D3-1	4	3.526	2.3	-13.8	0.01	-7.7	0.01	t0	0.66
D3-1	5	4.533	2.9	-14.6	0.00	-7.6	0.01	TL	11.08
D3-1	6	5.540	3.6	-12.8	0.00	-7.6	0.01		
D3-1	7	6.547	4.5	-9.6	0.01	-7.3	0.03		
D3-1	8	7.555	5.6	-10.9	0.00	-7.7	0.01		
D3-1	9	8.562	7.1	-11.6	0.01	-8.8	0.02		
D3-1	10	9.569	9.4	-10.7	0.01	-8.1	0.01		
D3-1	11	10.577	15.3	-10.0	0.01	-8.3	0.01		
C3-1A	0	0.000	0.0	-14.1	0.01	-7.2	0.00		
C3-1A	1	0.483	0.7	-13.9	0.01	-6.9	0.01	C3-1a	
C3-1A	2	1.449	1.0	-16.6	0.01	-7.9	0.01	Linf	8.23
C3-1A	3	2.414	1.4	-15.7	0.01	-7.6	0.00	K	0.37
C3-1A	4	3.380	1.9	-15.3	0.01	-8.1	0.01	t0	0.51
C3-1A	5	4.346	2.5	-13.8	0.01	-8.3	0.01	tl	7.73
C3-1A	6	5.311	3.3	-12.9	0.01	-8.0	0.01		
C3-1A	7	6.277	4.4	-12.7	0.01	-7.6	0.01		
C3-1A	8	7.243	6.2	-12.5	0.01	-7.4	0.01		
C3-1B	0	0.000	0.0	-14.1	0.01	-7.5	0.01		
C3-1B	1	0.522	0.3	-14.3	0.01	-7.6	0.01	C3-1b	
C3-1B	2	1.567	0.9	-15.6	0.02	-8.2	0.02	Linf	9.16
C3-1B	3	2.611	1.5	-13.7	0.01	-7.8	0.01	K	0.22
C3-1B	4	3.656	2.3	-14.5	0.00	-8.0	0.01	t0	0.02
C3-1B	5	4.701	3.3	-14.3	0.01	-7.7	0.01	TL	8.36
C3-1B	6	5.745	4.5	-11.8	0.01	-6.7	0.02		
C3-1B	7	6.790	6.2	-10.1	0.01	-7.4	0.01		
C3-1B	8	7.834	8.8	-9.2	0.01	-7.8	0.01		
F4-1B	0	0.000	0.0	-16.9	0.01	-7.2	0.01		

Specimen	Sample Number	Calculated Increment Distance	Calculated Age	$\delta^{13}C$‰ VPDB	±	$\delta^{18}O$‰ VPDB	±	Equation parameters	
F4-1B	1	0.647	0.7	-16.8	0.01	-7.5	0.01	F4-1b	
F4-1B	2	1.941	1.3	-16.6	0.01	-7.6	0.02	Linf	10.28
F4-1B	3	3.236	2.0	-14.5	0.01	-7.2	0.01	K	0.24
F4-1B	4	4.530	2.8	-15.6	0.00	-7.5	0.01	t0	0.41
F4-1b	5	5.824	3.9	-11.2	0.00	-7.8	0.02	tl	10.35
F4-1B	6	7.118	5.3	-10.1	0.01	-8.1	0.03		
F4-1b	7	8.413	7.5	-10.3	0.01	-8.1	0.00		
F4-1b	8	9.707	12.4	-10.1	0.00	-7.8	0.01		
C4-2*	0	0.000	0.0	-17.6	0.12	-15.4	0.07	C4-2 mm	
C4-2*	1	0.454	0.4	-16.6	0.02	-9.0	0.01	Linf	8.78
C4-2*	2	1.362	1.0	-15.4	0.02	-8.5	0.04	K	0.20
C4-2*	3	2.270	1.7	-13.4	0.01	-8.4	0.02	t0	0.17
C4-2*	4	3.179	2.4	-13.5	0.01	-8.5	0.05	tl	9.08
C4-2*	5	4.087	3.3	-10.8	0.01	-8.2	0.02		
C4-2*	6	4.995	4.4	-8.9	0.03	-8.3	0.03		
C4-2*	7	5.903	5.7	-8.3	0.01	-8.1	0.03		
C4-2*	8	6.811	7.6	-8.4	0.01	-8.0	0.02		
C4-2*	9	7.720	10.7	-7.6	0.01	-7.6	0.05		
C4-2*	10	8.628	20.4	-7.6	0.01	-7.7	0.02		
E4-2	0	0.000	0.0	-13.9	0.02	-7.5	0.01		
E4-2	1	0.470	0.4	-14.2	0.02	-7.5	0.02	E4-2	
E4-2	2	1.410	0.8	-13.7	0.01	-7.2	0.02	Linf	11.12
E4-2	3	2.350	1.2	-12.6	0.00	-7.5	0.02	K	0.22
E4-2	4	3.290	1.8	-12.6	0.01	-7.7	0.01	t0	0.17
E4-2	5	4.230	2.3	-13.5	0.00	-7.9	0.01	tl	9.40
E4-2	6	5.170	3.0	-14.0	0.00	-8.0	0.01		
E4-2	7	6.110	3.8						
E4-2	8	7.050	4.7	-13.2	0.01	-7.3	0.02		
E4-2	9	7.990	5.9	-12.8	0.01	-7.9	0.01		
E4-2	10	8.930	7.6	-10.9	0.01	-7.8	0.02		
C4-2	0	0.000	0.0	-13.7	0.00	-7.6	0.01		
C4-2	1	0.426	0.3	-14.0	0.01	-7.8	0.02	C4-2 nms	
C4-2	2	1.278	0.9	-14.1	0.02	-7.2	0.01	Linf	9.00
C4-2	3	2.130	1.5	-14.4	0.00	-7.3	0.01	K	0.18
C4-2	4	2.982	2.2	-14.2	0.01	-7.9	0.02	t0	0.01
C4-2	5	3.834	3.1	-15.5	0.01	-8.9	0.01	tl	9.37
C4-2	6	4.686	4.1	-14.4	0.01	-8.7	0.01		
C4-2	7	5.538	5.3	-14.4	0.01	-8.7	0.01		

Specimen	Sample Number	Calculated Increment Distance	Calculated Age	δ^{13}C‰ VPDB	±	δ^{18}O‰ VPDB	±	Equation parameters	
C4-2	8	6.390	6.9	-11.7	0.00	-8.0	0.01		
C4-2	9	7.242	9.1	-9.5	0.01	-7.8	0.01		
C4-2	10	8.094	12.8	-8.7	0.00	-7.5	0.02		
C4-2	11	8.945	28.4	-8.3	0.01	-7.6	0.01		
C3-2B	0	0.000	0.0	-15.7	0.01	-7.5	0.01		
C3-2B	1	0.511	1.3	-15.8	0.01	-7.6	0.01	C3-2b	
C3-2B	2	1.532	1.8	-16.0	0.03	-8.0	0.01	Linf	8.17
C3-2B	3	2.553	2.3	-14.0	0.01	-7.8	0.02	K	0.32
C3-2B	4	3.574	2.9	-13.8	0.01	-7.9	0.01	t0	1.11
C3-2B	5	4.596	3.7	-13.7	0.02	-7.8	0.03	tl	8.01
C3-2B	6	5.617	4.7	-13.3	0.02	-8.3	0.07		
C3-2B	7	6.638	6.3	-13.1	0.01	-7.2	0.04		
C3-2B	8	7.659	9.8	-11.0	0.02	-7.2	0.02		
C3-2A	0	0.000	0.0	-18.9	0.00	-7.5	0.00		
C3-2A	1	0.507	0.4	-18.7	0.00	-7.8	0.02	C3-2a	
C3-2A	2	1.522	1.1	-19.3	0.01	-7.9	0.01	Linf	9.42
C3-2A	3	2.537	1.8	-18.4	0.00	-8.0	0.02	K	0.17
C3-2A	4	3.552	2.5	-15.0	0.00	-7.1	0.00	t0	-0.57
C3-2A	5	4.567	3.3	-14.5	0.01	-8.0	0.01	tl	9.13
C3-2A	6	5.582	4.7	-13.5	0.01	-7.9	0.01	m	1.44
C3-2A	7	6.597	6.5	-11.8	0.01	-8.3	0.02	b	0.00
C3-2A	8	7.612	9.1	-11.3	0.01	-7.9	0.01		
C3-2A	9	8.627	14.0	-11.6	0.01	-7.7	0.01		
C3-2C	0			-15.0	0.01	-7.8	0.01	C3-2c	
C3-2C	1	0.444	0.5	-16.4	0.01	-8.5	0.01	Linf	8.03
C3-2C	2	1.333	0.7	-17.4	0.01	-8.8	0.02	K	0.44
C3-2C	3	2.221	1.1	-18.7	0.00	-9.3	0.02	t0	0.33
C3-2C	4	3.109	1.4	-17.2	0.01	-8.7	0.01	tl	8.00
C3-2C	5	3.998	1.9	-15.4	0.01	-8.4	0.02		
C3-2C	6	4.886	2.5	-14.0	0.01	-8.1	0.01		
C3-2C	7	5.774	3.2	-13.4	0.00	-8.1	0.02		
C3-2C	8	6.663	4.4	-12.8	0.01	-8.4	0.01		
C3-2C	9	7.551	6.7	-11.0	0.00	-8.2	0.01		
E4-3B	0	0.000	0.0	-17.8	0.00	-7.5	0.01	E4-3b	
E4-3B	1	0.503	0.1	-16.0	0.01	-7.1	0.02	Linf	9.02
E4-3B	2	1.510	0.8					K	0.18
E4-3B	3	2.516	1.6	-18.4	0.01	-8.0	0.01	t0	-0.21
E4-3B	4	3.523	2.5					tl	9.06

Specimen	Sample Number	Calculated Increment Distance	Calculated Age	$\delta^{13}C$‰ VPDB	±	$\delta^{18}O$‰ VPDB	±	Equation parameters	
E4-3B	5	4.530	3.7						
E4-3B	6	5.536	5.1						
E4-3B	7	6.543	7.0						
E4-3B	8	7.549	9.9	-11.2	0.01	-7.2	0.02		
E4-3B	9	8.556	16.3	-11.2	0.01	-7.1	0.01		
E4-3A	0	0.000	0.0	-19.9	0.00	-8.4	0.01	E4-3a	
E4-3A	1	0.723	0.4	-19.9	0.01	-8.7	0.01	Linf	11.97
E4-3A	2	2.168	1.2	-19.1	0.00	-7.7	0.01	K	0.16
E4-3A	3	3.613	2.0	-17.3	0.01	-8.6	0.01	t0	-0.46
E4-3A	4	5.058	3.0	-14.9	0.00	-7.9	0.01	tl	11.56
E4-3A	5	6.503	4.4	-12.9	0.01	-7.9	0.02	linear to	m
E4-3A	6	7.949	6.4	-11.9	0.01	-7.0	0.02	3.70	b
E4-3A	7	9.394	9.1	-11.1	0.01	-7.0	0.01		
E4-3A	8	10.839	14.3	-11.3	0.00	-7.7	0.01		
C4-3	0	0.000	0.0	-18.7	0.01	-8.0	0.02	C4-3	
C4-3	1	0.547	0.8	-17.4	0.01	-8.2	0.01	Linf	8.77
C4-3	2	1.640	1.2	-14.6	0.01	-7.1	0.02	K	0.33
C4-3	3	2.734	1.7	-13.0	0.01	-6.4	0.02	t0	0.60
C4-3	4	3.827	2.3	-13.7	0.01	-7.6	0.00	tl	7.65
C4-3	5	4.921	3.1	-11.5	0.01	-7.1	0.01		
C4-3	6	6.014	4.1	-11.0	0.01	-7.7	0.03		
C4-3	7	7.108	5.6						
B2-3D	0	0.000	0.0	-18.2	0.01	-8.0	0.02	B2-3d	
B2-3D	1	0.311	0.3	-18.7	0.01	-8.3	0.02	Linf	6.61
B2-3D	2	0.932	1.0	-18.6	0.01	-8.2	0.02	K	0.16
B2-3D	3	1.554	1.7	-17.7	0.01	-8.2	0.01	t0	-0.59
B2-3D	4	2.175	1.9	-12.9	0.02	-7.9	0.01	tl	6.84
B2-3D	5	2.797	2.8	-11.2	0.01	-7.9	0.02		
B2-3D	6	3.418	4.0	-10.8	0.01	-7.7	0.02	linear to 1.88	
B2-3D	7	4.040	5.3	-10.7	0.01	-7.5	0.02	m	0.94
B2-3D	8	4.661	7.0	-9.3	0.00	-7.9	0.01		
B2-3D	9	5.283	9.4	-8.5	0.01	-7.9	0.04		
B2-3D	10	5.904	13.4	-8.3	0.01	-7.9	0.01		
B2-3D	11	6.526	26.7	-8.3	0.01	-7.9	0.02		
B2-3C	0	0.000	0.0	-18.1	0.01	-11.2	0.02	B2-3C	
B2-3C	1	0.461	0.4	-17.3	0.01	-8.9	0.02	Linf	10.11
B2-3C	2	1.382	0.9	-17.5	0.02	-8.8	0.03	K	0.19
B2-3C	3	2.303	1.5	-15.5	0.01	-8.1	0.02	t0	0.11

Specimen	Sample Number	Calculated Increment Distance	Calculated Age	$\delta^{13}C$‰ VPDB	±	$\delta^{18}O$‰ VPDB	±	Equation parameters	
B2-3C	4	3.225	2.1	-14.7	0.01	-7.7	0.01	tl	10.13
B2-3C	5	4.146	2.9	-14.7	0.01	-8.1	0.01		
B2-3C	6	5.067	3.8	-13.0	0.01	-7.8	0.03		
B2-3C	7	5.988	4.8	-12.4	0.01	-7.4	0.01		
B2-3C	8	6.910	6.2	-10.4	0.01	-7.6	0.01		
B2-3C	9	7.831	8.0	-9.3	0.01	-8.1	0.01		
B2-3C	10	8.752	10.7	-9.3	0.01	-8.3	0.02		
B2-3C	11	9.674	16.7	-9.0	0.00	-8.1	0.00		
B2-3B	0	0.000	0.0	-14.8	0.00	-7.0	0.01	B2-3b	
B2-3B	1	0.753	0.5	-16.9	0.01	-7.2	0.02	Linf	17.23
B2-3B	2	2.259	0.9					K	0.27
B2-3B	3	3.765	1.3					t0	0.38
B2-3B	4	5.271	1.7					tl	15.06
B2-3B	5	6.777	2.2	-14.2	0.00	-7.4	0.02		
B2-3B	6	8.283	2.8	-13.3	0.02	-7.3	0.02		
B2-3B	7	9.789	3.5	-12.3	0.00	-7.8	0.02		
B2-3B	8	11.295	4.3	-11.8	0.01	-7.8	0.01		
B2-3B	9	12.801	5.4	-9.8	0.01	-7.6	0.01		
B2-3B	10	14.307	7.0	-8.2	0.00	-7.7	0.01		
B2-3A	0	0.000	0.0	-15.9	0.03	-7.3	0.07	B2-3a	
B2-3A	1	0.487	0.1	-14.3	0.01	-6.4	0.03	Linf	8.93
B2-3A	2	1.462	0.7	-14.4	0.01	-7.1	0.03	K	0.21
B2-3A	3	2.437	1.3	-15.7	0.00	-7.7	0.01	t0	-0.17
B2-3A	4	3.412	2.1	-15.8	0.00	-7.5	0.02	tl	7.80
B2-3A	5	4.386	3.0	-15.2	0.01	-7.7	0.01		
B2-3A	6	5.361	4.2	-12.4	0.01	-7.8	0.02		
B2-3A	7	6.336	5.7	-11.9	0.01	-8.1	0.01		
B2-3A	8	7.311	8.0	-10.8	0.00	-7.9	0.00		
D3-3	0	0.000	0.0	-18.6	0.01	-9.3	0.03	D3-3	
D3-3	1	0.407	0.8	-19.4	0.00	-9.7	0.02	Linf	9.11
D3-3	2	1.220	1.2	-19.3	0.00	-9.5	0.01	K	0.27
D3-3	3	2.033	1.6	-17.8	0.01	-8.7	0.01	t0	0.62
D3-3	4	2.847	2.0	-15.0	0.00	-7.2	0.02	tl	8.13
D3-3	5	3.660	2.5	-16.6	0.01	-8.4	0.02		
D3-3	6	4.473	3.1						
D3-3	7	5.287	3.8	-15.4	0.01	-7.7	0.02		
D3-3	8	6.100	4.7	-11.9	0.01	-7.8	0.01		
D3-3	9	6.913	5.9	-11.0	0.01	-8.0	0.02		

Specimen	Sample Number	Calculated Increment Distance	Calculated Age	$\delta^{13}C$‰ VPDB	±	$\delta^{18}O$‰ VPDB	±	Equation parameters	
D3-3	10	7.727	7.6	-10.5	0.01	-8.1	0.01		
C4-3C	0	0.000	0.0	-19.1	0.01	-11.6	0.05	C4-3c	
C4-3C	1	0.519	0.5					Linf	10.71
C4-3C	2	1.556	1.0	-18.3	0.01	-9.0	0.02	K	0.19
C4-3C	3	2.593	1.7					t0	0.21
C4-3C	4	3.630	2.4	-15.0	0.01	-6.8	0.02	tl	8.30
C4-3C	5	4.667	3.2						
C4-3C	6	5.704	4.2						
C4-3C	7	6.741	5.4	-11.9	0.01	-7.2	0.01		
C4-3C	8	7.778	7.0	-10.4	0.01	-7.6	0.02		
C3-4	0	0.000	0.0	-18.5	0.02	-8.6	0.03	C3-4	
C3-4	1	0.641	0.9	-17.8	0.03	-8.9	0.02	Used Log and linear regressions	
C3-4	2	1.922	1.8					0 to 4.66	m1 (log)
C3-4	3	3.203	3.6	-13.3	0.02	-7.7	0.01		b1
C3-4	4	4.484	7.4	-11.5	0.03	-7.0	0.01	4.66 and up	m2 (linear)
C3-4	5	5.765	9.9	-10.3	0.01	-8.0			b2
C3-4	6	7.046	12.9	-9.5	0.00	-8.2	0.01		tl
G3-4B	1	0.570	0.2	-15.4	0.01	-8.5	0.01	C3-4	Used 2 linear regressions
G3-4B	2	1.710	0.9	-14.8	0.01	-7.7	0.03	0 to 4.66	m1
G3-4B	3	2.850	1.5	-12.6	0.01	-7.3	0.03		b1
G3-4B	4	3.990	2.2	-13.2	0.01	-7.6	0.01	4.66 and up	m2
G3-4B	5	5.130	2.9	-12.7	0.01	-7.8	0.01		b2
G3-4B	6	6.270	3.6	-13.0	0.01	-7.3	0.02		tl
G3-4B	7	7.410	4.2	-11.5	0.01	-8.3	0.01		
G3-4B	8	8.550	4.6	-11.5	0.02	-8.5	0.02		
G3-4B	9	9.689	7.6	-11.2	0.01	-8.6	0.02		
G3-4B	10	10.829	10.5	-9.2	0.01	-7.9	0.02		
G3-4B	11	11.969	13.5	-8.7	0.02	-7.8	0.01		
G3-4B	12	13.109	16.5	-8.2	0.02	-9.0	0.05		
B2-4	0			-16.1	0.00	-7.7	0.01	B2-4	
B2-4	1	0.394	0.3	-16.0	0.01	-7.7	0.02	Linf	7.98
B2-4	2	1.181	0.7	-17.0	0.01	-7.9	0.01	K	0.23
B2-4	3	1.968	1.3	-16.8	0.01	-8.3	0.01	t0	0.04
B2-4	4	2.756	1.9	-15.9	0.01	-8.5	0.02	tl	7.09
B2-4	5	3.543	2.6	-15.2	0.00	-7.5	0.02		
B2-4	6	4.330	3.4	-13.2	0.01	-7.5	0.01		

Specimen	Sample Number	Calculated Increment Distance	Calculated Age	$\delta^{13}C$‰ VPDB	±	$\delta^{18}O$‰ VPDB	±	Equation parameters	
B2-4	7	5.118	4.5	-12.7	0.01	-7.5	0.02		
B2-4	8	5.905	5.9	-12.2	0.01	-7.8	0.02		
B2-4	9	6.692	8.0	-12.1	0.01	-7.9	0.01		
C3-4	0	0.000	0.0	-19.3	0.01	-8.3	0.02	C3-4	Used Linear and Log regressions
C3-4	1	0.533	0.2	-17.8	0.03	-8.9	0.04	0 to 6.62	m1 (Linear)
C3-4	2	1.598	0.8						b1
C3-4	3	2.663	1.5	-13.3	0.02	-7.7	0.02	6.62 and up	m2 (Log)
C3-4	4	3.728	2.1	-11.5	0.03	-7.0	0.01		b2
C3-4	5	4.793	2.7	-10.3	0.01	-8.0	0.03		tl
C3-4	6	5.858	3.4	-9.5	0.00	-8.2	0.03		
C3-4	7	6.923	4.3						
C3-4	8	7.988	6.6						
C3-4	9	9.053	10.2	-9.7	0.01	-7.3	0.02		
C3-4	10	10.118	15.7	-9.7	0.00	-7.7	0.02		
G3-4A	0	0.000	0.0	-14.1	0.01	-8.0	0.02	C3-4	Used Log and linear regressions
G3-4A	1	1.064	1.1	-18.1	0.01	-10.1	0.01	0 to 9.4	m1 (log)
G3-4A	2	3.193	1.8	-16.6	0.00	-8.2	0.01		b1
G3-4A	3	5.322	3.2	-17.4	0.01	-9.0	0.01	9.4 and up	m2 (Linear)
G3-4A	4	7.450	5.6	-14.1	0.00	-7.8	0.01		b2
G3-4A	5	9.579	8.8	-12.5	0.00	-7.6	0.01		tl
G3-4A	6	11.708	24.7	-10.4	0.01	-8.3	0.04		
G3-5	0	0.000	0.0	-14.4	0.00	-7.4	0.04	G3-5	
G3-5	1	0.755	0.1	-13.5	0.02	-7.0	0.01	Linf	11.75
G3-5	2	2.266	1.3	-14.1	0.01	-7.5	0.01	K	0.12
G3-5	3	3.777	2.8	-12.5	0.00	-7.8	0.03	t0	-0.46
G3-5	4	5.288	4.5	-11.6	0.00	-8.2	0.01	tl	9.07
G3-5	5	6.799	6.7	-9.4	0.01	-8.3	0.01		
G3-5	6	8.310	9.8	-9.7	0.01	-8.6	0.01		
C4-5B	0	0.000	0.0	-16.4	0.00	-7.8	0.02	C4-5b	
C4-5B	1	0.353	0.8	-18.0	0.03	-8.5	0.03	Linf	9.28
C4-5B	2	1.060	1.2					K	0.21
C4-5B	3	1.766	1.7	-17.2	0.00	-8.5	0.01	t0	0.65
C4-5B	4	2.472	2.1	-15.7	0.01	-8.4	0.01	tl	9.18
C4-5B	5	3.179	2.6	-13.8	0.00	-7.8	0.01		
C4-5B	6	3.885	3.2	-13.4	0.01	-7.4	0.02		

Specimen	Sample Number	Calculated Increment Distance	Calculated Age	$\delta^{13}C$‰ VPDB	±	$\delta^{18}O$‰ VPDB	±	Equation parameters	
C4-5B	7	4.591	3.9	-13.9	0.01	-7.6	0.03		
C4-5B	8	5.298	4.7	-13.5	0.01	-7.5	0.01		
C4-5B	9	6.004	5.6	-12.1	0.01	-7.7	0.01		
C4-5B	10	6.710	6.8	-10.9	0.01	-7.9	0.02		
C4-5B	11	7.417	8.3	-10.0	0.00	-8.1	0.01		
C4-5B	12	8.123	10.6	-10.2	0.01	-8.0	0.02		
C4-5B	13	8.829	15.1	-9.4	0.01	-8.1	0.02		
C4-5A	0	0.000	0.0	-13.4	0.01	-8.8	0.01	C4-5a	
C4-5A	1	0.467	0.6					Linf	13.13
C4-5A	2	1.402	1.3	-13.9	0.01	-10.3	0.02	K	0.11
C4-5A	3	2.336	2.0	-13.6	0.01	-9.3	0.01	t0	0.25
C4-5A	4	3.271	2.9	-13.9	0.02	-7.9	0.01	tl	10.28
C4-5A	5	4.206	3.8	-13.6	0.01	-8.1	0.02		
C4-5A	6	5.140	4.8	-13.4	0.04	-7.4	0.05		
C4-5A	7	6.075	5.9	-13.2	0.01	-8.1	0.03		
C4-5A	8	7.009	7.2	-12.4	0.01	-7.4	0.01		
C4-5A	9	7.944	8.7	-11.3	0.01	-7.5	0.03		
C4-5A	10	8.878	10.5	-7.2	0.01	-8.6	0.06		
C4-5A	11	9.813	12.8	-7.4	0.01	-7.8	0.02		
G3-5	0	0.000	0.0	-10.9	0.01	-8.7	0.04	G3-5	
G3-5	1	0.411	0.3	-11.6	0.01	-8.9	0.02	Linf	9.72
G3-5	2	1.233	0.8					K	0.31
G3-5	3	2.055	1.3	-12.2	0.01	-9.2	0.01	t0	0.75
G3-5	4	2.877	1.8	-15.2	0.01	-7.8	0.02	tl	9.04
G3-5	5	3.699	2.3	-16.4	0.02	-7.3	0.02		
G3-5	6	4.521	2.8	-14.6	0.01	-7.0	0.01	to 3.13	
G3-5	7	5.343	3.3	-13.8	0.01	-6.8	0.01	m	1.57
G3-5	8	6.165	4.0	-15.2	0.01	-6.9	0.01		
G3-5	9	6.987	4.8	-13.8	0.00	-6.8	0.01		
G3-5	10	7.809	6.0	-9.9	0.01	-5.0	0.02		
G3-5	11	8.631	7.8	-9.8	0.00	-6.0	0.01		
C3-6	0	0.000	0.0	-14.2	0.01	-7.7	0.01	Used 2 linear regressions	
C3-6	1	0.531	0.4	-17.8	0.02	-7.8	0.03	0-2.69	m1
C3-6	2	1.592	1.2	-13.6	0.01	-7.0	0.04		b1
C3-6	3	2.653	2.0	-12.6	0.02	-6.6	0.04	2.69 to 3.02	m2
C3-6	4	3.714	3.4	-12.5	0.01	-7.0	0.07		b2
C3-6	5	4.775	4.0	-12.7	0.02	-7.0	0.01	3.02 to4.85	m3

Specimen	Sample Number	Calculated Increment Distance	Calculated Age	$\delta^{13}C$‰ VPDB	±	$\delta^{18}O$‰ VPDB	±	Equation parameters	
C3-6	6	5.836	6.7	-12.6	0.01	-7.3	0.03		b3
								4.85 and up	m4
									b4
									tl
C4-6	0	0.000						C4-6	
C4-6	1	0.601	1.2	-15.7	0.01	-7.1	0.01	Linf	9.60
C4-6	2	1.802	1.6	-16.8	0.01	-11.3	0.03	K	0.37
C4-6	3	3.003	2.1	-13.6	0.02	-7.2	0.01	t0	1.04
C4-6	4	4.204	2.6	-12.9	0.02	-9.7	0.02	tl	9.61
C4-6	5	5.405	3.3	-10.9	0.02	-8.2	0.04		
C4-6	6	6.606	4.2	-9.7	0.01	-7.1	0.01		
C4-6	7	7.807	5.6	-9.1	0.02	-6.9	0.04		
C4-6	8	9.008	8.6	-8.7	0.00	-8.0	0.01		
G3-7*	0	0.000	0.0	-18.1	0.02	-9.6	0.04	G3-7 mm	
G3-7*	1	0.544	1.0	-16.0	0.00	-7.7	0.00	Linf	11.21
G3-7*	2	1.633	1.8	-14.9	0.01	-8.0	0.01	K	0.13
G3-7*	3	2.722	2.8	-14.1	0.01	-7.9	0.01	t0	0.62
G3-7*	4	3.811	3.8	-13.2	0.01	-7.7	0.01	tl	9.80
G3-7*	5	4.900	5.0	-11.4	0.00	-8.1	0.01		
G3-7*	6	5.989	6.5	-10.6	0.01	-8.3	0.01		
G3-7*	7	7.078	8.3	-9.7	0.01	-8.1	0.01		
G3-7*	8	8.167	10.7	-9.1	0.01	-7.9	0.01		
G3-7*	9	9.256	14.1	-10.4	0.01	-8.0	0.02		
E4-7	0		0.0	-15.5	0.01	-7.7	0.02	E4-7	
E4-7	1	0.713	1.7					Linf	9.28
E4-7	2	2.139	2.7	-15.3	0.02	-7.9	0.05	K	0.18
E4-7	3	3.564	4.0					t0	1.27
E4-7	4	4.990	5.6	-12.8	0.03	-6.8	0.04	tl	9.98
E4-7	5	6.416	7.8	-11.3	0.02	-6.5	0.03		
E4-7	6	7.841	11.6	-9.5	0.01	-7.7	0.01		
E4-7	7	9.267	20.0	-8.6	0.00	-7.8	0.01		
G3-8	0	0.000	0.0	-15.7	0.01	-7.3	0.03	G3-8	
G3-8	1	0.658	0.7	-16.0	0.01	-7.7	0.01	Used 2 linear regressions	
G3-8	2	1.973	1.7	-15.8	0.00	-7.9	0.01	0-1.93	m1
G3-8	3	3.288	4.5	-14.9	0.00	-7.8	0.01		b1
G3-8	4	4.603	7.3	-12.2	0.00	-7.6	0.01	1.93 up	m2
G3-8	5	5.918	10.1	-10.1	0.01	-7.2	0.01		b2

Specimen	Sample Number	Calculated Increment Distance	Calculated Age	$\delta^{13}C$‰ VPDB	±	$\delta^{18}O$‰ VPDB	±	Equation parameters	
G3-8	6	7.233	12.9	-8.3	0.02	-7.9	0.02		tl
D3-10	0	0.000	0.0	-17.9	0.01	-8.8	0.04	D3-10	
D3-10	1	0.536	0.6	-16.0	0.01	-10.0	0.02	Linf	6.25
D3-10	2	1.608	1.8	-15.1	0.01	-8.2	0.01	K	0.29
D3-10	3	2.680	3.2	-13.5	0.01	-7.7	0.00	t0	1.28
D3-10	4	3.752	4.4	-12.6	0.00	-8.1	0.01	tl	6.43
D3-10	5	4.824	6.4	-9.6	0.01	-7.5	0.01		
D3-10	6	5.896	11.2						
F4-11*	0	0.000	0.0	-14.2	0.01	-7.7	0.01	F4-11	
F4-11*	1	0.622	0.5	-17.8	0.01	-6.8	0.02	Used 2 linear regressions	
F4-11*	2	1.867	1.7	-17.6	0.01	-6.0	0.01	0-6.25	m1
F4-11*	3	3.112	2.8	-16.9	0.01	-5.8	0.01		b1
F4-11*	4	4.357	4.0					6.25 and up	m2
F4-11*	5	5.602	5.1	-11.5	0.01	-6.9	0.01		b2
F4-11*	6	6.846	8.7	-12.3	0.04	-13.9	0.04		tl
F4-11*	7	8.091	14.0	-9.1	0.00	-8.0	0.01		
H4-12*	0	0.000						H4-12	
H4-12*	1	0.510	0.4	-15.3	0.01	-7.3	0.02	Used 2 linear regressions	
H4-12*	2	1.530	1.3	-15.6	0.01	-8.8	0.01	0-5	m1
H4-12*	3	2.549	2.2	-13.7	0.01	-6.7	0.01		b1
H4-12*	4	3.569	3.0	-10.5	0.01	-6.9	0.02	5 to 21	m2
H4-12*	5	4.589	5.0	-10.4	0.01	-7.1	0.02		b2
H4-12*	6	5.609	7.0	-9.3	0.01	-6.5	0.01		tl
F4-16*	0							F4-16	
F4-16*	1	0.544	0.7	-17.6		-7.3		Used 2 linear regressions	
F4-16*	2	1.633	1.4	-15.4		-7.0		0-5	m1
F4-16*	3	2.721	2.2	-13.1		-6.1			b1
F4-16*	4	3.809	2.9					5 to 21	m2
F4-16*	5	4.898	3.7	-12.1		-7.3			b2
F4-16*	6	5.986	4.4	-10.3		-7.4			tl
F4-16*	7	7.074	7.3	-9.8		-7.0			
F4-16*	8	8.163	11.3	-9.7		-7.0			
F4-16*	9	9.251	15.4						
F4-16*	10	10.339	19.4	-8.8		-7.2			
G3-16*	0	0.000	0.0	-13.8	0.03	-7.7	0.02	G3-16	
G3-16*	1	0.509	0.1	-15.0	0.01	-6.8	0.02	Linf	8.09

Specimen	Sample Number	Calculated Increment Distance	Calculated Age	$\delta^{13}C$‰ VPDB	±	$\delta^{18}O$‰ VPDB	±	Equation parameters	
G3-16*	2	1.527	0.5	-15.5	0.01	-6.9	0.02	K	0.37
G3-16*	3	2.545	0.9	-12.5	0.00	-6.9	0.02	t0	-0.10
G3-16*	4	3.563	1.5	-11.4	0.01	-7.1	0.03	tl	8.14
G3-16*	5	4.581	2.2	-10.7	0.01	-7.2	0.03		
G3-16*	6	5.599	3.1	-10.4	0.02	-6.8	0.01		
G3-16*	7	6.617	4.5						
G3-16*	8	7.635	7.7	-9.7	0.01	-7.7	0.02		

Table A4—Tabulated high-resolution intra-otolith $\delta^{13}C$ values of *Aplodinotus grunniens* utilized in chapter 3.

Specimen/ Sample Number	Calc Age	$\delta^{13}C$‰ VPDB	±	$\delta^{18}O$‰ VPDB	±	Calc Age	$\delta^{13}C$‰ VPDB	±	$\delta^{18}O$‰ VPDB	±
F4-1										
14	0.36	-13.0	0.01	-6.4	0.01	0.00	-16.0	0.03	-8.8	0.02
18	0.39	-12.9	0.01	-6.7	0.01	0.17	-16.7	0.01	-9.2	0.05
21.5	0.42	-12.7	0.01	-6.8	0.02	0.24	-16.9	0.01	-9.1	0.03
30	0.50	-13.3	0.02	-7.3	0.04	0.29	-16.7	0.02	-9.4	0.02
38	0.59	-16.8	0.02	-8.6	0.03	0.34	-17.6	0.02	-9.4	0.03
40	0.61	-17.1	0.02	-8.6	0.01	0.38	-17.5	0.02	-9.4	0.04
41	0.63	-17.1	0.01	-8.6	0.01	0.42	-17.7	0.01	-9.4	0.02
42	0.64	-17.2	0.01	-8.4	0.02	0.50	-17.3	0.02	-9.3	0.02
44	0.66	-17.4	0.03	-8.6	0.01	0.52	-17.9	0.01	-9.3	0.02
45	0.68	-17.2	0.01	-8.6	0.02	0.54	-17.7	0.01	-9.2	0.02
46	0.69	-17.4	0.02	-8.7	0.03	0.57	-17.6	0.01	-9.1	0.05
51	0.77	-17.1	0.03	-8.4	0.04	0.59	-17.6	0.01	-9.2	0.01
60	0.92	-15.8	0.01	-7.2	0.02	0.61	-17.2	0.03	-9.3	0.02
64	1.00	-15.1	0.01	-6.7	0.03	0.63	-17.3	0.02	-9.3	0.02
65	1.02	-14.4	0.01	-6.5	0.04	0.67	-17.2	0.02	-9.0	0.03
66	1.05	-14.5	0.01	-6.6	0.02	0.70	-16.9	0.02	-9.2	0.02
67	1.07	-12.9	0.02	-6.6	0.01	0.74	-16.7	0.01	-8.8	0.04
68	1.09	-13.9	0.02	-6.8	0.02	0.76	-16.9	0.01	-8.6	0.04
70	1.14	-13.5	0.02	-6.9	0.02	0.80	-17.0	0.03	-8.5	0.04
72	1.18	-13.5	0.01	-7.3	0.02	0.83	-16.8	0.02	-8.5	0.02
76	1.29	-14.4	0.01	-7.9	0.02	0.85	-17.0	0.05	-8.2	0.01
78	1.34	-15.6	0.00	-8.5	0.02	0.87	-16.4	0.02	-8.4	0.04
79	1.37	-15.8	0.02	-8.3	0.03	0.89	-15.9	0.02	-8.0	0.01

Specimen/ Sample Number	Calc Age	$\delta^{13}C$‰ VPDB	±	$\delta^{18}O$‰ VPDB	±	Calc Age	$\delta^{13}C$‰ VPDB	±	$\delta^{18}O$‰ VPDB	±
80	1.40	-16.3	0.02	-8.5	0.01	0.91	-15.3	0.01	-7.7	0.03
81	1.42	-16.7	0.00	-8.5	0.02	0.93	-15.2	0.00	-7.2	0.02
82	1.43	-16.9	0.02	-8.3	0.08	0.96	-15.0	0.01	-7.0	0.03
85	1.50	-17.3	0.02	-8.5	0.03	0.98	-14.9	0.01	-6.8	0.04
88	1.56	-17.5	0.02	-8.3	0.04	1.00	-13.8	0.01	-6.7	0.02
90	1.61	-17.6	0.00	-8.2	0.04	1.02	-13.8	0.00	-6.8	0.02
92	1.65	-17.0	0.02	-8.0	0.04	1.04	-13.5	0.02	-7.0	0.06
98	1.80	-15.2	0.01	-7.2	0.04	1.07	-12.9	0.02	-7.4	0.05
100	1.85	-13.8	0.02	-7.2	0.02	1.09	-12.6	0.01	-7.8	0.05
101	1.87	-14.8	0.04	-6.8	0.03	1.11	-12.3	0.02	-7.8	0.02
103	1.93	-13.7	0.01	-7.0	0.02	1.13	-12.7	0.02	-8.4	0.04
104	1.95	-12.7	0.01	-7.0	0.01	1.15	-13.4	0.02	-9.0	0.05
105	1.98	-12.8	0.02	-7.1	0.01	1.17	-13.7	0.01	-8.7	0.03
108	2.07	-11.2	0.32	-7.2	0.03	1.20	-14.0	0.02	-9.1	0.01
110	2.12	-11.7	0.00	-7.6	0.01	1.22	-14.7	0.01	-9.3	0.04
112	2.18	-11.4	0.01	-7.5	0.03	1.24	-14.8	0.02	-9.0	0.02
115	2.28	-11.5	0.01	-7.7	0.03	1.26	-15.0	0.01	-9.4	0.02
120	2.44	-12.7	0.01	-8.0	0.03	1.28	-16.2	0.01	-9.8	0.05
125	2.52	-13.0	0.01	-8.0	0.03	1.30	-17.0	0.02	-9.7	0.02
129	2.58	-12.6	0.02	-7.9	0.02	1.37	-17.3	0.02	-9.8	0.01
131	2.61	-13.8	0.03	-8.2	0.03	1.52	-16.8	0.03	-10.2	0.02
134	2.66	-13.7	0.01	-8.0	0.02	1.54	-16.7	0.01	-10.1	0.05
140	2.76	-14.2	0.01	-7.9	0.02	1.57	-16.6	0.01	-9.8	0.02
145	2.85	-14.2	0.01	-7.8	0.04	1.59	-16.6	0.01	-9.6	0.02
150	2.94	-14.5	0.02	-7.8	0.01	1.61	-16.3	0.01	-9.5	0.03
158	3.09	-13.5	0.01	-7.2	0.01	1.63	-16.6	0.02	-9.4	0.02
159	3.11	-14.0	0.02	-7.2	0.02	1.65	-16.5	0.02	-9.2	0.03
160	3.13	-13.2	0.02	-7.1	0.02	1.67	-16.3	0.03	-9.2	0.03
161	3.15	-13.6	0.01	-7.2	0.01	1.70	-16.4	0.01	-8.9	0.02
162	3.18	-13.2	0.01	-7.2	0.01	1.72	-16.2	0.01	-8.7	0.01
167	3.31	-13.0	0.02	-7.5	0.02	1.78	-15.8	0.01	-8.6	0.02
170	3.40	-13.5	0.02	-8.2	0.04	1.80	-15.3	0.01	-7.5	0.01
177	3.60	-13.8	0.01	-8.3	0.02	1.89	-15.3	0.03	-7.0	0.01
178	3.63	-14.1	0.02	-8.4	0.04	1.91	-14.4	0.01	-6.9	0.01
179	3.66	-14.0	0.02	-8.4	0.05	1.93	-13.9	0.00	-6.7	0.02
180	3.69	-14.0	0.01	-8.4	0.03	1.98	-13.5	0.01	-6.7	0.02
181	3.72	-14.3	0.02	-8.0	0.03	2.00	-13.1	0.02	-6.4	0.01
182	3.75	-14.1	0.02	-8.3	0.03	2.02	-13.2	0.02	-6.8	0.02

Specimen/ Sample Number	Calc Age	$\delta^{13}C$‰ VPDB	±	$\delta^{18}O$‰ VPDB	±	Calc Age	$\delta^{13}C$‰ VPDB	±	$\delta^{18}O$‰ VPDB	±
191	4.04	-13.8	0.00	-7.9	0.07	2.04	-13.3	0.02	-7.5	0.02
200	4.35	-13.3	0.01	-7.5	0.02	2.07	-13.6	0.02	-7.7	0.03
205	4.47	-12.2	0.01	-7.6	0.02	2.11	-13.6	0.02	-8.2	0.03
210	4.61	-11.8	0.02	-7.5	0.02	2.16	-13.9	0.02	-8.8	0.03
220	4.88	-11.7	0.02	-7.0	0.03	2.22	-13.9	0.02	-8.6	0.03
227	5.08	-11.3	0.02	-6.9	0.06	2.24	-13.9	0.01	-9.1	0.01
228	5.11	-11.5	0.03	-7.1	0.03	2.29	-13.9	0.01	-9.0	0.02
230	5.17	-11.6	0.03	-7.2	0.01	2.31	-13.8	0.01	-9.0	0.02
232	5.23	-11.4	0.02	-7.1	0.04	2.36	-14.3	0.02	-9.0	0.02
234	5.29	-11.6	0.03	-7.0	0.02	2.38	-14.4	0.01	-9.0	0.04
236	5.35	-11.1	0.05	-6.9	0.04	2.40	-14.4	0.02	-8.9	0.04
238	5.41	-11.0	0.03	-6.5	0.02	2.42	-14.3	0.01	-8.8	0.02
239	5.44	-10.6	0.02	-7.2	0.03	2.44	-14.4	0.01	-8.5	0.03
240	5.48	-10.8	0.04	-6.7	0.02	2.47	-14.2	0.01	-8.6	0.02
241	5.58	-11.3	0.02	-6.4	0.02	2.49	-14.0	0.02	-8.6	0.02
242	5.70	-10.7	0.01	-8.3	0.03	2.51	-14.3	0.02	-8.6	0.02
244	5.93	-11.2	0.01	-7.2	0.03	2.51	-14.0	0.02	-8.7	0.01
250	6.67	-10.0	0.02	-7.2	0.02	2.53	-14.1	0.01	-8.6	0.03
251	6.80	-9.8	0.01	-7.1	0.02	2.56	-14.0	0.02	-8.3	0.04
252	6.94	-9.8	0.01	-7.2	0.04	2.58	-13.8	0.02	-8.5	0.03
253	7.08	-10.0	0.03	-7.4	0.05	2.60	-13.4	0.02	-8.5	0.02
						2.62	-13.3	0.01	-8.2	0.02
						2.64	-13.0	0.01	-8.3	0.03
						2.67	-12.8	0.03	-7.8	0.02
						2.69	-12.9	0.04	-8.2	0.03
						2.71	-12.7	0.02	-8.2	0.03
						2.73	-13.2	0.02	-8.3	0.01
						2.76	-13.1	0.01	-8.3	0.03
						2.78	-12.9	0.02	-8.0	0.02
						2.80	-13.1	0.01	-8.3	0.01
						2.82	-12.6	0.02	-8.0	0.03
						2.84	-12.7	0.02	-7.8	0.04
						2.87	-12.7	0.02	-7.9	0.05
						2.89	-12.4	0.02	-7.6	0.02
						2.91	-12.2	0.02	-7.2	0.04
						2.93	-11.8	0.02	-7.2	0.04
						2.96	-11.8	0.02	-7.5	0.03
						2.98	-11.4	0.01	-7.1	0.03

Specimen/ Sample Number	Calc Age	$\delta^{13}C$‰ VPDB	±	$\delta^{18}O$‰ VPDB	±	Calc Age	$\delta^{13}C$‰ VPDB	±	$\delta^{18}O$‰ VPDB	±
						3.00	-11.1	0.01	-6.5	0.02
						3.04	-10.7	0.02	-6.8	0.04
						3.07	-10.5	0.03	-7.1	0.02
						3.11	-10.5	0.03	-7.1	0.04
						3.14	-10.5	0.02	-7.9	0.02
						3.18	-10.3	0.02	-7.7	0.08
						3.21	-10.5	0.02	-8.1	0.02
						3.25	-10.3	0.03	-8.1	0.02
						3.29	-10.5	0.02	-8.5	0.03
						3.32	-10.5	0.02	-8.5	0.03
						3.36	-10.0	0.01	-8.6	0.03
						3.46	-10.1	0.01	-8.4	0.04
						3.57	-10.2	0.01	-8.6	0.04
						3.73	-9.7	0.04	-8.3	0.02
						3.80	-9.3	0.02	-7.8	0.02
						3.88	-9.0	0.03	-7.5	0.03
						3.93	-9.6	0.01	-6.8	0.02
						3.96	-9.5	0.01	-6.7	0.05
						4.00	-9.6	0.04	-6.3	0.03
						4.14	-9.1	0.02	-6.9	0.03
						4.22	-8.9	0.02	-8.0	0.04
						4.29	-8.8	0.02	-8.3	0.04
						4.29	-9.2	0.01	-8.3	0.03
						4.41	-9.2	0.03	-8.5	0.03
						4.45	-9.0	0.02	-8.4	0.06
						4.51	-8.9	0.02	-8.2	0.05
						4.59	-9.1	0.02	-8.2	0.03
						4.67	-9.0	0.02	-8.2	0.02
						4.84	-8.3	0.03	-7.3	0.04
						4.92	-9.1	0.03	-6.2	0.03
						5.00	-9.5	0.01	-6.3	0.05
						5.14	-9.8	0.02	-7.5	0.04
						5.29	-9.9	0.02	-8.1	0.02
						5.43	-9.5	0.02	-8.3	0.02
						5.57	-9.0	0.01	-8.1	0.04
						5.71	-8.8	0.01	-7.8	0.03
						5.86	-8.3	0.02	-7.3	0.04
						6.00	-8.6	0.02	-6.3	0.05

Specimen/ Sample Number	Calc Age	$\delta^{13}C$‰ VPDB	±	$\delta^{18}O$‰ VPDB	±	Calc Age	$\delta^{13}C$‰ VPDB	±	$\delta^{18}O$‰ VPDB	±
						6.20	-8.7	0.02	-7.0	0.02
						6.41	-8.7	0.02	-6.8	0.01
						6.61	-8.5	0.01	-7.8	0.03
						6.81	-8.2	0.01	-7.8	0.02
						7.01	-8.0	0.02	-7.5	0.02
						7.22	-8.2	0.01	-7.2	0.04
						7.42	-8.6	0.01	-6.8	0.04
						7.62	-8.5	0.02	-7.2	0.04
						7.82	-8.8	0.01	-7.3	0.02
						8.03	-8.9	0.02	-7.1	0.03
						8.63	-9.0	0.02	-7.3	0.01
						9.44	-9.2	0.01	-7.7	0.02
						10.05	-8.9	0.02	-7.7	0.03
						10.25	-8.6	0.01	-7.5	0.01
						10.46	-8.6	0.02	-6.8	0.01
						10.66	-8.5	0.03	-6.8	0.06
						10.86	-8.5	0.02	-7.1	0.04
						11.06	-8.1	0.01	-7.6	0.05
						11.27	-7.7	0.01	-7.1	0.03
						11.47	-8.4	0.01	-6.9	0.03
						11.67	-8.4	0.01	-7.2	0.05
						11.87	-9.0	0.02	-7.8	0.04
						12.08	-9.0	0.01	-8.2	0.07
						12.28	-9.3	0.01	-8.0	0.01
						12.48	-9.7	0.03	-7.7	0.04
						12.68	-9.4	0.02	-7.9	0.01
						12.89	-8.7	0.04	-8.2	0.04
						13.09	-8.7	0.03	-7.7	0.05
						13.29	-8.7	0.01	-7.0	0.06
						13.49	-8.9	0.03	-7.3	0.03
						13.70	-8.7	0.03	-7.5	0.02
						13.90	-7.8	0.01	-7.0	0.03
						14.10	-7.7	0.01	-6.5	0.03
						14.30	-8.3	0.01	-7.0	0.01
						14.51	-7.9	0.02	-7.3	0.03
						14.71	-7.4	0.02	-7.2	0.04
						14.91	-7.9	0.01	-6.7	0.06
						15.11	-7.9	0.01	-7.3	0.03

Specimen/ Sample Number	Calc Age	δ^{13}C‰ VPDB	±	δ^{18}O‰ VPDB	±	Calc Age	δ^{13}C‰ VPDB	±	δ^{18}O‰ VPDB	±
						15.52	-7.3	0.01	-7.3	0.04
						15.92	-7.9	0.02	-7.4	0.02
						16.13	-7.8	0.01	-6.9	0.01
						16.33	-7.8	0.01	-6.7	0.03
						16.63	-7.9	0.03	-8.1	0.05
						16.89	-8.6	0.02	-7.5	0.06
						16.99	-8.7	0.01	-7.6	0.03
						17.09	-8.8	0.06	-8.2	0.06
						17.39	-8.4	0.04	-8.0	0.05
						17.70	-8.6	0.02	-8.0	0.04
						17.80	-9.3	0.01	-7.7	0.03
						18.00	-9.4	0.03	-7.7	0.03

Specimen D3-3

Sample Number	Calc Age	δ^{13}C‰ VPDB	±	δ^{18}O‰VPDB	±	Calc Age	δ^{13}C‰ VPDB	±	δ^{18}O‰VPDB	±
2	0.11	-16.7	0.01	-8.3	0.03	0.55	-20.2	0.04	-8.8	0.03
6.5	0.36	-18.0	0.02	-8.5	0.03	0.68	-18.7	0.01	-8.6	0.03
9.5	0.53	-17.6	0.01	-8.4	0.03	0.78	-16.9	0.02	-8.3	0.02
13.5	0.76	-12.1	0.02	-8.3	0.05	0.83	-16.4	0.02	-8.3	0.01
17.5	0.98	-16.8	0.01	-8.3	0.01	0.89	-16.1	0.01	-8.2	0.02
25.5	1.43	-15.7	0.02	-8.3	0.05	1.00	-15.5	0.01	-7.6	0.00
35	1.96	-14.0	0.04	-7.1	0.02	1.01	-15.3	0.01	-7.4	0.03
43	2.41	-12.8	0.02	-6.4	0.05	1.02	-14.6	0.01	-7.2	0.03
45	2.52	-12.6	0.00	-6.3	0.01	1.03	-14.8	0.01	-7.3	0.02
45.5	2.55	-12.4	0.01	-6.1	0.01	1.05	-14.4	0.01	-7.3	0.02
48	2.69	-11.6	0.02	-5.8	0.03	1.06	-14.5	0.01	-7.3	0.06
49	2.74	-11.6	0.02	-6.0	0.01	1.07	-14.6	0.02	-7.5	0.04
50	2.80	-12.2	0.01	-6.6	0.02	1.08	-14.6	0.02	-7.5	0.03
51	2.84	-12.3	0.02	-6.9	0.02	1.10	-15.1	0.02	-7.7	0.03
55	3.01	-12.3	0.03	-7.6	0.01	1.11	-15.3	0.03	-7.8	0.01
56	3.05	-12.4	0.01	-7.7	0.02	1.13	-15.5	0.01	-7.8	0.01
57	3.09	-12.5	0.00	-7.8	0.04	1.14	-15.9	0.02	-8.0	0.02
58	3.13	-12.7	0.00	-7.8	0.05	1.16	-16.0	0.02	-7.9	0.02
59	3.17	-12.8	0.01	-7.6	0.04	1.17	-16.4	0.02	-8.0	0.03
60	3.21	-13.0	0.01	-7.6	0.02	1.25	-17.3	0.02	-8.3	0.02
67	3.50	-14.7	0.01	-7.0	0.02	1.29	-18.3	0.02	-8.6	0.02
70	3.62	-14.4	0.01	-7.0	0.00	1.31	-18.4	0.01	-8.6	0.04

Specimen/ Sample Number	Calc Age	$\delta^{13}C$‰ VPDB	±	$\delta^{18}O$‰ VPDB	±	Calc Age	$\delta^{13}C$‰ VPDB	±	$\delta^{18}O$‰ VPDB	±
78	3.95	-12.0	0.02	-6.6	0.02	1.32	-18.5	0.01	-8.8	0.01
79	3.99	-11.6	0.01	-6.4	0.02	1.33	-18.4	0.01	-8.8	0.04
80	4.03	-11.4	0.01	-5.7	0.02	1.35	-18.3	0.01	-8.8	0.04
81	4.07	-11.2	0.00	-6.2	0.02	1.36	-18.2	0.02	-8.7	0.02
82	4.11	-11.2	0.02	-6.0	0.01	1.38	-18.3	0.03	-8.7	0.03
83	4.15	-11.2	0.03	-5.8	0.03	1.39	-18.2	0.02	-8.6	0.01
84	4.19	-11.2	0.02	-5.6	0.03	1.47	-18.3	0.01	-8.6	0.04
85	4.24	-11.4	0.01	-5.5	0.01	1.55	-18.2	0.01	-8.6	0.02
86	4.28	-11.3	0.01	-5.4	0.03	1.63	-17.6	0.01	-8.2	0.01
87	4.32	-11.2	0.02	-5.2	0.01	1.72	-16.3	0.01	-7.8	0.01
89	4.40	-11.5	0.01	-5.3	0.02	1.81	-15.7	0.01	-7.1	0.03
90	4.44	-11.4	0.01	-5.2	0.02	1.89	-15.1	0.04	-6.9	0.03
91	4.47	-11.1	0.01	-5.9	0.02	1.91	-14.8	0.02	-6.9	0.02
95	4.59	-11.5	0.01	-6.7	0.02	1.93	-14.0	0.01	-6.9	0.03
96	4.62	-11.6	0.01	-6.4	0.05	1.96	-14.5	0.01	-7.0	0.02
97	4.65	-11.7	0.01	-7.0	0.01	2.00	-14.2	0.00	-7.4	0.01
98	4.68	-11.8	0.02	-7.2	0.04	2.05	-13.7	0.02	-7.5	0.06
102	4.80	-11.2	0.02	-6.5	0.05	2.07	-14.0	0.01	-7.4	0.02
103	4.83	-12.7	0.02	-7.6	0.02	2.15	-14.0	0.01	-8.0	0.02
104	4.86	-12.9	0.01	-7.6	0.06	2.24	-15.0	0.02	-8.0	0.03
105	4.89	-12.9	0.02	-7.5	0.04	2.33	-16.2	0.03	-8.6	0.03
106	4.92	-13.3	0.01	-7.5	0.02	2.33	-16.1	0.02	-8.5	0.02
107	4.95	-13.1	0.01	-7.1	0.02	2.37	-16.9	0.01	-8.6	0.01
111	5.07	-13.1	0.01	-7.0	0.03	2.42	-16.7	0.02	-8.6	0.02
111	5.07	-13.1	0.01	-7.0	0.03	2.44	-16.7	0.02	-8.5	0.03
113	5.13	-12.5	0.01	-6.9	0.02	2.46	-17.4	0.01	-8.3	0.05
114	5.16	-12.6	0.01	-6.9	0.02	2.48	-17.3	0.04	-8.1	0.05
115	5.19	-12.0	0.02	-7.1	0.02	2.52	-17.1	0.01	-8.0	0.01
119	5.31	-11.2	0.01	-7.3	0.02	2.62	-16.6	0.01	-7.8	0.02
120	5.34	-11.3	0.01	-7.2	0.02	2.66	-16.0	0.02	-7.6	0.02
120	5.34	-11.3	0.01	-7.2	0.02	2.76	-14.9	0.01	-6.9	0.04
121	5.37	-11.1	0.01	-7.1	0.02	2.81	-14.3	0.01	-6.6	0.03
123	5.43	-10.6	0.05	-7.0	0.03	2.83	-14.4	0.03	-6.7	0.02
124	5.46	-10.7	0.00	-6.9	0.02	2.85	-14.4	0.04	-6.7	0.03
125	5.49	-10.4	0.01	-6.9	0.01	2.95	-14.1	0.01	-6.7	0.04
127	5.55	-10.2	0.01	-7.1	0.01	3.07	-13.7	0.01	-6.8	0.03
128	5.58	-10.3	0.01	-7.4	0.01	3.20	-14.0	0.02	-6.8	0.02
129	5.61	-10.5	0.01	-7.6	0.02	3.28	-14.0	0.01	-6.8	0.03

Specimen/ Sample Number	Calc Age	$\delta^{13}C$‰ VPDB	±	$\delta^{18}O$‰ VPDB	±	Calc Age	$\delta^{13}C$‰ VPDB	±	$\delta^{18}O$‰ VPDB	±
129	5.61	-10.5	0.01	-7.6	0.02	3.34	-14.0	0.02	-6.9	0.04
130	5.64	-10.8	0.02	-7.4	0.03	3.36	-14.1	0.05	-6.9	0.04
130	5.64	-10.8	0.02	-7.4	0.03	3.39	-14.2	0.01	-6.9	0.03
131	5.67	-11.3	0.02	-7.9	0.04	3.42	-14.3	0.01	-6.8	0.02
131	5.67	-11.3	0.02	-7.9	0.04	3.53	-14.5	0.01	-6.7	0.02
132	5.70	-11.2	0.01	-8.0	0.01	3.59	-14.4	0.02	-6.7	0.04
133	5.73	-11.6	0.02	-8.2	0.05	3.77	-14.3	0.01	-6.5	0.03
134	5.76	-12.0	0.01	-8.3	0.02	3.90	-13.3	0.01	-6.4	0.04
135	5.79	-11.2	0.01	-8.8	0.02	3.99	-13.1	0.00	-6.7	0.01
138	5.83	-12.3	0.03	-8.5	0.04	4.05	-12.7	0.03	-6.6	0.03
139	5.85	-12.0	0.02	-8.3	0.02	4.10	-12.4	0.02	-6.3	0.04
140	5.86	-12.3	0.00	-8.2	0.04	4.16	-12.7	0.04	-7.0	0.02
143	5.90	-12.2	0.02	-8.0	0.02	4.22	-12.5	0.02	-7.2	0.01
145	5.93	-11.9	0.01	-7.4	0.02	4.25	-12.5	0.03	-7.2	0.05
148	5.97	-12.0	0.02	-7.1	0.03	4.31	-12.5	0.02	-7.8	0.03
150	6.00	-11.9	0.01	-7.0	0.02	4.37	-12.5	0.02	-8.0	0.01
152	6.03	-11.4	0.03	-6.3	0.05	4.44	-12.5	0.01	-8.4	0.02
153	6.04	-11.7	0.04	-6.4	0.03	4.53	-12.6	0.01	-8.5	0.03
154	6.06	-11.7	0.02	-6.9	0.02	4.59	-12.5	0.02	-8.4	0.04
155	6.07	-11.6	0.03	-6.2	0.04	4.66	-12.6	0.01	-8.5	0.03
156	6.08	-11.4	0.01	-6.3	0.04	4.69	-12.6	0.01	-8.6	0.04
157	6.10	-10.7	0.02	-6.6	0.03	4.76	-12.5	0.01	-8.2	0.02
160	6.14	-11.2	0.01	-6.6	0.02	4.79	-12.6	0.03	-8.4	0.04
165	6.21	-11.7	0.01	-7.0	0.01	4.90	-12.5	0.03	-7.8	0.03
						5.07	-11.9	0.02	-7.0	0.04
						5.14	-11.7	0.02	-6.9	0.05
						5.18	-11.8	0.02	-7.1	0.00
						5.22	-11.9	0.02	-7.2	0.03
						5.25	-11.8	0.02	-7.2	0.03

Specimen G3-5 Sample Number	Calc Age	$\delta^{13}C$‰ VPDB	±	$\delta^{18}O$‰VPDB	±	Calc Age	$\delta^{13}C$‰ VPDB	±	$\delta^{18}O$‰VPDB	±
3.5	0.59	-14.2	0.01	-8.4	0.03	0.39	-17.9	0.01	-7.5	0.03
8.5	0.65	-14.3	0.01	-8.0	0.01	0.40	-18.1	0.01	-7.6	0.03
11.5	0.69	-14.5	0.02	-7.6	0.01	0.44	-18.4	0.01	-7.4	0.01
13.5	0.71	-14.5	0.02	-7.6	0.01	0.48	-18.7	0.02	-7.6	0.02
15.5	0.74	-14.4	0.01	-7.5	0.01	0.51	-18.5	0.04	-7.9	0.02

Specimen/ Sample Number	Calc Age	$\delta^{13}C$‰ VPDB	±	$\delta^{18}O$‰ VPDB	±	Calc Age	$\delta^{13}C$‰ VPDB	±	$\delta^{18}O$‰ VPDB	±
19.5	0.80	-14.0	0.01	-7.4	0.02	0.54	-18.0	0.03	-7.9	0.04
29	0.95	-13.4	0.01	-7.1	0.04	0.60	-17.4	0.02	-8.0	0.01
30	0.96	-12.7	0.00	-6.0	0.01	0.63	-16.3	0.01	-7.9	0.02
39.5	1.15	-12.5	0.01	-6.2	0.04	0.67	-15.2	0.01	-7.8	0.02
41.5	1.19	-12.9	0.01	-6.7	0.01	0.70	-14.5	0.02	-7.7	0.02
43.5	1.23	-13.0	0.03	-6.5	0.02	0.73	-14.5	0.01	-7.7	0.03
45.5	1.28	-13.7	0.01	-7.5	0.03	0.77	-14.4	0.02	-7.6	0.02
48	1.34	-13.7	0.01	-7.7	0.03	0.81	-14.2	0.02	-7.5	0.04
49	1.36	-14.0	0.02	-8.1	0.03	0.88	-14.4	0.03	-7.4	0.04
50	1.39	-14.2	0.03	-8.2	0.03	0.96	-14.3	0.01	-7.2	0.01
51.5	1.43	-14.3	0.02	-8.3	0.02	0.98	-15.4	0.01	-6.4	0.03
53	1.47	-14.3	0.01	-8.4	0.04	1.01	-15.9	0.01	-6.5	0.03
56	1.55	-14.4	0.02	-8.0	0.02	1.04	-16.0	0.01	-6.4	0.03
62	1.73	-14.3	0.01	-7.3	0.03	1.07	-15.4	0.01	-6.2	0.04
69	1.96	-13.3	0.00	-6.4	0.03	1.09	-14.4	0.01	-5.7	0.04
70	2.00	-12.9	0.01	-6.1	0.01	1.12	-13.9	0.03	-5.5	0.05
72	2.04	-12.7	0.07	-5.6	0.06	1.15	-12.3	0.01	-5.0	0.02
73	2.06	-12.3	0.01	-5.3	0.01	1.25	-11.7	0.01	-5.5	0.02
74	2.07	-12.6	0.02	-6.0	0.05	1.34	-12.2	0.01	-6.8	0.01
80	2.19	-12.8	0.02	-6.6	0.02	1.34	-14.2	0.01	-7.9	0.02
85	2.29	-13.2	0.01	-7.2	0.05	1.36	-14.6	0.01	-8.0	0.03
90	2.39	-13.4	0.02	-7.6	0.01	1.38	-14.8	0.02	-8.0	0.01
91	2.42	-13.4	0.01	-7.8	0.03	1.40	-14.7	0.04	-8.0	0.08
92	2.44	-13.4	0.01	-7.9	0.02	1.42	-14.8	0.01	-8.0	0.02
93	2.46	-13.5	0.00	-8.0	0.04	1.45	-14.8	0.01	-7.9	0.03
94	2.48	-13.9	0.00	-8.2	0.02	1.56	-15.1	0.02	-8.0	0.05
97	2.55	-13.8	0.01	-7.7	0.02	1.67	-14.4	0.03	-7.5	0.04
98	2.57	-14.0	0.02	-7.8	0.01	1.75	-14.0	0.01	-7.1	0.01
99	2.59	-14.2	0.01	-7.9	0.01	1.77	-13.7	0.02	-6.9	0.01
100	2.62	-14.6	0.01	-8.0	0.03	1.80	-13.6	0.01	-7.0	0.02
100	2.62	-14.4	0.01	-8.0	0.01	1.83	-13.5	0.02	-6.8	0.03
102	2.67	-14.6	0.01	-8.0	0.02	1.85	-13.2	0.01	-6.7	0.04
104	2.71	-14.3	0.01	-7.8	0.03	1.88	-13.3	0.02	-6.9	0.04
104	2.71	-14.4	0.01	-7.6	0.01	1.94	-13.0	0.02	-6.8	0.01
110	2.86	-11.6	0.01	-6.2	0.03	2.02	-12.8	0.02	-6.9	0.01
112	2.91	-12.5	0.02	-6.6	0.03	2.12	-12.8	0.00	-6.9	0.02
114	2.96	-12.3	0.02	-6.8	0.02	2.15	-12.6	0.02	-7.0	0.01
116	3.01	-12.5	0.01	-6.7	0.06	2.18	-12.5	0.01	-7.1	0.02

Specimen/ Sample Number	Calc Age	$\delta^{13}C$‰ VPDB	±	$\delta^{18}O$‰ VPDB	±	Calc Age	$\delta^{13}C$‰ VPDB	±	$\delta^{18}O$‰ VPDB	±
118	3.06	-11.7	0.01	-6.8	0.02	2.21	-12.7	0.01	-7.2	0.02
120	3.11	-11.8	0.02	-6.9	0.01	2.24	-12.6	0.01	-7.2	0.06
123	3.19	-11.5	0.04	-7.7	0.04	2.28	-12.6	0.01	-6.7	0.04
125	3.24	-11.6	0.02	-7.8	0.07	2.31	-12.7	0.01	-7.2	0.04
130	3.38	-12.3	0.02	-8.3	0.02	2.34	-12.8	0.02	-7.1	0.06
133	3.47	-12.8	0.02	-8.3	0.03	2.45	-12.7	0.01	-7.0	0.01
134	3.50	-12.8	0.01	-8.4	0.01	2.52	-12.4	0.02	-6.9	0.04
135	3.52	-13.2	0.01	-8.3	0.01	2.60	-12.1	0.04	-6.9	0.04
136	3.55	-12.9	0.01	-8.4	0.01	2.64	-12.3	0.02	-7.3	0.03
137	3.58	-13.3	0.01	-8.3	0.03	2.88	-12.4	0.01	-7.4	0.03
140	3.67	-13.6	0.01	-8.2	0.01	2.92	-14.7	0.02	-8.1	0.02
145	3.83	-13.2	0.01	-7.9	0.03	2.96	-14.8	0.02	-7.6	0.04
149	3.96	-11.5	0.01	-7.0	0.01	3.01	-15.3	0.02	-8.3	0.01
150	3.99	-12.6	0.02	-6.9	0.04	3.05	-15.4	0.04	-8.3	0.04
152	4.04	-12.1	0.02	-6.8	0.01	3.14	-15.3	0.03	-8.2	0.04
153	4.07	-12.3	0.03	-6.8	0.02	3.28	-15.2	0.01	-8.2	0.01
154	4.09	-11.9	0.03	-6.4	0.06	3.48	-14.7	0.02	-7.8	0.01
155	4.12	-12.7	0.02	-6.9	0.05	3.64	-14.0	0.01	-7.2	0.02
156	4.15	-11.6	0.02	-6.7	0.02	3.80	-13.9	0.01	-6.5	0.02
157	4.17	-12.0	0.01	-6.7	0.02	3.86	-13.7	0.01	-5.6	0.03
158	4.20	-12.0	0.04	-6.7	0.04	3.91	-13.5	0.02	-5.3	0.01
159	4.23	-11.8	0.02	-7.0	0.06	3.97	-13.4	0.01	-5.2	0.01
160	4.25	-12.2	0.01	-7.2	0.01	4.03	-13.2	0.01	-5.2	0.02
165	4.39	-12.5	0.01	-7.5	0.01	4.15	-12.7	0.00	-5.3	0.02
170	4.53	-12.1	0.02	-8.0	0.01	4.35	-12.6	0.01	-5.6	0.01
176	4.70	-12.6	0.02	-8.2	0.03	4.40	-12.7	0.04	-6.5	0.04
177	4.73	-12.3	0.05	-8.4	0.05	4.59	-12.5	0.01	-6.9	0.02
178	4.76	-12.3	0.02	-8.1	0.02	4.90	-13.0	0.02	-8.1	0.05
179	4.79	-12.6	0.03	-8.3	0.05	5.00	-13.5	0.03	-8.4	0.03
180	4.82	-12.7	0.05	-8.2	0.02	5.06	-14.4	0.01	-8.6	0.05
181	4.85	-12.7	0.02	-8.0	0.00	5.11	-14.5	0.01	-8.7	0.02
185	4.98	-12.5	0.01	-7.6	0.03	5.19	-14.5	0.02	-8.6	0.03
189	5.11	-12.5	0.01	-7.4	0.02	5.28	-14.8	0.01	-8.7	0.03
190	5.14	-12.6	0.02	-7.3	0.02	5.34	-14.2	0.02	-8.1	0.05
191	5.17	-12.3	0.02	-7.4	0.02	5.39	-14.5	0.03	-8.4	0.03
192	5.20	-12.4	0.03	-7.3	0.03	5.69	-14.4	0.02	-8.0	0.03
						5.88	-13.8	0.02	-7.5	0.03
						5.94	-13.5	0.02	-7.3	0.06

Specimen/ Sample Number	Calc Age	$\delta^{13}C$‰ VPDB	±	$\delta^{18}O$‰ VPDB	±	Calc Age	$\delta^{13}C$‰ VPDB	±	$\delta^{18}O$‰ VPDB	±
						6.01	-13.3	0.01	-7.2	0.01
						6.07	-13.0	0.01	-6.9	0.07
						6.14	-13.5	0.03	-7.2	0.03
						6.34	-13.3	0.00	-7.3	0.04
						6.41	-13.3	0.03	-7.7	0.01
						6.47	-13.1	0.03	-7.5	0.02
							-13.2	0.01	-7.9	0.04

Specimen G3-7

Sample Number	Calc Age	$\delta^{13}C$‰ VPDB	±	$\delta^{18}O$‰VPDB	±	Calc Age	$\delta^{13}C$‰ VPDB	±	$\delta^{18}O$‰VPDB	±
2	0.42	-18.0	0.01	-8.1	0.04	0.97	-15.3	0.02	-7.4	0.02
7	0.48	-18.2	0.01	-8.1	0.02	1.02	-14.9	0.00	-7.0	0.03
13	0.56	-17.5	0.01	-8.3	0.03	1.07	-15.1	0.01	-7.0	0.01
15	0.59	-17.3	0.02	-8.3	0.03	1.11	-15.1	0.02	-7.0	0.02
17	0.62	-17.2	0.01	-8.5	0.02	1.15	-16.2	0.01	-7.4	0.03
18	0.63	-17.0	0.02	-8.5	0.01	1.17	-16.1	0.01	-7.4	0.02
25	0.76	-16.9	0.02	-7.5	0.02	1.19	-17.0	0.02	-7.7	0.01
29	0.84	-16.3	0.01	-7.2	0.02	1.27	-17.3	0.01	-8.1	0.02
34	0.95	-14.4	0.02	-6.7	0.02	1.29	-17.9	0.01	-8.3	0.02
36	0.98	-14.2	0.02	-6.3	0.01	1.32	-17.7	0.01	-8.2	0.01
38	1.01	-14.7	0.02	-6.7	0.01	1.35	-17.9	0.01	-8.2	0.03
46.5	1.12	-15.8	0.02	-8.0	0.02	1.38	-17.7	0.01	-8.0	0.06
50	1.18	-15.6	0.01	-7.7	0.03	1.40	-17.6	0.02	-8.0	0.02
51	1.19	-16.0	0.02	-8.4	0.04	1.46	-17.7	0.01	-7.9	0.02
53	1.22	-16.3	0.02	-8.4	0.03	1.72	-17.0	0.01	-7.7	0.01
54	1.24	-16.0	0.04	-8.2	0.04	1.83	-14.7	0.01	-7.3	0.03
55	1.25	-16.4	0.02	-8.2	0.02	1.87	-14.7	0.01	-7.4	0.03
56	1.27	-15.6	0.03	-7.9	0.05	1.91	-14.1	0.01	-7.3	0.03
58	1.30	-16.2	0.02	-7.9	0.01	1.99	-14.2	0.01	-7.5	0.02
60	1.34	-16.2	0.02	-7.9	0.01	2.03	-14.7	0.03	-7.7	0.03
62.5	1.38	-16.2	0.02	-7.8	0.02	2.11	-15.5	0.01	-8.0	0.02
64	1.41	-16.1	0.02	-7.9	0.04	2.16	-16.4	0.02	-8.4	0.01
65	1.43	-15.9	0.01	-7.8	0.02	2.18	-16.7	0.01	-8.6	0.01
67	1.47	-15.9	0.01	-7.7	0.01	2.23	-17.1	0.02	-8.5	0.02
68	1.49	-15.9	0.02	-7.8	0.03	2.26	-16.4	0.00	-8.3	0.03
69	1.51	-15.9	0.01	-7.8	0.01	2.31	-16.7	0.01	-8.3	0.02
70	1.53	-16.0	0.01	-7.9	0.04	2.36	-16.7	0.03	-8.2	0.03

Specimen/ Sample Number	Calc Age	$\delta^{13}C$‰ VPDB	±	$\delta^{18}O$‰ VPDB	±	Calc Age	$\delta^{13}C$‰ VPDB	±	$\delta^{18}O$‰ VPDB	±
72	1.57	-15.9	0.02	-8.0	0.02	2.41	-16.6	0.01	-7.9	0.06
75.5	1.64	-15.8	0.01	-8.1	0.03	2.63	-16.3	0.01	-8.1	0.02
77	1.67	-16.1	0.01	-8.4	0.02	2.69	-16.4	0.01	-7.8	0.03
78	1.69	-15.5	0.02	-8.1	0.02	2.87	-15.4	0.02	-7.6	0.03
79	1.72	-15.2	0.01	-8.0	0.01	2.90	-14.3	0.03	-6.7	0.02
80	1.74	-15.4	0.02	-8.1	0.02	2.94	-14.1	0.02	-6.5	0.04
82	1.78	-14.7	0.02	-7.8	0.01	2.97	-13.4	0.02	-5.9	0.03
84	1.83	-14.6	0.01	-7.7	0.03	3.00	-12.5	0.01	-5.8	0.00
86	1.88	-14.9	0.01	-7.5	0.04	3.03	-12.7	0.01	-6.1	0.03
92	2.03	-15.6	0.02	-6.8	0.02	3.14	-14.6	0.03	-7.5	0.02
93	2.06	-15.9	0.02	-6.7	0.06	3.28	-16.2	0.01	-7.8	0.03
94	2.08	-15.8	0.03	-6.6	0.04	3.32	-16.5	0.01	-7.8	0.02
95	2.11	-14.9	0.02	-6.4	0.01	3.36	-17.1	0.01	-7.8	0.02
97	2.15	-14.9	0.01	-6.7	0.03	3.38	-16.8	0.02	-7.8	0.01
98	2.17	-15.0	0.01	-6.8	0.03	3.40	-17.0	0.01	-7.8	0.03
100	2.20	-15.1	0.03	-7.2	0.03	3.42	-16.7	0.01	-7.7	0.02
106	2.32	-14.9	0.02	-7.9	0.01	3.48	-16.3	0.01	-7.5	0.03
108	2.36	-15.1	0.01	-8.0	0.04	3.68	-16.3	0.03	-6.6	0.03
110	2.40	-15.0	0.02	-8.0	0.03	3.70	-16.3	0.01	-6.6	0.02
112	2.44	-14.9	0.02	-8.1	0.02	3.73	-14.7	0.02	-5.6	0.01
113	2.46	-15.1	0.01	-8.1	0.03	3.75	-14.6	0.03	-5.9	0.03
114	2.48	-15.2	0.03	-8.1	0.04	3.77	-14.6	0.00	-5.9	0.01
115	2.51	-14.8	0.01	-7.8	0.03	3.80	-14.2	0.01	-5.9	0.02
116	2.53	-14.9	0.01	-7.9	0.01	3.82	-13.5	0.01	-5.8	0.02
118	2.57	-15.0	0.03	-7.8	0.02	3.84	-13.1	0.02	-5.7	0.02
120	2.62	-15.0	0.01	-7.6	0.02	3.87	-12.8	0.02	-6.1	0.03
125	2.73	-14.7	0.01	-7.1	0.02	3.89	-12.8	0.02	-6.5	0.02
128	2.80	-14.2	0.01	-6.7	0.02	3.94	-12.5	0.01	-7.1	0.03
130	2.85	-14.0	0.01	-6.9	0.04	4.01	-13.1	0.00	-7.4	0.01
131	2.87	-14.0	0.02	-6.6	0.03	4.09	-12.3	0.00	-7.4	0.01
132	2.90	-14.3	0.01	-6.5	0.02	4.19	-12.7	0.01	-8.1	0.03
133	2.92	-13.8	0.02	-6.7	0.03	4.22	-13.5	0.00	-8.3	0.03
134	2.95	-13.9	0.01	-6.8	0.01	4.25	-13.5	0.02	-8.3	0.01
135	2.97	-14.7	0.02	-6.9	0.01	4.29	-13.7	0.01	-8.4	0.03
136	2.99	-14.0	0.01	-6.8	0.03	4.32	-13.4	0.02	-8.2	0.03
137	3.01	-13.6	0.01	-7.1	0.03	4.36	-13.5	0.01	-8.3	0.02
139	3.05	-13.8	0.03	-6.6	0.01	4.53	-12.8	0.01	-7.7	0.01
140	3.07	-13.5	0.01	-7.3	0.01	4.64	-12.0	0.01	-6.9	0.03

Specimen/ Sample Number	Calc Age	$\delta^{13}C$‰ VPDB	±	$\delta^{18}O$‰ VPDB	±	Calc Age	$\delta^{13}C$‰ VPDB	±	$\delta^{18}O$‰ VPDB	±
141	3.09	-13.8	0.01	-6.7	0.02	4.71	-11.9	0.01	-6.8	0.01
142	3.11	-13.2	0.02	-7.2	0.03	4.75	-11.9	0.01	-6.9	0.03
143	3.13	-13.5	0.02	-6.9	0.03	4.79	-11.9	0.00	-6.6	0.02
144	3.15	-13.3	0.02	-6.9	0.01	4.83	-11.9	0.01	-6.7	0.01
145	3.17	-13.4	0.00	-7.0	0.00	4.90	-12.1	0.03	-7.8	0.03
146	3.19	-13.0	0.03	-7.3	0.02	5.18	-12.4	0.01	-8.3	0.00
149	3.25	-12.6	0.01	-6.9	0.02	5.22	-12.9	0.01	-8.4	0.03
150	3.27	-13.2	0.01	-6.5	0.02	5.27	-12.5	0.01	-8.2	0.02
151	3.29	-12.8	0.01	-7.2	0.01	5.31	-12.4	0.03	-8.0	0.02
152	3.31	-12.6	0.01	-7.0	0.02	5.39	-12.5	0.01	-7.8	0.03
153	3.33	-12.7	0.01	-6.9	0.03	5.74	-12.0	0.02	-7.1	0.04
154	3.35	-12.4	0.02	-7.1	0.02	6.11	-11.7	0.04	-6.9	0.01
155	3.37	-12.3	0.02	-7.3	0.02	6.15	-11.3	0.01	-6.6	0.03
156	3.40	-12.6	0.02	-6.9	0.03	6.15	-11.3	0.01	-6.6	0.03
157	3.42	-12.2	0.01	-7.2	0.03	6.20	-10.7	0.01	-6.1	0.03
158	3.44	-12.1	0.01	-7.2	0.01	6.25	-10.8	0.02	-6.0	0.02
159	3.46	-12.0	0.01	-7.1	0.02	6.30	-11.0	0.02	-5.9	0.01
160	3.48	-12.0	0.02	-6.9	0.02	6.35	-10.8	0.04	-5.8	0.02
165	3.59	-11.7	0.01	-7.2	0.01	6.39	-10.9	0.02	-6.0	0.02
173	3.78	-11.4	0.02	-7.6	0.03	6.44	-10.6	0.01	-6.6	0.03
174	3.81	-11.4	0.01	-7.6	0.01	6.57	-10.6	0.03	-7.3	0.02
175	3.83	-11.4	0.03	-7.6	0.02	6.69	-10.8	0.02	-7.6	0.01
176	3.86	-11.7	0.01	-7.7	0.02	6.75	-11.0	0.01	-7.6	0.02
177	3.89	-11.6	0.02	-7.8	0.02	6.80	-11.4	0.01	-7.7	0.01
180	3.97	-11.4	0.02	-8.0	0.05	6.85	-11.3	0.01	-7.5	0.02
183	4.06	-11.4	0.02	-7.9	0.02	6.90	-11.7	0.02	-7.6	0.01
184	4.09	-11.4	0.01	-8.1	0.02	6.90	-11.7	0.02	-7.6	0.01
185	4.13	-11.4	0.03	-8.1	0.01	7.23	-11.4	0.01	-7.3	0.03
187	4.19	-11.4	0.02	-8.2	0.01	7.34	-11.2	0.01	-6.7	0.02
190	4.28	-11.3	0.01	-8.1	0.02	7.45	-11.4	0.01	-6.1	0.05
194	4.41	-11.4	0.01	-8.1	0.03	7.51	-11.4	0.03	-5.8	0.01
198	4.54	-11.4	0.01	-8.2	0.02	7.57	-11.0	0.02	-6.1	0.04
199	4.58	-11.2	0.02	-8.1	0.02	7.63	-11.0	0.01	-5.9	0.02
200	4.61	-11.4	0.02	-8.2	0.02	7.68	-10.9	0.02	-6.3	0.03
201	4.65	-11.3	0.01	-8.3	0.03	7.86	-10.9	0.02	-7.1	0.02
202	4.68	-11.2	0.01	-8.1	0.04	8.31	-11.7	0.03	-8.0	0.01
203	4.72	-11.3	0.02	-8.3	0.03	8.36	-11.5	0.01	-8.2	0.02
204	4.75	-11.2	0.01	-8.2	0.01	8.42	-11.2	0.02	-7.8	0.04

Specimen/ Sample Number	Calc Age	$\delta^{13}C$‰ VPDB	±	$\delta^{18}O$‰ VPDB	±	Calc Age	$\delta^{13}C$‰ VPDB	±	$\delta^{18}O$‰ VPDB	±
205	4.79	-11.3	0.01	-8.1	0.04	8.48	-11.7	0.01	-7.3	0.05
207	4.86	-11.0	0.01	-8.0	0.02	8.54	-11.4	0.01	-8.0	0.03
208	4.89	-11.0	0.01	-7.9	0.02	8.60	-11.2	0.01	-8.0	0.02
209	4.93	-11.1	0.01	-7.9	0.02	8.66	-11.3	0.01	-7.8	0.01
210	4.97	-10.7	0.01	-7.6	0.02	8.84	-10.9	0.02	-8.0	0.02
211	5.01	-11.1	0.02	-7.8	0.04	8.90	-10.7	0.03	-8.2	0.02
212	5.04	-11.0	0.02	-7.9	0.02	8.96	-10.2	0.02	-8.7	0.01
213	5.08	-10.7	0.03	-7.9	0.01	9.02	-10.5	0.01	-8.3	0.02
214	5.12	-10.8	0.01	-7.6	0.03	9.09	-10.5	0.01	-8.1	0.03
215	5.16	-10.7	0.01	-7.4	0.02	9.60	-9.3	0.01	-8.1	0.02
						10.29	-9.1	0.02	-8.0	0.02
						10.65	-9.2	0.02	-7.7	0.02

Specimen D3-10

Sample Number	Calc Age	$\delta^{13}C$‰ VPDB	±	$\delta^{18}O$‰VPDB	±	Calc Age	$\delta^{13}C$‰ VPDB	±	$\delta^{18}O$‰VPDB	±
5	0.43	-19.2	0.03	-8.8	0.02	0.50	-18.6	0.02	-6.7	0.07
12.5	0.49	-23.4	0.02	-8.5	0.02	0.59	-18.2	0.03	-6.3	0.02
16	0.52	-22.9	0.03	-8.4	0.06	0.71	-18.3	0.02	-6.0	0.05
19	0.54	-20.9	0.01	-8.4	0.04	0.86	-17.7	0.01	-4.8	0.05
21.5	0.56	-20.2	0.01	-8.4	0.02	0.91	-17.4	0.01	-4.2	0.03
35	0.70	-18.1	0.03	-7.8	0.04	0.97	-17.6	0.01	-4.3	0.01
45	0.82	-16.0	0.02	-7.5	0.01	1.00	-17.9	0.03	-5.2	0.03
55	0.97	-15.0	0.01	-7.2	0.03	1.12	-19.6	0.02	-5.9	0.03
56	0.98	-14.7	0.03	-7.2	0.02	1.19	-19.9	0.03	-5.9	0.02
57	1.00	-14.3	0.01	-7.1	0.01	1.21	-21.4	0.02	-6.2	0.02
58	1.02	-14.3	0.01	-6.8	0.03	1.27	-22.1	0.02	-6.2	0.03
59	1.03	-13.2	0.03	-7.5	0.02	1.34	-22.1	0.01	-6.6	0.03
60	1.05	-12.3	0.01	-7.8	0.02	1.37	-21.4	0.02	-6.3	0.04
62	1.07	-12.2	0.01	-7.9	0.04	1.40	-21.6	0.00	-6.0	0.02
64	1.09	-13.5	0.02	-8.3	0.02	1.45	-20.8	0.03	-5.9	0.03
67	1.13	-14.5	0.01	-8.8	0.04	1.50	-21.3	0.01	-6.1	0.03
70	1.16	-15.5	0.02	-8.9	0.03	1.53	-21.7	0.01	-6.3	0.03
72	1.19	-15.6	0.01	-9.6	0.02	1.55	-21.1	0.02	-6.7	0.02
74	1.21	-15.5	0.00	-9.6	0.03	1.60	-20.3	0.03	-6.9	0.05
75	1.23	-15.8	0.01	-9.7	0.03	1.63	-20.0	0.01	-6.6	0.03
76	1.24	-16.6	0.01	-9.8	0.04	1.66	-19.5	0.01	-6.4	0.04
77	1.25	-16.8	0.01	-9.7	0.01	1.68	-19.4	0.02	-6.5	0.04

Specimen/ Sample Number	Calc Age	$\delta^{13}C$‰ VPDB	±	$\delta^{18}O$‰ VPDB	±	Calc Age	$\delta^{13}C$‰ VPDB	±	$\delta^{18}O$‰ VPDB	±
78	1.27	-16.8	0.02	-9.7	0.03	1.71	-21.3	0.06	-6.8	0.03
81	1.31	-18.0	0.03	-9.5	0.01	1.73	-19.9	0.02	-6.5	0.05
83	1.33	-18.2	0.01	-9.5	0.05	1.76	-19.8	0.01	-6.5	0.01
85	1.36	-18.5	0.02	-9.3	0.04	1.84	-19.5	0.02	-5.9	0.04
87	1.39	-18.5	0.02	-9.1	0.03	1.89	-15.9	0.00	-5.0	0.02
88	1.40	-18.0	0.01	-9.0	0.02	1.94	-15.6	0.02	-4.5	0.03
90	1.43	-17.4	0.03	-8.9	0.03	1.97	-15.3	0.03	-4.8	0.03
94	1.50	-16.0	0.01	-9.0	0.04	1.99	-14.2	0.02	-4.6	0.01
98	1.56	-14.6	0.01	-9.0	0.05	2.02	-13.4	0.02	-4.8	0.03
100	1.59	-14.4	0.01	-8.5	0.03	2.05	-12.7	0.01	-5.5	0.02
101.5	1.62	-14.9	0.02	-8.9	0.05	2.07	-12.5	0.02	-5.9	0.02
103	1.64	-14.8	0.04	-9.0	0.04	2.15	-12.2	0.02	-5.7	0.05
110	1.76	-13.9	0.02	-7.7	0.02	2.20	-14.2	0.02	-5.7	0.04
112	1.80	-13.7	0.01	-7.7	0.01	2.26	-16.9	0.01	-6.1	0.03
114	1.83	-13.8	0.02	-7.4	0.02	2.36	-18.9	0.02	-6.6	0.02
117	1.89	-14.2	0.00	-7.3	0.01	2.42	-20.0	0.01	-6.6	0.03
118	1.91	-13.9	0.01	-7.2	0.02	2.47	-20.1	0.02	-6.6	0.03
119	1.93	-13.3	0.02	-7.2	0.05	2.52	-20.1	0.02	-6.4	0.03
120	1.95	-12.4	0.02	-6.6	0.01	2.58	-20.3	0.01	-6.6	0.01
121	1.97	-12.8	0.01	-6.9	0.03	2.60	-20.7	0.01	-6.7	0.02
122	1.99	-12.1	0.03	-7.1	0.01	2.63	-21.5	0.02	-7.9	0.00
124	2.03	-13.0	0.01	-7.6	0.02	2.65	-20.7	0.02	-7.1	0.03
126	2.07	-13.1	0.02	-7.9	0.03	2.68	-20.9	0.01	-7.0	0.05
128	2.11	-13.5	0.03	-7.8	0.01	2.71	-21.0	0.01	-7.0	0.03
130	2.15	-14.1	0.02	-7.8	0.02	2.73	-21.2	0.01	-7.0	0.03
131	2.18	-14.1	0.03	-8.1	0.04	2.76	-21.4	0.01	-6.9	0.03
132	2.20	-14.2	0.02	-8.2	0.03	2.79	-21.0	0.02	-6.2	0.02
133	2.22	-14.5	0.01	-8.9	0.03	2.95	-18.8	0.01	-5.0	0.02
135	2.27	-14.4	0.01	-8.7	0.04	3.00	-16.9	0.01	-4.5	0.01
136	2.29	-14.3	0.01	-8.4	0.02	3.03	-13.8	0.01	-4.3	0.02
139	2.36	-15.1	0.01	-8.0	0.03	3.05	-11.8	0.01	-4.7	0.03
140	2.38	-14.9	0.02	-7.9	0.02	3.08	-11.6	0.02	-5.5	0.02
141	2.41	-14.6	0.01	-8.0	0.02	3.11	-10.7	0.01	-6.1	0.04
142	2.43	-15.1	0.02	-7.8	0.06	3.13	-10.5	0.01	-8.0	0.03
150	2.64	-14.3	0.01	-7.2	0.03	3.17	-10.5	0.03	-7.7	0.01
152	2.70	-13.8	0.02	-7.3	0.02	3.20	-10.9	0.01	-8.7	0.01
155	2.79	-14.1	0.03	-7.1	0.07	3.23	-11.9	0.01	-9.7	0.04
158	2.87	-14.4	0.01	-7.2	0.03	3.26	-12.8	0.01	-10.5	0.02

Specimen/ Sample Number	Calc Age	$\delta^{13}C$‰ VPDB	±	$\delta^{18}O$‰ VPDB	±	Calc Age	$\delta^{13}C$‰ VPDB	±	$\delta^{18}O$‰ VPDB	±
159	2.90	-13.8	0.02	-6.9	0.02	3.29	-13.1	0.01	-10.9	0.02
160	2.93	-13.8	0.02	-6.8	0.02	3.32	-13.0	0.02	-10.6	0.02
161	2.97	-13.8	0.03	-6.7	0.02	3.33	-12.4	0.01	-10.1	0.02
162	3.00	-14.8	0.01	-6.8	0.04	3.36	-12.1	0.02	-9.4	0.03
163	3.03	-15.7	0.01	-7.0	0.04	3.40	-11.5	0.05	-8.0	0.01
164	3.06	-16.2	0.03	-7.2	0.05	3.45	-11.5	0.04	-7.3	0.03
165	3.09	-14.8	0.01	-7.2	0.03	3.53	-11.8	0.01	-7.2	0.02
168	3.19	-14.0	0.02	-7.5	0.03	3.58	-11.8	0.01	-7.6	0.01
169	3.22	-13.8	0.01	-7.6	0.06	3.65	-11.9	0.02	-8.0	0.05
170	3.26	-13.9	0.02	-7.8	0.04	3.67	-10.5	0.02	-6.7	0.03
172	3.33	-13.6	0.02	-7.9	0.03	3.79	-10.6	0.02	-5.9	0.01
174	3.40	-13.6	0.02	-7.8	0.02	3.87	-10.8	0.03	-5.9	0.02
176	3.47	-13.5	0.01	-7.8	0.02	3.89	-10.6	0.01	-6.1	0.03
177	3.50	-13.6	0.01	-8.0	0.04	3.90	-10.6		-6.1	
178	3.54	-13.5	0.02	-8.2	0.03					
179	3.58	-13.3	0.03	-8.1	0.03					
180	3.61	-13.1	0.04	-7.8	0.03					
183	3.70	-12.8	0.02	-7.9	0.03					
184	3.73	-12.8	0.01	-7.8	0.03					
185	3.76	-12.6	0.02	-7.7	0.00					
187	3.82	-12.1	0.02	-7.6	0.01					
189	3.88	-12.2	0.02	-7.2	0.02					
190	3.91	-11.6	0.02	-6.8	0.04					
191	3.94	-11.4	0.01	-6.6	0.03					
192	3.97	-11.2	0.03	-6.5	0.01					
193	4.00	-10.9	0.04	-6.6	0.02					
196	4.09	-10.6	0.00	-6.5	0.02					
197	4.12	-10.4	0.01	-6.6	0.04					
198	4.15	-11.1	0.01	-6.9	0.03					
199	4.19	-11.1	0.01	-7.0	0.01					
200	4.22	-11.3	0.01	-7.2	0.01					
203	4.30	-11.6	0.01	-7.6	0.03					
204	4.32	-11.8	0.01	-7.9	0.04					
205	4.35	-11.5	0.03	-7.8	0.03					
208	4.43	-11.0	0.02	-7.7	0.03					
209	4.46	-11.0	0.02	-7.8	0.02					
210	4.48	-11.0	0.01	-7.9	0.02					
211	4.51	-11.6	0.04	-7.8	0.08					

Specimen/ Sample Number	Calc Age	$\delta^{13}C$‰ VPDB	±	$\delta^{18}O$‰ VPDB	±	Calc Age	$\delta^{13}C$‰ VPDB	±	$\delta^{18}O$‰ VPDB	±
213	4.56	-10.7	0.01	-7.4	0.03					
215	4.62	-11.2	0.03	-7.2	0.03					
216	4.65	-11.0	0.03	-7.6	0.03					
218	4.70	-10.9	0.03	-7.5	0.04					
220	4.76	-10.3	0.02	-7.5	0.05					
221	4.79	-10.5	0.02	-7.6	0.03					
222	4.82	-10.7	0.02	-7.4	0.02					
223	4.85	-10.9	0.04	-7.5	0.02					
224	4.88	-10.6	0.03	-7.6	0.03					
225	4.91	-10.4	0.01	-7.7	0.02					
227	4.97	-10.1	0.01	-7.7	0.02					
230	5.06	-9.8	0.01	-7.6	0.02					
236	5.25	-9.6	0.02	-7.9	0.02					
240	5.37	-9.7	0.02	-7.9	0.02					
243	5.47	-9.5	0.03	-8.1	0.01					
244	5.51	-9.3	0.01	-8.2	0.02					
245	5.54	-9.2	0.03	-8.0	0.05					
Specimen H4-12 Sample Number	Calc Age	$\delta^{13}C$‰ VPDB	±	$\delta^{18}O$‰VPDB	±	Calc Age	$\delta^{13}C$‰ VPDB	±	$\delta^{18}O$‰VPDB	±
2	0.25	-16.3	0.04	-8.0	0.01	0.40	-15.2	0.01	-6.5	0.03
3	0.37	-16.6	0.03	-8.1	0.01	0.47	-15.6	0.06	-7.0	0.05
4	0.41	-16.6	0.05	-8.2	0.01	0.51	-15.2	0.03	-6.9	0.03
6	0.45	-16.6	0.06	-8.2	0.01	0.53	-15.3	0.02	-6.9	0.07
7	0.49	-16.6	0.06	-8.3	0.01	0.57	-15.3	0.03	-6.8	0.01
8	0.54	-16.5	0.04	-8.2	0.02	0.61	-15.4	0.01	-7.2	0.04
10	0.58	-16.4	0.03	-8.2	0.01	0.64	-16.1	0.03	-7.5	0.05
11	0.62	-16.3	0.06	-8.3	0.02	0.65	-16.6	0.03	-7.5	0.03
12.5	0.66	-16.2	0.03	-8.3	0.01	0.68	-16.9	0.02	-7.5	0.01
14.5	0.69	-16.3	0.05	-8.3	0.02	0.70	-16.6	0.02	-7.5	0.05
16.5	0.71	-16.4	0.03	-8.3	0.01	0.71	-16.2	0.02	-7.6	0.01
18.5	0.73	-16.4	0.05	-8.3	0.01	0.73	-15.8	0.01	-7.5	0.03
20.5	0.80	-16.7	0.04	-8.2	0.01	0.74	-15.8	0.00	-7.6	0.06
22	0.82	-16.6	0.06	-7.9	0.01	0.78	-15.3	0.02	-7.3	0.03
25.5	0.83	-16.7	0.02	-8.3	0.01	0.83	-15.3	0.02	-7.1	0.02
26	0.85	-16.4	0.01	-8.3	0.01	0.85	-15.9	0.01	-7.1	0.03
27.5	0.87	-16.7	0.06	-8.2	0.00	0.89	-15.6	0.03	-6.0	0.05

Specimen/ Sample Number	Calc Age	$\delta^{13}C$‰ VPDB	±	$\delta^{18}O$‰ VPDB	±	Calc Age	$\delta^{13}C$‰ VPDB	±	$\delta^{18}O$‰ VPDB	±
29	0.89	-16.6	0.01	-8.1	0.00	0.94	-15.7	0.01	-6.3	0.04
32.5	0.90	-16.6	0.04	-7.9	0.01	1.00	-15.5	0.05	-5.7	0.04
34	0.96	-16.6	0.03	-7.9	0.01	1.02	-14.7	0.00	-5.6	0.01
35	0.98	-16.4	0.03	-7.6	0.01	1.03	-14.8	0.01	-5.5	0.01
36.5	1.01	-16.4	0.03	-7.5	0.01	1.05	-14.4	0.02	-5.2	0.02
38	1.03	-16.3	0.06	-7.5	0.02	1.09	-12.6	0.01	-6.3	0.01
39.5	1.05	-16.3	0.05	-7.3	0.01	1.14	-11.7	0.01	-7.9	0.06
41	1.06	-16.3	0.07	-7.2	0.01	1.18	-11.7	0.01	-8.3	0.03
43.5	1.08	-16.1	0.05	-6.8	0.01	1.20	-11.6	0.01	-8.1	0.03
45.5	1.13	-16.0	0.05	-6.9	0.01	1.22	-11.3	0.01	-7.9	0.03
48	1.15	-15.8	0.05	-6.4	0.01	1.26	-11.4	0.01	-7.7	0.04
49	1.17	-15.4	0.08	-6.7	0.02	1.30	-11.0	0.01	-7.4	0.01
50	1.19	-15.7	0.05	-6.4	0.01	1.41	-11.4	0.01	-6.3	0.02
51	1.22	-14.9	0.08	-6.7	0.02	1.47	-11.9	0.03	-6.4	0.04
52	1.28	-15.0	0.06	-6.3	0.01	1.53	-11.7	0.01	-6.0	0.02
53	1.29	-14.5	0.03	-6.4	0.01	1.63	-11.6	0.01	-6.1	0.04
54	1.30	-14.4	0.04	-6.4	0.01	1.74	-11.4	0.04	-5.7	0.02
55	1.31	-14.1	0.04	-6.5	0.01	1.79	-11.2	0.03	-5.6	0.01
56	1.34	-13.9	0.02	-6.7	0.01	1.84	-11.8	0.03	-4.3	0.01
57	1.36	-14.0	0.05	-6.9	0.00	1.86	-12.5	0.07	-5.1	0.06
58	1.38	-14.0	0.04	-7.0	0.01	1.94	-10.9	0.01	-5.9	0.01
61	1.39	-13.9	0.05	-7.3	0.01	2.00	-10.2	0.00	-6.5	0.01
63	1.40	-15.0	0.08	-7.9	0.01	2.09	-9.9	0.02	-7.1	0.05
66	1.41	-15.2	0.04	-8.3	0.01	2.15	-9.6	0.01	-7.5	0.02
67.5	1.43	-15.3	0.05	-8.9	0.01	2.19	-9.7	0.03	-7.6	0.04
69	1.45	-15.5	0.04	-8.8	0.01	2.21	-9.9	0.01	-7.8	0.08
71	1.47	-15.8	0.01	-9.4	0.01	2.23	-9.9	0.04	-7.9	0.04
76	1.49	-15.9	0.08	-9.2	0.01	2.25	-9.8	0.01	-7.6	0.05
78.5	1.51	-15.8	0.05	-8.9	0.01	2.31	-9.7	0.04	-7.3	0.02
81	1.55	-15.6	0.07	-9.0	0.01	2.36	-9.7	0.03	-7.4	0.03
82.5	1.58	-15.6	0.05	-8.9	0.02	2.44	-9.9	0.01	-7.2	0.03
86.5	1.59	-15.1	0.04	-8.8	0.01	2.51	-10.4	0.03	-7.0	0.03
88	1.60	-15.0	0.07	-8.8	0.02	2.58	-10.1	0.03	-6.8	0.03
91.5	1.61	-14.1	0.03	-8.6	0.00	2.71	-11.0	0.03	-5.8	0.01
94	1.64	-13.6	0.04	-8.5	0.01	2.78	-11.3	0.02	-5.4	0.02
96.5	1.66	-13.4	0.02	-8.4	0.01	2.84	-11.4	0.02	-5.2	0.02
99	1.68	-12.9	0.01	-7.8	0.01	2.86	-11.5	0.03	-5.1	0.01
101	1.69	-12.7	0.07	-7.9	0.01	2.89	-11.7	0.01	-4.5	0.02

Specimen/ Sample Number	Calc Age	$\delta^{13}C$‰ VPDB	±	$\delta^{18}O$‰ VPDB	±	Calc Age	$\delta^{13}C$‰ VPDB	±	$\delta^{18}O$‰ VPDB	±
102	1.70	-12.5	0.05	-7.6	0.01	2.92	-11.3	0.03	-4.7	0.03
103.5	1.72	-12.5	0.02	-7.3	0.01	3.00	-10.3	0.03	-5.1	0.03
108.5	1.78	-12.0	0.05	-6.5	0.01	3.11	-9.2	0.02	-5.9	0.04
114	1.80	-12.7	0.06	-6.6	0.01	3.23	-8.7	0.01	-7.1	0.03
116	1.88	-12.9	0.06	-7.3	0.01	3.29	-8.6	0.01	-7.5	0.02
117	1.93	-12.9	0.01	-7.4	0.01	3.32	-8.7	0.04	-7.6	0.03
119	1.94	-12.7	0.04	-7.6	0.01	3.35	-8.7	0.01	-7.6	0.02
120	1.95	-12.9	0.07	-7.7	0.01	3.38	-8.7	0.01	-7.6	0.02
123	1.96	-12.4	0.01	-7.8	0.00	3.41	-8.2	0.02	-7.6	0.04
124	2.03	-12.8	0.03	-8.2	0.00	3.44	-8.8	0.01	-7.4	0.04
125	2.06	-13.0	0.01	-8.5	0.01	3.47	-9.0	0.02	-7.0	0.04
126	2.12	-12.7	0.02	-8.6	0.01	3.51	-9.0	0.03	-7.3	0.02
127	2.14	-12.6	0.02	-8.6	0.01	3.60	-9.2	0.01	-6.7	0.01
128	2.16	-12.2	0.01	-8.7	0.00	3.73	-9.4	0.02	-6.4	0.03
129	2.19	-12.2	0.03	-8.5	0.01	3.90	-10.4	0.02	-6.1	0.01
130	2.21	-12.1	0.02	-8.8	0.01	4.08	-11.7	0.03	-5.2	0.04
131	2.23	-11.8	0.03	-8.8	0.00	4.15	-12.0	0.01	-4.8	0.04
132	2.26	-11.4	0.02	-8.7	0.01	4.22	-12.0	0.02	-4.2	0.03
133	2.28	-11.3	0.03	-8.5	0.01	4.26	-12.0	0.02	-3.8	0.04
136	2.30	-11.1	0.02	-8.4	0.00	4.30	-12.1	0.02	-3.4	0.02
137	2.32	-10.9	0.05	-8.2	0.01	4.34	-11.9	0.03	-3.7	0.04
138	2.35	-10.8	0.03	-8.1	0.00	4.38	-11.7	0.03	-3.7	0.03
139	2.37	-10.7	0.02	-8.0	0.01	4.42	-11.1	0.02	-3.9	0.04
140	2.39	-10.9	0.03	-8.1	0.01	4.45	-10.9	0.01	-4.5	0.02
141	2.42	-11.0	0.07	-7.2	0.01	4.58	-9.9	0.01	-5.9	0.01
142	2.44	-10.7	0.02	-8.1	0.00	4.70	-9.2	0.01	-7.3	0.01
143	2.46	-10.6	0.04	-7.9	0.00	4.78	-9.0	0.02	-8.1	0.05
144	2.48	-10.6	0.01	-7.9	0.02	4.87	-9.1	0.02	-8.4	0.02
145	2.51	-10.4	0.04	-7.7	0.01	4.91	-9.1	0.01	-8.5	0.03
146	2.53	-10.4	0.01	-7.7	0.01	4.96	-9.1	0.03	-8.6	0.03
147	2.55	-10.3	0.02	-7.2	0.01	5.00	-9.2	0.00	-8.5	0.03
148	2.58	-10.4	0.04	-7.2	0.01	5.04	-9.2	0.01	-8.5	0.03
149	2.64	-10.3	0.05	-6.9	0.00	5.09	-9.5	0.02	-8.6	0.02
150	2.67	-10.3	0.02	-5.9	0.01					
151	2.69	-10.0	0.02	-5.6	0.01					
152	2.71	-9.5	0.03	-6.0	0.01					
153	2.74	-9.6	0.03	-6.4	0.01					
154	2.76	-9.7	0.06	-6.7	0.02					

Specimen/ Sample Number	Calc Age	$\delta^{13}C$‰ VPDB	±	$\delta^{18}O$‰ VPDB	±	Calc Age	$\delta^{13}C$‰ VPDB	±	$\delta^{18}O$‰ VPDB	±
155	2.78	-10.3	0.03	-7.2	0.01					
156	2.80	-11.0	0.04	-7.6	0.01					
158.5	2.83	-12.3	0.01	-8.0	0.00					
160	2.85	-12.8	0.07	-8.3	0.01					
168	2.94	-13.4	0.05	-8.6	0.01					
169	2.99	-13.5	0.02	-8.9	0.01					
170	3.01	-13.3	0.01	-8.7	0.01					
171	3.05	-13.3	0.04	-8.7	0.00					
175	3.06	-12.8	0.07	-8.7	0.02					
181	3.10	-12.5	0.07	-8.5	0.01					
183	3.19	-12.6	0.04	-8.4	0.00					
187.5	3.28	-12.6	0.08	-8.1	0.02					
189	3.31	-12.9	0.01	-8.5	0.00					
190	3.33	-13.0	0.04	-8.4	0.00					
191	3.36	-13.0	0.04	-8.4	0.00					
192	3.40	-13.0	0.05	-8.4	0.01					
194	3.45	-12.9	0.04	-8.3	0.01					
196	3.49	-12.2	0.02	-7.9	0.01					
197	3.55	-12.7	0.08	-8.1	0.01					
198	3.58	-12.4	0.04	-7.9	0.01					
199	3.65	-12.3	0.06	-7.9	0.01					
201	3.67	-11.9	0.02	-7.4	0.01					
204	3.72	-11.8	0.02	-7.0	0.01					
205.5	3.76	-11.5	0.03	-6.6	0.00					
207.5	3.85	-11.9	0.03	-6.9	0.01					
209	3.88	-11.4	0.07	-6.9	0.00					
210.5	3.91	-11.3	0.06	-6.6	0.00					
212	3.94	-10.1	0.04	-7.6	0.01					
213	3.99	-11.6	0.07	-6.3	0.01					
214	4.05	-11.6	0.02	-6.3	0.01					
215	4.14	-11.7	0.03	-5.8	0.01					
216	4.17	-11.8	0.06	-6.2	0.01					
218	4.20	-11.8	0.08	-6.8	0.01					
220	4.23	-12.1	0.07	-6.6	0.01					
221	4.26	-12.7	0.03	-7.5	0.01					
222	4.29	-12.8	0.03	-7.6	0.00					
223	4.32	-12.2	0.04	-7.9	0.01					
226	4.35	-12.2	0.01	-8.1	0.01					

Specimen/ Sample Number	Calc Age	δ^{13}C‰ VPDB	±	δ^{18}O‰ VPDB	±	Calc Age	δ^{13}C‰ VPDB	±	δ^{18}O‰ VPDB	±
228	4.38	-12.0	0.05	-8.3	0.00					
229	4.41	-12.0	0.03	-8.3	0.00					
230	4.44	-11.9	0.03	-8.2	0.01					
231	4.51	-11.8	0.07	-8.1	0.01					
234	4.57	-11.3	0.06	-7.9	0.01					
235	4.65	-11.1	0.02	-7.8	0.01					
236	4.69	-11.1	0.03	-7.6	0.02					
237	4.73	-11.1	0.05	-7.5	0.00					
238	4.78	-11.1	0.03	-7.3	0.00					
240	4.82	-11.0	0.02	-7.2	0.01					
241	4.85	-11.1	0.03	-6.9	0.01					
244	4.90	-11.6	0.03	-6.7	0.01					
245	5.00	-10.9	0.01	-6.4	0.01					
246	5.05	-11.0	0.03	-6.3	0.01					
247	5.09	-10.7	0.04	-6.4	0.01					
248	5.11	-10.8	0.04	-6.3	0.00					
249	5.21	-10.8	0.05	-6.6	0.01					
250	5.26	-10.7	0.08	-6.7	0.01					
254	5.32	-10.8	0.07	-7.3	0.01					
255	5.38	-11.1	0.07	-7.8	0.01					
256	5.44	-10.9	0.03	-7.6	0.01					
258	5.50	-11.7	0.03	-8.0	0.00					
259	5.54	-12.2	0.07	-8.3	0.01					
260	5.57	-12.2	0.01	-8.4	0.01					
261	5.63	-12.3	0.05	-8.4	0.00					
262	5.66	-12.2	0.04	-8.3	0.00					
263	5.69	-12.3	0.05	-8.5	0.00					
264	5.75	-12.2	0.06	-8.4	0.00					
265	5.78	-12.4	0.07	-8.4	0.00					
268	5.81	-11.6	0.03	-6.8	0.01					
Specimen F4-16 Sample Number	Calc Age	δ^{13}C‰ VPDB	±	δ^{18}O‰VPDB	±	Calc Age	δ^{13}C‰ VPDB	±	δ^{18}O‰VPDB	±
3	0.59	-17.2	0.02	-7.4	0.02	0.76	-18.1	0.02	-7.9	0.03
10	0.66	-17.0	0.01	-7.5	0.02	1.04	-17.4	0.01	-7.4	0.03
13.5	0.70	-17.4	0.01	-7.7	0.03	1.34	-17.2	0.01	-7.1	0.02
15.5	0.72	-17.9	0.02	-7.7	0.04	1.51	-16.5	0.02	-6.9	0.03

Specimen/ Sample Number	Calc Age	$\delta^{13}C$‰ VPDB	±	$\delta^{18}O$‰ VPDB	±	Calc Age	$\delta^{13}C$‰ VPDB	±	$\delta^{18}O$‰ VPDB	±
17.5	0.74	-17.8	0.02	-7.3	0.02	1.57	-15.7	0.02	-6.2	0.06
19.5	0.76	-17.6	0.02	-7.1	0.03	1.65	-14.6	0.02	-6.3	0.01
21.5	0.79	-16.9	0.01	-6.8	0.01	1.68	-12.4	0.02	-6.1	0.03
23	0.81	-16.5	0.01	-6.8	0.01	1.79	-11.9	0.02	-5.2	0.03
24	0.82	-15.7	0.03	-6.6	0.02	1.85	-10.6	0.01	-6.3	0.06
25	0.83	-15.1	0.01	-6.8	0.03	2.07	-12.9	0.00	-7.1	0.01
26	0.85	-15.0	0.01	-6.3	0.02	2.50	-13.1	0.01	-7.9	0.03
28	0.87	-13.0	0.02	-6.4	0.01	2.56	-13.2	0.01	-8.3	0.04
29	0.89	-12.7	0.04	-6.8	0.04	2.56	-13.2	0.01	-8.3	0.04
30	0.90	-13.4	0.03	-6.4	0.02	2.61	-13.3	0.01	-8.2	0.02
32	0.93	-13.1	0.02	-6.5	0.02	2.67	-13.0	0.02	-8.0	0.03
38	1.02	-12.7	0.02	-7.1	0.02	2.72	-13.3	0.02	-7.9	0.04
45	1.13	-13.4	0.03	-7.3	0.04	2.88	-12.8	0.01	-7.5	0.03
47	1.17	-13.4	0.02	-7.5	0.01	3.04	-14.3	0.01	-6.4	0.03
50	1.23	-12.9	0.01	-7.7	0.03	3.10	-14.3	0.02	-6.3	0.03
55	1.32	-13.1	0.01	-7.5	0.01	3.15	-14.3	0.02	-6.4	0.01
56	1.34	-13.2	0.01	-7.3	0.02	3.21	-14.0	0.02	-6.5	0.02
58	1.39	-13.3	0.01	-7.0	0.03	3.21	-14.0	0.02	-6.5	0.02
60	1.43	-13.0	0.01	-7.8	0.02	3.31	-13.1	0.01	-6.8	0.02
62	1.48	-13.4	0.01	-6.7	0.01	3.53	-12.2	0.02	-7.2	0.04
65	1.55	-13.5	0.01	-6.6	0.01	3.53	-12.2	0.02	-7.2	0.04
70	1.67	-13.2	0.02	-6.6	0.02	3.58	-12.3	0.02	-7.4	0.08
75	1.80	-12.5	0.02	-6.9	0.03	3.75	-12.0	0.02	-7.0	0.02
80	1.95	-12.1	0.00	-6.6	0.01	3.85	-12.3	0.01	-6.6	0.04
85	2.11	-11.4	0.00	-6.1	0.02	4.07	-11.1	0.02	-6.0	0.04
90	2.28	-11.2	0.01	-5.7	0.02	4.23	-10.9	0.02	-5.6	0.01
92.5	2.31	-10.6	0.02	-5.6	0.03	4.29	-12.5	0.07	-4.6	0.03
95	2.35	-10.9	0.02	-5.8	0.03	4.34	-10.7	0.04	-5.0	0.02
96	2.37	-10.9	0.01	-5.9	0.00	4.39	-10.2	0.01	-5.6	0.02
100	2.43	-11.2	0.02	-6.3	0.01	4.43	-10.5	0.03	-6.1	0.06
105	2.51	-12.1	0.02	-7.3	0.04	4.46	-11.3	0.01	-6.6	0.04
110	2.60	-12.7	0.01	-7.5	0.05	4.66	-12.4	0.01	-7.6	0.02
115	2.69	-12.9	0.01	-7.9	0.03	4.76	-13.3	0.02	-8.3	0.03
119	2.76	-13.0	0.02	-7.9	0.02	4.79	-13.0	0.02	-8.0	0.03
121	2.79	-13.0	0.01	-7.9	0.03	4.82	-13.3	0.01	-8.3	0.04
123	2.83	-13.0	0.01	-7.5	0.01	4.86	-13.1	0.01	-8.4	0.04
125	2.87	-13.1	0.02	-7.5	0.02	4.96	-13.1	0.03	-8.3	0.02
127	2.91	-13.3	0.01	-7.5	0.02	5.05	-13.1	0.02	-8.2	0.03

Specimen/ Sample Number	Calc Age	$\delta^{13}C$‰ VPDB	±	$\delta^{18}O$‰ VPDB	±	Calc Age	$\delta^{13}C$‰ VPDB	±	$\delta^{18}O$‰ VPDB	±
129	2.95	-13.6	0.01	-7.3	0.03	5.32	-13.4	0.01	-7.6	0.01
130	2.97	-13.5	0.02	-7.4	0.01	5.38	-13.9	0.02	-7.8	0.02
135	3.07	-13.4	0.02	-7.0	0.00	5.58	-13.0	0.04	-6.1	0.05
139	3.15	-13.4	0.01	-6.7	0.03	5.62	-13.1	0.01	-5.3	0.02
140	3.17	-11.9	0.01	-6.4	0.02	5.65	-13.4	0.00	-5.7	0.02
141	3.19	-13.1	0.02	-6.5	0.03	5.68	-13.0	0.01	-6.0	0.02
142	3.21	-12.9	0.02	-6.5	0.02	5.71	-12.3	0.01	-6.7	0.03
143	3.24	-12.4	0.01	-6.7	0.06	5.77	-11.8	0.01	-7.1	0.01
145	3.28	-12.8	0.01	-6.6	0.00	5.90	-11.4	0.01	-8.2	0.02
146	3.30	-12.6	0.01	-6.8	0.02	5.92	-11.6	0.01	-8.4	0.02
150	3.40	-11.7	0.01	-7.4	0.01	5.94	-11.6	0.02	-8.4	0.04
155	3.52	-11.6	0.01	-8.0	0.01	5.97	-11.2	0.02	-8.3	0.04
160	3.64	-11.2	0.02	-8.1	0.01	5.97	-11.2	0.02	-8.3	0.04
161	3.66	-11.0	0.03	-8.1	0.02	5.99	-11.3	0.01	-8.4	0.02
162	3.69	-11.0	0.02	-8.0	0.01	6.06	-11.4	0.02	-8.4	0.02
163	3.72	-10.8	0.01	-8.0	0.02	6.11	-11.2	0.01	-8.4	0.02
165	3.77	-10.8	0.02	-8.2	0.02	6.11	-11.2	0.01	-8.4	0.02
166	3.79	-10.8	0.02	-8.1	0.03	6.13	-11.2	0.01	-8.4	0.01
168	3.85	-10.4	0.02	-7.9	0.02	6.15	-11.0	0.01	-8.3	0.02
170	3.90	-10.2	0.00	-7.6	0.04	6.17	-10.8	0.01	-8.3	0.01
175	4.04	-10.0	0.01	-7.2	0.03	6.27	-11.3	0.03	-8.3	0.02
179	4.15	-9.9	0.01	-7.0	0.03	6.29	-10.9	0.02	-8.5	0.03
180	4.18	-9.9	0.03	-7.1	0.04	6.32	-10.7	0.01	-8.4	0.04
181	4.21	-9.9	0.02	-7.1	0.04	6.40	-10.6	0.01	-8.2	0.05
185	4.32	-10.0	0.03	-7.2	0.03	6.47	-10.1	0.02	-7.6	0.01
194	4.58	-9.6	0.01	-7.8	0.04	6.59	-10.9	0.03	-6.7	0.05
195	4.62	-9.5	0.01	-7.9	0.03	6.61	-10.0	0.01	-6.4	0.04
196	4.65	-9.7	0.03	-8.0	0.05	6.63	-10.1	0.01	-6.1	0.03
197	4.68	-9.9	0.02	-8.0	0.02	6.65	-9.8	0.02	-6.5	0.04
198	4.71	-9.5	0.01	-7.9	0.02	6.67	-10.0	0.04	-6.6	0.02
202	4.83	-9.2	0.02	-7.7	0.01	6.81	-10.3	0.03	-7.8	0.07
203	4.87	-9.2	0.01	-7.7	0.04	6.98	-10.0	0.01	-8.3	0.01
204	4.90	-9.2	0.01	-7.6	0.02	7.01	-10.1	0.02	-8.3	0.02
205	4.93	-9.3	0.02	-7.4	0.02	7.03	-10.2	0.01	-8.6	0.02
206	4.97	-9.2	0.03	-7.6	0.05	7.05	-10.1	0.01	-8.5	0.02
207	5.01	-9.4	0.01	-7.4	0.03	7.07	-10.0	0.01	-8.4	0.02
210	5.12	-9.4	0.01	-7.5	0.02	7.09	-10.1	0.02	-8.3	0.04
211	5.16	-9.6	0.02	-7.6	0.02	7.09	-10.1	0.02	-8.3	0.04

Specimen/ Sample Number	Calc Age	$\delta^{13}C$‰ VPDB	±	$\delta^{18}O$‰ VPDB	±	Calc Age	$\delta^{13}C$‰ VPDB	±	$\delta^{18}O$‰ VPDB	±
212	5.20	-9.5	0.02	-7.6	0.03	7.20	-9.2	0.00	-7.6	0.02
213	5.23	-9.4	0.02	-7.5	0.01	7.32	-9.0	0.01	-6.7	0.02
215	5.31	-9.5	0.03	-7.4	0.03	7.32	-9.0	0.01	-6.7	0.02
220	5.52	-9.6	0.02	-7.5	0.02	7.34	-9.2	0.01	-6.7	0.01
221	5.56	-9.3	0.03	-7.2	0.02	7.36	-9.6	0.02	-6.6	0.04
222	5.60	-9.3	0.01	-7.1	0.03	7.38	-10.0	0.01	-6.9	0.03
223	5.64	-9.3	0.02	-7.1	0.02	7.39	-10.0	0.02	-7.0	0.01
224	5.68	-9.3	0.02	-7.1	0.02	7.41	-10.2	0.02	-7.4	0.01
225	5.72	-9.4	0.01	-7.1	0.05	7.43	-10.2	0.02	-7.4	0.02
227	5.81	-9.1	0.01	-7.1	0.01	7.45	-10.4	0.02	-8.0	0.04
228	5.85	-9.0	0.01	-7.2	0.02					
230	5.94	-9.2	0.02	-7.1	0.02					
231	5.99	-9.3	0.01	-7.1	0.02					
232	6.03	-9.4	0.02	-7.2	0.04					
233	6.08	-9.3	0.02	-7.2	0.03					
234	6.12	-9.5	0.02	-7.2	0.02					
235	6.17	-9.4	0.01	-7.3	0.04					
237	6.26	-9.6	0.02	-7.4	0.01					
238	6.31	-9.6	0.01	-7.5	0.02					
240	6.40	-9.6	0.02	-7.5	0.03					
241	6.45	-9.6	0.02	-7.6	0.01					
242	6.50	-9.6	0.02	-7.6	0.03					
243	6.55	-9.7	0.01	-7.5	0.03					
245	6.65	-9.6	0.01	-7.3	0.02					
246	6.70	-9.5	0.00	-7.2	0.02					
247	6.75	-9.4	0.02	-7.5	0.02					
248	6.80	-9.7	0.01	-7.7	0.01					
249	6.85	-9.6	0.01	-7.5	0.03					
253	7.05	-9.6	0.02	-7.3	0.03					
254	7.11	-9.6	0.01	-7.3	0.01					
255	7.16	-9.8	0.02	-7.1	0.02					
256	7.21	-9.7	0.02	-7.4	0.04					
258	7.32	-9.8	0.01	-7.4	0.02					
259	7.38	-9.7	0.01	-7.3	0.02					
260	7.43	-9.7	0.00	-7.4	0.01					
261	7.49	-9.7	0.01	-7.4	0.04					
264	7.66	-10.1	0.01	-7.4	0.02					
265	7.71	-10.1	0.01	-7.3	0.02					

Specimen/ Sample Number	Calc Age	$\delta^{13}C$‰ VPDB	±	$\delta^{18}O$‰ VPDB	±	Calc Age	$\delta^{13}C$‰ VPDB	±	$\delta^{18}O$‰ VPDB	±
266	7.77	-10.2	0.00	-7.3	0.02					
267	7.83	-10.2	0.01	-7.3	0.03					
268	7.89	-10.2	0.01	-7.3	0.04					
270	8.01	-10.2	0.01	-7.5	0.03					
271	8.07	-10.1	0.01	-7.5	0.02					
272	8.13	-10.3	0.02	-7.5	0.02					
273	8.19	-10.4	0.01	-7.4	0.03					
274	8.25	-10.2	0.01	-7.3	0.04					
275	8.31	-10.2	0.02	-7.3	0.03					
276	8.37	-10.1	0.01	-7.2	0.05					
277	8.44	-9.2	0.01	-6.9	0.03					
278	8.50	-9.4	0.01	-7.0	0.01					
282	8.76	-8.9	0.02	-7.1	0.01					
283	8.82	-8.8	0.02	-7.0	0.01					
284	8.89	-8.7	0.01	-6.9	0.02					
285	8.96	-8.7	0.01	-6.9	0.03					
295	9.97	-9.3	0.02	-7.1	0.02					
304.5	11.05	-10.4	0.02	-7.4	0.02					
310	11.72	-10.1	0.00	-7.6	0.02					
314	12.24	-9.8	0.02	-7.6	0.01					
315	12.37	-9.7	0.02	-7.7	0.02					
316	12.51	-9.5	0.02	-7.7	0.04					
317	12.64	-9.5	0.01	-7.6	0.01					
323	13.49	-10.2	0.01	-7.0	0.03					
325	13.78	-9.8	0.01	-6.7	0.03					

Table A5—Weakfish predator energy density (joules• g wet weight $^{-1}$) for bioenergetic simulation and incorporated into chapter 3.

Values from Hartman and Brandt 1995a.

Day	Age 0+	Age 1+	Age 2+
150	2707	3819	6276
165	2836	4112	6276
180	2970	4422	5795
195	3108	4757	5125
210	3255	5117	4853
225	3409	5506	4602
240	3573	5924	4916
255	3740	6372	5021
270	3920	6858	5858

Day	Age 0+	Age 1+	Age 2+
285	4105	7376	6276
300	4297	7933	6694
315	4502	8535	7113

Table A6—Prey proportions incorporated into bioenergetic simulation of weakfish described in chapter 3.

Day	Bay anchovy	Atlantic menhaden	Atlantic croaker	Spot	Other fish	Crangon	Neomysis	Other invertebrates
Age 0+								
151	0.737	0	0	0	0	0.111	0.13	0.022
212	0.737	0	0	0	0	0.111	0.13	0.022
273	0.979	0	0	0	0.002	0.001	0.015	0.003
334	0.582	0	0.374	0	0	0	0.044	0
Age 1+								
1	0.727	0.037	0	0.029	0.036	0.017	0.134	0.02
151	0.727	0.037	0	0.029	0.036	0.017	0.134	0.02
211	0.703	0.072	0.002	0	0.096	0.059	0.037	0.031
273	0.174	0.537	0.115	0.137	0.023	0.004	0.001	0.009
365	0.174	0.537	0.115	0.137	0.023	0.004	0.001	0.009
Age 2+								
1	0.078	0.221	0.017	0.432	0.142	0.021	0	0.089
151	0.078	0.221	0.017	0.432	0.142	0.021	0	0.089
273	0.009	0.642	0	0.304	0.044	0.001	0	0
365	0.009	0.642	0	0.304	0.044	0.001	0	0

Table A7—Growth (g wet weight) of two cohorts of weakfish incorporated in bioenergetic simulation described in chapter 3.

Cohort *a* reaches 1 g at day 183; Cohort *b* reaches 1 g at day 210. Data from Hartman and Brandt, 1995a.

Age class	a	b
0+	42	20
1+	311	135
2+	640	341

Table A8—Energy density (joules• g wet weight $^{-1}$) of weakfish prey items incorporated into bioenergetic simulation and described in chapter 3.

Data from Hartman and Brandt, 1995a.

Day	Bay anchovy	Atlantic menhaden	Atlantic croaker	Spot	Other fish	Crangon	Neomysis	Other invertebrates
1	4586	4602	7222	10544	5029	3975	4816	3138
60	4435	4602	7222	10544	5502	3975	4816	3138
121	4289	4602	3226	8259	5234	3975	4816	3138
182	4146	3933	5159	7163	5021	3975	4816	3138
244	4004	4197	7222	6464	5008	3975	4816	3138
305	3870	4439	7222	5971	5017	3975	4816	3138
365	3745	4594	7222	5611	5029	3975	4816	3138

Table A9—Energy density (joules• g wet weight $^{-1}$), prey proportions and growth input (grams wet weight) parameters of bioenergetic simulation for yellow perch incorporated into chapter 3.

Values from Kitchell et al., 1977.

Energy density	Prey Energy		Predator Energy		
Day	Fish	Invertebrate	Yellow Perch		
1	4184	1673.6	4184		
365	4185	1673.6	4184		
Prey Proportions	Age 0+		Age 1+		Age 2+
Day	Fish	Invertebrate	Fish	Invertebrate	Fish
1	0	1	0.5	0.5	1
365	0	1	0.5	0.5	1
Growth	Age 0+	Age 1+	Age 2+	Age 3+	Age 4+
Start Day	156	139	139	139	139
End Day	323	323	323	323	323
Start Growth	1	9	58	119	172
End Growth	9	58	119	172	224

Table A10—Prey proportions incorporated into bioenergetic simulation of steelhead salmon described in chapter 3.

Day	Invertebrate	Zooplankton	Other	Smelt	$Alwife_{small}$	$Alewife_{large}$
Age 1+						
1	0.83	0.05	0.12	0	0	0
60	0.83	0.05	0.12	0	0	0
61	0.83	0.05	0.12	0	0	0
91	0.83	0.05	0.12	0	0	0
92	0.32	0.05	0.12	0.01	0.5	0
122	0.32	0.05	0.12	0.01	0.5	0
123	0.06	0.06	0	0.3	0.29	0.29
152	0.06	0.06	0	0.3	0.29	0.29
153	0.06	0.06	0	0.3	0.29	0.29
183	0.06	0.06	0	0.3	0.29	0.29
184	0.31	0.07	0	0.2	0.21	0.21
333	0.31	0.07	0	0.2	0.21	0.21
334	0.31	0.07	0	0.2	0.21	0.21
365	0.31	0.07	0	0.2	0.21	0.21
Age 2+						
1	0.31	0.07	0	0.09	0.1	0.43
60	0.31	0.07	0	0.09	0.1	0.43
61	0.08	0.31	0	0.15	0.1	0.36
91	0.08	0.31	0	0.15	0.1	0.36
92	0.06	0.06	0	0.22	0.13	0.53
122	0.06	0.06	0	0.22	0.13	0.53
123	0.06	0.06	0	0.22	0.13	0.53

Day	Invertebrate	Zooplankton	Other	Smelt	$Alwife_{small}$	$Alewife_{large}$
152	0.06	0.06	0	0.22	0.13	0.53
153	0.06	0.06	0	0.22	0.13	0.53
183	0.06	0.06	0	0.22	0.13	0.53
184	0.18	0	0	0.38	0.1	0.34
333	0.18	0	0	0.38	0.1	0.34
334	0.18	0	0	0.38	0.1	0.34
365	0.18	0	0	0.38	0.1	0.34
Age 3,4+						
1	0.18	0	0	0.13	0.16	0.53
60	0.18	0	0	0.13	0.16	0.53
61	0.2	0.08	0	0	0.04	0.68
91	0.2	0.08	0	0	0.04	0.68
92	0.18	0.31	0	0.31	0.07	0.13
122	0.18	0.31	0	0.31	0.07	0.13
123	0.18	0.31	0	0.31	0.07	0.13
152	0.18	0.31	0	0.31	0.07	0.13
153	0.18	0.31	0	0.31	0.07	0.13
183	0.18	0.31	0	0.31	0.07	0.13
184	0.18	0	0	0.13	0.16	0.53
333	0.18	0	0	0.13	0.16	0.53
334	0.18	0	0	0.13	0.16	0.53
365	0.18	0	0	0.13	0.16	0.53

Table A11—Energy density (joules• g wet weight $^{-1}$) of steelhead trout prey items incorporated into bioenergetic simulation and described in chapter 3.

Data from Rand et al., 1993.

Day	Invertebrate	Zooplankton	Other	Smelt	$Alwife_{small}$	$Alewife_{large}$
1	4184	1674	5700	4069.5	4258	5709
32	4184	1674	5700	4038.5	5560	5083
62	4184	1674	5700	4143.5	5620	5165
93	4184	1674	5700	3943.5		4834
124	4184	1674	5700	4030.5	5612	4583
154	4184	1674	5700	4842	5564	7059
189	4184	1674	5700	4669	5870	6997

Table A12—Temperatures of weakfish, yellow perch, and steelhead trout simulated in a bioenergetic model described in chapter 3.

Temperatures from Hartman and Brandt 1995a (weakfish), Kitchell et al., 1977 (yellow Perch), and Rand et al., 1993 (steelhead trout).

	Weakfish *Cynoscion regalis*	Yellow Perch *Perca flavescens*	Steelhead trout *Oncorhynchus mykiss*	
Day	T (°C)	T (°C)	T (°C)	
1	4	4	3	
2	4	4	3	
3	4.1	4	3	

Weakfish *Cynoscion regalis*	Yellow Perch *Perca flavescens*	Steelhead trout *Oncorhynchus mykiss*	
4	4.1	4	3
5	4.2	4	3
6	4.3	4	3
7	4.3	5	3
8	4.4	5	3
9	4.4	6	3
10	4.4	6	3
11	4.5	6	3
12	4.5	6	3
13	4.6	5	3
14	4.6	5	3
15	4.7	6	3
16	4.8	6	2
17	4.7	6	2
18	4.8	6	2
19	4.8	7	2
20	4.8	7	2
21	4.8	7	2
22	4.8	6	2
23	4.8	7	2
24	4.8	7	2
25	4.8	7	2
26	4.9	7	2
27	4.9	8	2
28	4.9	8	2
29	4.9	8	2
30	5	8	2
31	5	8	2
32	5	7	2
33	5.1	7	1
34	5.2	8	1
35	5.3	9	1
36	5.4	9	1
37	5.5	9	2
38	5.5	11	2
39	5.6	11	2
40	5.7	11	2
41	5.8	11	2
42	5.9	11	2
43	6	12	1
44	6	13	1
45	6.1	14	1
46	6.1	14	1
47	6.1	14	2
48	6.1	14	2

Weakfish *Cynoscion regalis*	Yellow Perch *Perca flavescens*	Steelhead trout *Oncorhynchus mykiss*	
49	6.2	14	2
50	6.2	15	2
51	6.2	15	1
52	6.2	16	1
53	6.1	16	1
54	6.2	16	1
55	6.2	16	1
56	6.2	16	1
57	6.2	17	1
58	6.2	17	1
59	6.2	18	1
60	6.2	18	1
61	6.2	18	1
62	6.3	18	1
63	6.3	17	1
64	6.4	17	1
65	6.5	17	1
66	6.6	17	1
67	6.7	17	1
68	6.8	17	1
69	6.9	17	1
70	7	17	1
71	7	17	1
72	7.1	17	1
73	7.2	17	1
74	7.3	19	1
75	7.4	18	1
76	7.5	19	1
77	7.6	20	1
78	7.8	20	1
79	8.1	20	1
80	8.3	20	1
81	8.4	20	1
82	8.7	19	1
83	9	20	1
84	9.2	21	1
85	9.3	20	2
86	9.8	20	1
87	9.8	21	1
88	10	21	2
89	10	20	2
90	10	20	1
91	10	21	2
92	10	21	2
93	10	21	2

Weakfish *Cynoscion regalis*	Yellow Perch *Perca flavescens*	Steelhead trout *Oncorhynchus mykiss*	
94	10	21	2
95	10	21	2
96	11	22	2
97	12	22	2
98	12	22	2
99	12	22	2
100	12	22	3
101	12	23	2
102	12	22	3
103	12	22	3
104	12	22	3
105	13	22	3
106	13	22	3
107	13	22	3
108	13	22	3
109	13	22	3
110	14	22	4
111	14	21	4
112	14	21	4
113	14	21	5
114	15	21	5
115	15	21	4
116	15	21	4
117	15	21	4
118	15	21	5
119	16	22	4
120	16	21	5
121	16	21	5
122	16	21	5
123	16	21	6
124	17	21	5
125	17	21	6
126	17	21	7
127	17	21	7
128	18	21	8
129	18	21	8
130	18	21	8
131	18	20	8
132	18	20	7
133	19	20	7
134	19	20	7
135	19	20	9
136	19	19	8
137	20	19	8
138	20	19	8

Weakfish *Cynoscion regalis*	Yellow Perch *Perca flavescens*	Steelhead trout *Oncorhynchus mykiss*	
139	20	19	10
140	20	19	10
141	20	19	9
142	21	18	10
143	21	18	10
144	21	19	10
145	21	18	10
146	22	17	10
147	22	17	11
148	23	17	11
149	23	17	11
150	23	16	11
151	23	16	11
152	23	16	10
153	23	16	10
154	23	16	11
155	23	16	12
156	24	15	12
157	24	15	12
158	24	15	13
159	24	15	14
160	24	15	14
161	24	14	14
162	24	14	15
163	25	14	15
164	25	14	15
165	25	14	16
166	25	14	17
167	25	14	18
168	25	14	17
169	25	14	17
170	26	13	17
171	26	13	18
172	27	13	18
173	27	13	19
174	27	13	18
175	27	12	19
176	28	12	19
177	28	12	19
178	28	12	19
179	28	12	20
180	28	12	20
181	28	12	20
182	28	12	20
183	28	11	19

Weakfish *Cynoscion regalis*	Yellow Perch *Perca flavescens*	Steelhead trout *Oncorhynchus mykiss*	
184	28	11	19
185	28	11	19
186	28	10	19
187	28	10	19
188	28	10	19
189	28	10	19
190	28	10	19
191	28	9	19
192	28	10	20
193	28	10	20
194	28	10	21
195	28	10	21
196	28	9	21
197	28	9	22
198	28	9	21
199	28	9	21
200	28	9	21
201	28	9	22
202	28	9	22
203	29	9	22
204	29	9	22
205	29	9	22
206	29	8	22
207	29	8	22
208	29	8	22
209	29	8	22
210	29	8	22
211	29	8	23
212	29	8	22
213	29	8	22
214	28	8	22
215	28	8	23
216	28	8	23
217	28	8	23
218	28	7	23
219	28	7	23
220	28	7	23
221	28	6	23
222	28	6	23
223	28	6	23
224	28	6	23
225	28	6	23
226	28	6	23
227	27	6	24
228	27	6	23

Weakfish *Cynoscion regalis*	Yellow Perch *Perca flavescens*	Steelhead trout *Oncorhynchus mykiss*	
229	27	6	23
230	27	5	22
231	27	5	22
232	27	5	22
233	27	5	22
234	27	5	22
235	27	5	23
236	27	5	23
237	27	5	22
238	27	5	22
239	27	5	23
240	27	4	22
241	27	4	22
242	27	4	22
243	27	4	22
244	27	4	22
245	27	4	22
246	27	4	22
247	27	4	22
248	27	4	22
249	27	4	22
250	27	4	22
251	27	4	22
252	27	4	21
253	27	4	21
254	27	4	21
255	26	3	21
256	26	3	21
257	26	3	21
258	26	3	21
259	26	3	21
260	25	3	21
261	25	3	21
262	25	3	20
263	25	3	20
264	24	3	20
265	24	2	19
266	24	2	18
267	24	2	18
268	24	2	18
269	23	2	18
270	23	2	18
271	23	2	18
272	23	2	18
273	23	2	18

Weakfish *Cynoscion regalis*	Yellow Perch *Perca flavescens*	Steelhead trout *Oncorhynchus mykiss*	
274	22	2	17
275	22	2	17
276	22	2	17
277	22	2	17
278	22	2	17
279	22	2	17
280	22	2	17
281	22	2	16
282	21	2	16
283	21	2	16
284	21	2	16
285	21	2	16
286	21	2	15
287	21	2	16
288	20	2	15
289	20	2	15
290	20	2	15
291	20	2	15
292	20	2	15
293	19	2	15
294	19	2	14
295	19	2	14
296	19	2	14
297	18	2	14
298	18	2	14
299	18	1	14
300	18	1	14
301	18	2	14
302	17	2	13
303	17	2	12
304	17	2	12
305	17	2	12
306	16	2	12
307	16	2	12
308	16	1	12
309	16	1	12
310	15	1	12
311	15	1	12
312	15	1	12
313	15	1	12
314	14	1	12
315	14	1	12
316	14	1	12
317	14	1	12
318	13	1	12

Weakfish *Cynoscion regalis*	Yellow Perch *Perca flavescens*	Steelhead trout *Oncorhynchus mykiss*	
319	13	1	11
320	13	1	11
321	13	1	11
322	13	1	10
323	12	1	10
324	12	1	10
325	12	1	10
326	12	1	9
327	12	1	9
328	11	2	9
329	11	2	9
330	11	2	9
331	11	2	9
332	10	2	9
333	10	2	9
334	10.68	2	8
335	9.8	2	8
336	9.7	2	8
337	9.5	2	8
338	9.2	2	7
339	9	2	7
340	8.8	2	6
341	8.6	2	6
342	8.3	2	6
343	8.2	2	6
344	8	2	6
345	7.7	2	6
346	7.6	2	6
347	7.4	2	6
348	7.3	2	6
349	7.1	2	6
350	7	2	5
351	6.8	3	4
352	6.7	3	4
353	6.6	2	4
354	6.5	2	4
355	6.3	3	4
356	6.1	3	4
357	6	3	4
358	5.9	3	4
359	5.7	3	4
360	5.6	3	3
361	5.4	3	3
362	5.1	2	3
363	4.7	3	3

Weakfish *Cynoscion regalis*	Yellow Perch *Perca flavescens*	Steelhead trout *Oncorhynchus mykiss*	
364	4.5	3	3
365	4.5	3	3

Table A13—Temperatures of chinook salmon incorporated into bioenergetic simulations described in chapter 4.

Day 1 = May 1.

Day	T °C nominal	T °C otolith thermometry
1	4	4
15	4	4
30	5	5
45	10.3	10.3
61	11	14.2
76	11	15.6
92	11	19
137	11	19
153	11	15.2
168	11	15.6
183	10	10
198	6.9	6.9
214	6.6	6.6
229	5	5
365	4	4

Table A14—Proportions of prey consumed by chinook salmon incorporated into bioenergetic simulations and described in chapter 4.

Day 1 = May 1.

Day	Invertebrate Diet 1	Other Diet 2	Smelt Diet 3	$Alewife_{small}$ Diet 4	$Alewife_{large}$ Diet 5
Age1+	Stewart and Ibarra, 1991				
1	0	0	0.41	0.2	0.39
31	0	0	0.41	0.2	0.39
61	0	0	0.21	0	0.79
62	0	0	0.21	0	0.79
92	0	0	0.21	0	0.79
93	0	0	0.21	0	0.79
153	0	0	0.21	0	0.79
334	0	0	0.41	0.2	0.39
335	0	0	0.41	0.2	0.39
365	0	0	0.41	0.2	0.39
Age2+	Rand, 1993				
Day	Diet 1	Diet 2	Diet 3	Diet 4	Diet 5
1	0	0	0.28	0.12	0.6
31	0	0	0.28	0.12	0.6

	Invertebrate	Other	Smelt	$Alewife_{small}$	$Alewife_{large}$
61	0	0	0.17	0.05	0.78
62	0	0	0.17	0.05	0.78
123	0	0	0.17	0.05	0.78
124	0	0	0	0.05	0.95
153	0	0	0	0.05	0.95
334	0	0	0.44	0.01	0.55
335	0	0	0.44	0.01	0.55
365	0	0	0.44	0.01	0.55

Age3+ Day	Diet 1	Diet 2	Diet 3	Diet 4	Diet 5
1	0	0	0.03	0	0.97
31	0	0	0.03	0	0.97
61	0	0.01	0.08	0.08	0.83
62	0	0.01	0.08	0.08	0.83
92	0	0.01	0.08	0.08	0.83
123	0	0	0.04	0.15	0.81
124	0	0	0.04	0.15	0.81
153	0	0	0.04	0.15	0.81
334	0	0	0.03	0	0.97
335	0	0	0.03	0	0.97
365	0	0	0.03	0	0.97

Table A15—Energy density (Joules• g wet weight $^{-1}$) of chinook prey items incorporated into bioenergetic simulations described in chapter 4.

Day 1 = May 1, from Rand and Stewart, 1998b.

Day	Diet 1	Diet 2	Diet 3	Diet 4	Diet 5
1	3176	5674	4448	4247	5732
30	3176	5674	4109	5289	5012
61	3176	5674	4167	5510	5075
92	3176	5674	4121	5360	5012
123	3176	5674	3916	5213	5816
153	3176	5674	4268	5435	6820
184	3176	5674	4109	5812	6841
214	3176	5674	4255	5665	6561
245	3176	5674	4402	5477	6255
276	3176	5674	4548	5284	5950
304	3176	5674	4690	5113	5669
334	3176	5674	4573	4782	5577
365	3176	5674	4448	4263	5724

Table A16—Chinook salmon growth (grams) input into bioenergetic model described in chapter 4.

Growth is separated into two life forms dependent on time spent in Lake Ontario from the late 1990s and late 1980s. Day 1 = May 1, from Rand and Stewart, 1998b

Cohort	Day	Growth late 1990s	Growth late 1980s

Cohort	Day	Growth late 1990s	Growth late 1980s
1+	1	332	332
	365	1978	1977
2+	1	1978	1977
1+	1	212	212
	365	1428	1428
2+	1	1428	1428
	365	5441	5442
3+	1	5441	5442
	184	9583	9580

Table A17—Tabulated bioenergetic model output of total specific respiration rate (TRR j • g^{-1} • day^{-1}) for weakfish, yellow perch, and steelhead trout incorporated in chapter 3.

Day	Temperature	TRR	Day	Temperature	TRR	Day	Temperature	TRR
183	28	660	156	12	159	38	11	94
184	28	660	157	12	162	39	11	99
185	28	660	158	13	164	40	11	93
186	28	660	159	14	174	41	11	92
187	28	660	160	14	176	42	11	96
188	28	660	161	14	180	43	12	106
189	28	660	162	15	182	44	13	113
190	28	661	163	15	191	45	14	119
191	28	661	164	15	189	46	14	121
192	28	661	165	16	193	47	14	122
193	28	661	166	17	205	48	14	116
194	28	661	167	18	211	49	14	114
195	28	662	168	17	197	50	15	127
196	28	662	169	17	195	51	15	131
197	28	662	170	17	198	52	16	131
198	28	662	171	18	203	53	16	136
199	28	662	172	18	199	54	16	135
200	28	663	173	19	211	55	16	139
201	28	663	174	18	194	56	16	135
202	28	663	175	19	206	57	17	146
203	29	654	176	19	205	58	17	141
204	29	694	177	19	206	59	18	157
205	29	736	178	19	202	60	18	158
206	29	781	179	20	210	61	18	157
207	29	827	180	20	210	62	18	152
208	29	875	181	20	202	63	17	142
209	29	924	182	20	203	64	17	139
210	29	973	183	19	194	65	17	141
211	29	1021	184	19	185	66	17	139
212	29	1068	185	19	182	67	17	138
213	29	1113	186	19	176	68	17	138
214	28	1246	187	19	175	69	17	138
215	28	1143	188	19	182	70	17	142

Day	Temperature	TRR	Day	Temperature	TRR	Day	Temperature	TRR
216	28	1065	189	19	179	71	17	142
217	28	1006	190	19	179	72	17	139
218	28	958	191	19	174	73	17	144
219	28	920	192	20	180	74	19	157
220	28	889	193	20	182	75	18	152
221	28	863	194	21	184	76	19	163
222	28	841	195	21	183	77	20	172
223	28	823	196	21	192	78	20	171
224	28	807	197	22	194	79	20	172
225	28	793	198	21	186	80	20	169
226	28	781	199	21	185	81	20	173
227	27	798	200	21	183	82	19	160
228	27	746	201	22	188	83	20	170
229	27	705	202	22	182	84	21	180
230	27	671	203	22	179	85	20	176
231	27	643	204	22	182	86	20	176
232	27	619	205	22	175	87	21	187
233	27	599	206	22	174	88	21	188
234	27	581	207	22	175	89	20	170
235	27	566	208	22	177	90	20	176
236	27	552	209	22	170	91	21	180
237	27	541	210	22	175	92	21	195
238	27	530	211	23	176	93	21	196
239	27	520	212	22	171	94	21	191
240	27	512	213	22	169	95	21	198
241	27	504	214	22	168	96	22	204
242	27	497	215	23	169	97	22	205
243	27	491	216	23	175	98	22	204
244	27	485	217	23	174	99	22	202
245	27	480	218	23	168	100	22	202
246	27	475	219	23	169	101	23	206
247	27	470	220	23	168	102	22	204
248	27	466	221	23	167	103	22	205
249	27	462	222	23	162	104	22	201
250	27	459	223	23	165	105	22	200
251	27	456	224	23	162	106	22	201
252	27	453	225	23	159	107	22	205
253	27	450	226	23	161	108	22	204
254	27	447	227	24	161	109	22	205
255	26	432	228	23	155	110	22	202
256	26	424	229	23	154	111	21	199
257	26	416	230	22	145	112	21	198
258	26	408	231	22	145	113	21	196
259	26	401	232	22	142	114	21	195
260	25	376	233	22	141	115	21	194
261	25	367	234	22	142	116	21	196
262	25	360	235	23	141	117	21	197
263	25	353	236	23	140	118	21	192

Day	Temperature	TRR	Day	Temperature	TRR	Day	Temperature	TRR
264	24	325	237	22	136	119	22	200
265	24	319	238	22	136	120	21	195
266	24	313	239	23	139	121	21	197
267	24	307	240	22	133	122	21	195
268	24	302	241	22	134	123	21	193
269	23	276	242	22	133	124	21	191
270	23	272	243	22	130	125	21	194
271	23	267	244	22	131	126	21	188
272	23	263	245	22	131	127	21	190
273	23	259	246	22	127	128	21	190
274	22	236	247	22	125	129	21	187
275	22	233	248	22	124	130	21	186
276	22	230	249	22	124	131	20	180
277	22	228	250	22	122	132	20	181
278	22	225	251	22	122	133	20	178
279	22	223	252	21	115	134	20	172
280	22	221	253	21	112	135	20	172
281	22	219	254	21	109	136	19	172
282	21	196	255	21	109	137	19	169
283	21	195	256	21	110	138	19	171
284	21	193	257	21	109	139	19	171
285	21	192	258	21	108	140	19	165
286	21	191	259	21	111	141	19	170
287	21	189	260	21	108	142	18	155
288	20	167	261	21	106	143	18	159
289	20	166	262	20	98	144	19	161
290	20	166	263	20	98	145	18	155
291	20	165	264	20	96	146	17	145
292	20	165	265	19	93	147	17	142
293	19	142	266	18	88	148	17	141
294	19	142	267	18	87	149	17	138
295	19	142	268	18	85	150	16	134
296	19	143	269	18	86	151	16	132
297	18	122	270	18	85	152	16	130
298	18	123	271	18	84	153	16	133
299	18	123	272	18	82	154	16	129
300	18	124	273	18	81	155	16	132
301	18	125	274	17	77	156	15	124
302	17	108	275	17	79	157	15	120
303	17	109	276	17	78	158	15	123
304	17	109	277	17	77	159	15	120
305	17	110	278	17	78	160	15	120
306	16	97	279	17	75	161	14	114
307	16	98	280	17	73	162	14	113
308	16	99	281	16	70	163	14	109
309	16	99	282	16	68	164	14	111
310	15	89	283	16	68	165	14	109
311	15	90	284	16	68	166	14	111

Day	Temperature	TRR	Day	Temperature	TRR	Day	Temperature	TRR
312	15	91	285	16	67	167	14	108
313	15	91	286	15	66	168	14	109
314	14	83	287	16	67	169	14	108
315	14	83	288	15	65	170	13	103
316	14	84	289	15	64	171	13	100
317	14	85	290	15	63	172	13	99
318	13	77	291	15	62	173	13	97
319	13	78	292	15	61	174	13	97
320	13	78	293	15	61	175	12	91
321	13	79	294	14	60	176	12	93
322	13	80	295	14	59	177	12	92
323	12	73	296	14	57	178	12	90
324	12	73	297	14	57	179	12	88
325	12	74	298	14	56	180	12	89
326	12	75	299	14	56	181	12	88
327	12	75	300	14	56	182	12	85
328	11	69	301	14	56	183	11	80
329	11	69	302	13	54	184	11	76
330	11	70	303	12	50	185	11	75
331	11	70	304	12	50	186	10	73
332	10	65	305	12	49	187	10	72
333	10	65	306	12	49	188	10	70
453	10	95	307	12	48	403	11	79
454	10	95	308	12	49	404	11	83
455	10	96	309	12	48	405	11	78
456	10	96	310	12	49	406	11	77
457	10	96	311	12	48	407	11	81
458	10	97	312	12	49	408	12	89
459	10	97	313	12	48	409	13	96
460	10	97	314	12	48	410	14	101
461	11	104	315	12	47	411	14	103
462	12	112	316	12	46	412	14	104
463	12	112	317	12	46	413	14	99
464	12	112	318	12	46	414	14	97
465	12	113	319	11	45	415	15	109
466	12	113	320	11	45	416	15	112
467	12	114	321	11	43	417	16	112
468	12	114	322	10	40	418	16	117
469	12	114	323	10	40	419	16	116
470	13	124	511	10	48	420	16	119
471	13	124	512	11	51	421	16	116
472	13	124	513	11	49	422	17	126
473	13	125	514	11	49	423	17	122
474	13	125	515	11	49	424	18	137
475	14	137	516	11	50	425	18	138
476	14	137	517	10	48	426	18	131
477	14	137	518	10	48	427	18	127
478	14	138	519	11	49	428	17	118

Day	Temperature	TRR	Day	Temperature	TRR	Day	Temperature	TRR
479	15	152	520	12	56	429	17	115
480	15	152	521	12	54	430	17	117
481	15	152	522	12	56	431	17	115
482	15	153	523	13	57	432	17	115
483	15	153	524	14	61	433	17	115
484	16	170	525	14	63	434	17	115
485	16	170	526	14	65	435	17	119
486	16	170	527	15	66	436	17	119
487	16	170	528	15	71	437	17	116
488	16	170	529	15	71	438	17	121
489	17	189	530	16	73	439	19	133
490	17	189	531	17	78	440	18	128
491	17	188	532	18	82	441	19	138
492	17	188	533	17	77	442	20	147
493	18	208	534	17	77	443	20	147
494	18	207	535	17	79	444	20	147
495	18	206	536	18	82	445	20	145
496	18	205	537	18	81	446	20	148
497	18	204	538	19	87	447	19	136
498	19	223	539	18	81	448	20	145
499	19	221	540	19	86	449	21	156
500	19	220	541	19	87	450	20	151
501	19	219	542	19	88	451	20	151
502	20	235	543	19	87	452	21	162
503	20	233	544	20	91	453	21	164
504	20	231	545	20	92	454	20	146
505	20	230	546	20	90	455	20	151
506	20	228	547	20	91	456	21	155
507	21	241	548	19	88	457	21	168
508	21	240	549	19	85	458	21	169
509	21	238	550	19	84	459	21	164
510	21	236	551	19	82	460	21	171
511	22	247	552	19	83	461	22	180
512	22	245	553	19	86	462	22	180
513	23	255	554	19	85	463	22	179
514	23	253	555	19	86	464	22	176
515	23	251	556	19	85	465	22	176
516	23	250	557	20	88	466	23	182
517	23	248	558	20	89	467	22	179
518	23	246	559	21	91	468	22	181
519	23	244	560	21	91	469	22	175
520	23	243	561	21	95	470	22	174
521	24	252	562	22	96	471	22	175
522	24	250	563	21	94	472	22	180
523	24	248	564	21	94	473	22	179
524	24	247	565	21	94	474	22	180
525	24	245	566	22	96	475	22	176
526	24	244	567	22	94	476	21	172

Day	Temperature	TRR	Day	Temperature	TRR	Day	Temperature	TRR
527	24	243	568	22	94	477	21	172
528	25	251	569	22	95	478	21	169
529	25	250	570	22	93	479	21	169
530	25	248	571	22	93	480	21	168
531	25	247	572	22	94	481	21	170
532	25	246	573	22	95	482	21	171
533	25	245	574	22	93	483	21	166
534	25	243	575	22	95	484	22	174
535	26	252	576	23	96	485	21	170
536	26	251	577	22	94	486	21	171
537	27	259	578	22	94	487	21	169
538	27	258	579	22	94	488	21	171
539	27	257	580	23	95	489	21	169
540	27	257	581	23	97	490	21	172
541	28	266	582	23	97	491	21	166
542	28	265	583	23	95	492	21	168
543	28	264	584	23	96	493	21	168
544	28	263	585	23	96	494	21	166
545	28	262	586	23	96	495	21	165
546	28	262	587	23	95	496	20	160
547	28	261	588	23	96	497	20	160
548	28	260	589	23	95	498	20	158
549	28	260	590	23	94	499	20	152
550	28	259	591	23	95	500	20	153
551	28	258	592	24	95	501	19	152
552	28	257	593	23	94	502	19	150
553	28	257	594	23	94	503	19	152
554	28	256	595	22	90	504	19	153
555	28	256	596	22	90	505	19	147
556	28	255	597	22	90	506	19	152
557	28	254	598	22	89	507	18	138
558	28	254	599	22	90	508	18	142
559	28	253	600	23	90	509	19	143
560	28	253	601	23	90	510	18	139
561	28	252	602	22	88	511	17	129
562	28	251	603	22	88	512	17	126
563	28	251	604	23	90	513	17	126
564	28	250	605	22	87	514	17	123
565	28	250	606	22	88	515	16	120
566	28	249	607	22	88	516	16	118
567	28	249	608	22	87	517	16	116
568	29	258	609	22	87	518	16	119
569	29	258	610	22	87	519	16	115
570	29	258	611	22	86	520	16	119
571	29	257	612	22	85	521	15	112
572	29	257	613	22	85	522	15	108
573	29	256	614	22	85	523	15	111
574	29	256	615	22	84	524	15	108

Day	Temperature	TRR	Day	Temperature	TRR	Day	Temperature	TRR
575	29	256	616	22	84	525	15	108
576	29	255	617	21	81	526	14	103
577	29	255	618	21	79	527	14	102
578	29	255	619	21	77	528	14	98
579	28	245	620	21	78	529	14	99
580	28	244	621	21	79	530	14	98
581	28	244	622	21	78	531	14	100
582	28	244	623	21	78	532	14	97
583	28	244	624	21	79	533	14	98
584	28	243	625	21	78	534	14	97
585	28	243	626	21	77	535	13	92
586	28	243	627	20	72	536	13	90
587	28	242	628	20	72	537	13	89
588	28	242	629	20	71	538	13	87
589	28	242	630	19	69	539	13	87
590	28	242	631	18	66	540	12	81
591	28	241	632	18	65	541	12	83
592	27	232	633	18	64	542	12	83
593	27	231	634	18	64	543	12	81
594	27	231	635	18	64	544	12	79
595	27	231	636	18	63	545	12	79
596	27	231	637	18	62	546	12	79
597	27	230	638	18	61	547	12	76
598	27	230	639	17	58	548	11	72
599	27	230	640	17	60	549	11	69
600	27	229	641	17	60	550	11	67
601	27	229	642	17	59	551	10	66
602	27	229	643	17	59	552	10	65
603	27	228	644	17	57	553	10	63
604	27	228	645	17	56	768	11	76
605	27	228	646	16	53	769	11	79
606	27	228	647	16	52	770	11	74
607	27	227	648	16	52	771	11	74
608	27	227	649	16	52	772	11	77
609	27	227	650	16	52	773	12	85
610	27	226	651	15	51	774	13	92
611	27	226	652	16	51	775	14	97
612	27	226	653	15	50	776	14	99
613	27	226	654	15	49	777	14	100
614	27	225	655	15	48	778	14	95
615	27	225	656	15	48	779	14	93
616	27	225	657	15	47	780	15	104
617	27	224	658	15	47	781	15	107
618	27	224	659	14	46	782	16	108
619	27	224	660	14	45	783	16	112
620	26	215	661	14	44	784	16	111
621	26	215	662	14	44	785	16	115
622	26	214	663	14	44	786	16	112

Day	Temperature	TRR	Day	Temperature	TRR	Day	Temperature	TRR
623	26	214	664	14	43	787	17	121
624	26	214	665	14	43	788	17	117
625	25	205	666	14	43	789	18	131
626	25	205	667	13	41	790	18	132
627	25	205	668	12	39	791	18	129
628	25	204	669	12	39	792	18	125
629	24	196	670	12	38	793	17	116
630	24	196	671	12	38	794	17	113
631	24	195	672	12	37	795	17	115
632	24	195	673	12	38	796	17	113
633	24	195	674	12	37	797	17	113
634	23	186	675	12	38	798	17	112
635	23	186	676	12	37	799	17	112
636	23	186	677	12	38	800	17	116
637	23	185	678	12	37	801	17	116
638	23	185	679	12	37	802	17	113
639	22	176	680	12	36	803	17	118
640	22	176	681	12	36	804	19	130
641	22	175	682	12	36	805	18	125
642	22	175	683	12	36	806	19	135
643	22	175	684	11	35	807	20	143
644	22	174	685	11	35	808	20	143
645	22	174	686	11	33	809	20	143
646	22	173	876	10	30	810	20	141
647	21	164	877	11	32	811	20	144
648	21	164	878	11	31	812	19	132
649	21	164	879	11	31	813	20	141
650	21	163	880	11	31	814	21	151
651	21	163	881	11	32	815	20	147
652	21	163	882	10	30	816	20	147
653	20	153	883	10	30	817	21	158
654	20	152	884	11	31	818	21	159
655	20	152	885	12	35	819	20	141
656	20	152	886	12	34	820	20	146
657	20	152	887	12	35	821	21	150
658	19	141	888	13	36	822	21	150
659	19	141	889	14	39	823	21	151
660	19	140	890	14	40	824	21	146
661	19	140	891	14	41	825	21	154
662	18	129	892	15	42	826	22	164
663	18	129	893	15	45	827	22	165
664	18	129	894	15	45	828	22	163
665	18	129	895	16	47	829	22	160
666	18	129	896	17	50	830	22	159
667	17	117	897	18	53	831	23	167
668	17	117	898	17	50	832	22	164
669	17	117	899	17	50	833	22	165
670	17	117	900	17	51	834	22	158

Day	Temperature	TRR	Day	Temperature	TRR	Day	Temperature	TRR
671	16	106	901	18	53	835	22	156
672	16	106	902	18	53	836	22	158
673	16	106	903	19	57	837	22	165
674	16	106	904	18	53	838	22	163
675	15	97	905	19	57	839	22	164
676	15	97	906	19	57	840	22	159
677	15	97	907	19	58	841	21	155
678	15	97	908	19	58	842	21	154
679	14	89	909	20	60	843	21	152
680	14	89	910	20	61	844	21	151
681	14	89	911	20	60	845	21	150
682	14	89	912	20	61	846	21	152
683	13	83	913	19	59	847	21	154
684	13	83	914	19	57	848	21	149
685	13	83	915	19	56	849	22	158
686	13	83	916	19	55	850	21	153
687	13	83	917	19	56	851	21	154
688	12	78	918	19	58	852	21	152
689	12	78	919	19	58	853	21	154
690	12	78	920	19	59	854	21	152
691	12	78	921	19	57	855	21	155
692	12	78	922	20	60	856	21	149
693	11	73	923	20	61	857	21	150
694	11	73	924	21	62	858	21	151
695	11	73	925	21	62	859	21	148
696	11	74	926	21	65	860	21	147
697	10	69	927	22	67	861	20	141
698	10	69	928	21	65	862	20	141
818	10	70	929	21	65	863	20	139
819	10	70	930	21	65	864	20	133
820	10	70	931	22	67	865	20	133
821	10	70	932	22	66	866	19	133
822	10	70	933	22	65	867	19	130
823	10	70	934	22	67	868	19	133
824	10	70	935	22	65	869	19	133
825	10	70	936	22	65	870	19	127
826	11	75	937	22	66	871	19	132
827	12	80	938	22	67	872	18	118
828	12	80	939	22	66	873	18	122
829	12	80	940	22	67	874	19	124
830	12	81	941	23	68	875	18	119
831	12	81	942	22	67	876	17	110
832	12	81	943	22	67	877	17	107
833	12	81	944	22	67	878	17	107
834	12	81	945	23	68	879	17	104
835	13	87	946	23	70	880	16	101
836	13	87	947	23	70	881	16	99
837	13	88	948	23	69	882	16	97

Day	Temperature	TRR	Day	Temperature	TRR	Day	Temperature	TRR
838	13	88	949	23	69	883	16	100
839	13	88	950	23	69	884	16	97
840	14	95	951	23	69	885	16	100
841	14	96	952	23	69	886	15	93
842	14	96	953	23	70	887	15	90
843	14	96	954	23	69	888	15	93
844	15	105	955	23	69	889	15	90
845	15	105	956	23	70	890	15	91
846	15	105	957	24	70	891	14	86
847	15	105	958	23	69	892	14	85
848	15	105	959	23	69	893	14	82
849	16	116	960	22	66	894	14	83
850	16	116	961	22	66	895	14	82
851	16	116	962	22	66	896	14	84
852	16	116	963	22	66	897	14	82
853	16	116	964	22	66	898	14	83
854	17	129	965	23	66	899	14	82
855	17	129	966	23	66	900	13	78
856	17	129	967	22	65	901	13	75
857	17	128	968	22	65	902	13	75
858	18	142	969	23	67	903	13	73
859	18	141	970	22	65	904	13	73
860	18	141	971	22	66	905	12	68
861	18	141	972	22	66	906	12	70
862	18	141	973	22	65	907	12	70
863	19	153	974	22	65	908	12	68
864	19	153	975	22	66	909	12	66
865	19	152	976	22	64	910	12	67
866	19	152	977	22	64	911	12	67
867	20	163	978	22	64	912	12	64
868	20	163	979	22	64	913	11	61
869	20	162	980	22	63	914	11	71
870	20	162	981	22	64	915	11	69
871	20	161	982	21	61	916	10	68
872	21	171	983	21	60	917	10	67
873	21	171	984	21	59	918	10	65
874	21	170	985	21	59	1133	11	65
875	21	170	986	21	60	1134	11	68
876	22	178	987	21	59	1135	11	64
877	22	178	988	21	59	1136	11	63
878	23	185	989	21	61	1137	11	67
879	23	185	990	21	60	1138	12	74
880	23	184	991	21	59	1139	13	80
881	23	184	992	20	55	1140	14	85
882	23	183	993	20	55	1141	14	87
883	23	182	994	20	55	1142	14	88
884	23	182	995	19	53	1143	14	83
885	23	181	996	18	51	1144	14	82

Day	Temperature	TRR	Day	Temperature	TRR	Day	Temperature	TRR
886	24	188	997	18	50	1145	15	92
887	24	188	998	18	49	1146	15	96
888	24	187	999	18	50	1147	16	96
889	24	187	1000	18	50	1148	16	100
890	24	186	1001	18	49	1149	16	100
891	24	185	1002	18	48	1150	16	103
892	24	185	1003	18	48	1151	16	100
893	25	192	1004	17	45	1152	17	110
894	25	191	1005	17	47	1153	17	105
895	25	191	1006	17	46	1154	18	120
896	25	190	1007	17	46	1155	18	121
897	25	190	1008	17	46	1156	18	118
898	25	189	1009	17	45	1157	18	114
899	25	189	1010	17	44	1158	17	105
900	26	196	1011	16	42	1159	17	103
901	26	196	1012	16	41	1160	17	105
902	27	203	1013	16	41	1161	17	103
903	27	202	1014	16	41	1162	17	103
904	27	202	1015	16	41	1163	17	103
905	27	202	1016	15	40	1164	17	103
906	28	209	1017	16	40	1165	17	107
907	28	209	1018	15	40	1166	17	107
908	28	209	1019	15	39	1167	17	104
909	28	208	1020	15	38	1168	17	109
910	28	208	1021	15	38	1169	19	120
911	28	207	1022	15	37	1170	18	116
912	28	207	1023	15	37	1171	19	126
913	28	207	1024	14	37	1172	20	135
914	28	206	1025	14	36	1173	20	134
915	28	206	1026	14	35	1174	20	134
916	28	206	1027	14	35	1175	20	132
917	28	206	1028	14	35	1176	20	136
918	28	205	1029	14	34	1177	19	124
919	28	205	1030	14	34	1178	20	133
920	28	205	1031	14	34	1179	21	143
921	28	204	1032	13	33	1180	20	139
922	28	204	1033	12	31	1181	20	139
923	28	204	1034	12	31	1182	21	150
924	28	204	1035	12	30	1183	21	152
925	28	203	1036	12	30	1184	20	133
926	28	203	1037	12	30	1185	20	138
927	28	203	1038	12	30	1186	21	143
928	28	203	1039	12	30	1187	21	143
929	28	202	1040	12	30	1188	21	145
930	28	202	1041	12	30	1189	21	139
931	28	202	1042	12	30	1190	21	148
932	28	202	1043	12	30	1191	22	159
933	29	210	1044	12	30	1192	22	160

Day	Temperature	TRR	Day	Temperature	TRR	Day	Temperature	TRR
934	29	209	1045	12	29	1193	22	158
935	29	209	1046	12	29	1194	22	154
936	29	209	1047	12	29	1195	22	154
937	29	209	1048	12	29	1196	23	163
938	29	209	1049	11	28	1197	22	158
939	29	208	1050	11	28	1198	22	160
940	29	208	1051	11	27	1199	22	152
941	29	208	1241	10	26	1200	22	150
942	29	208	1242	11	28	1201	22	152
943	29	208	1243	11	27	1202	22	159
944	28	199	1244	11	27	1203	22	158
945	28	199	1245	11	26	1204	22	159
946	28	199	1246	11	28	1205	22	153
947	28	199	1247	10	26	1206	21	148
948	28	199	1248	10	26	1207	21	148
949	28	198	1249	11	27	1208	21	145
950	28	198	1250	12	31	1209	21	145
951	28	198	1251	12	30	1210	21	144
952	28	198	1252	12	31	1211	21	146
953	28	197	1253	13	31	1212	21	147
954	28	197	1254	14	34	1213	21	142
955	28	197	1255	14	35	1214	22	152
956	28	197	1256	14	36	1215	21	146
957	27	189	1257	15	37	1216	21	148
958	27	189	1258	15	39	1217	21	145
959	27	188	1259	15	39	1218	21	148
960	27	188	1260	16	41	1219	21	146
961	27	188	1261	17	44	1220	21	149
962	27	188	1262	18	46	1221	21	142
963	27	188	1263	17	43	1222	21	144
964	27	187	1264	17	43	1223	21	144
965	27	187	1265	17	45	1224	21	141
966	27	187	1266	18	46	1225	21	140
967	27	187	1267	18	46	1226	20	134
968	27	186	1268	19	49	1227	20	134
969	27	186	1269	18	46	1228	20	132
970	27	186	1270	19	49	1229	20	126
971	27	186	1271	19	50	1230	20	126
972	27	186	1272	19	51	1231	19	126
973	27	185	1273	19	50	1232	19	123
974	27	185	1274	20	53	1233	19	126
975	27	185	1275	20	53	1234	19	126
976	27	185	1276	20	52	1235	19	120
977	27	185	1277	20	53	1236	19	125
978	27	185	1278	19	51	1237	18	111
979	27	184	1279	19	49	1238	18	115
980	27	184	1280	19	49	1239	19	116
981	27	184	1281	19	48	1240	18	112

Day	Temperature	TRR	Day	Temperature	TRR	Day	Temperature	TRR
982	27	184	1282	19	48	1241	17	103
983	27	184	1283	19	51	1242	17	100
984	27	184	1284	19	50	1243	17	100
985	26	176	1285	19	51	1244	17	97
986	26	176	1286	19	50	1245	16	94
987	26	176	1287	20	52	1246	16	92
988	26	175	1288	20	53	1247	16	90
989	26	175	1289	21	54	1248	16	93
990	25	168	1290	21	54	1249	16	90
991	25	168	1291	21	57	1250	16	93
992	25	168	1292	22	58	1251	15	87
993	25	167	1293	21	56	1252	15	84
994	24	160	1294	21	57	1253	15	86
995	24	160	1295	21	57	1254	15	84
996	24	160	1296	22	58	1255	15	85
997	24	160	1297	22	57	1256	14	80
998	24	160	1298	22	57	1257	14	79
999	23	153	1299	22	58	1258	14	76
1000	23	152	1300	22	57	1259	14	77
1001	23	152	1301	22	57	1260	14	76
1002	23	152	1302	22	58	1261	14	78
1003	23	152	1303	22	59	1262	14	76
1004	22	145	1304	22	57	1263	14	77
1005	22	144	1305	22	59	1264	14	77
1006	22	144	1306	23	59	1265	13	72
1007	22	144	1307	22	59	1266	13	70
1008	22	144	1308	22	59	1267	13	70
1009	22	144	1309	22	59	1268	13	68
1010	22	144	1310	23	59	1269	13	68
1011	22	143	1311	23	61	1270	12	64
1012	21	136	1312	23	61	1271	12	65
1013	21	136	1313	23	60	1272	12	65
1014	21	136	1314	23	60	1273	12	64
1015	21	136	1315	23	61	1274	12	62
1016	21	135	1316	23	61	1275	12	63
1017	21	135	1317	23	60	1276	12	62
1018	20	127	1318	23	61	1277	12	60
1019	20	127	1319	23	61	1278	11	56
1020	20	127	1320	23	60	1279	11	66
1021	20	127	1321	23	61	1280	11	64
1022	20	127	1322	24	61	1281	10	63
1023	19	118	1323	23	60	1282	10	62
1024	19	118	1324	23	60	1283	10	60
1025	19	118	1325	22	58			
1026	19	118	1326	22	58			
1027	18	109	1327	22	58			
1028	18	109	1328	22	58			
1029	18	109	1329	22	58			

Day	Temperature	TRR	Day	Temperature	TRR	Day	Temperature	TRR
1030	18	109	1330	23	58			
1031	18	109	1331	23	58			
1032	17	100	1332	22	57			
1033	17	100	1333	22	57			
1034	17	100	1334	23	59			
1035	17	100	1335	22	57			
1036	16	92	1336	22	58			
1037	16	92	1337	22	57			
1038	16	92	1338	22	57			
1039	16	92	1339	22	57			
1040	15	84	1340	22	57			
1041	15	84	1341	22	56			
1042	15	85	1342	22	56			
1043	15	85	1343	22	56			
1044	14	78	1344	22	56			
1045	14	78	1345	22	56			
1046	14	78	1346	22	56			
1047	14	79	1347	21	53			
1048	13	73	1348	21	53			
1049	13	73	1349	21	52			
1050	13	73	1350	21	52			
1051	13	73	1351	21	53			
1052	13	73	1352	21	52			
1053	12	69	1353	21	52			
1054	12	69	1354	21	53			
1055	12	69	1355	21	52			
1056	12	69	1356	21	52			
1057	12	69	1357	20	48			
1058	11	65	1358	20	49			
1059	11	65	1359	20	48			
1060	11	65	1360	19	47			
1061	11	65	1361	18	45			
1062	10	62	1362	18	44			
1063	10	62	1363	18	43			
			1364	18	44			
			1365	18	44			
			1366	18	43			
			1367	18	42			
			1368	18	42			
			1369	17	40			
			1370	17	41			
			1371	17	41			
			1372	17	40			
			1373	17	41			
			1374	17	39			
			1375	17	39			
			1376	16	37			
			1377	16	36			

Day	Temperature	TRR	Day	Temperature	TRR	Day	Temperature	TRR
			1378		16	36		
			1379		16	36		
			1380		16	36		
			1381		15	35		
			1382		16	36		
			1383		15	35		
			1384		15	34		
			1385		15	34		
			1386		15	33		
			1387		15	33		
			1388		15	33		
			1389		14	32		
			1390		14	32		
			1391		14	31		
			1392		14	31		
			1393		14	31		
			1394		14	30		
			1395		14	30		
			1396		14	30		
			1397		13	29		
			1398		12	27		
			1399		12	27		
			1400		12	27		
			1401		12	26		
			1402		12	26		
			1403		12	27		
			1404		12	26		
			1405		12	27		
			1406		12	27		
			1407		12	27		
			1408		12	26		
			1409		12	26		
			1410		12	26		
			1411		12	25		
			1412		12	25		
			1413		12	25		
			1414		11	25		
			1415		11	25		
			1416		11	24		

Table A18—Tabulated bioenergetic model output of Specific Growth Rate (SGR) in $j \cdot g^{-1} \cdot day^{-1}$ and Gross Conversion Efficiency for chinook salmon described in chapter 4.

Day	SGR_{2+oto}	SGR_{2+nom}	$SGR3_{+oto}$	SGR_{3+nom}	GCE_{2+oto}	GCE_{2+nom}	GCE_{3+oto}	GCE_{3+nom}
1	15.7	10.9	16.3	11.3	0.25	0.20	0.25	0.20
2	15.7	10.8	16.2	11.2	0.25	0.20	0.24	0.20
3	15.6	10.8	16.1	11.1	0.25	0.20	0.24	0.19
4	15.5	10.7	16.1	11.1	0.24	0.20	0.24	0.19

Day	SGR_{2+oto}	SGR_{2+nom}	$SGR3_{+oto}$	SGR_{3+nom}	GCE_{2+oto}	GCE_{2+nom}	GCE_{3+oto}	GCE_{3+nom}
5	15.4	10.7	16.0	11.0	0.24	0.20	0.24	0.19
6	15.4	10.6	15.9	10.9	0.24	0.20	0.24	0.19
7	15.3	10.5	15.8	10.9	0.24	0.19	0.24	0.19
8	15.2	10.5	15.7	10.8	0.24	0.19	0.24	0.19
9	15.1	10.4	15.7	10.7	0.24	0.19	0.24	0.19
10	15.0	10.3	15.6	10.7	0.24	0.19	0.24	0.19
11	15.0	10.3	15.5	10.6	0.24	0.19	0.24	0.19
12	14.9	10.2	15.4	10.5	0.24	0.19	0.24	0.19
13	14.8	10.2	15.3	10.5	0.24	0.19	0.24	0.19
14	14.7	10.1	15.3	10.4	0.24	0.19	0.24	0.19
15	14.7	10.0	15.2	10.4	0.24	0.19	0.24	0.19
16	15.3	10.6	15.9	10.9	0.24	0.19	0.24	0.19
17	16.0	11.1	16.5	11.5	0.25	0.20	0.25	0.20
18	16.6	11.7	17.2	12.1	0.25	0.21	0.25	0.20
19	17.3	12.3	17.9	12.7	0.26	0.21	0.26	0.21
20	17.9	12.8	18.6	13.3	0.26	0.22	0.26	0.22
21	18.6	13.4	19.3	13.9	0.27	0.22	0.27	0.22
22	19.3	14.0	20.0	14.5	0.27	0.23	0.27	0.23
23	20.0	14.6	20.7	15.1	0.28	0.23	0.28	0.23
24	20.7	15.2	21.5	15.7	0.28	0.24	0.28	0.24
25	21.3	15.8	22.2	16.4	0.29	0.24	0.29	0.24
26	22.0	16.3	22.9	17.0	0.29	0.25	0.29	0.25
27	22.7	16.9	23.6	17.6	0.29	0.25	0.29	0.25
28	23.4	17.5	24.4	18.2	0.30	0.26	0.30	0.26
29	24.1	18.1	25.1	18.9	0.30	0.26	0.30	0.26
30	24.8	18.7	25.8	19.5	0.31	0.27	0.31	0.27
31	29.2	22.5	30.4	23.5	0.33	0.29	0.33	0.29
32	33.8	26.4	35.3	27.6	0.34	0.31	0.35	0.31
33	38.5	30.4	40.1	31.8	0.36	0.33	0.36	0.33
34	43.1	34.4	45.0	36.0	0.37	0.34	0.37	0.34
35	47.7	38.3	49.8	40.0	0.38	0.35	0.38	0.36
36	52.1	42.0	54.4	44.0	0.39	0.36	0.39	0.36
37	56.3	45.6	58.7	47.7	0.40	0.37	0.40	0.37
38	60.2	48.9	62.8	51.2	0.40	0.38	0.40	0.38
39	63.8	51.9	66.5	54.3	0.41	0.38	0.41	0.38
40	66.9	54.6	69.8	57.1	0.41	0.38	0.41	0.38
41	69.7	56.9	72.8	59.6	0.41	0.38	0.41	0.39
42	72.1	58.9	75.2	61.6	0.41	0.38	0.41	0.39
43	74.1	60.5	77.3	63.3	0.41	0.38	0.41	0.38
44	75.6	61.7	78.9	64.6	0.41	0.38	0.41	0.38
45	76.8	62.6	80.0	65.5	0.40	0.38	0.41	0.38
46	77.3	62.6	80.6	65.5	0.40	0.38	0.40	0.38
47	77.7	62.5	80.9	65.4	0.40	0.38	0.40	0.38
48	77.8	62.5	81.0	65.4	0.40	0.38	0.40	0.38
49	77.8	62.5	81.0	65.4	0.39	0.38	0.39	0.38
50	77.7	62.5	80.9	65.3	0.39	0.38	0.39	0.38
51	77.4	62.4	80.5	65.3	0.38	0.37	0.39	0.38
52	77.0	62.4	80.1	65.2	0.38	0.37	0.38	0.37

Day	SGR_{2+oto}	SGR_{2+nom}	$SGR3_{+oto}$	SGR_{3+nom}	GCE_{2+oto}	GCE_{2+nom}	GCE_{3+oto}	GCE_{3+nom}
53	76.4	62.3	79.5	65.1	0.37	0.37	0.38	0.37
54	75.7	62.3	78.7	65.0	0.37	0.37	0.37	0.37
55	74.9	62.2	77.9	65.0	0.36	0.37	0.37	0.37
56	74.0	62.1	76.9	64.9	0.36	0.37	0.36	0.37
57	73.0	62.0	75.8	64.8	0.35	0.37	0.35	0.37
58	71.9	62.0	74.7	64.7	0.35	0.37	0.35	0.37
59	70.7	61.9	73.4	64.6	0.34	0.37	0.34	0.37
60	69.4	61.8	72.0	64.4	0.33	0.37	0.33	0.37
61	68.0	61.7	70.6	64.3	0.33	0.37	0.33	0.37
62	67.1	61.4	69.7	64.0	0.32	0.37	0.32	0.37
63	66.3	61.1	68.8	63.7	0.32	0.37	0.32	0.37
64	65.4	60.8	67.9	63.4	0.32	0.37	0.32	0.37
65	64.5	60.6	67.0	63.1	0.31	0.37	0.31	0.37
66	63.7	60.3	66.1	62.8	0.31	0.36	0.31	0.37
67	62.8	60.0	65.1	62.5	0.31	0.36	0.31	0.36
68	61.9	59.8	64.2	62.2	0.30	0.36	0.30	0.36
69	61.0	59.5	63.2	61.9	0.30	0.36	0.30	0.36
70	60.1	59.2	62.3	61.7	0.29	0.36	0.30	0.36
71	59.2	59.0	61.3	61.4	0.29	0.36	0.29	0.36
72	58.2	58.7	60.4	61.1	0.29	0.36	0.29	0.36
73	57.3	58.5	59.4	60.8	0.28	0.36	0.28	0.36
74	56.4	58.2	58.4	60.5	0.28	0.36	0.28	0.36
75	55.4	58.0	57.5	60.3	0.27	0.36	0.28	0.36
76	54.5	57.7	56.5	60.0	0.27	0.36	0.27	0.36
77	52.7	57.5	54.6	59.7	0.26	0.36	0.26	0.36
78	50.8	57.2	52.6	59.4	0.25	0.36	0.25	0.36
79	48.8	57.0	50.6	59.2	0.24	0.36	0.24	0.36
80	46.8	56.7	48.5	58.9	0.23	0.36	0.24	0.36
81	44.7	56.5	46.4	58.6	0.22	0.36	0.23	0.36
82	42.5	56.2	44.2	58.4	0.21	0.36	0.22	0.36
83	40.3	56.0	41.8	58.1	0.20	0.36	0.20	0.36
84	37.9	55.8	39.4	57.9	0.19	0.36	0.19	0.36
85	35.4	55.5	36.8	57.6	0.18	0.36	0.18	0.36
86	32.7	55.3	34.1	57.4	0.17	0.35	0.17	0.35
87	29.9	55.1	31.2	57.1	0.15	0.35	0.16	0.35
88	26.8	54.8	28.0	56.8	0.14	0.35	0.14	0.35
89	23.4	54.6	24.5	56.6	0.12	0.35	0.12	0.35
90	19.6	54.4	20.7	56.4	0.10	0.35	0.11	0.35
91	15.4	54.2	16.3	56.1	0.08	0.35	0.09	0.35
92	10.5	53.9	11.4	55.9	0.06	0.35	0.06	0.35
93	10.9	54.1	11.8	56.1	0.06	0.35	0.06	0.35
94	11.3	54.3	12.2	56.2	0.06	0.35	0.06	0.35
95	11.7	54.5	12.6	56.4	0.06	0.35	0.07	0.35
96	12.1	54.7	13.0	56.6	0.07	0.35	0.07	0.35
97	12.5	54.9	13.4	56.8	0.07	0.36	0.07	0.36
98	12.9	55.1	13.8	57.0	0.07	0.36	0.07	0.36
99	13.3	55.3	14.2	57.2	0.07	0.36	0.07	0.36
100	13.7	55.5	14.6	57.4	0.07	0.36	0.08	0.36

Day	SGR_{2+oto}	SGR_{2+nom}	$SGR3_{+oto}$	SGR_{3+nom}	GCE_{2+oto}	GCE_{2+nom}	GCE_{3+oto}	GCE_{3+nom}
101	14.1	55.6	15.0	57.5	0.07	0.36	0.08	0.36
102	14.4	55.8	15.4	57.7	0.08	0.36	0.08	0.36
103	14.8	56.0	15.8	57.9	0.08	0.36	0.08	0.36
104	15.2	56.2	16.2	58.1	0.08	0.36	0.08	0.36
105	15.6	56.4	16.6	58.2	0.08	0.36	0.08	0.36
106	16.0	56.5	16.9	58.4	0.08	0.36	0.09	0.36
107	16.3	56.7	17.3	58.6	0.09	0.36	0.09	0.36
108	16.7	56.9	17.7	58.7	0.09	0.36	0.09	0.36
109	17.1	57.0	18.1	58.9	0.09	0.36	0.09	0.36
110	17.4	57.2	18.4	59.1	0.09	0.36	0.09	0.36
111	17.8	57.4	18.8	59.2	0.09	0.36	0.09	0.36
112	18.2	57.5	19.2	59.4	0.09	0.36	0.10	0.36
113	18.5	57.7	19.6	59.5	0.10	0.37	0.10	0.37
114	18.9	57.9	19.9	59.7	0.10	0.37	0.10	0.37
115	19.2	58.0	20.3	59.8	0.10	0.37	0.10	0.37
116	19.6	58.2	20.6	60.0	0.10	0.37	0.10	0.37
117	19.9	58.3	21.0	60.1	0.10	0.37	0.10	0.37
118	20.3	58.5	21.4	60.3	0.10	0.37	0.11	0.37
119	20.6	58.6	21.7	60.4	0.10	0.37	0.11	0.37
120	21.0	58.8	22.1	60.6	0.11	0.37	0.11	0.37
121	21.3	58.9	22.4	60.7	0.11	0.37	0.11	0.37
122	21.7	59.1	22.8	60.9	0.11	0.37	0.11	0.37
123	22.0	59.2	23.1	61.0	0.11	0.37	0.11	0.37
124	22.6	59.6	23.7	61.3	0.11	0.37	0.11	0.37
125	23.1	59.9	24.2	61.6	0.11	0.37	0.12	0.37
126	23.7	60.2	24.8	62.0	0.12	0.37	0.12	0.37
127	24.2	60.5	25.4	62.3	0.12	0.37	0.12	0.37
128	24.8	60.8	25.9	62.6	0.12	0.38	0.12	0.38
129	25.3	61.1	26.5	62.9	0.12	0.38	0.13	0.38
130	25.8	61.4	27.0	63.2	0.13	0.38	0.13	0.38
131	26.4	61.8	27.6	63.5	0.13	0.38	0.13	0.38
132	26.9	62.1	28.1	63.8	0.13	0.38	0.13	0.38
133	27.4	62.4	28.6	64.1	0.13	0.38	0.13	0.38
134	27.9	62.7	29.2	64.4	0.13	0.38	0.14	0.38
135	28.5	62.9	29.7	64.7	0.14	0.38	0.14	0.38
136	29.0	63.2	30.2	65.0	0.14	0.38	0.14	0.38
137	29.5	63.5	30.7	65.3	0.14	0.38	0.14	0.38
138	35.6	63.8	37.0	65.5	0.16	0.38	0.17	0.38
139	40.9	64.1	42.4	65.8	0.18	0.39	0.19	0.38
140	45.6	64.4	47.2	66.1	0.20	0.39	0.20	0.39
141	49.7	64.7	51.3	66.4	0.22	0.39	0.22	0.39
142	53.3	64.9	55.1	66.6	0.23	0.39	0.23	0.39
143	56.7	65.2	58.4	66.9	0.25	0.39	0.25	0.39
144	59.7	65.5	61.6	67.2	0.26	0.39	0.26	0.39
145	62.6	65.7	64.4	67.4	0.27	0.39	0.27	0.39
146	65.2	66.0	67.1	67.7	0.28	0.39	0.28	0.39
147	67.7	66.3	69.7	67.9	0.29	0.39	0.29	0.39
148	70.1	66.5	72.1	68.2	0.30	0.39	0.30	0.39

Day	SGR_{2+oto}	SGR_{2+nom}	$SGR3_{+oto}$	SGR_{3+nom}	GCE_{2+oto}	GCE_{2+nom}	GCE_{3+oto}	GCE_{3+nom}
149	72.3	66.8	74.3	68.4	0.31	0.39	0.31	0.39
150	74.5	67.0	76.5	68.7	0.32	0.39	0.32	0.39
151	76.5	67.3	78.5	68.9	0.33	0.39	0.33	0.39
152	78.4	67.5	80.4	69.1	0.33	0.39	0.33	0.39
153	80.2	67.8	82.3	69.4	0.34	0.40	0.34	0.40
154	80.9	67.4	82.9	69.0	0.35	0.39	0.35	0.39
155	81.5	67.1	83.5	68.7	0.35	0.39	0.35	0.39
156	82.0	66.8	84.1	68.3	0.36	0.39	0.36	0.39
157	82.5	66.4	84.6	67.9	0.36	0.39	0.36	0.39
158	83.0	66.1	85.0	67.6	0.36	0.39	0.36	0.39
159	83.4	65.8	85.3	67.2	0.37	0.39	0.37	0.39
160	83.7	65.5	85.7	66.9	0.37	0.39	0.37	0.39
161	84.0	65.2	85.9	66.6	0.38	0.39	0.38	0.39
162	84.2	64.8	86.1	66.2	0.38	0.39	0.38	0.39
163	84.3	64.5	86.2	65.9	0.38	0.39	0.38	0.39
164	84.4	64.2	86.3	65.6	0.39	0.39	0.39	0.39
165	84.5	63.9	86.3	65.2	0.39	0.39	0.39	0.39
166	84.4	63.6	86.3	64.9	0.39	0.39	0.39	0.39
167	84.3	63.3	86.1	64.6	0.40	0.39	0.40	0.39
168	84.1	63.0	85.9	64.3	0.40	0.39	0.40	0.39
169	83.9	62.7	85.6	63.9	0.40	0.39	0.40	0.39
170	83.5	62.3	85.3	63.5	0.40	0.39	0.40	0.39
171	83.2	62.0	84.9	63.2	0.41	0.39	0.41	0.39
172	82.8	61.6	84.4	62.8	0.41	0.39	0.41	0.39
173	82.3	61.3	83.9	62.4	0.41	0.39	0.41	0.39
174	81.8	60.9	83.4	62.0	0.41	0.39	0.41	0.39
175	81.2	60.5	82.8	61.6	0.41	0.39	0.41	0.39
176	80.6	60.2	82.2	61.2	0.41	0.39	0.41	0.39
177	80.0	59.8	81.5	60.8	0.42	0.39	0.42	0.39
178	79.3	59.4	80.8	60.4	0.42	0.39	0.42	0.39
179	78.5	59.0	80.0	60.0	0.42	0.39	0.42	0.39
180	77.7	58.6	79.1	59.6	0.42	0.39	0.42	0.39
181	76.9	58.2	78.2	59.1	0.42	0.39	0.42	0.39
182	75.9	57.7	77.3	58.7	0.42	0.39	0.42	0.39
183	75.0	57.3	76.3	58.2	0.42	0.39	0.42	0.39
184	73.7	56.5	75.0	57.4	0.42	0.39	0.42	0.39
185	72.2	55.4	73.5	56.3	0.42	0.39	0.42	0.39
186	70.7	54.3	71.9	55.1	0.42	0.39	0.42	0.39
187	69.0	53.1	70.1	53.9	0.42	0.39	0.42	0.39
188	67.2	51.8	68.3	52.5	0.42	0.39	0.42	0.39
189	65.4	50.3	66.4	51.1	0.42	0.39	0.42	0.39
190	63.4	48.9	64.4	49.5	0.42	0.39	0.42	0.39
191	61.3	47.3	62.3	47.9	0.42	0.39	0.42	0.39
192	59.2	45.6	60.1	46.2	0.42	0.39	0.42	0.39
193	57.0	43.9	57.8	44.5	0.41	0.39	0.41	0.38
194	54.7	42.1	55.4	42.6	0.41	0.38	0.41	0.38
195	52.3	40.2	53.0	40.7	0.41	0.38	0.41	0.38
196	49.9	38.3	50.5	38.7	0.41	0.37	0.40	0.37

Day	SGR_{2+oto}	SGR_{2+nom}	$SGR3_{+oto}$	SGR_{3+nom}	GCE_{2+oto}	GCE_{2+nom}	GCE_{3+oto}	GCE_{3+nom}
197	47.4	36.3	48.0	36.7	0.40	0.37	0.40	0.37
198	44.9	34.3	45.5	34.7	0.40	0.36	0.40	0.36
199	44.5	34.0	45.0	34.4	0.40	0.36	0.39	0.36
200	44.0	33.7	44.6	34.0	0.39	0.36	0.39	0.36
201	43.6	33.4	44.2	33.7	0.39	0.36	0.39	0.36
202	43.2	33.0	43.7	33.4	0.39	0.36	0.39	0.36
203	42.8	32.7	43.3	33.0	0.39	0.36	0.39	0.36
204	42.4	32.4	42.9	32.7	0.39	0.36	0.39	0.36
205	42.0	32.1	42.5	32.4	0.39	0.36	0.39	0.35
206	41.6	31.8	42.1	32.1	0.39	0.36	0.39	0.35
207	41.2	31.5	41.7	31.8	0.39	0.35	0.39	0.35
208	40.8	31.2	41.3	31.4	0.39	0.35	0.39	0.35
209	40.4	30.9	40.9	31.1	0.38	0.35	0.38	0.35
210	40.1	30.6	40.5	30.8	0.38	0.35	0.38	0.35
211	39.7	30.3	40.1	30.5	0.38	0.35	0.38	0.35
212	39.3	30.0	39.7	30.2	0.38	0.35	0.38	0.35
213	38.9	29.7	39.3	29.9	0.38	0.35	0.38	0.34
214	38.5	29.4	38.9	29.6	0.38	0.35	0.38	0.34
215	37.2	28.3	37.5	28.5	0.38	0.34	0.37	0.34
216	35.9	27.3	36.2	27.4	0.37	0.34	0.37	0.33
217	34.6	26.2	34.9	26.3	0.37	0.33	0.37	0.33
218	33.3	25.2	33.5	25.3	0.36	0.33	0.36	0.33
219	32.0	24.1	32.2	24.2	0.36	0.32	0.36	0.32
220	30.7	23.1	30.9	23.1	0.35	0.32	0.35	0.31
221	29.4	22.0	29.6	22.1	0.35	0.31	0.35	0.31
222	28.2	21.0	28.3	21.0	0.34	0.31	0.34	0.30
223	26.9	20.0	27.0	20.0	0.34	0.30	0.34	0.30
224	25.7	19.0	25.8	19.0	0.33	0.29	0.33	0.29
225	24.5	18.0	24.5	18.0	0.33	0.29	0.33	0.28
226	23.3	17.0	23.3	17.0	0.32	0.28	0.32	0.28
227	22.1	16.0	22.1	16.0	0.31	0.27	0.31	0.27
228	20.9	15.1	20.9	15.0	0.31	0.26	0.31	0.26
229	19.8	14.1	19.8	14.1	0.30	0.26	0.30	0.25
230	19.6	14.0	19.6	13.9	0.30	0.25	0.30	0.25
231	19.5	13.9	19.5	13.8	0.30	0.25	0.30	0.25
232	19.3	13.8	19.3	13.7	0.30	0.25	0.29	0.25
233	19.2	13.7	19.1	13.5	0.30	0.25	0.29	0.25
234	19.0	13.5	19.0	13.4	0.30	0.25	0.29	0.24
235	18.9	13.4	18.8	13.3	0.29	0.25	0.29	0.24
236	18.7	13.3	18.7	13.2	0.29	0.25	0.29	0.24
237	18.6	13.2	18.5	13.1	0.29	0.25	0.29	0.24
238	18.4	13.1	18.4	12.9	0.29	0.25	0.29	0.24
239	18.3	12.9	18.2	12.8	0.29	0.24	0.29	0.24
240	18.1	12.8	18.1	12.7	0.29	0.24	0.29	0.24
241	18.0	12.7	17.9	12.6	0.29	0.24	0.28	0.24
242	17.8	12.6	17.8	12.5	0.29	0.24	0.28	0.23
243	17.7	12.5	17.6	12.3	0.29	0.24	0.28	0.23
244	17.5	12.4	17.5	12.2	0.28	0.24	0.28	0.23

Day	SGR_{2+oto}	SGR_{2+nom}	$SGR3_{+oto}$	SGR_{3+nom}	GCE_{2+oto}	GCE_{2+nom}	GCE_{3+oto}	GCE_{3+nom}
245	17.4	12.3	17.3	12.1	0.28	0.24	0.28	0.23
246	17.3	12.1	17.2	12.0	0.28	0.24	0.28	0.23
247	17.1	12.0	17.1	11.9	0.28	0.23	0.28	0.23
248	17.0	11.9	16.9	11.8	0.28	0.23	0.28	0.23
249	16.9	11.8	16.8	11.7	0.28	0.23	0.28	0.23
250	16.7	11.7	16.6	11.5	0.28	0.23	0.27	0.22
251	16.6	11.6	16.5	11.4	0.28	0.23	0.27	0.22
252	16.5	11.5	16.4	11.3	0.28	0.23	0.27	0.22
253	16.3	11.4	16.2	11.2	0.27	0.23	0.27	0.22
254	16.2	11.3	16.1	11.1	0.27	0.23	0.27	0.22
255	16.1	11.2	16.0	11.0	0.27	0.22	0.27	0.22
256	15.9	11.1	15.8	10.9	0.27	0.22	0.27	0.22
257	15.8	10.9	15.7	10.8	0.27	0.22	0.27	0.22
258	15.7	10.8	15.6	10.7	0.27	0.22	0.26	0.21
259	15.5	10.7	15.4	10.6	0.27	0.22	0.26	0.21
260	15.4	10.6	15.3	10.5	0.27	0.22	0.26	0.21
261	15.3	10.5	15.2	10.4	0.27	0.22	0.26	0.21
262	15.2	10.4	15.0	10.3	0.26	0.22	0.26	0.21
263	15.0	10.3	14.9	10.1	0.26	0.21	0.26	0.21
264	14.9	10.2	14.8	10.0	0.26	0.21	0.26	0.21
265	14.8	10.1	14.7	9.9	0.26	0.21	0.26	0.21
266	14.7	10.0	14.5	9.8	0.26	0.21	0.26	0.20
267	14.5	9.9	14.4	9.7	0.26	0.21	0.25	0.20
268	14.4	9.8	14.3	9.6	0.26	0.21	0.25	0.20
269	14.3	9.7	14.2	9.5	0.26	0.21	0.25	0.20
270	14.2	9.6	14.0	9.4	0.26	0.21	0.25	0.20
271	14.1	9.5	13.9	9.3	0.25	0.20	0.25	0.20
272	13.9	9.4	13.8	9.2	0.25	0.20	0.25	0.20
273	13.8	9.4	13.7	9.2	0.25	0.20	0.25	0.19
274	13.7	9.3	13.6	9.1	0.25	0.20	0.25	0.19
275	13.6	9.2	13.4	9.0	0.25	0.20	0.25	0.19
276	13.5	9.1	13.3	8.9	0.25	0.20	0.24	0.19
277	13.4	9.0	13.2	8.8	0.25	0.20	0.24	0.19
278	13.2	8.9	13.1	8.7	0.25	0.20	0.24	0.19
279	13.1	8.8	13.0	8.6	0.25	0.19	0.24	0.19
280	13.0	8.7	12.9	8.5	0.24	0.19	0.24	0.19
281	12.9	8.6	12.7	8.4	0.24	0.19	0.24	0.18
282	12.8	8.5	12.6	8.3	0.24	0.19	0.24	0.18
283	12.7	8.4	12.5	8.2	0.24	0.19	0.24	0.18
284	12.6	8.3	12.4	8.1	0.24	0.19	0.23	0.18
285	12.5	8.3	12.3	8.0	0.24	0.19	0.23	0.18
286	12.4	8.2	12.2	7.9	0.24	0.18	0.23	0.18
287	12.3	8.1	12.1	7.9	0.24	0.18	0.23	0.18
288	12.2	8.0	12.0	7.8	0.24	0.18	0.23	0.17
289	12.0	7.9	11.9	7.7	0.23	0.18	0.23	0.17
290	11.9	7.8	11.8	7.6	0.23	0.18	0.23	0.17
291	11.8	7.7	11.7	7.5	0.23	0.18	0.23	0.17
292	11.7	7.7	11.5	7.4	0.23	0.18	0.23	0.17

Day	SGR_{2+oto}	SGR_{2+nom}	$SGR3_{+oto}$	SGR_{3+nom}	GCE_{2+oto}	GCE_{2+nom}	GCE_{3+oto}	GCE_{3+nom}
293	11.6	7.6	11.4	7.3	0.23	0.18	0.22	0.17
294	11.5	7.5	11.3	7.3	0.23	0.17	0.22	0.17
295	11.4	7.4	11.2	7.2	0.23	0.17	0.22	0.17
296	11.3	7.3	11.1	7.1	0.23	0.17	0.22	0.16
297	11.2	7.2	11.0	7.0	0.22	0.17	0.22	0.16
298	11.1	7.2	10.9	6.9	0.22	0.17	0.22	0.16
299	11.0	7.1	10.8	6.8	0.22	0.17	0.22	0.16
300	10.9	7.0	10.7	6.8	0.22	0.17	0.22	0.16
301	10.8	6.9	10.6	6.7	0.22	0.17	0.21	0.16
302	10.7	6.8	10.5	6.6	0.22	0.16	0.21	0.16
303	10.6	6.8	10.4	6.5	0.22	0.16	0.21	0.15
304	10.5	6.7	10.3	6.4	0.22	0.16	0.21	0.15
305	10.4	6.6	10.2	6.3	0.22	0.16	0.21	0.15
306	10.3	6.5	10.1	6.3	0.21	0.16	0.21	0.15
307	10.2	6.4	10.0	6.2	0.21	0.16	0.21	0.15
308	10.1	6.4	9.9	6.1	0.21	0.16	0.21	0.15
309	10.0	6.3	9.8	6.0	0.21	0.15	0.20	0.15
310	9.9	6.2	9.7	5.9	0.21	0.15	0.20	0.14
311	9.8	6.1	9.6	5.8	0.21	0.15	0.20	0.14
312	9.7	6.0	9.5	5.8	0.21	0.15	0.20	0.14
313	9.6	5.9	9.4	5.7	0.21	0.15	0.20	0.14
314	9.5	5.9	9.3	5.6	0.20	0.15	0.20	0.14
315	9.5	5.8	9.2	5.5	0.20	0.15	0.20	0.14
316	9.4	5.7	9.1	5.4	0.20	0.14	0.19	0.14
317	9.3	5.6	9.0	5.4	0.20	0.14	0.19	0.13
318	9.2	5.5	8.9	5.3	0.20	0.14	0.19	0.13
319	9.1	5.5	8.8	5.2	0.20	0.14	0.19	0.13
320	9.0	5.4	8.7	5.1	0.20	0.14	0.19	0.13
321	8.9	5.3	8.6	5.0	0.19	0.14	0.19	0.13
322	8.8	5.2	8.5	4.9	0.19	0.14	0.19	0.13
323	8.7	5.1	8.4	4.9	0.19	0.13	0.19	0.12
324	8.6	5.1	8.3	4.8	0.19	0.13	0.18	0.12
325	8.5	5.0	8.2	4.7	0.19	0.13	0.18	0.12
326	8.4	4.9	8.1	4.6	0.19	0.13	0.18	0.12
327	8.3	4.8	8.0	4.5	0.19	0.13	0.18	0.12
328	8.2	4.8	7.9	4.5	0.19	0.13	0.18	0.12
329	8.1	4.7	7.8	4.4	0.18	0.12	0.18	0.12
330	8.0	4.6	7.8	4.3	0.18	0.12	0.18	0.11
331	7.9	4.5	7.7	4.2	0.18	0.12	0.17	0.11
332	7.8	4.4	7.6	4.2	0.18	0.12	0.17	0.11
333	7.7	4.4	7.5	4.1	0.18	0.12	0.17	0.11
334	7.6	4.3	7.4	4.0	0.18	0.12	0.17	0.11
335	7.6	4.2	7.3	3.9	0.18	0.11	0.17	0.11
336	7.5	4.2	7.2	3.9	0.17	0.11	0.17	0.10
337	7.4	4.1	7.2	3.8	0.17	0.11	0.17	0.10
338	7.4	4.1	7.1	3.8	0.17	0.11	0.16	0.10
339	7.3	4.0	7.0	3.7	0.17	0.11	0.16	0.10
340	7.2	3.9	6.9	3.6	0.17	0.11	0.16	0.10

Day	SGR_{2+oto}	SGR_{2+nom}	$SGR3_{+oto}$	SGR_{3+nom}	GCE_{2+oto}	GCE_{2+nom}	GCE_{3+oto}	GCE_{3+nom}
341	7.1	3.9	6.9	3.6	0.17	0.11	0.16	0.10
342	7.1	3.8	6.8	3.5	0.17	0.11	0.16	0.10
343	7.0	3.8	6.7	3.5	0.17	0.10	0.16	0.10
344	6.9	3.7	6.7	3.4	0.17	0.10	0.16	0.09
345	6.9	3.7	6.6	3.3	0.16	0.10	0.16	0.09
346	6.8	3.6	6.5	3.3	0.16	0.10	0.16	0.09
347	6.7	3.5	6.4	3.2	0.16	0.10	0.15	0.09
348	6.7	3.5	6.4	3.2	0.16	0.10	0.15	0.09
349	6.6	3.4	6.3	3.1	0.16	0.10	0.15	0.09
350	6.5	3.4	6.2	3.1	0.16	0.10	0.15	0.09
351	6.4	3.3	6.2	3.0	0.16	0.09	0.15	0.08
352	6.4	3.3	6.1	2.9	0.16	0.09	0.15	0.08
353	6.3	3.2	6.0	2.9	0.16	0.09	0.15	0.08
354	6.2	3.1	6.0	2.8	0.15	0.09	0.15	0.08
355	6.2	3.1	5.9	2.8	0.15	0.09	0.14	0.08
356	6.1	3.0	5.8	2.7	0.15	0.09	0.14	0.08
357	6.0	3.0	5.8	2.7	0.15	0.09	0.14	0.08
358	6.0	2.9	5.7	2.6	0.15	0.09	0.14	0.08
359	5.9	2.9	5.6	2.6	0.15	0.08	0.14	0.07
360	5.8	2.8	5.5	2.5	0.15	0.08	0.14	0.07
361	5.8	2.8	5.5	2.4	0.15	0.08	0.14	0.07
362	5.7	2.7	5.4	2.4	0.14	0.08	0.14	0.07
363	5.6	2.7	5.3	2.3	0.14	0.08	0.14	0.07
364	5.6	2.6	5.3	2.3	0.14	0.08	0.13	0.07
365	5.5	2.5	5.2	2.2	0.14	0.08	0.13	0.07
366			14.2	10.7	0.26	0.28	0.24	0.22
367			14.2	10.6			0.24	0.21
368			14.1	10.5			0.24	0.21
369			14.1	10.4			0.24	0.21
370			14.0	10.3			0.24	0.21
371			13.9	10.2			0.24	0.21
372			13.9	10.1			0.24	0.21
373			13.8	10.0			0.24	0.21
374			13.7	10.0			0.24	0.21
375			13.7	9.9			0.24	0.21
376			13.6	9.8			0.24	0.20
377			13.6	9.7			0.24	0.20
378			13.5	9.6			0.24	0.20
379			13.4	9.5			0.24	0.20
380			13.4	9.4			0.24	0.20
381			13.9	9.9			0.24	0.20
382			14.5	10.3			0.25	0.21
383			15.1	10.8			0.25	0.22
384			15.7	11.2			0.26	0.22
385			16.3	11.7			0.26	0.23
386			16.9	12.1			0.27	0.23
387			17.5	12.6			0.27	0.23
388			18.1	13.0			0.27	0.24

Day	SGR_{2+oto}	SGR_{2+nom}	$SGR3_{+oto}$	SGR_{3+nom}	GCE_{2+oto}	GCE_{2+nom}	GCE_{3+oto}	GCE_{3+nom}
389			18.7	13.5			0.28	0.24
390			19.3	14.0			0.28	0.25
391			19.9	14.4			0.29	0.25
392			20.5	14.9			0.29	0.26
393			21.1	15.4			0.29	0.26
394			21.7	15.8			0.30	0.26
395			22.4	16.3			0.30	0.27
396			26.3	19.5			0.32	0.29
397			30.3	22.8			0.34	0.31
398			34.5	26.2			0.35	0.32
399			38.6	29.6			0.36	0.34
400			42.7	32.9			0.37	0.35
401			46.6	36.0			0.38	0.36
402			50.4	39.1			0.39	0.36
403			53.9	41.9			0.39	0.37
404			57.1	44.4			0.39	0.37
405			60.0	46.7			0.40	0.38
406			62.6	48.7			0.40	0.38
407			64.8	50.4			0.40	0.38
408			66.7	51.7			0.40	0.38
409			68.2	52.8			0.40	0.37
410			69.3	53.5			0.39	0.37
411			69.9	53.6			0.39	0.37
412			70.3	53.6			0.39	0.37
413			70.5	53.6			0.39	0.37
414			70.6	53.6			0.38	0.37
415			70.6	53.6			0.38	0.37
416			70.4	53.6			0.38	0.37
417			70.1	53.6			0.37	0.37
418			69.7	53.5			0.37	0.36
419			69.2	53.5			0.36	0.36
420			68.5	53.5			0.36	0.36
421			67.8	53.5			0.35	0.36
422			66.9	53.4			0.35	0.36
423			66.0	53.4			0.34	0.36
424			64.9	53.3			0.33	0.36
425			63.8	53.3			0.33	0.36
426			62.6	53.2			0.32	0.36
427			61.9	53.0			0.32	0.36
428			61.2	52.9			0.31	0.36
429			60.4	52.7			0.31	0.36
430			59.7	52.5			0.31	0.36
431			58.9	52.3			0.30	0.36
432			58.2	52.1			0.30	0.36
433			57.4	51.9			0.30	0.36
434			56.6	51.8			0.29	0.36
435			55.8	51.6			0.29	0.35
436			55.1	51.4			0.29	0.35

Day	SGR_{2+oto}	SGR_{2+nom}	$SGR3_{+oto}$	SGR_{3+nom}	GCE_{2+oto}	GCE_{2+nom}	GCE_{3+oto}	GCE_{3+nom}
437			54.2	51.2			0.28	0.35
438			53.4	51.0			0.28	0.35
439			52.6	50.9			0.27	0.35
440			51.8	50.7			0.27	0.35
441			50.9	50.5			0.27	0.35
442			49.3	50.3			0.26	0.35
443			47.5	50.2			0.25	0.35
444			45.7	50.0			0.24	0.35
445			43.9	49.8			0.23	0.35
446			41.9	49.7			0.22	0.35
447			39.9	49.5			0.21	0.35
448			37.7	49.3			0.20	0.35
449			35.5	49.2			0.19	0.35
450			33.1	49.0			0.18	0.35
451			30.6	48.8			0.16	0.35
452			27.9	48.7			0.15	0.35
453			24.9	48.5			0.14	0.35
454			21.7	48.4			0.12	0.35
455			18.1	48.2			0.10	0.35
456			14.1	48.0			0.08	0.35
457			9.5	47.9			0.05	0.35
458			9.9	48.1			0.06	0.35
459			10.2	48.3			0.06	0.35
460			10.6	48.5			0.06	0.35
461			11.0	48.7			0.06	0.35
462			11.4	48.9			0.06	0.35
463			11.7	49.1			0.07	0.35
464			12.1	49.3			0.07	0.35
465			12.5	49.5			0.07	0.35
466			12.8	49.7			0.07	0.35
467			13.2	49.9			0.07	0.35
468			13.6	50.1			0.07	0.35
469			13.9	50.3			0.08	0.35
470			14.3	50.5			0.08	0.35
471			14.6	50.7			0.08	0.36
472			15.0	50.9			0.08	0.36
473			15.3	51.1			0.08	0.36
474			15.7	51.3			0.09	0.36
475			16.0	51.5			0.09	0.36
476			16.4	51.7			0.09	0.36
477			16.7	51.8			0.09	0.36
478			17.1	52.0			0.09	0.36
479			17.4	52.2			0.09	0.36
480			17.8	52.4			0.09	0.36
481			18.1	52.6			0.10	0.36
482			18.5	52.8			0.10	0.36
483			18.8	52.9			0.10	0.36
484			19.2	53.1			0.10	0.36

Day	SGR_{2+oto}	SGR_{2+nom}	$SGR3_{+oto}$	SGR_{3+nom}	GCE_{2+oto}	GCE_{2+nom}	GCE_{3+oto}	GCE_{3+nom}
485			19.5	53.3			0.10	0.36
486			19.8	53.5			0.10	0.36
487			20.2	53.6			0.11	0.37
488			20.5	53.8			0.11	0.37
489			21.0	59.6			0.11	0.38
490			21.6	59.9			0.11	0.38
491			22.1	60.3			0.11	0.38
492			22.6	60.7			0.12	0.38
493			23.1	61.0			0.12	0.38
494			23.7	61.4			0.12	0.39
495			24.2	61.7			0.12	0.39
496			24.7	62.1			0.12	0.39
497			25.2	62.4			0.13	0.39
498			25.7	62.8			0.13	0.39
499			26.2	63.1			0.13	0.39
500			26.8	63.5			0.13	0.39
501			27.3	63.8			0.13	0.39
502			27.8	64.2			0.14	0.39
503			33.7	64.5			0.16	0.39
504			38.8	64.8			0.18	0.39
505			43.3	65.2			0.20	0.40
506			47.3	65.5			0.22	0.40
507			50.8	65.8			0.23	0.40
508			54.1	66.2			0.24	0.40
509			57.1	66.5			0.25	0.40
510			59.9	66.8			0.27	0.40
511			62.5	67.1			0.28	0.40
512			64.9	67.4			0.29	0.40
513			67.3	67.8			0.30	0.40
514			69.5	68.1			0.30	0.40
515			71.6	68.4			0.31	0.40
516			73.5	68.7			0.32	0.40
517			75.4	69.0			0.33	0.40
518			77.2	69.3			0.34	0.40
519			77.9	69.0			0.34	0.40
520			78.6	68.8			0.35	0.40
521			79.2	68.5			0.35	0.40
522			79.7	68.2			0.36	0.40
523			80.2	68.0			0.36	0.40
524			80.7	67.7			0.36	0.40
525			81.1	67.4			0.37	0.40
526			81.4	67.2			0.37	0.40
527			81.7	66.9			0.38	0.40
528			81.9	66.7			0.38	0.40
529			82.0	66.4			0.38	0.40
530			82.1	66.2			0.39	0.40
531			82.1	65.9			0.39	0.40
532			82.1	65.7			0.39	0.40

Day	SGR_{2+oto}	SGR_{2+nom}	$SGR3_{+oto}$	SGR_{3+nom}	GCE_{2+oto}	GCE_{2+nom}	GCE_{3+oto}	GCE_{3+nom}
533			82.0	65.4			0.39	0.40
534			81.8	65.1			0.40	0.40
535			81.5	64.8			0.40	0.40
536			81.2	64.5			0.40	0.40
537			80.9	64.1			0.40	0.40
538			80.5	63.8			0.40	0.40
539			80.0	63.4			0.41	0.40
540			79.6	63.1			0.41	0.40
541			79.0	62.7			0.41	0.40
542			78.4	62.4			0.41	0.40
543			77.8	62.0			0.41	0.40
544			77.1	61.6			0.41	0.40
545			76.4	61.2			0.41	0.40
546			75.6	60.8			0.41	0.40
547			74.8	60.4			0.41	0.40
548			73.9	60.0			0.42	0.40
549			72.7	59.1			0.42	0.40
550			71.3	58.0			0.42	0.40
551			69.8	56.8			0.42	0.41
552			68.1	55.5			0.42	0.41
553			66.4	54.1			0.42	0.40
554			64.6	52.7			0.42	0.40
555			62.7	51.1			0.41	0.40
556			60.8	49.5			0.41	0.40
557			58.7	47.8			0.41	0.40
558			56.5	46.0			0.41	0.40
559			54.3	44.1			0.41	0.39
560			52.0	42.2			0.40	0.39
561			49.6	40.2			0.40	0.39
562			47.2	38.2			0.40	0.38
563			44.8	36.2			0.39	0.38
564			44.4	35.8			0.39	0.38
565			44.0	35.5			0.39	0.38
566			43.7	35.2			0.39	0.38
567			43.3	34.8			0.39	0.37
568			42.9	34.5			0.39	0.37
569			42.5	34.1			0.39	0.37
570			42.2	33.8			0.39	0.37
571			41.8	33.5			0.38	0.37
572			41.4	33.2			0.38	0.37
573			41.1	32.8			0.38	0.37
574			40.7	32.5			0.38	0.37
575			40.4	32.2			0.38	0.37
576			40.0	31.9			0.38	0.36
577			39.6	31.6			0.38	0.36
578			39.3	31.2			0.38	0.36
579			38.9	30.9			0.38	0.36
580			37.7	29.8			0.37	0.36

Day	SGR_{2+oto}	SGR_{2+nom}	$SGR3_{+oto}$	SGR_{3+nom}	GCE_{2+oto}	GCE_{2+nom}	GCE_{3+oto}	GCE_{3+nom}
581			36.4	28.8			0.37	0.35
582			35.1	27.7			0.37	0.35
583			33.8	26.6			0.36	0.34
584			32.5	25.5			0.36	0.34
585			31.3	24.5			0.35	0.34
586			30.0	23.4			0.35	0.33
587			28.8	22.4			0.35	0.32
588			27.6	21.4			0.34	0.32
589			26.4	20.3			0.34	0.31
590			25.2	19.3			0.33	0.31
591			24.0	18.3			0.33	0.30
592			22.8	17.4			0.32	0.29
593			21.7	16.4			0.31	0.29
594			20.6	15.5			0.31	0.28
595			20.4	15.3			0.31	0.28
596			20.3	15.2			0.30	0.28
597			20.1	15.1			0.30	0.28
598			20.0	14.9			0.30	0.27
599			19.9	14.8			0.30	0.27
600			19.7	14.7			0.30	0.27
601			19.6	14.5			0.30	0.27
602			19.4	14.4			0.30	0.27
603			19.3	14.3			0.30	0.27
604			19.2	14.1			0.30	0.27
605			19.0	14.0			0.30	0.27
606			18.9	13.9			0.30	0.26
607			18.7	13.8			0.29	0.26
608			18.6	13.6			0.29	0.26
609			18.5	13.5			0.29	0.26
610			18.3	13.4			0.29	0.26
611			18.2	13.3			0.29	0.26
612			18.1	13.1			0.29	0.26
613			17.9	13.0			0.29	0.26
614			17.8	12.9			0.29	0.25
615			17.7	12.8			0.29	0.25
616			17.6	12.7			0.29	0.25
617			17.4	12.5			0.29	0.25
618			17.3	12.4			0.28	0.25
619			17.2	12.3			0.28	0.25
620			17.0	12.2			0.28	0.25
621			16.9	12.1			0.28	0.25
622			16.8	12.0			0.28	0.24
623			16.7	11.9			0.28	0.24
624			16.5	11.7			0.28	0.24
625			16.4	11.6			0.28	0.24
626			16.3	11.5			0.28	0.24
627			16.2	11.4			0.28	0.24
628			16.1	11.3			0.27	0.24

Day	SGR_{2+oto}	SGR_{2+nom}	$SGR3_{+oto}$	SGR_{3+nom}	GCE_{2+oto}	GCE_{2+nom}	GCE_{3+oto}	GCE_{3+nom}
629			15.9	11.2			0.27	0.24
630			15.8	11.1			0.27	0.23
631			15.7	11.0			0.27	0.23
632			15.6	10.9			0.27	0.23
633			15.5	10.8			0.27	0.23
634			15.4	10.7			0.27	0.23
635			15.2	10.6			0.27	0.23
636			15.1	10.5			0.27	0.23
637			15.0	10.4			0.27	0.22
638			14.9	10.3			0.26	0.22
639			14.8	10.2			0.26	0.22
640			14.7	10.1			0.26	0.22
641			14.6	10.0			0.26	0.22
642			14.5	9.9			0.26	0.22
643			14.3	9.8			0.26	0.22
644			14.2	9.7			0.26	0.22
645			14.1	9.6			0.26	0.21
646			14.0	9.5			0.26	0.21
647			13.9	9.4			0.26	0.21
648			13.8	9.3			0.25	0.21
649			13.7	9.2			0.25	0.21
650			13.6	9.1			0.25	0.21
651			13.5	9.0			0.25	0.21
652			13.4	8.9			0.25	0.21
653			13.3	8.8			0.25	0.20
654			13.2	8.7			0.25	0.20
655			13.1	8.6			0.25	0.20
656			13.0	8.6			0.25	0.20
657			12.9	8.5			0.25	0.20
658			12.8	8.4			0.24	0.20
659			12.7	8.3			0.24	0.20
660			12.6	8.2			0.24	0.20
661			12.5	8.1			0.24	0.19
662			12.4	8.0			0.24	0.19
663			12.3	8.0			0.24	0.19
664			12.2	7.9			0.24	0.19
665			12.1	7.8			0.24	0.19
666			12.0	7.7			0.24	0.19
667			11.9	7.6			0.24	0.19
668			11.8	7.5			0.23	0.19
669			11.7	7.5			0.23	0.18
670			11.6	7.4			0.23	0.18
671			11.5	7.3			0.23	0.18
672			11.4	7.2			0.23	0.18
673			11.3	7.2			0.23	0.18
674			11.2	7.1			0.23	0.18
675			11.1	7.0			0.23	0.18
676			11.0	6.9			0.23	0.18

Day	SGR_{2+oto}	SGR_{2+nom}	$SGR3_{+oto}$	SGR_{3+nom}	GCE_{2+oto}	GCE_{2+nom}	GCE_{3+oto}	GCE_{3+nom}
677			10.9	6.9			0.23	0.17
678			10.8	6.8			0.22	0.17
679			10.7	6.7			0.22	0.17
680			10.7	6.7			0.22	0.17
681			10.6	6.6			0.22	0.17
682			10.5	6.5			0.22	0.17
683			10.4	6.4			0.22	0.17
684			10.3	6.4			0.22	0.17
685			10.2	6.3			0.22	0.16
686			10.1	6.2			0.21	0.16
687			10.0	6.2			0.21	0.16
688			9.9	6.1			0.21	0.16
689			9.8	6.0			0.21	0.16
690			9.7	5.9			0.21	0.16
691			9.6	5.9			0.21	0.16
692			9.5	5.8			0.21	0.15
693			9.4	5.7			0.21	0.15
694			9.3	5.7			0.21	0.15
695			9.2	5.6			0.20	0.15
696			9.2	5.5			0.20	0.15
697			9.1	5.5			0.20	0.15
698			9.0	5.4			0.20	0.15
699			8.9	5.3			0.20	0.15
700			8.8	5.3			0.20	0.14
701			8.7	5.2			0.20	0.14
702			8.7	5.2			0.20	0.14
703			8.6	5.2			0.20	0.14
704			8.5	5.1			0.19	0.14
705			8.5	5.1			0.19	0.14
706			8.4	5.0			0.19	0.14
707			8.3	5.0			0.19	0.14
708			8.2	5.0			0.19	0.14
709			8.2	4.9			0.19	0.14
710			8.1	4.9			0.19	0.14
711			8.0	4.8			0.19	0.14
712			8.0	4.8			0.19	0.14
713			7.9	4.8			0.19	0.13
714			7.8	4.7			0.18	0.13
715			7.8	4.7			0.18	0.13
716			7.7	4.6			0.18	0.13
717			7.6	4.6			0.18	0.13
718			7.6	4.6			0.18	0.13
719			7.5	4.5			0.18	0.13
720			7.4	4.5			0.18	0.13
721			7.4	4.4			0.18	0.13
722			7.3	4.4			0.18	0.13
723			7.2	4.4			0.18	0.13
724			7.2	4.3			0.17	0.13

Day	SGR_{2+oto}	SGR_{2+nom}	$SGR3_{+oto}$	SGR_{3+nom}	GCE_{2+oto}	GCE_{2+nom}	GCE_{3+oto}	GCE_{3+nom}
725			7.1	4.3			0.17	0.13
726			7.0	4.3			0.17	0.12
727			7.0	4.2			0.17	0.12
728			6.9	4.2			0.17	0.12
729			6.8	4.1			0.17	0.12
730			6.8	4.1			0.17	0.12

Table A19—Tabulated intra-otolith $\delta^{18}O$ and $\delta^{13}C$ values for chinook salmon utilized in chapter 4. Temperatures are calculated using $\delta^{18}O$ water value of –6.8‰VSMOW and temperature-fractionation equations of Patt (Patterson et al., 1993), Kim (Kim and O'Neil, 1997), and Thor (Thorrold et al., 1997). SN indicates Sample Number from otolith core.

SN	Specimen	$\delta^{13}C$ ‰ VPDB	±	$\delta^{18}O$ ‰ VPDB	±	Patt °C	Kim °C	Thor °C
8.5	SAM108	-8.6	0.00	-8.1	0.02	23.4	22.7	27.8
11.5	SAM108	-9.5	0.01	-7.9	0.02	22.5	21.8	26.9
15.5	SAM108	-7.8	0.01	-7.2	0.05	19.4	18.7	23.7
17	SAM108	-7.9	0.01	-7.5	0.02	20.6	19.9	25.0
18	SAM108	-7.1	0.02	-7.3	0.03	19.8	19.1	24.1
19	SAM108	-7.1	0.02	-7.1	0.01	18.9	18.1	23.2
20	SAM108	-6.1	0.04	-7.4	0.08	20.2	19.5	24.5
21	SAM108	-6.3	0.01	-7.3	0.02	19.7	19.0	24.0
22	SAM108	-6.2	0.02	-6.9	0.03	17.9	17.1	22.2
23	SAM108	-5.8	0.03	-6.8	0.02	17.7	16.9	21.9
25	SAM108	-5.6	0.01	-6.7	0.01	16.9	16.1	21.1
26	SAM108	-5.3	0.01	-6.3	0.02	15.2	14.3	19.3
27	SAM108	-5.7	0.02	-6.0	0.02	14.0	13.1	18.1
28	SAM108	-5.5	0.02	-6.0	0.01	14.0	13.2	18.2
29	SAM108	-5.5	0.01	-6.0	0.01	13.9	13.1	18.1
30	SAM108	-5.7	0.02	-5.9	0.05	13.3	12.4	17.4
31	SAM108	-6.0	0.01	-6.1	0.01	14.5	13.6	18.6
32	SAM108	-6.8	0.01	-6.5	0.03	15.9	15.1	20.1
33	SAM108	-7.5	0.01	-6.8	0.02	17.3	16.5	21.5
34	SAM108	-8.1	0.01	-7.1	0.02	19.0	18.3	23.3
35	SAM108	-8.4	0.01	-7.3	0.02	19.7	19.0	24.0
36	SAM108	-8.9	0.01	-7.6	0.03	21.2	20.5	25.6
37	SAM108	-8.7	0.03	-7.6	0.02	21.2	20.6	25.6
38	SAM108	-9.6	0.01	-7.5	0.04	20.8	20.1	25.1
39	SAM108	-8.9	0.00	-7.9	0.02	22.4	21.7	26.8
40	SAM108	-9.0	0.01	-7.7	0.04	21.5	20.8	25.9
41	SAM108	-9.0	0.03	-7.8	0.05	21.9	21.2	26.2

SN	Specimen	$\delta^{13}C$ ‰ VPDB	±	$\delta^{18}O$ ‰ VPDB	±	Patt °C	Kim °C	Thor °C
42	SAM108	-9.2	0.02	-7.8	0.03	21.9	21.2	26.3
43	SAM108	-8.9	0.01	-7.7	0.02	21.6	21.0	26.0
44	SAM108	-8.8	0.01	-7.8	0.01	22.2	21.5	26.6
45	SAM108	-8.9	0.02	-7.9	0.04	22.4	21.7	26.8
46	SAM108	-8.6	0.01	-7.6	0.01	21.3	20.6	25.7
47	SAM108	-8.5	0.01	-7.7	0.01	21.9	21.2	26.2
48	SAM108	-8.5	0.01	-7.8	0.01	22.3	21.7	26.7
49	SAM108	-8.2	0.01	-7.7	0.01	21.4	20.7	25.8
50	SAM108	-7.9	0.01	-7.6	0.01	21.4	20.7	25.7
51	SAM108	-7.6	0.01	-7.1	0.02	18.9	18.2	23.2
52	SAM108	-7.1	0.01	-6.8	0.01	17.6	16.8	21.8
53	SAM108	-7.0	0.01	-6.7	0.02	17.2	16.4	21.4
54	SAM108	-6.7	0.01	-6.5	0.02	15.9	15.0	20.1
55	SAM108	-6.3	0.00	-6.3	0.02	15.0	14.1	19.1
56	SAM108	-6.3	0.01	-6.2	0.03	14.5	13.7	18.7
57	SAM108	-6.1	0.01	-6.1	0.01	14.2	13.3	18.3
58	SAM108	-5.9	0.01	-5.9	0.02	13.5	12.6	17.6
59	SAM108	-5.8	0.01	-5.7	0.02	12.4	11.5	16.5
60	SAM108	-6.0	0.02	-5.5	0.07	11.8	10.8	15.8
61	SAM108	-6.1	0.00	-5.8	0.01	13.1	12.2	17.2
62	SAM108	-6.1	0.01	-5.8	0.02	13.0	12.1	17.1
63	SAM108	-6.4	0.00	-6.1	0.02	14.4	13.6	18.6
64	SAM108	-7.1	0.06	-6.4	0.10	15.4	14.6	19.6
65	SAM108	-7.0	0.01	-6.3	0.02	15.2	14.3	19.3
66	SAM108	-7.9	0.01	-6.9	0.01	17.8	17.0	22.1
68	SAM108	-8.0	0.01	-7.1	0.03	18.7	17.9	22.9
70.5	SAM108	-8.9	0.02	-7.2	0.08	19.5	18.8	23.8
72	SAM108	-9.0	0.03	-7.5	0.06	20.7	20.0	25.0
73.5	SAM108	-9.3	0.01	-7.2	0.01	19.2	18.5	23.5
75.5	SAM108	-8.3	0.01	-7.6	0.01	21.3	20.6	25.6
78.5	SAM108	-7.7	0.02	-7.2	0.03	19.5	18.8	23.8
81	SAM108	-7.7	0.01	-7.4	0.01	20.4	19.7	24.7
82.5	SAM108	-6.9	0.01	-7.0	0.03	18.3	17.5	22.5
84.5	SAM108	-7.0	0.02	-6.8	0.02	17.4	16.6	21.6
86	SAM108	-6.1	0.01	-6.4	0.03	15.4	14.6	19.6
87	SAM108	-5.7	0.02	-6.3	0.04	15.2	14.3	19.3
88.5	SAM108	-5.7	0.01	-5.9	0.01	13.2	12.3	17.3
90	SAM108	-5.6	0.11	-5.9	0.23	13.3	12.4	17.4
91	SAM108	-5.6	0.01	-5.8	0.01	13.2	12.3	17.3

SN	Specimen	$\delta^{13}C$ ‰ VPDB	±	$\delta^{18}O$ ‰ VPDB	±	Patt °C	Kim °C	Thor °C
92	SAM108	-6.4	0.01	-5.8	0.02	13.1	12.2	17.2
94	SAM108	-6.1	0.01	-5.9	0.02	13.4	12.6	17.5
98.5	SAM108	-7.3	0.01	-6.3	0.02	15.3	14.5	19.5
101.5	SAM108	-8.6	0.02	-7.0	0.03	18.1	17.4	22.4
104	SAM108	-9.0	0.01	-7.2	0.02	19.1	18.4	23.4
105	SAM108	-9.5	0.01	-7.3	0.01	19.7	18.9	24.0
106	SAM108	-9.0	0.01	-7.3	0.03	19.6	18.9	23.9
108	SAM108	-9.2	0.02	-7.3	0.05	19.6	18.9	23.9
109.5	SAM108	-8.7	0.02	-7.0	0.06	18.3	17.6	22.6
1.5	SAM54	-4.6	0.02	-5.1	0.04	9.9	9.0	13.9
5	SAM54	-5.5	0.02	-5.6	0.06	11.9	11.0	15.9
7.5	SAM54	-6.4	0.03	-5.9	0.05	13.3	12.4	17.4
10	SAM54	-7.3	0.01	-6.3	0.04	15.2	14.4	19.4
12.5	SAM54	-8.3	0.01	-6.8	0.03	17.5	16.7	21.7
14	SAM54	-8.6	0.02	-6.9	0.01	17.9	17.1	22.2
15	SAM54	-8.6	0.03	-6.9	0.03	18.0	17.3	22.3
16	SAM54	-8.9	0.02	-7.1	0.03	18.8	18.1	23.1
17	SAM54	-8.9	0.02	-7.0	0.13	18.6	17.8	22.8
18	SAM54	-8.9	0.01	-7.1	0.03	18.7	17.9	22.9
19	SAM54	-9.1	0.03	-7.3	0.01	19.6	18.9	23.9
20	SAM54	-9.0	0.02	-7.1	0.04	19.0	18.3	23.3
21	SAM54	-9.0	0.02	-7.1	0.03	19.0	18.3	23.3
22	SAM54	-9.2	0.02	-7.3	0.03	19.7	19.0	24.0
23	SAM54	-9.2	0.02	-7.2	0.03	19.3	18.5	23.5
24	SAM54	-9.0	0.02	-7.3	0.05	19.6	18.9	23.9
25	SAM54	-8.7	0.03	-6.9	0.01	17.9	17.1	22.1
26	SAM54	-8.5	0.01	-6.9	0.03	18.1	17.3	22.3
27	SAM54	-8.1	0.02	-6.6	0.05	16.4	15.6	20.6
28.5	SAM54	-7.9	0.01	-6.2	0.03	14.9	14.1	19.1
30	SAM54	-7.4	0.01	-6.0	0.04	13.8	12.9	17.9
31	SAM54	-7.4	0.02	-6.3	0.04	15.0	14.1	19.1
32	SAM54	-7.5	0.01	-6.0	0.05	13.7	12.9	17.9
33	SAM54	-7.5	0.01	-6.1	0.02	14.3	13.5	18.4
34	SAM54	-8.2	0.02	-6.3	0.03	15.0	14.2	19.2
37	SAM54	-7.6	0.01	-6.0	0.08	13.9	13.0	18.0
38	SAM54	-8.2	0.01	-6.2	0.01	14.7	13.8	18.8
39	SAM54	-7.9	0.01	-6.1	0.06	14.4	13.5	18.5
41	SAM54	-8.1	0.02	-6.3	0.02	15.0	14.2	19.2
42	SAM54	-8.4	0.02	-6.3	0.02	15.4	14.5	19.5

SN	Specimen	$\delta^{13}C$ ‰ VPDB	±	$\delta^{18}O$ ‰ VPDB	±	Patt °C	Kim °C	Thor °C
43	SAM54	-9.1	0.04	-6.5	0.05	16.3	15.5	20.5
44	SAM54	-8.9	0.03	-6.6	0.05	16.6	15.8	20.9
45	SAM54	-9.2	0.01	-6.8	0.01	17.4	16.6	21.6
46	SAM54	-9.6	0.02	-6.9	0.03	17.7	17.0	22.0
47	SAM54	-10.0	0.02	-7.1	0.04	19.0	18.2	23.3
48	SAM54	-10.1	0.01	-7.1	0.04	19.0	18.3	23.3
49	SAM54	-10.1	0.01	-7.3	0.02	19.9	19.2	24.2
50	SAM54	-9.8	0.01	-7.1	0.03	19.0	18.2	23.2
51	SAM54	-9.5	0.01	-7.1	0.04	19.0	18.2	23.2
52	SAM54	-9.6	0.03	-7.2	0.02	19.4	18.7	23.7
53	SAM54	-9.1	0.02	-7.0	0.04	18.3	17.6	22.6
54	SAM54	-9.5	0.03	-7.2	0.01	19.2	18.4	23.4
55	SAM54	-9.2	0.02	-7.1	0.06	18.9	18.1	23.2
56	SAM54	-8.9	0.02	-6.9	0.05	18.1	17.4	22.4
57	SAM54	-8.7	0.03	-7.0	0.02	18.2	17.4	22.4
58	SAM54	-8.2	0.02	-6.8	0.02	17.5	16.7	21.7
59	SAM54	-7.6	0.02	-6.6	0.04	16.6	15.8	20.8
60	SAM54	-7.5	0.02	-6.7	0.03	16.8	16.0	21.0
61	SAM54	-7.4	0.02	-6.4	0.03	15.7	14.9	19.9
62	SAM54	-6.3	0.02	-6.0	0.02	13.7	12.8	17.8
64	SAM54	-5.4	0.02	-5.3	0.02	10.9	10.0	15.0
65	SAM54	-5.3	0.02	-5.4	0.05	11.3	10.4	15.4
69	SAM54	-6.3	0.01	-5.6	0.04	12.3	11.4	16.3
70	SAM54	-6.5	0.02	-6.0	0.02	13.9	13.0	18.0
71	SAM54	-6.8	0.02	-6.1	0.02	14.2	13.3	18.3
72	SAM54	-7.4	0.01	-6.4	0.04	15.6	14.8	19.8
73	SAM54	-7.8	0.01	-6.6	0.04	16.6	15.8	20.8
74	SAM54	-8.5	0.02	-7.1	0.02	18.8	18.0	23.1
75	SAM54	-9.0	0.01	-7.3	0.03	19.9	19.2	24.2
76	SAM54	-9.4	0.01	-7.6	0.02	21.2	20.6	25.6
77	SAM54	-9.8	0.01	-7.6	0.05	21.0	20.3	25.3
78	SAM54	-10.0	0.02	-7.9	0.04	22.8	22.1	27.2
79	SAM54	-9.9	0.01	-7.8	0.04	21.9	21.3	26.3
80	SAM54	-9.9	0.01	-7.8	0.02	22.0	21.4	26.4
81	SAM54	-10.0	0.02	-8.0	0.03	22.9	22.2	27.3
82	SAM54	-9.2	0.01	-7.5	0.05	20.6	19.9	24.9
83	SAM54	-8.8	0.01	-7.2	0.05	19.4	18.7	23.7
84	SAM54	-8.4	0.02	-7.0	0.03	18.5	17.8	22.8
85	SAM54	-7.4	0.02	-6.6	0.02	16.4	15.6	20.6

SN	Specimen	$\delta^{13}C$ ‰ VPDB	±	$\delta^{18}O$ ‰ VPDB	±	Patt °C	Kim °C	Thor °C
86	SAM54	-6.8	0.02	-6.2	0.03	14.7	13.8	18.8
87	SAM54	-6.3	0.05	-6.0	0.07	13.6	12.7	17.7
88	SAM54	-6.6	0.02	-6.1	0.05	14.4	13.6	18.6
89	SAM54	-6.7	0.02	-6.1	0.04	14.2	13.4	18.4
90	SAM54	-7.2	0.03	-6.5	0.03	15.9	15.1	20.1
91	SAM54	-7.7	0.01	-6.8	0.03	17.2	16.4	21.4
92	SAM54	-8.4	0.02	-7.0	0.05	18.6	17.8	22.9
93	SAM54	-6.5	0.02	-6.3	0.04	15.1	14.2	19.2
94	SAM54	-8.7	0.00	-7.1	0.03	19.0	18.3	23.3
100	SAM54	-3.8	0.01	-5.1	0.06	10.0	9.0	14.0
2.5	SAM12	-4.4	0.03	-5.3	10.95	10.9	10.0	15.0
6.5	SAM12	-6.5	0.02	-6.4	15.77	15.8	15.0	20.0
9.5	SAM12	-6.1	0.01	-6.3	15.31	15.3	14.5	19.5
11.5	SAM12	-6.6	0.00	-6.7	16.96	17.0	16.2	21.2
15.5	SAM12	-6.5	0.02	-6.4	15.67	15.7	14.9	19.9
17	SAM12	-6.0	0.02	-6.3	14.98	15.0	14.1	19.1
18	SAM12	-6.0	0.01	-6.1	14.20	14.2	13.3	18.3
19	SAM12	-5.5	0.02	-5.6	11.92	11.9	11.0	16.0
20	SAM12	-5.3	0.04	-5.4	11.32	11.3	10.4	15.4
21	SAM12	-5.2	0.02	-5.1	10.01	10.0	9.1	14.0
22	SAM12	-5.3	0.02	-5.4	11.13	11.1	10.2	15.2
23	SAM12	-5.4	0.01	-5.3	10.55	10.6	9.6	14.6
24	SAM12	-5.3	0.02	-5.2	10.47	10.5	9.5	14.5
25	SAM12	-5.6	0.03	-5.4	11.12	11.1	10.2	15.2
26	SAM12	-5.8	0.01	-5.4	11.25	11.2	10.3	15.3
27	SAM12	-6.0	0.02	-5.7	12.41	12.4	11.5	16.5
28	SAM12	-6.8	0.01	-5.9	13.51	13.5	12.6	17.6
29	SAM12	-7.5	0.02	-6.3	15.28	15.3	14.5	19.5
30	SAM12	-7.6	0.01	-6.3	15.38	15.4	14.6	19.6
31	SAM12	-8.1	0.02	-6.8	17.23	17.2	16.4	21.5
32	SAM12	-8.7	0.01	-6.9	18.02	18.0	17.3	22.3
33	SAM12	-9.2	0.03	-7.1	18.92	18.9	18.2	23.2
34	SAM12	-9.5	0.02	-7.2	19.40	19.4	18.7	23.7
36	SAM12	-9.7	0.02	-7.2	19.49	19.5	18.8	23.8
37	SAM12	-9.8	0.01	-7.3	19.87	19.9	19.1	24.2
38	SAM12	-9.8	0.03	-7.3	19.76	19.8	19.0	24.1
39	SAM12	-9.8	0.02	-7.2	19.09	19.1	18.3	23.4
40	SAM12	-9.7	0.01	-7.2	19.42	19.4	18.7	23.7
41	SAM12	-9.8	0.03	-7.3	19.63	19.6	18.9	23.9

SN	Specimen	$\delta^{13}C$ ‰ VPDB	±	$\delta^{18}O$ ‰ VPDB	±	Patt °C	Kim °C	Thor °C
42	SAM12	-9.5	0.01	-7.1	18.87	18.9	18.1	23.2
43	SAM12	-9.0	0.01	-7.0	18.44	18.4	17.7	22.7
44	SAM12	-9.3	0.02	-7.1	18.65	18.7	17.9	22.9
45	SAM12	-9.2	0.01	-7.1	18.61	18.6	17.9	22.9
46	SAM12	-9.7	0.02	-7.5	20.49	20.5	19.8	24.8
47	SAM12	-8.6	0.04	-7.3	19.72	19.7	19.0	24.0
48	SAM12	-9.4	0.01	-7.4	20.10	20.1	19.4	24.4
49	SAM12	-9.5	0.03	-7.4	20.41	20.4	19.7	24.7
50	SAM12	-9.6	0.03	-7.5	20.47	20.5	19.8	24.8
51	SAM12	-8.3	0.02	-7.0	18.58	18.6	17.8	22.8
52	SAM12	-9.1	0.02	-7.3	19.59	19.6	18.9	23.9
53	SAM12	-9.2	0.01	-7.1	19.04	19.0	18.3	23.3
54	SAM12	-8.2	0.01	-7.0	18.15	18.1	17.4	22.4
55	SAM12	-8.0	0.01	-6.8	17.49	17.5	16.7	21.7
56	SAM12	-8.2	0.03	-6.8	17.35	17.3	16.6	21.6
57	SAM12	-8.3	0.02	-6.6	16.73	16.7	15.9	20.9
58	SAM12	-8.0	0.02	-6.5	15.95	15.9	15.1	20.1
59	SAM12	-7.1	0.02	-6.0	13.88	13.9	13.0	18.0
60	SAM12	-6.8	0.01	-5.8	12.81	12.8	11.9	16.9
61	SAM12	-7.0	0.01	-5.8	12.84	12.8	12.0	16.9
62	SAM12	-6.3	0.02	-5.6	12.26	12.3	11.4	16.3
63	SAM12	-5.4	0.01	-5.1	9.70	9.7	8.7	13.7
64	SAM12	-6.1	0.02	-5.3	10.56	10.6	9.6	14.6
65	SAM12	-6.2	0.01	-5.3	10.58	10.6	9.6	14.6
66	SAM12	-6.0	0.03	-5.3	10.64	10.6	9.7	14.7
67	SAM12	-5.6	0.02	-5.2	10.11	10.1	9.2	14.1
68	SAM12	-6.6	0.01	-5.6	12.17	12.2	11.3	16.2
69	SAM12	-6.4	0.02	-5.5	11.69	11.7	10.8	15.8
70	SAM12	-6.8	0.02	-5.8	12.77	12.8	11.9	16.9
71	SAM12	-7.0	0.02	-5.9	13.27	13.3	12.4	17.4
73	SAM12	-8.2	0.02	-6.7	17.07	17.1	16.3	21.3
74	SAM12	-8.5	0.01	-6.9	18.04	18.0	17.3	22.3
75	SAM12	-7.7	0.02	-6.7	16.81	16.8	16.0	21.0
77	SAM12	-9.4	0.01	-7.4	20.20	20.2	19.5	24.5
78	SAM12	-8.5	0.02	-7.2	19.12	19.1	18.4	23.4
79	SAM12	-8.9	0.01	-7.2	19.15	19.1	18.4	23.4
81	SAM12	-7.6	0.02	-6.9	17.77	17.8	17.0	22.0
82	SAM12	-8.3	0.02	-7.2	19.09	19.1	18.4	23.4
84	SAM12	-8.2	0.02	-7.1	18.88	18.9	18.1	23.2

SN	Specimen	$\delta^{13}C$ ‰ VPDB	±	$\delta^{18}O$ ‰ VPDB	±	Patt °C	Kim °C	Thor °C
85	SAM12	-8.0	0.00	-7.0	18.59	18.6	17.8	22.9
86	SAM12	-7.3	0.02	-6.6	16.66	16.7	15.9	20.9
87	SAM12	-8.1	0.02	-7.0	18.43	18.4	17.7	22.7
89	SAM12	-8.1	0.01	-7.0	18.54	18.5	17.8	22.8
90	SAM12	-8.0	0.03	-6.9	17.80	17.8	17.0	22.0
91	SAM12	-8.2	0.06	-6.9	18.06	18.1	17.3	22.3
92	SAM12	-8.4	0.01	-7.1	18.75	18.8	18.0	23.0
93	SAM12	-8.0	0.03	-6.9	17.99	18.0	17.2	22.2
94	SAM12	-7.5	0.02	-6.8	17.31	17.3	16.5	21.5
95	SAM12	-7.9	0.01	-6.9	17.96	18.0	17.2	22.2
96	SAM12	-7.2	0.03	-6.6	16.48	16.5	15.7	20.7
97	SAM12	-7.5	0.01	-6.6	16.45	16.5	15.6	20.7
98	SAM12	-7.5	0.01	-6.6	16.61	16.6	15.8	20.8
99	SAM12	-7.2	0.01	-6.4	15.75	15.8	14.9	19.9
100	SAM12	-6.7	0.01	-6.1	14.40	14.4	13.5	18.5
101	SAM12	-7.5	0.01	-6.3	15.16	15.2	14.3	19.3
102	SAM12	-7.1	0.01	-6.1	14.28	14.3	13.4	18.4
103	SAM12	-6.6	0.02	-5.7	12.51	12.5	11.6	16.6
105	SAM12	-5.7	0.01	-5.1	9.70	9.7	8.7	13.7
108	SAM12	-6.5	0.04	-5.4	11.31	11.3	10.4	15.4
109	SAM12	-6.6	0.02	-5.7	12.49	12.5	11.6	16.6
110	SAM12	-7.9	0.01	-6.4	15.66	15.7	14.8	19.8
114.5	SAM12	-9.1	0.01	-7.3	19.57	19.6	18.8	23.9
116	SAM12	-8.9	0.02	-7.3	19.64	19.6	18.9	23.9
117	SAM12	-8.4	0.03	-6.7	17.18	17.2	16.4	21.4
118	SAM12	-7.4	0.00	-7.1	18.89	18.9	18.1	23.2
120.5	SAM12	-8.3	0.02	-7.1	18.72	18.7	18.0	23.0
129	SAM12	-6.1	0.01	-5.6	12.00	12.0	11.1	16.1
130	SAM12	-5.9	0.02	-5.3	10.58	10.6	9.6	14.6
131	SAM12	-5.4	0.01	-5.0	9.53	9.5	8.6	13.5
132	SAM12	-5.0	0.03	-4.7	8.15	8.1	7.2	12.1
133	SAM12	-4.8	0.02	-4.7	8.20	8.2	7.2	12.2
134	SAM12	-4.4	0.06	-4.4	6.85	6.8	5.8	10.8
7.5	SAM84	-7.9	0.00	-6.6	0.01	16.7	15.9	20.9
9.5	SAM84	-7.3	0.02	-5.9	0.08	13.4	12.5	17.5
11.5	SAM84	-6.3	0.01	-5.3	0.02	10.6	9.7	14.6
13	SAM84	-5.5	0.02	-4.7	0.03	8.3	7.3	12.3
14	SAM84	-5.4	0.01	-4.5	0.03	7.2	6.2	11.2
15.5	SAM84	-5.0	0.01	-4.3	0.01	6.6	5.6	10.5

SN	Specimen	$\delta^{13}C$ ‰ VPDB	±	$\delta^{18}O$ ‰ VPDB	±	Patt °C	Kim °C	Thor °C
17	SAM84	-6.3	0.01	-4.7	0.01	8.1	7.1	12.1
18	SAM84	-8.1	0.01	-5.6	0.01	12.1	11.2	16.1
19	SAM84	-8.9	0.02	-5.8	0.06	13.1	12.2	17.2
20	SAM84	-10.2	0.01	-6.6	0.02	16.7	15.9	20.9
21	SAM84	-11.5	0.01	-7.1	0.01	18.6	17.9	22.9
22	SAM84	-12.2	0.01	-7.2	0.01	19.1	18.3	23.4
23	SAM84	-11.6	0.01	-7.0	0.01	18.3	17.5	22.5
24	SAM84	-11.7	0.02	-7.2	0.02	19.1	18.4	23.4
25	SAM84	-11.8	0.02	-7.3	0.03	19.8	19.1	24.1
26	SAM84	-11.1	0.01	-7.1	0.03	18.9	18.1	23.2
27	SAM84	-10.7	0.01	-7.2	0.01	19.1	18.4	23.4
28	SAM84	-11.0	0.02	-7.3	0.02	19.5	18.8	23.8
29.5	SAM84	-10.7	0.00	-7.2	0.02	19.1	18.4	23.4
31.5	SAM84	-9.7	0.01	-6.9	0.02	17.8	17.0	22.0
33.5	SAM84	-9.2	0.02	-6.8	0.01	17.5	16.7	21.7
35.5	SAM84	-8.6	0.02	-6.5	0.02	15.9	15.1	20.1
37.5	SAM84	-7.9	0.01	-6.2	0.01	14.6	13.7	18.7
39	SAM84	-7.2	0.02	-5.8	0.05	13.1	12.2	17.2
41.5	SAM84	-5.8	0.03	-5.1	0.01	9.7	8.8	13.7
48	SAM84	-8.7	0.06	-5.7	0.02	12.4	11.5	16.5
49	SAM84	-7.6	0.05	-5.5	0.03	11.8	10.9	15.9
50	SAM84	-9.4	0.06	-6.0	0.03	13.8	12.9	17.9
51.5	SAM84	-8.2	0.01	-6.0	0.01	13.7	12.8	17.8
56	SAM84	-9.2	0.01	-6.7	0.02	17.2	16.4	21.4
0	SAM92	-4.4	0.04	-5.7	0.04	12.4	11.5	16.5
4.5	SAM92	-5.4	0.05	-6.0	0.02	13.8	12.9	17.9
7	SAM92	-7.3	0.04	-7.0	0.01	18.4	17.7	22.7
8	SAM92	-8.0	0.02	-7.2	0.02	19.5	18.8	23.8
9	SAM92	-9.0	0.02	-7.5	0.03	20.9	20.2	25.2
10	SAM92	-8.0	0.01	-7.2	0.02	19.2	18.5	23.5
11	SAM92	-7.6	0.02	-7.6	0.01	21.1	20.4	25.4
12	SAM92	-7.1	0.02	-7.2	0.03	19.3	18.5	23.5
13	SAM92	-8.6	0.01	-7.8	0.02	22.1	21.4	26.5
14.5	SAM92	-9.6	0.01	-8.6	0.02	25.9	25.3	30.4
16	SAM92	-10.4	0.01	-8.6	0.03	26.0	25.5	30.5
17	SAM92	-10.5	0.01	-9.2	0.04	28.8	28.3	33.4
18	SAM92	-7.2	0.09	-6.0	0.02	14.0	13.2	18.1
23	SAM92	-8.4	0.01	-7.6	0.02	20.9	20.3	25.3
24.5	SAM92	-7.9	0.01	-7.3	0.02	19.9	19.2	24.2

SN	Specimen	$\delta^{13}C$ ‰ VPDB	±	$\delta^{18}O$ ‰ VPDB	±	Patt °C	Kim °C	Thor °C
26	SAM92	-8.4	0.02	-7.5	0.04	20.6	19.9	24.9
27	SAM92	-8.1	0.01	-7.5	0.03	20.7	20.0	25.0
28	SAM92	-7.2	0.01	-7.1	0.01	18.9	18.1	23.1
29	SAM92	-6.8	0.02	-7.0	0.03	18.1	17.4	22.4
30	SAM92	-6.6	0.01	-6.8	0.02	17.6	16.9	21.9
32	SAM92	-8.2	0.04	-7.2	0.03	19.3	18.5	23.6
33	SAM92	-7.3	0.03	-7.1	0.03	18.9	18.2	23.2
34	SAM92	-7.7	0.01	-7.0	0.03	18.1	17.4	22.4
35	SAM92	-7.4	0.01	-6.8	0.01	17.5	16.7	21.7
36	SAM92	-6.5	0.01	-6.4	0.06	15.7	14.9	19.9
37	SAM92	-6.4	0.07	-6.4	0.08	15.7	14.9	19.9
38	SAM92	-6.8	0.00	-6.3	0.01	15.1	14.2	19.2
39	SAM92	-6.5	0.00	-6.0	0.01	13.8	13.0	18.0
40	SAM92	-5.8	0.01	-5.9	0.02	13.4	12.5	17.5
41.5	SAM92	-6.0	0.01	-6.0	0.03	13.9	13.0	18.0
43.5	SAM92	-5.9	0.01	-6.0	0.01	13.7	12.9	17.8
45	SAM92	-6.0	0.01	-6.1	0.02	14.3	13.4	18.4
47.5	SAM92	-6.7	0.01	-6.6	0.04	16.7	15.9	20.9
49	SAM92	-6.9	0.01	-6.7	0.01	16.8	16.0	21.0
50.5	SAM92	-7.1	0.01	-6.7	0.02	16.8	16.0	21.0
52	SAM92	-7.1	0.02	-7.0	0.02	18.3	17.5	22.5
53	SAM92	-7.4	0.02	-7.1	0.03	18.7	18.0	23.0
54	SAM92	-7.2	0.01	-7.1	0.02	18.8	18.1	23.1
55	SAM92	-7.7	0.01	-7.3	0.01	19.7	18.9	24.0
56	SAM92	-7.8	0.01	-7.2	0.03	19.4	18.7	23.7
57	SAM92	-7.5	0.01	-7.2	0.02	19.2	18.4	23.5
58	SAM92	-7.6	0.02	-7.0	0.04	18.5	17.7	22.7
59	SAM92	-7.4	0.01	-7.1	0.01	18.7	18.0	23.0
60.5	SAM92	-6.9	0.01	-6.9	0.01	17.9	17.2	22.2
62	SAM92	-6.9	0.01	-7.0	0.02	18.3	17.5	22.5
63.5	SAM92	-6.3	0.00	-6.7	0.01	16.9	16.1	21.1
65	SAM92	-6.1	0.01	-6.4	0.02	15.4	14.6	19.6
66.5	SAM92	-6.2	0.00	-6.5	0.01	16.2	15.4	20.4
68	SAM92	-5.8	0.00	-6.3	0.01	15.0	14.2	19.2
69.5	SAM92	-5.6	0.01	-6.1	0.01	14.5	13.6	18.6
71.5	SAM92	-5.3	0.02	-6.1	0.02	14.1	13.2	18.2
73.5	SAM92	-6.0	0.01	-6.0	0.02	13.7	12.9	17.9
75.5	SAM92	-6.4	0.08	-5.9	0.01	13.6	12.7	17.7
80	SAM92	-7.3	0.01	-7.1	0.03	18.6	17.9	22.9

SN	Specimen	$\delta^{13}C$ ‰ VPDB	±	$\delta^{18}O$ ‰ VPDB	±	Patt °C	Kim °C	Thor °C
81	SAM92	-8.1	0.02	-7.4	0.04	20.0	19.3	24.3
83	SAM92	-7.5	0.01	-7.3	0.03	19.9	19.1	24.2
85	SAM92	-7.6	0.02	-7.4	0.02	20.1	19.4	24.4
86	SAM92	-7.2	0.00	-7.2	0.01	19.3	18.5	23.6
87	SAM92	-6.8	0.01	-7.0	0.02	18.5	17.7	22.7
88.5	SAM92	-6.5	0.00	-6.8	0.02	17.6	16.9	21.9
90	SAM92	-6.9	0.01	-7.1	0.02	18.8	18.1	23.1
91	SAM92	-6.6	0.01	-6.9	0.01	18.0	17.2	22.2
92	SAM92	-6.4	0.01	-6.9	0.01	18.0	17.3	22.3
93.5	SAM92	-6.0	0.01	-6.8	0.01	17.3	16.5	21.5
95	SAM92	-6.2	0.02	-6.7	0.04	16.8	16.1	21.1
96	SAM92	-5.8	0.01	-6.4	0.01	15.8	15.0	20.0
97	SAM92	-5.4	0.01	-6.5	0.02	16.2	15.4	20.4
98	SAM92	-5.2	0.01	-6.4	0.03	15.5	14.7	19.7
99.5	SAM92	-5.6	0.01	-6.3	0.02	15.0	14.2	19.2
101.5	SAM92	-4.6	0.00	-6.0	0.03	13.6	12.8	17.7
104	SAM92	-5.2	0.01	-5.7	0.03	12.3	11.4	16.4
105.5	SAM92	-5.8	0.01	-6.1	0.01	14.4	13.6	18.5
107.5	SAM92	-7.2	0.01	-6.8	0.02	17.6	16.9	21.9
2.5	SAM93	-9.7	0.05	-6.8	0.06	17.6	16.9	21.9
5.5	SAM93	-10.6	0.02	-8.0	0.03	22.8	22.2	27.2
8	SAM93	-9.0	0.04	-6.8	0.03	17.3	16.5	21.5
10.5	SAM93	-8.5	0.02	-6.6	0.03	16.4	15.6	20.6
12.5	SAM93	-7.8	0.03	-6.5	0.05	15.9	15.1	20.1
14	SAM93	-7.6	0.03	-6.4	0.04	15.7	14.9	19.9
15	SAM93	-9.8	0.07	-9.6	0.16	31.0	30.6	35.6
16	SAM93	-7.6	0.02	-6.2	0.06	14.8	13.9	18.9
17	SAM93	-7.6	0.03	-6.1	0.03	14.3	13.5	18.5
18	SAM93	-7.6	0.02	-5.9	0.03	13.2	12.3	17.3
19	SAM93	-7.6	0.03	-5.8	0.05	12.9	12.0	17.0
20	SAM93	-6.9	0.01	-5.4	0.02	11.2	10.3	15.2
21.5	SAM93	-6.2	0.01	-5.1	0.02	10.1	9.1	14.1
23	SAM93	-5.6	0.02	-4.8	0.05	8.6	7.6	12.5
24	SAM93	-5.5	0.03	-4.6	0.03	7.8	6.8	11.7
25	SAM93	-5.4	0.02	-4.6	0.04	7.9	6.9	11.8
26.5	SAM93	-5.4	0.02	-4.5	0.03	7.2	6.1	11.1
32	SAM93	-8.9	0.01	-6.5	0.02	15.9	15.1	20.1
34	SAM93	-9.5	0.01	-6.8	0.03	17.3	16.5	21.5
35	SAM93	-9.8	0.02	-6.9	0.04	18.1	17.4	22.4

SN	Specimen	$\delta^{13}C$ ‰ VPDB	±	$\delta^{18}O$ ‰ VPDB	±	Patt °C	Kim °C	Thor °C
40	SAM93	-9.3	0.00	-6.8	0.03	17.6	16.8	21.8
44	SAM93	-9.2	0.02	-7.0	0.04	18.3	17.5	22.5
46	SAM93	-8.6	0.03	-6.9	0.07	17.9	17.1	22.2
47	SAM93	-8.3	0.02	-6.8	0.03	17.5	16.7	21.7
48	SAM93	-8.3	0.01	-6.8	0.04	17.3	16.5	21.5
49	SAM93	-7.9	0.01	-6.7	0.01	16.8	16.0	21.0
50	SAM93	-7.8	0.02	-6.6	0.08	16.4	15.6	20.6
51	SAM93	-7.8	0.02	-6.7	0.02	16.9	16.1	21.2
52	SAM93	-7.5	0.02	-6.6	0.05	16.7	15.9	20.9
53	SAM93	-7.6	0.02	-6.5	0.04	16.2	15.4	20.4
54	SAM93	-7.1	0.02	-6.5	0.05	16.0	15.1	20.1
55	SAM93	-7.0	0.02	-6.3	0.04	15.3	14.5	19.5
57	SAM93	-6.7	0.03	-6.0	0.01	14.1	13.2	18.2
59	SAM93	-6.4	0.02	-5.8	0.02	13.1	12.2	17.2
60	SAM93	-6.2	0.03	-5.6	0.04	12.0	11.1	16.1
61	SAM93	-5.9	0.01	-5.4	0.03	11.2	10.3	15.2
62	SAM93	-5.6	0.02	-5.3	0.03	10.6	9.6	14.6
63	SAM93	-5.3	0.01	-5.1	0.05	9.9	8.9	13.9
64	SAM93	-5.0	0.02	-4.8	0.04	8.6	7.7	12.6
65	SAM93	-4.8	0.02	-4.5	0.04	7.4	6.4	11.3
68	SAM93	-5.4	0.01	-4.8	0.02	8.5	7.5	12.4
71	SAM93	-6.3	0.03	-5.6	0.03	11.9	10.9	15.9
72	SAM93	-6.8	0.01	-5.8	0.05	13.0	12.1	17.1
75	SAM93	-8.6	0.03	-6.6	0.06	16.4	15.6	20.6
76	SAM93	-10.6	0.03	-7.4	0.05	20.1	19.3	24.4
78	SAM93	-9.4	0.02	-7.0	0.04	18.6	17.8	22.9
79	SAM93	-8.7	0.01	-7.0	0.02	18.2	17.4	22.4
80	SAM93	-8.4	0.02	-7.0	0.04	18.3	17.5	22.5
82	SAM93	-8.3	0.03	-6.8	0.05	17.3	16.5	21.6
83	SAM93	-8.5	0.02	-6.9	0.03	17.9	17.1	22.1
84	SAM93	-8.3	0.02	-6.6	0.02	16.8	16.0	21.0
86	SAM93	-6.8	0.04	-5.5	0.02	11.8	10.9	15.9
87	SAM93	-6.1	0.02	-5.1	0.03	10.0	9.1	14.1
88	SAM93	-6.0	0.01	-5.1	0.06	9.9	9.0	13.9
90	SAM93	-7.0	0.02	-5.4	0.07	11.3	10.4	15.4
91	SAM93	-8.5	0.01	-6.3	0.03	15.0	14.2	19.2
92	SAM93	-9.2	0.01	-6.5	0.02	16.2	15.4	20.4
93.5	SAM93	-9.2	0.02	-6.7	0.05	17.0	16.2	21.3
1	CHK1	-7.8	0.00	-7.5	0.05	20.8	20.1	25.1

SN	Specimen	$\delta^{13}C$ ‰ VPDB	±	$\delta^{18}O$ ‰ VPDB	±	Patt °C	Kim °C	Thor °C
2	CHK1	-7.8	0.02	-7.4	0.04	20.2	19.5	24.5
3	CHK1	-7.6	0.01	-7.5	0.06	20.6	19.9	24.9
4	CHK1	-7.7	0.02	-7.5	0.03	20.5	19.8	24.9
5	CHK1	-7.7	0.01	-7.3	0.02	19.8	19.1	24.2
6	CHK1	-7.7	0.01	-7.3	0.03	19.8	19.1	24.2
7	CHK1	-7.7	0.01	-7.3	0.04	19.7	18.9	24.0
8	CHK1	-7.8	0.01	-7.3	0.02	19.7	18.9	24.0
9	CHK1	-7.9	0.00	-7.5	0.02	20.6	19.9	25.0
11	CHK1	-7.9	0.00	-7.4	0.01	20.1	19.4	24.4
12	CHK1	-7.7	0.01	-7.3	0.02	19.6	18.9	23.9
13	CHK1	-7.6	0.01	-7.2	0.02	19.3	18.6	23.6
14	CHK1	-7.5	0.01	-7.1	0.02	18.8	18.0	23.1
15	CHK1	-7.4	0.01	-6.9	0.02	18.1	17.3	22.3
17	CHK1	-6.9	0.00	-6.6	0.01	16.5	15.7	20.7
18	CHK1	-6.6	0.01	-6.5	0.01	15.9	15.1	20.1
20	CHK1	-6.1	0.00	-6.2	0.01	14.9	14.0	19.0
21	CHK1	-6.0	0.00	-6.1	0.01	14.3	13.4	18.4
22	CHK1	-5.8	0.01	-6.0	0.01	13.7	12.8	17.8
23	CHK1	-5.7	0.01	-5.9	0.01	13.2	12.3	17.3
24	CHK1	-5.4	0.01	-5.8	0.01	12.9	12.1	17.0
25	CHK1	-5.3	0.00	-5.4	0.01	11.4	10.4	15.4
26	CHK1	-5.3	0.01	-5.4	0.01	11.2	10.3	15.2
27	CHK1	-5.1	0.01	-5.3	0.01	10.5	9.6	14.6
28	CHK1	-5.4	0.01	-5.4	0.02	11.3	10.3	15.3
29	CHK1	-5.7	0.02	-5.8	0.04	13.1	12.2	17.2
30	CHK1	-5.7	0.01	-5.6	0.02	12.1	11.1	16.1
31	CHK1	-5.9	0.01	-5.8	0.02	13.1	12.2	17.2
32	CHK1	-6.0	0.00	-5.7	0.01	12.6	11.7	16.7
33	CHK1	-6.0	0.01	-5.9	0.03	13.2	12.3	17.3
34	CHK1	-6.8	0.00	-6.1	0.02	14.1	13.2	18.2
35	CHK1	-6.4	0.01	-6.0	0.01	13.7	12.8	17.8
36	CHK1	-6.8	0.01	-6.1	0.01	14.3	13.5	18.5
37	CHK1	-7.0	0.00	-6.1	0.01	14.3	13.4	18.4
38	CHK1	-7.3	0.01	-6.4	0.01	15.6	14.8	19.8
39	CHK1	-7.5	0.01	-6.6	0.02	16.4	15.6	20.6
40	CHK1	-6.9	0.01	-6.3	0.01	15.3	14.4	19.4
41	CHK1	-8.1	0.01	-6.9	0.00	17.7	16.9	22.0
42	CHK1	-7.8	0.00	-6.7	0.00	16.8	16.0	21.0
43	CHK1	-7.7	0.01	-6.6	0.01	16.5	15.7	20.7

SN	Specimen	$\delta^{13}C$ ‰ VPDB	±	$\delta^{18}O$ ‰ VPDB	±	Patt °C	Kim °C	Thor °C
44	CHK1	-8.0	0.01	-6.8	0.01	17.4	16.7	21.7
45	CHK1	-8.1	0.01	-6.8	0.01	17.4	16.6	21.6
46	CHK1	-7.9	0.00	-7.0	0.01	18.2	17.4	22.4
48	CHK1	-7.9	0.00	-6.9	0.01	17.9	17.1	22.2
49	CHK1	-8.1	0.01	-7.2	0.01	19.2	18.4	23.4
50	CHK1	-7.4	0.01	-6.9	0.01	17.8	17.0	22.0
52	CHK1	-7.8	0.01	-7.2	0.02	19.5	18.7	23.8
53	CHK1	-8.0	0.01	-7.3	0.02	19.7	18.9	24.0
54	CHK1	-7.4	0.01	-7.2	0.01	19.4	18.7	23.7
55	CHK1	-7.2	0.01	-7.1	0.01	18.7	18.0	23.0
56	CHK1	-7.1	0.01	-7.1	0.01	18.6	17.8	22.9
57	CHK1	-5.8	0.00	-7.4	0.02	20.0	19.3	24.3
58	CHK1	-7.3	0.00	-7.2	0.00	19.2	18.4	23.4
59	CHK1	-7.4	0.01	-7.1	0.01	18.9	18.1	23.1
60	CHK1	-6.7	0.00	-6.9	0.01	18.0	17.3	22.3
63	CHK1	-6.3	0.01	-6.6	0.01	16.3	15.5	20.5
64	CHK1	-6.2	0.00	-6.5	0.01	16.2	15.4	20.4
65	CHK1	-6.2	0.00	-6.4	0.01	15.4	14.6	19.6
66	CHK1	-5.3	0.00	-6.0	0.01	13.9	13.1	18.0
68	CHK1	-5.2	0.01	-5.9	0.02	13.6	12.7	17.7
72	CHK1	-5.2	0.01	-5.8	0.01	13.1	12.2	17.2
73	CHK1	-5.6	0.01	-5.9	0.01	13.6	12.7	17.7
75	CHK1	-7.6	0.02	-7.0	0.01	18.3	17.6	22.6
76	CHK1	-8.1	0.00	-7.2	0.00	19.2	18.5	23.5
77	CHK1	-7.3	0.00	-7.0	0.01	18.1	17.4	22.4
3.5	CHK13	-7.3	0.04	-7.9	0.05	22.5	21.9	26.9
5.5	CHK13	-8.4	0.00	-8.3	0.02	24.6	24.0	29.1
8	CHK13	-8.9	0.02	-8.0	0.04	23.0	22.3	27.4
9.5	CHK13	-9.1	0.01	-7.7	0.01	21.7	21.1	26.1
11.5	CHK13	-8.9	0.02	-7.7	0.02	21.6	20.9	26.0
14.5	CHK13	-9.1	0.01	-7.8	0.04	22.2	21.6	26.6
17.5	CHK13	-9.1	0.02	-7.9	0.07	22.4	21.7	26.8
20.5	CHK13	-9.0	0.01	-8.1	0.03	23.3	22.7	27.7
24	CHK13	-8.9	0.01	-8.3	0.02	24.3	23.7	28.7
26.5	CHK13	-8.2	0.01	-8.0	0.02	23.1	22.4	27.5
30	CHK13	-8.1	0.08	-8.2	0.06	24.1	23.5	28.5
32.5	CHK13	-7.6	0.01	-8.1	0.01	23.6	23.0	28.0
35	CHK13	-7.4	0.03	-7.9	0.04	22.5	21.8	26.9
36	CHK13	-7.3	0.01	-7.8	0.02	22.3	21.6	26.7

SN	Specimen	$\delta^{13}C$ ‰ VPDB	±	$\delta^{18}O$ ‰ VPDB	±	Patt °C	Kim °C	Thor °C
37.5	CHK13	-6.8	0.01	-6.7	0.02	16.9	16.1	21.1
41	CHK13	-6.9	0.01	-7.6	0.02	21.4	20.7	25.7
44.5	CHK13	-6.5	0.03	-7.5	0.02	20.8	20.1	25.1
48.5	CHK13	-6.0	0.01	-7.1	0.01	18.8	18.1	23.1
52.5	CHK13	-5.7	0.01	-6.6	0.02	16.5	15.7	20.7
57	CHK13	-4.9	0.01	-5.7	0.01	12.6	11.7	16.7
62.5	CHK13	-4.2	0.01	-5.4	0.05	11.2	10.2	15.2
64	CHK13	-4.2	0.03	-4.6	0.02	7.8	6.8	11.7
65	CHK13	-4.5	0.02	-4.8	0.03	8.5	7.5	12.5
67.5	CHK13	-4.3	0.01	-4.7	0.02	8.2	7.2	12.2
71.5	CHK13	-4.9	0.01	-5.2	0.04	10.1	9.1	14.1
74	CHK13	-5.3	0.04	-5.4	0.05	11.2	10.2	15.2
77	CHK13	-6.7	0.01	-6.6	0.02	16.4	15.6	20.6
79.5	CHK13	-7.0	0.02	-6.7	0.02	17.0	16.2	21.2
81	CHK13	-7.3	0.01	-6.8	0.03	17.7	16.9	21.9
82.5	CHK13	-7.4	0.01	-6.8	0.01	17.7	16.9	21.9
84.5	CHK13	-7.4	0.01	-6.9	0.04	18.1	17.3	22.3
88.5	CHK13	-7.1	0.01	-7.1	0.04	18.7	18.0	23.0
92.5	CHK13	-6.6	0.01	-7.1	0.02	18.7	17.9	22.9
94.5	CHK13	-6.6	0.01	-7.3	0.02	19.6	18.9	23.9
96.5	CHK13	-6.5	0.01	-7.4	0.03	20.2	19.5	24.5
98	CHK13	-7.1	0.01	-7.2	0.00	19.5	18.8	23.8
99	CHK13	-6.9	0.06	-7.4	0.10	20.2	19.5	24.6
100.5	CHK13	-6.7	0.02	-7.5	0.03	20.6	19.9	24.9
102	CHK13	-6.7	0.04	-7.3	0.09	19.6	18.8	23.9
3.5	CHK14	-6.9	0.01	-7.2	0.03	19.1	18.4	23.4
7.5	CHK14	-6.0	0.01	-6.7	0.02	17.1	16.3	21.4
10	CHK14	-5.9	0.02	-6.8	0.01	17.3	16.5	21.5
12	CHK14	-5.6	0.02	-6.6	0.02	16.5	15.7	20.7
14	CHK14	-6.0	0.01	-6.9	0.01	18.0	17.2	22.2
16	CHK14	-6.3	0.01	-6.8	0.02	17.6	16.8	21.8
18	CHK14	-6.2	0.02	-6.8	0.02	17.6	16.8	21.9
20	CHK14	-6.4	0.02	-7.0	0.03	18.4	17.6	22.6
22	CHK14	-6.1	0.02	-6.6	0.02	16.7	15.9	20.9
38	CHK14	-5.3	0.01	-6.6	0.02	16.5	15.7	20.7
24	CHK14	-5.8	0.01	-6.6	0.02	16.5	15.7	20.7
36	CHK14	-5.1	0.02	-6.2	0.02	14.6	13.8	18.8
48	CHK14	-7.0	0.02	-8.0	0.07	23.2	22.6	27.6
50	CHK14	-7.3	0.01	-8.1	0.03	23.3	22.7	27.7

SN	Specimen	$\delta^{13}C$ ‰ VPDB	±	$\delta^{18}O$ ‰ VPDB	±	Patt °C	Kim °C	Thor °C
52	CHK14	-7.5	0.03	-8.1	0.03	23.4	22.8	27.8
54	CHK14	-8.0	0.02	-8.3	0.06	24.6	24.0	29.0
56	CHK14	-8.6	0.04	-8.7	0.04	26.3	25.8	30.8
58	CHK14	-8.9	0.01	-8.4	0.04	24.9	24.3	29.4
63.5	CHK14	-9.2	0.03	-9.2	0.05	28.8	28.3	33.4
44	CHK14	-6.7	0.01	-8.0	0.04	23.1	22.5	27.5
38.5	CHK15	-6.1	0.01	-6.7	0.03	16.9	16.1	21.1
41	CHK15	-6.2	0.03	-6.7	0.01	16.8	16.0	21.0
45	CHK15	-5.8	0.01	-6.2	0.03	14.7	13.8	18.8
49	CHK15	-5.1	0.02	-5.6	0.02	12.0	11.1	16.1
50	CHK15	-5.1	0.01	-5.5	0.03	11.6	10.7	15.6
51	CHK15	-5.0	0.04	-5.5	0.02	11.4	10.5	15.5
52	CHK15	-5.3	0.02	-5.5	0.01	11.6	10.7	15.7
53	CHK15	-5.0	0.01	-5.4	0.02	11.1	10.2	15.1
54	CHK15	-5.2	0.01	-5.5	0.02	11.7	10.8	15.8
55	CHK15	-5.1	0.01	-5.5	0.01	11.5	10.6	15.5
56	CHK15	-5.1	0.01	-5.5	0.02	11.7	10.7	15.7
58	CHK15	-6.0	0.00	-5.8	0.00	12.9	12.0	16.9
59	CHK15	-5.6	0.01	-5.8	0.03	13.0	12.1	17.1
60	CHK15	-6.0	0.01	-5.8	0.02	13.1	12.2	17.2
61	CHK15	-6.1	0.01	-5.9	0.03	13.2	12.3	17.3
62	CHK15	-6.1	0.01	-6.0	0.01	13.6	12.7	17.7
63	CHK15	-6.1	0.01	-5.9	0.02	13.6	12.7	17.7
64	CHK15	-6.4	0.02	-6.3	0.01	14.9	14.1	19.1
65	CHK15	-6.7	0.01	-6.4	0.00	15.4	14.6	19.6
66.5	CHK15	-6.6	0.02	-6.3	0.02	15.3	14.4	19.4
68	CHK15	-7.3	0.03	-6.6	0.02	16.4	15.6	20.6
69	CHK15	-7.5	0.03	-6.8	0.01	17.4	16.6	21.6
70	CHK15	-7.7	0.01	-7.0	0.03	18.3	17.5	22.5
71	CHK15	-7.6	0.01	-7.1	0.02	18.8	18.1	23.1
72	CHK15	-7.8	0.01	-6.8	0.01	17.5	16.7	21.7
73	CHK15	-7.5	0.01	-7.2	0.02	19.1	18.3	23.3
74	CHK15	-7.6	0.01	-7.1	0.03	19.0	18.3	23.3
75	CHK15	-8.2	0.01	-7.5	0.01	20.5	19.7	24.8
76	CHK15	-8.1	0.02	-7.4	0.02	20.4	19.7	24.7
77	CHK15	-8.0	0.01	-7.4	0.02	20.2	19.5	24.5
78	CHK15	-7.8	0.01	-7.5	0.01	20.6	19.9	24.9
79	CHK15	-7.9	0.01	-7.5	0.01	20.7	20.0	25.1
80	CHK15	-7.5	0.01	-7.2	0.03	19.4	18.7	23.7

SN	Specimen	$\delta^{13}C$ ‰ VPDB	±	$\delta^{18}O$ ‰ VPDB	±	Patt °C	Kim °C	Thor °C
81	CHK15	-7.4	0.00	-7.2	0.02	19.4	18.7	23.7
82	CHK15	-7.2	0.01	-7.3	0.02	19.9	19.2	24.2
83	CHK15	-7.2	0.01	-7.3	0.02	19.8	19.1	24.1
85	CHK15	-7.0	0.01	-7.3	0.01	19.5	18.8	23.8
86.5	CHK15	-6.7	0.02	-7.0	0.01	18.5	17.8	22.8
91	CHK15	-6.0	0.01	-6.5	0.02	16.2	15.4	20.4
94.5	CHK15	-5.8	0.01	-6.5	0.01	15.9	15.1	20.1
96	CHK15	-5.9	0.02	-6.4	0.01	15.4	14.6	19.6
98	CHK15	-5.8	0.02	-6.4	0.01	15.4	14.6	19.6
99.5	CHK15	-5.4	0.02	-6.0	0.00	13.9	13.0	18.0
101	CHK15	-5.2	0.03	-5.8	0.01	13.1	12.2	17.2
102.5	CHK15	-5.3	0.01	-5.8	0.01	13.0	12.1	17.1
104	CHK15	-5.2	0.01	-5.6	0.01	11.9	11.0	16.0
105.5	CHK15	-5.4	0.02	-5.7	0.01	12.4	11.5	16.5
107	CHK15	-5.2	0.02	-5.8	0.02	13.1	12.2	17.2
108	CHK15	-5.3	0.01	-5.6	0.01	12.2	11.3	16.3
110	CHK15	-5.5	0.03	-5.6	0.01	12.2	11.3	16.3
111.5	CHK15	-5.6	0.02	-5.8	0.01	13.1	12.2	17.2
113	CHK15	-6.0	0.01	-5.9	0.01	13.4	12.5	17.5
114	CHK15	-5.7	0.02	-5.6	0.01	12.1	11.1	16.1
115.5	CHK15	-6.3	0.03	-6.1	0.01	14.2	13.3	18.3
117.5	CHK15	-6.2	0.01	-6.0	0.03	13.8	12.9	17.9
119	CHK15	-6.3	0.02	-6.1	0.03	14.4	13.6	18.6
120	CHK15	-6.3	0.02	-6.1	0.02	14.3	13.5	18.5
121	CHK15	-6.5	0.00	-6.2	0.01	14.8	13.9	18.9
122.5	CHK15	-7.0	0.01	-6.5	0.02	15.9	15.1	20.1
124.5	CHK15	-7.2	0.02	-6.9	0.01	17.7	16.9	22.0
126	CHK15	-7.5	0.01	-6.9	0.01	17.9	17.1	22.1
127	CHK15	-7.8	0.03	-7.0	0.01	18.5	17.8	22.8
128	CHK15	-7.8	0.02	-7.2	0.01	19.1	18.3	23.3
129	CHK15	-8.0	0.03	-7.2	0.01	19.4	18.7	23.7
130	CHK15	-7.9	0.00	-7.2	0.00	19.3	18.6	23.6
131.5	CHK15	-7.7	0.02	-7.1	0.01	18.8	18.1	23.1
133.5	CHK15	-8.4	0.01	-7.4	0.01	20.2	19.5	24.5
135.5	CHK15	-7.8	0.02	-7.4	0.01	20.2	19.5	24.5
137.5	CHK15	-8.7	0.02	-7.7	0.01	21.6	20.9	25.9
139.5	CHK15	-8.2	0.01	-7.7	0.02	21.6	21.0	26.0
141.5	CHK15	-8.8	0.02	-7.9	0.04	22.4	21.8	26.8
143.3	CHK15	-9.1	0.03	-8.0	0.01	22.9	22.2	27.3

SN	Specimen	$\delta^{13}C$ ‰ VPDB	±	$\delta^{18}O$ ‰ VPDB	±	Patt °C	Kim °C	Thor °C
145.5	CHK15	-9.1	0.02	-8.1	0.02	23.7	23.0	28.1
147	CHK15	-10.4	0.03	-8.5	0.01	25.5	24.9	29.9
148	CHK15	-10.7	0.01	-8.6	0.03	25.9	25.4	30.4
149	CHK15	-10.6	0.03	-8.8	0.01	26.8	26.3	31.3
12	CHK20	-5.1	0.01	-6.2	0.01	14.7	13.8	18.8
19	CHK20	-6.9	0.01	-6.3	0.02	15.2	14.3	19.3
25	CHK20	-8.6	0.02	-6.9	0.02	18.0	17.2	22.2
28	CHK20	-9.5	0.02	-7.1	0.03	18.9	18.2	23.2
37	CHK20	-9.1	0.04	-6.7	0.06	16.8	16.0	21.0
42	CHK20	-8.5	0.01	-6.7	0.02	16.9	16.1	21.1
44.5	CHK20	-8.3	0.01	-6.3	0.01	15.4	14.6	19.6
46.5	CHK20	-9.6	0.01	-6.8	0.01	17.6	16.9	21.9
48	CHK20	-12.0	0.01	-8.4	0.06	25.2	24.6	29.6
49	CHK20	-12.0	0.02	-9.6	0.06	31.0	30.5	35.6
55.5	CHK20	-11.8	0.02	-8.6	0.06	26.1	25.6	30.6
57	CHK20	-12.0	0.02	-9.4	0.05	30.1	29.6	34.7
60	CHK20	-11.7	0.01	-9.4	0.02	29.7	29.2	34.3
61	CHK20	-11.7	0.01	-9.4	0.00	29.7	29.2	34.3
62	CHK20	-11.2	0.02	-9.2	0.04	28.9	28.4	33.5
63	CHK20	-10.7	0.02	-8.9	0.04	27.4	26.9	31.9
64	CHK20	-9.2	0.03	-7.8	0.04	22.3	21.6	26.6
65	CHK20	-8.7	0.02	-7.9	0.04	22.4	21.8	26.8
66	CHK20	-8.1	0.01	-7.4	0.02	20.4	19.7	24.8
67	CHK20	-7.7	0.04	-7.2	0.01	19.2	18.5	23.5
68.5	CHK20	-7.3	0.02	-7.0	0.03	18.3	17.6	22.6
70	CHK20	-6.9	0.01	-6.4	0.01	15.4	14.6	19.6
71	CHK20	-6.4	0.01	-6.3	0.03	15.1	14.3	19.3
72	CHK20	-6.8	0.01	-6.3	0.02	15.1	14.3	19.3
73	CHK20	-7.2	0.01	-6.4	0.01	15.8	14.9	19.9
74	CHK20	-7.6	0.01	-6.5	0.00	16.0	15.2	20.2
75	CHK20	-7.3	0.00	-6.4	0.01	15.5	14.6	19.6
76	CHK20	-7.6	0.00	-6.5	0.01	16.0	15.2	20.2
78	CHK20	-7.6	0.02	-6.5	0.02	16.3	15.5	20.5
79	CHK20	-7.5	0.01	-6.3	0.03	15.2	14.3	19.3
81	CHK20	-8.2	0.02	-6.9	0.05	17.8	17.0	22.0
82	CHK20	-8.2	0.01	-7.0	0.04	18.2	17.4	22.4
83	CHK20	-8.4	0.00	-7.0	0.01	18.5	17.7	22.8
84	CHK20	-8.1	0.03	-6.8	0.06	17.6	16.9	21.9
85	CHK20	-7.7	0.03	-7.0	0.06	18.2	17.5	22.5

SN	Specimen	$\delta^{13}C$ ‰ VPDB	±	$\delta^{18}O$ ‰ VPDB	±	Patt °C	Kim °C	Thor °C
86	CHK20	-8.6	0.01	-7.3	0.01	19.8	19.1	24.1
87	CHK20	-8.8	0.01	-7.6	0.03	21.4	20.7	25.7
88	CHK20	-9.0	0.02	-7.8	0.03	22.0	21.3	26.4
89	CHK20	-8.7	0.01	-7.7	0.01	21.7	21.0	26.1
90	CHK20	-8.4	0.01	-7.5	0.02	20.9	20.2	25.2
91	CHK20	-8.8	0.01	-7.8	0.02	22.2	21.6	26.6
92	CHK20	-8.0	0.01	-7.1	0.01	19.0	18.2	23.2
93	CHK20	-8.7	0.02	-7.8	0.06	22.2	21.5	26.6
94	CHK20	-9.2	0.01	-8.0	0.01	23.2	22.6	27.6
95	CHK20	-8.2	0.01	-7.5	0.01	20.5	19.8	24.8
96	CHK20	-8.9	0.03	-7.5	0.06	20.6	19.9	24.9
97	CHK20	-9.4	0.01	-8.4	0.02	24.8	24.2	29.2
98	CHK20	-9.6	0.03	-8.5	0.07	25.5	24.9	29.9
99	CHK20	-9.8	0.02	-8.5	0.04	25.3	24.7	29.8
101	CHK20	-9.6	0.01	-8.5	0.02	25.4	24.8	29.9
102	CHK20	-9.7	0.02	-8.6	0.05	25.7	25.2	30.2
103	CHK20	-9.5	0.01	-8.4	0.01	25.1	24.5	29.5
105	CHK20	-10.2	0.03	-9.1	0.07	28.2	27.7	32.8
106	CHK20	-9.3	0.05	-8.7	0.08	26.5	25.9	31.0
107	CHK20	-8.8	0.02	-8.3	0.04	24.6	24.0	29.0
108.5	CHK20	-7.8	0.01	-7.8	0.04	21.9	21.3	26.3
110	CHK20	-9.3	0.01	-8.4	0.02	25.0	24.4	29.4
1	CHK23	-10.7	0.02	-10.5	0.04	35.3	35.0	40.1
5.5	CHK23	-9.8	0.02	-8.0	0.02	23.1	22.4	27.5
9	CHK23	-7.7	0.01	-7.5	0.01	20.7	20.1	25.1
13.5	CHK23	-5.8	0.03	-6.2	0.04	14.7	13.9	18.9
15.5	CHK23	-4.6	0.01	-4.8	0.02	8.5	7.5	12.4
17.5	CHK23	-6.4	0.01	-6.0	0.02	13.6	12.8	17.8
19	CHK23	-8.5	0.03	-7.3	0.02	19.7	19.0	24.0
20	CHK23	-8.3	0.02	-7.2	0.02	19.4	18.7	23.7
21	CHK23	-7.3	0.02	-7.2	0.02	19.2	18.4	23.5
22	CHK23	-7.6	0.02	-7.3	0.03	19.8	19.1	24.1
23	CHK23	-7.8	0.02	-7.5	0.02	20.7	20.0	25.0
24	CHK23	-7.6	0.01	-7.4	0.03	20.1	19.3	24.4
26	CHK23	-6.2	0.02	-6.3	0.05	15.2	14.4	19.4
28	CHK23	-4.7	0.01	-4.9	0.03	8.9	7.9	12.8
29	CHK23	-5.5	0.01	-5.0	0.02	9.6	8.6	13.6
30	CHK23	-7.6	0.02	-6.6	0.05	16.4	15.6	20.6
31	CHK23	-8.4	0.02	-7.4	0.02	20.3	19.6	24.6

SN	Specimen	$\delta^{13}C$ ‰ VPDB	±	$\delta^{18}O$ ‰ VPDB	±	Patt °C	Kim °C	Thor °C
32	CHK23	-7.4	0.02	-7.1	0.02	19.0	18.2	23.2
33	CHK23	-7.3	0.01	-7.3	0.06	19.6	18.8	23.9
34	CHK23	-7.4	0.02	-7.4	0.00	20.2	19.5	24.5
35	CHK23	-7.6	0.01	-7.6	0.00	21.2	20.5	25.5
36	CHK23	-7.3	0.01	-7.2	0.02	19.1	18.4	23.4
37	CHK23	-6.3	0.02	-6.3	0.02	15.4	14.5	19.5
38	CHK23	-5.7	0.02	-5.7	0.01	12.4	11.5	16.5
39	CHK23	-4.8	0.01	-5.1	0.02	10.0	9.1	14.0
40	CHK23	-4.4	0.02	-4.8	0.03	8.7	7.7	12.7
41	CHK23	-5.5	0.02	-5.8	0.03	12.8	11.9	16.9
42	CHK23	-6.6	0.02	-6.5	0.02	16.2	15.4	20.4
43	CHK23	-7.0	0.01	-6.6	0.03	16.6	15.8	20.8
44	CHK23	-7.8	0.01	-7.1	0.02	18.6	17.9	22.9
45	CHK23	-9.3	0.01	-7.5	0.03	20.5	19.8	24.8
46	CHK23	-10.6	0.01	-7.8	0.02	22.1	21.4	26.5
47	CHK23	-12.4	0.01	-8.7	0.02	26.4	25.8	30.9
48	CHK23	-12.8	0.01	-9.0	0.05	27.8	27.3	32.4
6	CHK7	-11.1	0.02	-10.0	0.03	33.0	32.7	37.7
9	CHK7	-10.8	0.02	-9.8	0.03	32.1	31.7	36.8
12	CHK7	-10.0	0.02	-10.2	0.05	34.0	33.6	38.7
17	CHK7	-8.3	0.02	-8.4	0.03	25.1	24.5	29.6
19	CHK7	-7.7	0.03	-7.7	0.03	21.8	21.1	26.2
20	CHK7	-7.9	0.01	-7.5	0.04	20.5	19.8	24.9
21	CHK7	-7.3	0.02	-6.9	0.03	18.1	17.3	22.4
22	CHK7	-6.7	0.01	-6.5	0.01	16.2	15.4	20.4
23	CHK7	-7.0	0.01	-6.6	0.04	16.5	15.6	20.7
24	CHK7	-6.2	0.01	-6.1	0.04	14.5	13.6	18.6
25	CHK7	-6.2	0.01	-6.1	0.06	14.3	13.5	18.5
26	CHK7	-6.1	0.01	-6.2	0.03	14.7	13.8	18.8
27	CHK7	-6.0	0.01	-6.3	0.02	15.0	14.2	19.2
28	CHK7	-6.1	0.02	-6.4	0.03	15.7	14.9	19.9
30	CHK7	-6.8	0.01	-6.8	0.03	17.6	16.9	21.9
31.5	CHK7	-6.4	0.01	-6.3	0.04	15.4	14.5	19.5
34	CHK7	-6.2	0.02	-6.2	0.03	14.8	13.9	18.9
36	CHK7	-5.9	0.02	-5.8	0.04	12.8	11.9	16.9
37	CHK7	-5.8	0.00	-5.6	0.02	12.3	11.4	16.3
38	CHK7	-5.7	0.01	-5.6	0.04	11.9	11.0	16.0
39	CHK7	-5.6	0.01	-5.4	0.02	11.0	10.0	15.0
40	CHK7	-5.9	0.01	-5.3	0.03	10.8	9.9	14.8

SN	Specimen	$\delta^{13}C$ ‰ VPDB	±	$\delta^{18}O$ ‰ VPDB	±	Patt °C	Kim °C	Thor °C
41	CHK7	-6.2	0.02	-5.4	0.02	11.3	10.4	15.3
42	CHK7	-6.9	0.01	-5.8	0.01	12.9	12.0	17.0
43	CHK7	-7.0	0.01	-6.0	0.01	13.7	12.8	17.8
44	CHK7	-7.3	0.01	-6.0	0.02	14.0	13.1	18.1
45	CHK7	-7.4	0.01	-6.5	0.02	15.9	15.0	20.0
47	CHK7	-7.6	0.01	-6.5	0.02	16.0	15.2	20.2
49	CHK7	-8.0	0.01	-6.7	0.02	17.2	16.4	21.4
50	CHK7	-8.4	0.01	-7.2	0.02	19.3	18.6	23.6
51	CHK7	-7.8	0.01	-7.0	0.02	18.2	17.5	22.5
52	CHK7	-8.4	0.01	-7.4	0.02	20.3	19.6	24.6
53	CHK7	-8.1	0.01	-7.3	0.02	19.8	19.1	24.2
54	CHK7	-7.8	0.02	-6.6	0.01	16.4	15.6	20.6
55	CHK7	-7.5	0.01	-7.0	0.01	18.2	17.5	22.5
56	CHK7	-7.2	0.00	-6.5	0.02	16.3	15.5	20.5
57	CHK7	-7.0	0.01	-6.6	0.02	16.3	15.5	20.5
58	CHK7	-6.6	0.01	-6.2	0.03	14.5	13.7	18.6
59	CHK7	-6.5	0.01	-6.3	0.02	15.2	14.4	19.4
60	CHK7	-6.2	0.00	-6.1	0.01	14.1	13.2	18.2
62	CHK7	-5.7	0.01	-5.9	0.01	13.3	12.4	17.4
63	CHK7	-5.7	0.01	-5.7	0.02	12.7	11.8	16.8
64	CHK7	-5.9	0.01	-6.0	0.02	13.9	13.1	18.0
65	CHK7	-5.7	0.02	-6.1	0.02	14.2	13.4	18.4
66	CHK7	-5.7	0.02	-5.9	0.02	13.2	12.3	17.3
67	CHK7	-5.2	0.00	-5.4	0.02	11.0	10.0	15.0
68	CHK7	-5.4	0.01	-5.4	0.02	11.3	10.3	15.3
69	CHK7	-6.6	0.01	-6.3	0.03	15.1	14.3	19.3
70	CHK7	-8.3	0.02	-6.8	0.05	17.6	16.8	21.8
71	CHK7	-7.6	0.03	-6.5	0.03	16.1	15.3	20.3
72	CHK7	-6.7	0.01	-6.2	0.02	14.7	13.9	18.9
73	CHK7	-7.4	0.02	-6.6	0.01	16.4	15.6	20.6
74	CHK7	-7.8	0.01	-6.8	0.01	17.3	16.5	21.5
75	CHK7	-8.7	0.01	-7.1	0.01	18.9	18.2	23.2
76	CHK7	-8.7	0.02	-7.0	0.01	18.2	17.5	22.5
77	CHK7	-9.0	0.01	-7.4	0.01	20.4	19.7	24.7
78	CHK7	-8.2	0.02	-6.8	0.01	17.3	16.5	21.5
79	CHK7	-9.2	0.01	-7.6	0.01	21.2	20.5	25.6
80	CHK7	-9.1	0.02	-7.5	0.02	20.9	20.2	25.2
1	CHK4	-6.6	0.02	-6.5	0.01	16.0	15.2	20.2
2	CHK4	-7.3	0.03	-6.9	0.02	18.0	17.2	22.2

SN	Specimen	$\delta^{13}C$ ‰ VPDB	±	$\delta^{18}O$ ‰ VPDB	±	Patt °C	Kim °C	Thor °C
3	CHK4	-7.2	0.01	-6.6	0.02	16.4	15.6	20.6
4	CHK4	-9.5	0.01	-7.8	0.01	21.9	21.2	26.2
5	CHK4	-9.8	0.01	-7.9	0.01	22.6	22.0	27.0
6	CHK4	-8.8	0.00	-7.1	0.01	19.0	18.2	23.2
7	CHK4	-7.1	0.02	-6.1	0.02	14.2	13.4	18.4
8	CHK4	-7.3	0.01	-6.1	0.01	14.4	13.5	18.5
9	CHK4	-8.2	0.01	-6.6	0.01	16.7	15.9	20.9
10	CHK4	-8.8	0.01	-7.2	0.02	19.4	18.7	23.7
11	CHK4	-8.8	0.01	-7.2	0.02	19.5	18.7	23.8
12	CHK4	-8.8	0.01	-7.5	0.02	20.8	20.1	25.1
13	CHK4	-8.2	0.02	-7.5	0.02	20.5	19.8	24.8
14	CHK4	-8.9	0.01	-7.6	0.02	21.0	20.3	25.4
15	CHK4	-8.8	0.02	-7.6	0.01	21.0	20.3	25.4
16	CHK4	-8.6	0.02	-7.5	0.02	20.7	20.0	25.1
17	CHK4	-8.6	0.02	-7.3	0.01	19.7	19.0	24.0
18	CHK4	-7.4	0.02	-6.8	0.01	17.5	16.8	21.8
19	CHK4	-7.4	0.02	-6.7	0.01	16.9	16.1	21.1
20	CHK4	-6.6	0.01	-6.1	0.01	14.3	13.5	18.5
21	CHK4	-6.7	0.01	-6.2	0.01	14.6	13.8	18.8
22	CHK4	-6.5	0.02	-6.1	0.02	14.2	13.4	18.4
23	CHK4	-6.4	0.01	-6.0	0.00	13.9	13.1	18.0
24	CHK4	-6.5	0.01	-6.2	0.01	14.9	14.0	19.0
25	CHK4	-6.2	0.01	-6.8	0.01	17.3	16.5	21.5
26	CHK4	-5.4	0.02	-6.5	0.01	16.1	15.3	20.3
27	CHK4	-5.7	0.02	-6.5	0.03	16.0	15.2	20.2
28	CHK4	-5.1	0.01	-5.6	0.02	12.1	11.1	16.1

Table A20—Fish collection and otolith information for specimens utilized in chapter 4.

Sample number	Sex	Fish	Date collected	Location	Total Length (mm)	Age
84		1	7/28/91	St. Catharines	1026	3+
93		8	8/6/91	Brighton	1024	3+
54		1	7/3/91	Port Credit	1020	5+
108		15	8/18/91	St. Catharines	1019	3+
12		1	5/12/91	St. Catharines	995	3+
92		1	8/4/91	Port Credit	947	3+
1	FM		10/31/97	Salmon R.	830	
4	FM		10/31/97	Salmon R.	855	

Sample number	Sex	Fish	Date collected	Location	Total Length (mm)	Age
7	FM		10/31/97	Salmon R.	805	
13	M		10/31/97	Salmon R.	555	
14	M		10/31/97	Salmon R.	595	
15	M		10/31/97	Salmon R.	880	
23	M		10/31/97	Salmon R.	980	
20	M		10/31/97	Salmon R.	905	

Table A21—$\delta^{18}O_{(H_2O)}$ value of Lake Ontario.

Methods used include water equilibrator (WE) and high-temperature pyrolysis (TCEA).

Sample	Date Collected	$\delta^{18}O$‰ VSMOW	Method
Lake Ontario	8/21/02	-6.9	WE
Lake Ontario	8/29/02	-6.9	TCEA
Lake Ontario	8/21/02	-6.9	TCEA
Lake Ontario	6/13/00	-6.8	TCEA
Lake Ontario - Montori Point	9/30/03	-7.9	TCEA
Salmon River Hatchery	5/19/98	-12.5	WE
Salmon River Hatchery	10/16/98	-9.2	WE
Salmon River Hatchery	10/17/02	-9.0	TCEA
Salmon River Hatchery	5/19/02	-11.7	WE
Sodus Bay	8/2/97	-7.0	WE
Sodus Bay	6/7/98	-7.8	WE
Sodus Bay	6/7/98	-7.8	WE
Sodus Bay	7/5/98	-7.4	WE
Sodus Bay	7/5/98	-7.5	WE
Sodus Bay	7/19/98	-7.1	WE
Sodus Bay	7/19/98	-7.5	WE
Sodus Bay	7/27/98	-7.0	WE
Sodus Bay	7/27/98	-7.0	WE
Sodus Bay	7/28/98	-7.4	WE
Sodus Bay	8/10/98	-6.9	WE
Sodus Bay	8/10/98	-6.9	WE
Sodus Bay	8/17/98	-7.1	WE
Sodus Bay	8/24/98	-7.1	WE
Sodus Bay	05/25/99	-8.9	WE
Sodus Bay	7/13/02	-8.3	TCEA
Sodus Bay	8/18/02	-7.1	TCEA

Table A22—Lake Ontario chinook salmon condition factor.

MONTH		Round Weight	Round Weight	Round Weight
	N	-95.00%	+95.00%	Mean
Apr	106	2.80	3.05	2.92
May	140	2.86	3.02	2.94
Jun	154	2.70	2.84	2.77
Jul	774	2.71	2.78	2.74
Aug	938	2.79	2.87	2.83
Sep	356	2.78	2.93	2.85

Table A23—Isotope values of various chemical extracts from guano core 96-04.
Subscripts GE, CE, and L indicate guano, chitin, and solvent chemical extracts, respectively. $\delta^{13}C$ values are reported relative to VPDB, $\delta^{15}N$ are reported relative to AIR, and δD values are reported relative to VSMOW. Average values and 1 standard deviation on at least two samples are normally shown. No standard deviation indicates only 1 or no analysis was performed. ^{14}C and calendar ages are determined from linear interpolations between dated samples. Calibration of ^{14}C Age to calendar age was done using Calib 5.0 (Stuiver and Reimer, 1998; Reimer et al., 2004). * indicates contemporary sample ^{14}C dated.

Sample Number	^{14}C Age YBP	Calendar Age YBP	$\delta^{13}C_{ge}$ ‰	±	$\delta^{13}C_{ce}$ ‰	±	$\delta^{15}N_{ge}$ ‰	±	$\delta^{15}N_{ce}$ ‰	±	$\delta^{13}C_{l}$ ‰	±	δD_{l} ‰	±	δD_{ce} ‰	±
1*	5650	6416	-25.5		-24.1	0.1	12.0				-24.9					
2	5773	6559	-25.5	0.6	-24.3	0.2	13.1	2.7								
3	5896	6703	-25.9	0.0	-24.2	0.6	14.9	0.6			-25.8	0.3				
4	6019	6847	-25.8	0.0	-24.2	0.2	14.5	0.2			-26.0		-145		-162	7
5	6141	6990	-25.1	0.1			14.6									
6	6264	7134			-23.5	0.1			18.0	0.0	-25.3		-139	6	-150	0
7	6387	7277	-25.8	0.2	-24.0	0.1	16.3	0.1			-25.8		-149	0		
8	6509	7421	-25.5	0.2	-24.5	0.2	16.7	0.1	15.5	0.1	-26.4		-143	1	-156	
9	6632	7565	-25.0	0.0	-24.1	0.0	15.5	0.1	15.3		-25.8		-141		-151	
10	6755	7708	-24.8	0.1	-24.0	0.2	16.4	0.2	16.2	0.2	-25.6		-146	3	-143	1
11	6878	7852	-25.4	0.1	-24.3	0.1	16.0	0.1	15.9	0.5	-26.2		-148	1	-147	3
12	7000	7995	-25.3	0.0	-24.0	0.0	16.0	0.1	16.0		-25.7				-148	
13	7123	8139	-23.1	0.1		0.2	16.0	0.0	16.2	0.4	-24.4	0.3	-150	1		4
14	7246	8283	-24.3	0.1	-23.6	0.1	16.7	0.1	15.9	0.7	-25.4	0.1	-153		-142	
15	7368	8426	-25.2	0.1	-24.1	0.2	17.3	0.0	17.5	0.0	-25.8	0.1	-158		-153	3
16	7491	8570	-25.5	0.5	-24.2	0.2	17.1	0.0	16.8	0.0	-26.5	0.1	-158	0	-159	0
17	7614	8713	-25.4	0.2	-24.1	0.2	17.0	0.1	17.4	0.0	-26.0	0.0	-157	1	-160	2
18	7737	8857	-26.1	0.1	-25.0	0.2	16.7	0.4	17.7	0.1	-26.5	0.1	-161	3	-167	3
19	7859	9001	-25.4	0.2	-24.0	0.2	17.8	0.2	18.2	0.1	-26.2	0.0	-154	1	-152	0
20	7982	9144	-26.5	0.2	-24.8	0.1	19.9	0.1	21.0	0.4	-26.6				-157	
21	8105	9288	-25.8	0.2	-24.0	0.3	17.3	1.4	18.3	0.3	-26.6	0.2	-131	2	-158	1
22	8227	9431	-26.2	0.1	-24.6	0.1	16.9	0.1	16.7	0.3	-26.9	0.1	-157	1	-162	0
23	8350	9575	-26.4	0.2	-24.5	0.3	21.3	0.8	21.3	0.1	-26.1	0.9	-158	1	-152	5

Sample Number	^{14}C Age YBP	Calendar Age YBP	$\delta^{13}C_{ge}$ ‰	±	$\delta^{13}C_{ce}$ ‰	±	$\delta^{15}N_{ge}$ ‰	±	$\delta^{15}N_{ce}$ ‰	±	$\delta^{13}C_l$ ‰	±	δD_l ‰	±	δD_{ce} ‰	±
24	8473	9719	-25.9	0.1	-24.8	0.1	17.7	0.1	17.6	0.1	-26.5	0.0	-158	1	-159	4
25	8596	9862	-25.6	0.2	-23.9	0.1	16.8	0.4	16.7	0.2	-26.8	0.1	-162	1	-156	3
26	8718	10006	-25.9	0.1	-24.3	0.1	16.6	0.0	16.9	0.2	-26.6	0.0	-158		-164	2
27	8841	10149	-26.2	0.1	-24.7	0.1	16.4	0.0	16.7	0.0	-26.7	0.0	-162	3	-160	1
28	8964	10293	-26.1	0.1	-24.3	0.1	16.5	0.1	16.3	0.1	-26.2	0.0	-151	3	-156	5
29	9087	10437	-26.8	0.2	-25.1	0.0	16.2	0.0	16.3	0.3	-27.3	0.0	-164	1	-165	1
30	9209	10580	-26.7	0.0	-24.7	0.1	16.1	0.0	16.4	0.1	-27.2	0.2	-159	4	-161	
31	9332	10724	-26.3	0.1	-24.5	0.1	16.6	0.6	17.4	0.1	-27.1	0.1	-151	1	-146	3
32	9455	10867	-26.1	0.1	-24.3		17.0	0.2	17.1		-26.7	0.0	-152	1	-163	
33	9577	11011	-26.2	0.1	-24.0	0.0	17.1	0.1	17.3	0.0	-27.3	0.0	-164	1	-150	2
34	9700	11155	-26.3	0.0	-24.3	0.1	16.8	0.1	17.3	0.1	-26.7	0.0	-158	3	-162	4
35	9823	11298	-26.5	0.1	-24.6	0.0	16.4	0.2	16.3	0.2	-26.7	0.1	-159	1	-167	3
36	9946	11442	-26.1	0.0	-24.2	0.1	16.4	0.1	16.5	0.3	-27.2	0.0	-162	3	-160	4
37	10068	11585	-26.9	0.5	-24.6	0.0	15.6	0.0	15.4	0.1	-27.3	0.2	-154	1	-162	1
38*	10133	11675	-26.3	0.0	-23.7	0.5	17.6	0.1			-26.6	0.1	-159	0	-139	1
39	10140	11699	-25.6	0.6	-23.8	0.0	17.6	0.5	17.8	0.1	-26.3	0.0	-157	2	-154	2
40	10147	11723	-25.0	0.2	-23.5	0.2	17.0	0.1			-25.6	0.0	-156	6	-141	1
41	10154	11747	-25.6	0.2	-24.6	0.2	17.1	0.2	17.7	0.3	-26.8	0.0	-157	2	-156	4
42	10161	11771	-25.6	0.0	-24.5	0.0	18.4	0.2	16.6	0.4	-26.5	0.2	-154	1	-153	3
43	10168	11795	-25.6	0.1	-24.4	0.0	16.7	0.2	19.1	0.1	-26.8	0.0	-141	2	-159	4
44	10175	11819	-25.8	0.5	-24.3	0.0	17.3	0.1	17.8	0.2	-26.4	0.2	-152	3	-166	3
45	10182	11842	-26.8	0.3	-25.0	0.3	15.9	0.3	15.5	0.7	-27.7	0.0	-165	0	-163	2
46	10189	11866	-26.7	0.2	-24.3	0.1	19.1	0.1	22.6	1.1	-27.7	0.1	-160	2	-160	2
47	10196	11890	-27.1	0.2	-25.2	0.1	15.0	0.2	14.9	0.2	-27.8	0.1	-168	2	-167	1
48	10204	11914	-27.2	0.1	-25.2	0.1	17.5	0.3	18.7	0.5	-27.8	0.1	-166	2	-172	3
49	10211	11938	-27.7	0.0	-26.1	0.0	18.5	0.0	21.9	0.2	-28.4	0.2	-164	2	-187	1
50	10218	11962	-27.8	0.1	-25.5	0.1	18.1	1.0	23.2	1.0	-28.5	0.0	-164	2	-161	2
51	10225	11986	-28.0	0.2	-26.3	0.1	17.5	0.2	20.7	1.1	-28.9	0.0	-169	0	-188	0
52*	10232	12009	-28.1	0.2	-26.3	0.1	17.7	0.5	22.1	0.4	-28.3	0.2	-166	0	-179	2
53	10451	12221	-27.9	0.1	-26.1	0.0	18.0	0.3	22.9	0.5	-28.2	0.0	-170	1	-176	2
54	10629	12395	-27.9	0.1	-26.5	0.1	20.1	1.5	23.8	0.7	-28.3	0.0	-170	1	-181	2
55	10806	12569	-28.0	0.1	-26.2	0.1	19.2	0.5	25.4	1.6	-28.3	0.2	-168	0	-177	1
56	10983	12743	-28.1	0.2			19.6	0.3								

Sample Number	^{14}C Age YBP	Calendar Age YBP	$\delta^{13}C_{ge}$ ‰	±	$\delta^{13}C_{ce}$ ‰	±	$\delta^{15}N_{ge}$ ‰	±	$\delta^{15}N_{ce}$ ‰	±	$\delta^{13}C_l$ ‰	±	δD_l ‰	±	δD_{ce} ‰	±
57	11160	12917	-27.7	0.4	-26.4	0.2	17.9	0.8	24.1	0.9	-28.4	0.0	-172	2	-182	0
58	11337	13091	-27.9	0.0	-26.0	0.1	18.2	1.4	21.7	1.4	-27.9	0.2	-172	2	-188	1
59	11514	13265	-27.9	0.0	-26.1	0.0	17.1	1.1	20.6	2.1	-27.9	0.0	-169	1	-178	4
60	11692	13438	-27.7	0.0	-26.1	0.1	17.2	0.3	20.8	1.6	-28.3	0.1	-171	0	-185	2
61	11869	13612	-27.8	0.0	-25.6	0.2	14.7	0.5	14.9	1.0	-28.6	0.6	-172	1	-181	2
62	12046	13786	-27.9	0.0	-25.7	0.0	13.8	0.6	14.0	0.2	-27.7	0.1	-169	3	-182	1
63*	12223	13960	-27.5	0.1	-25.4	0.0	16.9	0.2	18.3	0.5	-27.8	0.1	-165	0	-183	

Table A24—Average C, N, and H weight percent and elemental ratios of various chemical extracts from guano core 96-04.

Subscripts GE, CE, indicate guano, and chitin chemical extracts, respectively.

Sample Number	$\%C_{ce}$	$\%N_{ce}$	$\%H_{ce}$	$C:H_{ce}$	$N:H_{ce}$	$C:N_{ce}$	$C:N_{ge}$
1							12.5
2							13.4
3							13.4
4			2.1				12.5
5							13.2
6	19.5	4.0	1.6	12.3	2.5	4.9	
7			0.0				10.7
8	11.1	1.5	1.6	6.9	0.9	7.6	9.8
9	14.0	1.9	2.5	5.5	0.7	7.4	10.2
10	17.3	2.6	1.9	9.1	1.4	6.7	8.5
11	9.6	1.4	1.8	5.5	0.8	7.0	10.3
12	13.0	1.8	1.4	9.1	1.3	7.2	10.2
13	5.0	1.2	0.7	7.0	1.7	4.1	5
14	11.5	2.0	1.5	7.7	1.3	5.7	7
15	15.0	2.5	1.5	9.8	1.7	5.9	7.7
16	10.7	1.6	1.8	5.8	0.9	6.6	10.5
17	9.8	1.6	1.5	6.4	1.0	6.2	9.3
18	14.6	1.9	1.9	7.8	1.0	7.5	10.6
19	11.5	2.1	1.4	8.1	1.5	5.5	8.2
20	5.6	0.9	1.2	4.6	0.7	6.3	11.7
21	11.5	2.0	1.6	7.1	1.2	5.8	9.5
22	8.5	1.2	1.4	5.9	0.8	7.4	12.6
23	3.8	0.6	1.0	3.9	0.6	6.3	11.7
24	11.5	1.6	2.0	5.7	0.8	7.0	9.2
25	11.1	1.9	1.6	6.8	1.2	5.9	9.8

Sample Number	$\%C_{ce}$	$\%N_{ce}$	$\%H_{ce}$	$C:H_{ce}$	$N:H_{ce}$	$C:N_{ce}$	$C:N_{ge}$
26	15.0	2.2	2.3	6.6	1.0	6.7	10.7
27	15.9	2.1	1.8	9.0	1.2	7.5	11.4
28	12.5	1.9	1.2	10.0	1.5	6.7	11.1
29	14.2	1.7	1.5	9.6	1.2	8.2	13.3
30	15.0	2.0	0.9			7.4	13.2
31	11.0	1.6	1.2	9.3	1.4	6.7	12.2
32	22.1	3.3	1.4			6.7	11.3
33	12.4	2.1	1.4	8.6	1.5	5.8	10
34	15.7	2.6	1.4	11.1	1.9	6.0	10.4
35	12.5	1.7	1.4	8.7	1.2	7.5	11.2
36	20.0	2.9	1.3	14.9	2.2	6.8	10.7
37	10.2	1.4	0.8	12.1	1.7	7.2	12.8
38	2.3	0.6	0.6	4.0	1.1	3.8	9.4
39	11.7	2.2	1.4	8.1	1.5	5.3	7
40	9.0	2.0	0.9	9.5	2.1	4.6	6.8
41	9.6	1.6	1.6	6.1	1.0	6.1	8.5
42	8.2	1.3	1.4	5.7	0.9	6.3	8
43	7.0	1.3	0.8	8.6	1.6	5.3	8.9
44	8.7	1.4	1.2	7.1	1.2	6.1	8.8
45	5.4	0.9	0.7	7.5	1.2	6.2	11.8
46	2.5	0.7	0.7	3.6	1.0	3.4	9.4
47	10.8	1.4	0.6	17.7	2.3	7.7	13.4
48	4.8	0.8	0.9	5.6	1.0	5.7	13.1
49	5.7	0.9	1.3	4.5	0.7	6.4	18.5
50	3.8	0.9	1.1	3.3	0.7	4.5	17.6
51	6.1	0.8	1.5	4.1	0.5	7.5	22.2
52	6.0	0.8	1.1	5.5	0.8	7.1	20.1
53	5.1	0.8	1.2	4.3	0.7	6.2	20.5
54	6.8	1.0	1.6	4.4	0.7	6.6	15.8
55	4.3	1.0	1.2	3.7	0.9	4.3	17.2
56							18.7
57	5.2	1.0	1.2	4.3	0.8	5.3	19.6
58	6.4	1.1	1.3	4.8	0.8	6.0	19.4
59	5.5	1.0	1.4	3.8	0.7	5.7	20.2
60	6.6	1.0	1.5	4.4	0.7	6.4	20.6
61	5.6	0.8	0.9	5.9	0.9	6.9	18.8
62	8.1	1.1	1.2	6.8	0.9	7.4	18.7
63	8.3	1.4	1.1	7.2	1.2	6.1	14.2

Appendix B. Fish bioenergetics models

B-1 Introduction

Fish Bioenergetics 3.0 is a computer application for the Windows 95 operating system that enables a user to input parameters into previously developed and published fish bioenergetic models for output of a host of energetic parameters. This appendix relies heavily on Hanson et al. (1997), the instructional manual incorporated with *Fish Bioenergetics 3.0*. The discussion, however is limited to a general description of bioenergetic models, with reference to the particular fish energetic models used herein.

The computer application *Fish Bioenergetics 3.0* was used to implement energetic models of yellow perch (*Perca flavescens*), weakfish (*Cynoscion regalis*), steelhead trout (*Oncorhynchus mykiss*), and chinook salmon (*Oncorhynchus tshawytscha*). A bioenergetic model is simply an energy mass balance equation in which energy consumed by a fish is balanced by total metabolism, waste losses, and growth. *Fish Bioenergetics 3.0* incorporates species-specific physiological estimates of components of an energetic mass balance equation. The basis of an energy model begins with the tenant:

Energy In = Energy Out + Growth, or Consumption = Metabolism + Wastes + Growth.

Each of these components can be described by a species-specific set of physiological equations, some more simple and others more complex. This appendix begins by describing individual equations describing the energy budget of fishes. Table 1 lists the species-specific physiological parameters used in the bioenergetic models employed by this study with the appropriate references. This appendix concludes with a description of site-specific variables incorporated into the models; tabulated data of these variables input into *Fish Bioenergetics 3.0*, and output used in separate chapters are incorporated in appendix A.

B-2 Consumption

Consumption is estimated as the proportion of maximum daily ration for a fish at a particular mass and temperature.

$$C = C_{max} \bullet p \bullet f(T)$$

$$C_{max} = CA \bullet W^{CB}$$

Therefore, maximum consumption (C_{max}) is an allometric function of body mass (W) empirically derived for a given species at optimal temperature. This maximum consumption rate is then adjusted according to a water temperature (T) dependence function and an additional proportionality constant (*p*-value). This *p*-value represents ecological constraints on the maximum feeding rate. Two separate temperature function equations are employed in bioenergetic models for fishes used in this study.

Consumption equation 1 (temperature dependence for warm water species from Kitchell et al., 1977):

$$f(T) = Vx \bullet e^{(X \bullet (1-V))}$$

where:

$$V = (CTM - T) / (CTM - CTO)$$
$$X = Z^2 \bullet (1+(1+40/Y)^{0.5})^2/400$$
$$Z = \ln(CQ) \bullet (CTM-CTO)$$
$$Y = \ln(CQ) \bullet (CTM-CTO+2)$$

where CTM is maximum water temp above which consumption ceases, CTO is final laboratory temperature preferendum, CA is the intercept of the mass dependence function for a 1 gram fish at CTO, CB is the coefficient of the mass dependence, CQ approximates a Q_{10} (the rate at which the function increases over relatively low water temperature.

Consumption equation 2 (temperature dependence for cool and cold water species from Thornton and Lessem, 1978):

The Thornton and Lessem temperature function equation is essentially the product of two sigmoid curves, the first describes an increasing temperature function (K_A) and the second describes a decreasing function (K_B).

$$f(T) = K_A \bullet K_B$$

where:

$$K_A = (CK1 \bullet e^{(G1 \bullet (T-CQ))}) / (1 + CK1 \bullet (e^{(G1 \bullet (T-CQ))} - 1))$$
$$G1 = (1/(CTO-CQ)) \bullet \ln((0.98 \bullet (1-CK4))/(CK4 \bullet 0.02))$$

$$K_B = (CK4 \bullet e^{(G2 \bullet (CTL-T))}) / (1 + CK4 \bullet (e^{(G2 \bullet (CTL-T))} - 1))$$
$$G2 = (1/(CTL-CTM)) \bullet \ln((0.98 \bullet (1-CK4))/(CK4 \bullet 0.02))$$

where CQ is the lower water temperature at which the temperature dependence is a small fraction (CK1) of the maximum rate, and CTO is the water temperature corresponding to 0.98 of the maximum consumption rate. CTM is the water temperature at which dependence is still 0.98 of the maximum, and CTL is the temperature at which dependence is some reduced fraction (CK4) of the maximum rate.

B-3 Respiration

Respiration is the amount of energy used by the fish for routine metabolism. Respiration is dependent on fish size, water temperature and fish activity. Total metabolism includes respiration, activity, and energy cost associated with the process of digestion (Specific Dynamic Action). Specific dynamic action (SDA) is estimated as a constant proportion of assimilated energy (consumption – egestion), and usually ranges between 0.15 and 0.2.

$R = RA \bullet W^{RB} \bullet f(T) \bullet Activity$

$S = SDA \bullet (C - F)$

Equation 1: Exponential with swimming speed (Stewart et al. 1983)

This equation uses a simple exponential relationship to describe the temperature dependence of metabolism and activity is a function of swimming speed.

$f(T) = e^{(RQ \bullet T)}$

$Activity = e^{(RTO \bullet VEL)}$

Where $VEL = RK1 \bullet W^{RK4}$, when $T > RTL$, or

$VEL = ACT \bullet W^{RK4} \bullet e^{(BACT \bullet T)}$, when $T \leq RTL$

where RA is the specific weight of oxygen consumed by a 1 gram fish at 0°C and zero swimming speed, RB is the slope of the allometric mass function for standard metabolism, and RQ approximates the Q_{10} (the rate at which the function increases over relatively low water temperatures). RTO is the coefficient of swimming speed dependence on metabolism, RTL is the cutoff temperature at which the activity relationship changes, RK1 is the intercept for swimming speed at all water temperatures, ACT is the intercept of the relationship for swimming speed versus mass at water temperatures less than RTL, and BACT is the water temperature dependence coefficient of swimming speed at water temperatures below RTL.

Equation 2 Temperature dependent with activity multiplier (Kitchell et al. 1977).

For this equation, the temperature dependence of respiration is simply adjusted by an activity multiplier (ACT)

$f(T) = V^{X} \bullet e^{(X \bullet (1-X))}$

$Activity = ACT$

where:

$V = (RTM - T)/(RTM - RTO)$

$X = (Z^2 \bullet (1 + (1 + 40 / Y)^{0.5})^2 / 400$

$Z = \ln(RQ) \bullet (RTM - RTO)$

$Y = \ln(RQ) \bullet (RTM - RTO + 2)$

where RTO is the optimum temperature for respiration, RTM is the maximum (lethal) water temperature, and RQ approximates the Q_{10}. RA is the number of grams of oxygen consumed by a 1 gram fish at RTO, and RB is the slope of the allometric mass function for standard metabolism, used to estimate maximum respiration. Activity is simply a constant multiplied by the resting metabolism.

B-4 Waste Losses

Egestion (Fecal Waste, F), and excretion (metabolic waste, U) can be estimated as a simple proportion of consumption or as functions of water temperature and consumption.

Equation Set 1: As a proportion of consumption (Kitchell et al., 1977)

Egestion: $F = FA \bullet C$

Excretion: $U = UA \bullet (C - F)$

where FA and UA are a constant to estimate the proportion of consumed energy or assimilated energy (C – F).

Equation Set 2: Dependent on mass, temperature, and ration (Elliot, 1976)

Egestion $F = FA \bullet T^{FB} \bullet e^{(FG \bullet p)} \bullet C$

Excretion $U = UA \bullet T^{UB} \bullet e^{(UG \bullet p)} \bullet (C - F)$

This equation is most appropriate if the consumption is almost all invertebrate or all fish. FA (UA) is the intercept of the proportion of consumed energy egested (excreted)

versus water temperature and ration and FB (UB) is the coefficient of water temperature dependence of egestion (excretion). FG (UG) is the coefficient for feeding level dependence (*p*-value) of egestion (excretion).

B-5 Predator Energy Density

Predator Energy density can be directly input into Fish Bioenergetic 3.0 as a site-specific variable or as a function of body mass

$$ED = \alpha + \beta W$$

where ED is the predator energy density, α is the intercept of the allometric mass function, and β is the slope of the allometric mass function. *Fish bioenergetic 3.0* will switch from “equation 1” to “equation 2” at a specified “mass cutoff”.

Table B1—Fish physiological parameters (after Hanson et al., 1997).

Species	Yellow perch	Weakfish	Weakfish	Steelhead	Chinook salmon
	Perca flavescens	*Cynoscion regalis*		*Oncorhynchus mykiss*	*Oncorhynchus tshawytscha*
Age	juvenile, adult	Age-0	Age-1 +	Adult	Adult
Source	Kitchell et al., 1977.	Hartman and Brandt, 1995	Hartman and Brandt, 1995	Rand et al. 1993	Stewart and Ibarra (1991)
Consumption					
Equation	1	2	2	2	2
CA	0.25	0.492	0.492	0.628	0.303
CB	-0.27	-0.2680	-0.2680	-0.3	-0.275
CQ	2.3	14.87	14.8	5	5
CTO	22	24.3	25	20	15
CTM	28	24.3	25	20	18
CTL	*	27.7	29	24	24
CK1	*	0.0334	0.195	0.33	0.36
CK4	*	0.561	0.970	0.2	0.01
Respiration					
equation	2	1	1	1	1
RA	0.0108	0.0009	0.003	0.00264	0.00264
RB	-0.2	-0.1254	-0.155	-0.217	-0.217
RQ	2.1	0.0912	0.0508	0.06818	0.06818
RTO	27	1.2326	0.9022	0.0234	0.0234
RTM	32	0	0	0	0
RTL	*	0	0	25	25
RK1	*	1	1	1	1
RK4	*	0	0	0.13	0.13
ACT	1	1	1	9.7	9.7
BACT	*	0	0	0.0405	0.0405
SDA	0.172	0.172	0.172	0.172	0.172
Egestion/Excretion					
Equation	2	1	1	3	3
FA	0.158	0.104	0.104	0.212	0.212
FB	-0.222	*	*	-0.222	-0.222
FG	0.631	*	*	0.631	0.631
UA	0.0253	0.068	0.068	0.0314	0.0314
UB	0.58	*	*	0.58	0.58
UG	-0.299	*	*	-0.299	-0.299
Predator Energy Density					
Equation	1	1	1	2	2
Energy Density	4186	3558	5860	*	*
1	*	*	*	5764	5764
1	*	*	*	0.9862	0.9862
Cutoff	*	*	*	4000	4000
2	*	*	*	7602	5674
2	*	*	*	0.5266	0.9862

B-6 Site-specific variables

Therefore the energetic equations rely on species-specific variables (empirically derived in laboratory studies), and site-specific variables. Two options are open to the user: 1) to estimate Consumption by inputting growth or 2) to estimate growth by inputting consumption. The first option is less prone to error as growth can be directly measured in the field. In this case, fish mass is a variable and a *p*-value is estimated by an iterative best-fit to estimate prey consumption. The other key site-specific variable directly input into the models are 1) temperature, 2) diet proportion, 3) energy values of prey, 4) and energy value of the predator, (if not estimated by an empirical equation). Tabulated data used as input for bioenergetic models, and output of bioenergetic simulations is incorporated in appendix A.

Appendix C. Detailed description of methods for processing, analysis, and diagenetic evaluation of ancient bat guano

C-1 Introduction

In the past few decades, many studies have demonstrated the utility of several different naturally occurring stable isotopes of organic matter to investigate ecological, paleoclimatic, and archaeological questions (Rundel et al., 1989; Schimmelmann et al., 1993; Wassenaar and Hobson, 2000). Recent advances in continuous-flow isotope ratio mass spectrometry (CF-IRMS) enable rapid throughput of minute samples with high precision thus extending research potentials. Such technological advances coupled with equilibration techniques (Wassenaar and Hobson, 2000, 2003), pave the way for studies using both $\delta^{13}C$ and δD values to investigate past environmental changes at high-resolution. However, research using ancient organic matter must be concerned with diagenesis and resulting isotopic changes (e.g., Schimmelmann and DeNiro, 1986a,b). Therefore, for any investigation using stable isotopes values, it is necessary to isolate organic matter originally deposited or to find a suitable biomarker using appropriate analytical techniques (e.g., Schimmelmann and DeNiro, 1986a).

An overlooked, but potentially valuable paleoenvironmental record, is archived in stable isotope ratios of bat guano, for which extended Holocene cave deposits are known to exist (Mizutani et al., 1992a,b; McFarlane et al., 2002). Today, several studies have shown animal feces $\delta^{13}C$ and $\delta^{15}N$ values to be a faithful tracer of dietary sources (e.g., Webb et al., 1998; Sponheimer et al., 2003). Perhaps more importantly, guano from insectivorous bats is composed mostly of insect exoskeletons containing chitin, and chitin is known to be a resistant biopolymer found as long ago as 25 million years (Stankiewicz et al., 1997). $\delta^{13}C$ and δD values of chitin are reasonably well-studied and found to record dietary and local water sources (e.g., Schimmelmann and DeNiro, 1986a,b; Miller et al., 1988; Webb et al., 1998; Motz, 2000).

This appendix details the chemical extraction of guano utilized in chapter 5 for $\delta^{13}C$ and δD values of a chitin extract. The primary goal of this appendix is to determine the nature and extent of diagenesis, and to evaluate the best out of several chemical extraction techniques examined.

C-2 Materials and Methods

C-2.1 Core and sample collection

Dr. Donald A. McFarlane directed the recovery of two consecutive bat guano cores from Bat Cave, a *Tadarida brasiliensis* (Mexican free-tailed bat) maternity roost located ~700 m above the Colorado River in Grand Canyon National Park, U.S.A. in 1996 (see Figure 5.1). Cores were sampled in a continuous fashion with Core 96-05 sampled just below 96-04 using methods described by Mizutani et al. (1992b). Each core was opened, wetted with deionized H_2O (DI-H_2O), and scraped until distinct stratigraphy was obvious (Figure C1). Two series of samples were collected and are termed Pass 1 and Pass 2. Pass 1 included collection of samples from both core 96-04 and 96-05, but only core 96-04 was resampled in Pass 2. Between each pass the core was scraped again to reveal distinct stratigraphy. To prevent mixing during sample collection, cores were wetted with DI-H_2O and razor blades placed between measured distances. Samples were not spot-collected, rather material was fully collected between each razor blade placed consecutively, and homogenized to prevent aliasing of data. Samples were collected at 8 mm intervals for Pass 1. For Pass 2, samples were taken at 4 mm intervals from 0-260 mm, and then continued at 8 mm increments. Some representative samples were chosen for visual examination of contents using binocular and petrographic microscopes, and others were chosen for application of X-ray diffraction.

C-2.2 Chemical extraction

Several chemical techniques were used to isolate various organic matter extracts from collected core material.

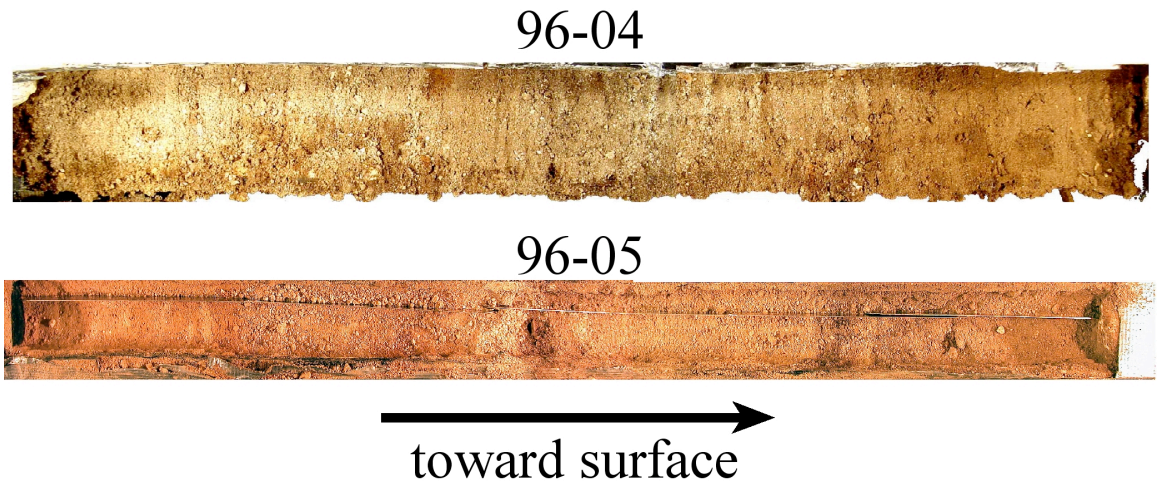

Figure C1—Opened guano core images

1. Initially, chemistry was performed following the methods described by Mizutani et al. (1992a) for analysis of bat guano $\delta^{13}C$ values. This consisted simply of first decarbonating samples for at least three hours in 2N HCl, subsequently followed by rinsing to neutrality with DI-H_2O, and finally lypholization of neutral sample. Between each step in this technique, and the other chemical extraction steps described below, samples were sonicated several times in ~15-minute cycles. Samples analyzed using this chemical technique are termed "guano extract without density separation".

2. Another chemical technique was applied to attempt to separate the organic portion from the mineral fraction using density separation. This technique consisted of first adding enough $ZnCl_2$ to 2N HCl to reach a specific gravity of 2.0. Samples were then decarbonated in this acid mix, paying close attention that the organic portion at the surface remained saturated. After at least three hours, the sample was centrifuged for three minutes and the floatant poured onto a 12-µm metal sieve. Excessive centrifugation resulted in a substantial loss of organic material recovered. The organic portion was then rinsed to neutrality with DI-H_2O, moved to a test tube and lypholized. Material recovered using this technique is termed the "guano extract".

3. Natural chitin was isolated using methods suggested by A. Schimmelmann and L. Wassenaar (personal communication). Samples are begun as in the guano extract but continued by treatment in 1N NaOH at 100 °C for 30 minutes followed by neutralization in DI-H_2O. Finally, solvent extraction was performed using 1x wash in methanol followed by 3x wash in chloroform/methanol 2:1 (v/v). Best results were found if the first chloroform/methanol wash was left overnight. After completion of solvent extraction, samples were lypholized. It was later determined that the NaOH step resulted in almost a total loss of organic material. Therefore, this chemical extraction was performed on later steps without use of NaOH step. Samples using this chemical technique are termed the "chitin extract".

4. Finally, each sample's solvent wash was placed in a fume hood and permitted to fully evaporate. The left over extract was collected and termed the "solvent extract".

C-2.3 Analysis of $\delta^{13}C$ and δD values, and C:N and N:H elemental ratios

$\delta^{13}C$, $\delta^{15}N$, and weight percent organic carbon (C%) and nitrogen (N%) were determined via continuous flow-isotope ratio mass spectrometry (CF-IRMS) using a ThermoFinnigan Flash 1112 Elemental Analyzer coupled by a ConFlo III to a ThermoFinnigan Delta XL Plus mass spectrometer. Samples were massed in tin foil capsules and loaded in a Flash MAS200 autosampler. Samples were dropped in a combustion chamber and first oxidized at 1000 °C and subsequently reduced at 680 °C to produce CO_2 and N_2 gases, which were then separated in a 5 Å Gas Chromatograph (GC) column kept at 50 °C. The column flow rate was set to 120 ml He/min. All $\delta^{13}C$ and $\delta^{15}N$ values are reported relative to VPDB and AIR standard scales, respectively, standardized using three internal laboratory standards. C% and N% were determined by comparison of gas pulse peak area and mass to that of a known standard. Repeated analyses of internal laboratory standards, yielded an external reproducibility of better than ±0.2‰ and 0.3‰ for $\delta^{13}C$ and $\delta^{15}N$ values, respectively.

δD values and weight percent H (H%) were determined via high-temperature flash pyrolysis CF-IRMS using a ThermoFinnigan High-Temperature Conversion Elemental Analyzer (TC/EA) coupled through a ThermoFinnigan ConFlo III to a ThermoFinnigan Delta XL Plus mass spectrometer. Samples were wrapped in silver foil and admitted into a combustion chamber using a Costech zero blank autosampler where atmosphere is initially purged and replaced with He. In the combustion chamber, samples were reduced at 1270 °C to H_2 gas (and N_2 and CO) and passed through and separated by a 5 Å GC column held at 90 °C. The column flow rate was set to 110-120 ml He/min. All δD values are reported relative to VSMOW-SLAP standard scale. Repeated analyses of international material IAEA CH-7, NBS-22, and three internal laboratory standards, yielded an external reproducibility of better than ±3‰.

$\delta^{13}C$ values were determined on samples from each chemical extract. For samples from Pass 1, the guano extract without density separation, $\delta^{13}C$ analyses were performed on 10-15 mg of sample without He dilution, and it was not possible to recover neither $\delta^{15}N$ values nor N% due to very low percent organics. On guano and chitin extracts from Pass 2 samples, both $\delta^{13}C$ and $\delta^{15}N$ analyses were performed, however sample size was minimized for Nitrogen. He flow was kept at 1.0 bar to obtain 700 mV of Nitrogen

decreasing reproducibility of $\delta^{15}N$ value and N%. $\delta^{13}C$ and $\delta^{15}N$ values are corrected relative to VPDB and AIR scales, respectively, using three internal laboratory standards. All samples were analyzed at least twice on separate runs, except where not enough material was collected. Sample size was adjusted to perform analyses with similar gas amounts.

δD values were analyzed only on samples taken from Pass 2 chitin and solvent extracts, which are the most chemically homogenous extracts in this study. However, to perform δD analyses on chitin extracts, correction for labile hydrogen exchange with atmospheric H_2O vapor was required because some hydrogen in complex organic matter—that bonded to N or O is potentially available to exchange with the atmosphere (e.g., Schimmelmann, 1991). To correct for this exchangeable hydrogen, two natural chitin standards were analyzed for δD_n value (non-exchangeable δD value), permitted to air-equilibrate with chitin extract samples, run together using high-temperature pyrolysis CF-IRMS, and the standard δD_n value was used to correct for δD_n values of samples (after Wassenaar and Hobson, 2000, 2003).

Specifically, grasshoppers were collected from Saskatoon in September and October of 2002 for one standard, and bat guano was purchased from a fertilizer company (most likely guano collected from a *Tadarida brasiliensis* roost in Texas or Northwestern Mexico) for the second standard. Visual examination of bat guano fertilizer confirmed that the guano was composed mostly of insect exoskeletons. Natural chitin from each standard was isolated using the chitin extract method described above with the NaOH step included. Unfortunately, time and equipment constraints did not permit proper determination of the percent of labile hydrogen of standards by appropriate steam equilibration techniques (Wassenaar and Hobson, 2000). However, many types of complex organic matter have similar percent labile hydrogen (Wassenaar and Hobson, 2000). In particular, chitin and keratin share very similar percent labile hydrogen at 130°C; 15.3±2.9% and 15±3%, respectively (Schimmelmann et al., 1993; Wassenaar and Hobson, 2003). Therefore, preliminary chitin standard δD_n values were constrained by air-equilibration with known keratin standards, determined to be –128±0.9‰ and –56.5±2.3‰ (assuming 80‰ α between atmospheric water vapor and organic matter

Table C1—Water equilibration results for chitin standards.

Standard	δD_n value relative to keratin standards	δD_n value 25°C equilibration
Guano Standard	-56.5±2‰ VSMOW	-59±2‰ VSMOW
Grasshopper Standard	-128±1‰ VSMOW	-123±4‰ VSMOW

Table C2—Water equilibration calculations for chitin standards at 25°C.

GH and Guano represent Saskatchewan Grasshopper and fertilizer guano chitin standards, respectively. Subscripts t, w, n, a, and b, refer to total, water, non-exchangeable, and reference a and b, respectively. All δD values reported relative to VSMOW in ‰ units. Calculations are performed using equations (3) and (4) in Hobson and Wassenaar (2000) assuming α = 1.251.

GH δD_{ta} (‰)	GH δD_{tb}	Equilibration water δD_{wa} (‰)	Equilibration water δD_{wb} (‰)		δD_n (‰)	δD_n (‰)		f_e
34	-106	1168	7		-119	-120		0.10
-133	-106	-171	7		-123	-123		0.12
34	-133	1168	-171		-129	-124		0.10
				Avg.	-124	-122	**-123±4**	0.11±0.01
Guano δD_{ta} (‰)	Guano δD_{tb} (‰)	Equilibration water δD_{wa} (‰)	Equilibration water δD_{wa} (‰)		δD_n	δD_n		f_e
70	-54	1168	7		-60	-60		0.09
-69	-54	-171	7		-59	-59		0.07
70	-69	1168	-171		-60	-56		0.09
				Avg.	-59	-58	**-59±2**	0.08±0.01

labile hydrogen) for "Grasshopper" and "Guano" standards, respectively (Table C1). As an additional test, these standards were equilibrated with liquid water with known δD value for three weeks at 25°C. After full equilibration was deemed complete, samples were immediately frozen using liquid nitrogen upon removal from the water bath. Frozen samples were then placed under vacuum and lypholized. After freeze-drying was complete, samples were kept frozen, removed from vacuum and quickly transferred to a zero-blank autosampler where He was introduced to immediately replace atmospheric water vapor and subsequently analyzed for δD values using the high-temperature pyrolysis method described above. Via this procedure, δD_n values of –123±4‰ and –59±2‰, and percent labile hydrogen values of 11±1% and 8±1% were determined for the grasshopper and guano standards, respectively (Table C2). δD values were calculated using a provisional α value of 224‰ estimated assuming a linear interpolation between assumed chitin α values of 80‰ at 130°C (after Schimmelmann et al., 1993; Wassenaar and Hobson, 2001), and 256‰ at 0°C (Motz, 2000). Although this test may allow a chance for atmospheric water vapor to exchange with equilibrated labile hydrogen, the consistency in determined standard values of this experiment with those determined with equilibration of keratin experiments argues against significant exchange occurring and confirms the use of these standard values. Additionally, the percent labile hydrogen agrees with Motz's (2000) finding of 11% at 0°C. δD_n values of samples were determined using δD_n values of standards determined by air-equilibration with keratin standards. Ten repeat measurements on selected samples analyzed a year apart confirmed that the air-equilibration technique enabled precise measurements. All repeat measurements corrected using guano and grasshopper chitin standards were within reported analytical precision.

C-2.4 Radiocarbon dating

Two samples were taken at the time the core was collected, at the surface and at 1.3 meters down (corresponding to the surface and end of core 96-04), and sent for AMS radiocarbon dating at Beta Analytic. At a later time, after initial examination of $\delta^{13}C$ values analyzed from Pass 1, six additional samples were taken from determined key depths from both cores 96-04 and 96-05 and sent to Gliwice radiocarbon laboratory for

AMS radiocarbon dates (Goslar et al., 2004) on total organic carbon (TOC). Radiocarbon dates are normalized according to $\delta^{13}C$ values.

C-3 Results

C-3.1 Visual examination of core material

The contents of both guano cores were very dry, and color varied from a deep dark brown to almost white (Figure C1). Visual examination of the organic fraction included what is interpreted as insect parts covered in brown clay, fossil guano pellets, bat hair, beetle cuticles, and in a few places very minute quantities of fungi. Bat hair, when scales were present, were identified from the genus *Tadarida* (Nason, 1948), however this is from a limited sample as hair was rarely found, and most shafts lacked scales (Figure C2). Samples were weight dominated by the mineral fraction, consisting mostly of quartz sand, aragonite, and calcite determined by optical light microscopy and X-ray diffraction (I. González-Alvarez and J. J. Scott, personal communication). In many cases silica was imbedded within, and clay particles were encrusted onto insect cuticles eliminating the potential for complete separation of the mineral and organic components.

C-3.2 Isotope profiles

The most salient feature for both $\delta^{13}C$ and δD values from all chemical extracts is a stepwise increase in values from 148 mm to 260 mm, which will be termed the transition (Figure C3). $\delta^{13}C$ values from the guano extract without density separation from Pass 1 is generally more positive than those from other chemical extracts. $\delta^{13}C$ values from the same samples repeated using density separation also have more negative $\delta^{13}C$ values by 1-2‰, but were similar to $\delta^{13}C$ measurements on guano extract samples from Pass 2 recovered from the same depth. Although $\delta^{13}C$ profiles from Pass 1 and Pass 2 are generally similar, all extracts from Pass 2 display a large spike in $\delta^{13}C$ values at 48-52 mm, and may exhibit more noise than $\delta^{13}C$ values analyzed from Pass 1. As expected, the solvent extract (lipid fraction) has the most negative $\delta^{13}C$ values (Figure C3). δD values on chitin and solvent extracts from Pass 2 also display this stepwise increase (transition), although this is not as obvious a feature in the solvent extract. Although δD values

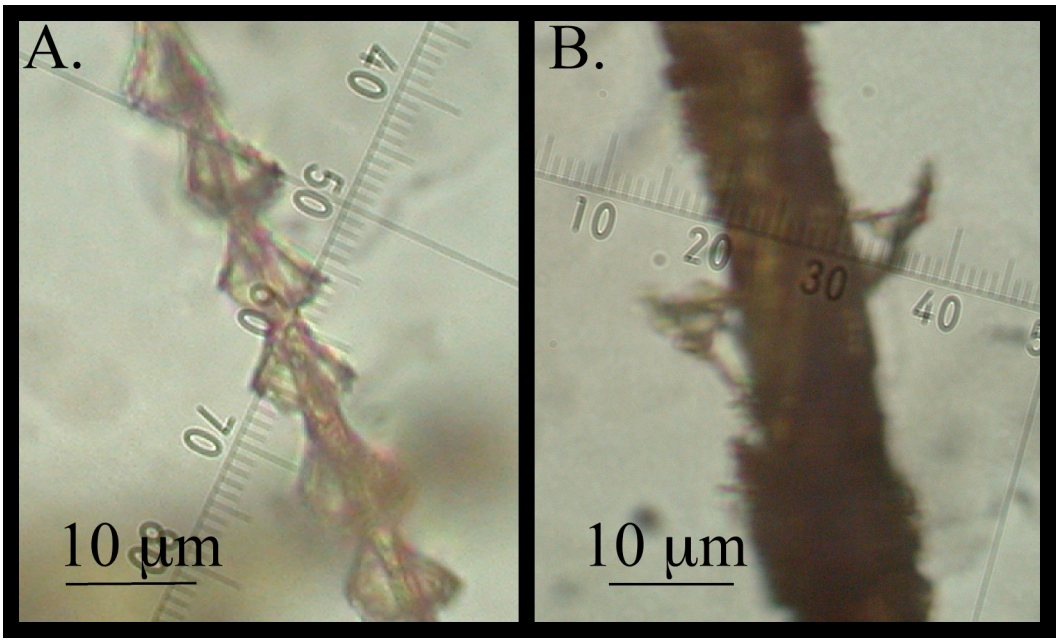

Figure C2—Two digital images of example bat hair recovered from guano core 96-04.

A. is identified to the genus *Tadarida* and recovered from a Holocene sample. B. identification is less certain due to lack of scales.

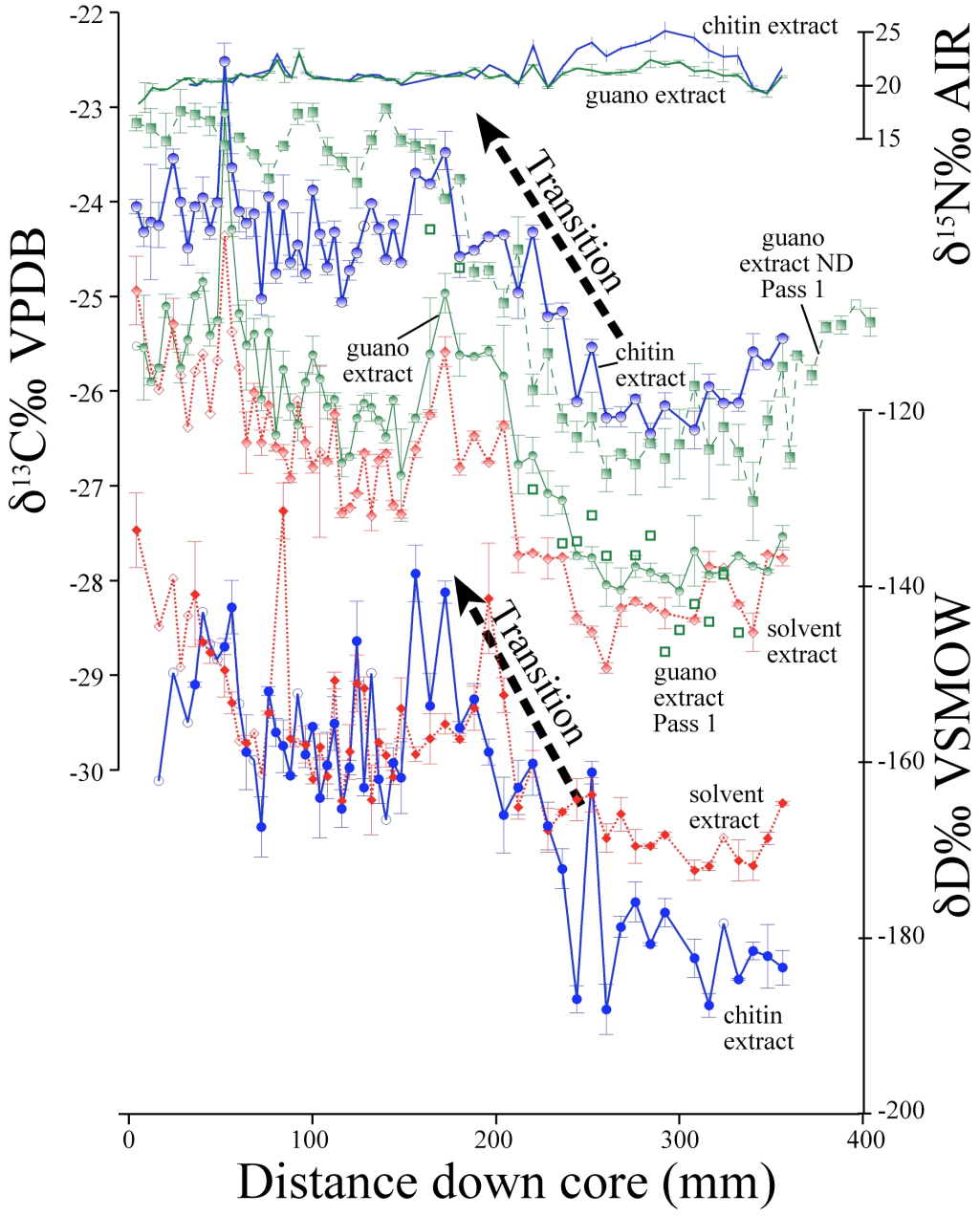

Figure C3—Isotope profiles for various chemical extracts of guano core material recovered from Bat Cave, Grand Canyon National Park.

Solid symbols refer to □D values, graded symbols refer to □^{13}C values, and no symbols refer to □^{15}N values. Green (squares) indicate guano extract, blue (circles) refer to chitin extract, and red diamonds indicate solvent extract. Open symbols denote single sample analysis due to limited supply. In particular, open green squares refer to single sample analysis on repeats of guano extract from Pass 1 originally analyzed without using density separation. Replicates utilized density separation chemical techniques.

Table C3—Correlation among Pass 2 chemical extract isotope profiles.

A * indicates significant correlation at the 1% level. N.S. signifies non-significance. A † denotes that outlier(s) were removed. Subscripts GE, CE, and L indicate guano, chitin, and solvent chemical extracts, respectively. Pre-T, T, and Post-T indicate covariates split by pre-transition, transition, and post-transition, respectively.

Covariates	r^2	slope	intercept	N	t
$\delta^{13}C_{ge}$ vs. $\delta^{13}C_{ce}$*	0.86	0.74	-5.2	60	18.8
$\delta^{13}C_{ge}$ vs. $\delta^{13}C_{l}$*	0.86	0.89	-4.1	59	19.95
$\delta^{13}C_{ce}$ vs. $\delta^{13}C_{l}$*	0.78	1.03	-1.2	60	14.47
ΔD_{ce} vs. ΔD_{l}*†	0.59	0.42	-91.4	45	7.87
ΔD_{ce} vs. $\delta^{13}C_{ce}$*†	0.81	0.06	-15.3	56	14.93
ΔD_{l} vs. $\delta^{13}C_{l}$*†	0.69	0.09	-12.9	55	10.66
$\delta^{15}N_{ge}$ vs. $\delta^{15}N_{ce}$*	0.63	1.66	-10.2	53	9.24
ΔD_{ce} vs. $\delta^{13}C_{ce}$*† Post-T	0.42	0.03	-18.9	28	4.36
ΔD_{ce} vs. $\delta^{13}C_{ce}$* T	0.82	0.05	-15.95	15	7.72
ΔD_{ce} vs. $\delta^{13}C_{ce}$ Pre-T (N.S.)	0.09	-0.03	-31.17	11	-0.97

compare favorably with $\delta^{13}C$ values, there is no apparent spike at 48-52 mm, rather δD values increase less distinctly near this point. Interestingly, solvent extract δD values are more positive than chitin extract values prior to the transition, but overlap post-transition (Figure C3). There are strong covariations among $\delta^{13}C$ and δD values from the varying chemical derivatives (Table C3). In contrast to $\delta^{13}C$ and δD values, $\delta^{15}N$ values of guano and chitin extracts are relatively constant and are more positive than most organic $\delta^{15}N$ values.

C-3.3 C, N, and H weight percent and C:N and N:H elemental ratios

Samples were split for different chemical extracts and isotope analyses, necessitating minimal amounts of material used in each analysis. Although isotope analyses were generally reproducible at acceptable precisions, amount percents were not as reproducible. In particular, N% for many samples are very small, ranging from 0.6 to 4.0% with an average of 1.6%. The case was similar for H%, which ranged from 0.6 to 2.5%, with an average of 1.3%. Percent organic carbon and nitrogen varied in some repeated samples, indicating varying mineral components. Therefore elemental ratios are only a rough guide to chemical purity and substance, and are expected to have relatively large errors. C:N ratios are expected to be the best indicator as they are determined in same run. N% and H% are similar in magnitude and therefore sample N:H ratios are considered the next best chemical indicator. However, C% and H% differ by an order of magnitude and are determined via different methods on different runs and are not considered as reliable.

To determine if isotopic values are a result of varying organic components, C:N and N:H ratios were compared to $\delta^{13}C$ and δD values (Table C4). It is clear that the guano extract's $\delta^{13}C$ values have a strong and significant relationship with C:N ratios. However, the chitin extract's $\delta^{13}C$ values display a weak and generally non-significant relationship with C:N and N:H ratios (Table C4). If only samples with C:N ratios between 6 and 8 are examined, no significant relationship is observed. As a further test of diagenesis on the chitin extract, C:N and N:H ratios were split among different time periods: (1) prior to the transition, (2) within the transition, and (3) after the transition (Table C5). Neither C:N

Table C4—Correlation among Pass 2 chemical extract elemental ratio and isotope value covariates.

A * indicates significant correlation at the 1% level, N.S. signifies non-significance. Subscripts GE and CE, indicate guano and chitin chemical extracts, respectively. T indicates only covariates within the transition are considered.

Covariates	r^2	N	t
C:N vs. $\delta^{13}C_{ge}$*	0.78	62	-14.58
C:N vs. $\delta^{13}C_{ce}$ (N.S.)	0.03	55	-1.2
N:H vs. $\delta^{13}C_{ce}$*	0.32	53	4.9
C:N vs. δD_{ce} (N.S.)	0.04	53	-1.45
N:H vs. δD_{ce}*	0.21	52	3.68
C:N vs. $\delta^{13}C_{ce}$ T (N.S.)	0.32	15	-2.44
C:N vs. δD_{ce} T (N.S.)	0.36	15	-2.68
N:H vs. $\delta^{13}C_{ce}$ T (N.S.)	0.26	15	2.12
N:H vs. δD_{ce} T (N.S.)	0.18	15	1.69

Table C5—C:N and N:H ratios of sample material used in chapter 5.
Elemental ratios of only samples with C:N ratios between 6 and 8 are presented in the "selected" category.

Elemental Ratio		Pre-Transition	Transition	Post-Transition	All samples	Idealized chitin
C:N	all	6.6±1.1	5.7±1.3	6.6±0.8	6.2±1.1	6.9
	selected	6.7±0.7	6.7±0.7	7.0±0.5	6.8±0.6	
N:H	all	0.8±0.2	1.0±0.3	1.1±0.3	1.0±0.3	1.2
	selected	0.8±0.2	1.2±0.6	1.1±0.1	1.1±0.4	

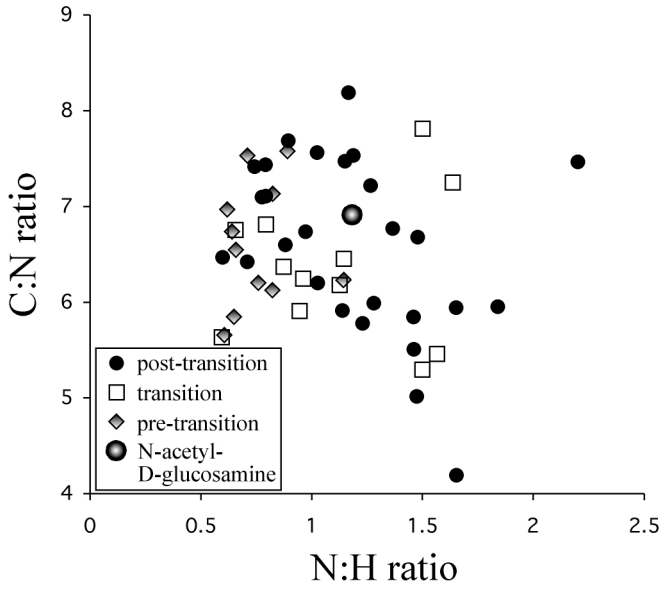

Figure C4—C:N and N:H ratios of individual samples.

Table C6—Information on Radiocarbon dating.

Core Location	Core	$\delta^{13}C$ value ‰ VPDB	Radiocarbon Years BP	Laboratory Number	Laboratory
Surface	96-04	-24.4	5620±70	Beta #95152	Beta Analytic
56-60 mm	96-04		6490±50	GdA-494	Gliwice
144-152 mm	96-04	-25.9	10130±60	GdA-319	Gliwice
256-264 mm	96-04	-27.2	10230±60	GdA-321	Gliwice
End	96-04	-22.5	12400±90	Beta #95153	Beta Analytic
96-104 mm	96-05	-24.0	7550±40	GdA-318	Gliwice
184-192 mm	96-05	-28.9	9490±50	GdA-320	Gliwice
274-280 mm	96-05	-32.1	15300±100	GdA-322	Gliwice

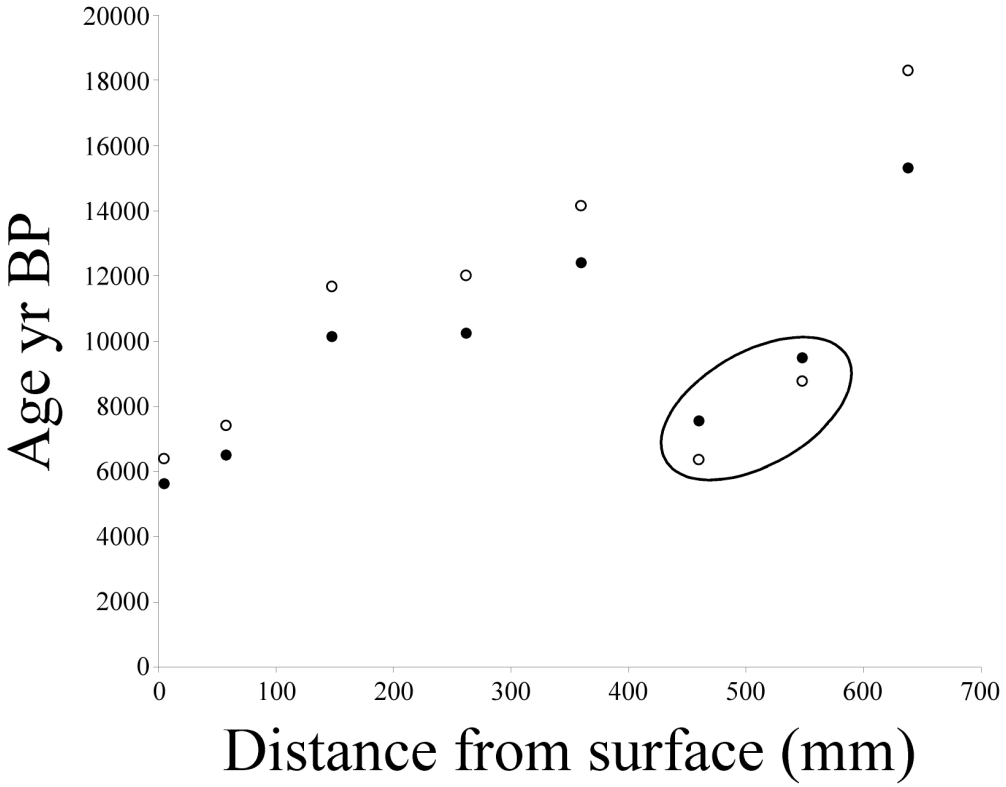

Figure C5—Age vs. depth in guano cores

Filled circles indicate radiocarbon age, open circles indicate most probable calendar age, calibrated by Calib 5.0 (Stuiver and Reimer, 1998; Reimer et al., 2004). Two dates (circled) appear young.

nor N:H ratios were significantly different among these time periods (Kruskal-Wallis test, $\alpha = 0.01$; $H_{[2,56]} = 5.99$; $H_{[2,56]} = 8.12$); however, N:H ratios were significantly different at the 5% level. No significant relationship was found using only samples with C:N ratios between 6 and 8 (Kruskal-Wallis test, $\alpha = 0.05$, $H_{[2,33]} = 5.45$). A plot of C:N as a function of N:H ratio shows that the elemental ratios of most samples are near the theoretical chitin value (N-acetyl-D-glucosamine), when considering the potential error, although a few are notably different in both C:N and N:H ratio (Figure C4).

C-3.4 Radiocarbon dates

Six of eight radiocarbon dates on TOC samples taken from both cores 96-05 and 96-04 fall in line with a reasonably constant deposition rate (Figure C5), although two dates from core 96-05 are conspicuously young (Table C6). All five dates from 96-04 monotonically increase with depth. Notably, two dates correspond to the end of the Younger Dryas event, and were from taken from samples representing the beginning and end of the transition, suggesting a rapid deposition rate at this time.

C-4 Discussion

C-4.1 $\delta^{13}C$ and δD values of chemical extracts

The most pertinent question herein regards the faithfulness of $\delta^{13}C$ and δD values as a biomarker for original values at the time of deposition or, in other words, what is the nature of diagenesis on the isotopic values. This question must be evaluated before inferring any past environmental conditions. Toward this goal, isotopic profiles from different chemical derivatives and elemental ratios were compared and assessed.

$\delta^{13}C$ values on all chemical derivatives show a similar pattern with strong covariation. δD values measured on the chitin extract, and to a more limited extent the solvent extract, also exhibit a similar pattern with strong covariations. In particular, each isotopic profile shows a distinct stepwise increase at 10.1 to 10.2 ^{14}C kyr BP. The similarity and especially the timing of this transition in each isotopic profile regardless of chemical makeup argues to some extent that this rise is an environmental signal and not

diagenetic, or at least is climatically driven. Mizutani and Wada (1988) found little overall fractionation in $\delta^{13}C$ during soil organic matter decomposition, in stark contrast to $\delta^{15}N$ values. In this study, $\delta^{15}N$ values are relatively constant and more positive than originally deposited values are expected to have had; this finding is consistent with volitization of ammonia described previously for seabird guano (Mizutani and Wada, 1988). Additionally, nitrogen in insect chitin incorporates recycled urea during production and therefore, $\delta^{15}N$ values do not trace insect diet nor trophic level (Webb et al., 1998).

It is almost surprising that δD values so strongly mirrors $\delta^{13}C$ values as they were expected to be much more prone to error. To begin, δD values are much more negative than expected, more negative than the grasshopper chitin δD value collected in Saskatchewan, Canada, and used as a standard forcing extrapolation of calculated chitin extract δD_n value. Secondly, some contamination was expected from hydrogen released from the mineral component as samples were not completely organic. Nonetheless, the strong correlation between δD and $\delta^{13}C$ covariates infers that the δD profile is not overly influenced by degradation nor contamination.

Although the same general pattern is repeated among the isotope profiles of various chemical extracts, there is a difference in the magnitude of change. $\delta^{13}C$ values are more negative by using density separation as evidenced on repeated samples from Pass 1. There may be a number of reasons for this observation. First, the density separation liquid or the sieve size may fractionate the material. Additionally, the samples were re-suspended in HCl. It was observed that HCl became cloudy and brown after suspension of samples indicating potential dissolution of an organic fraction. However, $\delta^{13}C$ values from Pass 1 guano extract with density separation and Pass 2 guano extract (also with density separation) are similar at the same location in the core.

C-4.2 Diagenesis and elemental ratios

The guano extract from Pass 2 had higher C:N ratios toward the bottom of the core, and was significantly and strongly correlated with $\delta^{13}C$ values. However, after a complete solvent wash, there was a general lack of significant covariations between isotope values ($\delta^{13}C$ and δD) and elemental ratios (C:N and N:H), most notably over the transition. Both

C:N and N:H ratios of chitin extract are close to theoretical chitin especially when considering potential error. It was difficult to determine, because of inherent errors in C%, N%, and H%, if values of certain samples are not reliable. The N% and H% of several samples were near detection limits, based on one value only, or repeats were not reproducible.

To further test influence of chemical changes, a non-parametric Kruskal-Wallis test was performed by splitting C:N and N:H ratios in three groups: pre-transition, transition, and post-transition. No significant difference was found between these groups and C:N ratios. However, a significant difference was noted between N:H ratio divided in groups at the 5% level, though not at the 1% level. This finding may simply be an artifact of error and a low sample size for the pre-transition. However, there may be more of a hydrogen component present prior to the transition. This might explain the weak but significant correlations between δD and $\delta^{13}C$ values and N:H ratio. This additional hydrogen may be a contribution of a background mineral component, and may explain why there is no significant correlation between $\delta^{13}C$ and δD values for this grouping. However, when repeating the Kruskal-Wallis test using only samples with C:N ratios between 6 and 8 no significance is found at either the 1% or 5% levels.

Chemical variance is also expected in part because natural chitin is partially de-acetylated, and tightly bound to protein, especially in schlerotized insect cuticles (Schimmelmann and DeNiro, 1986a,b; Schimmelmann et al., 1993; Schimmelmann and Miller, 2002). Both serve to decrease the C:N ratio from 6.9 of theoretical N-acetyl D-glucosamine. The presence of lipids, however will serve to increase the C:N ratio. Both the acetyl group of chitin and lipids have more negative $\delta^{13}C$ values compared to the N-acetyl D-glucosamine polysaccharide (Schimmelmann and DeNiro, 1986a). Therefore, chemical changes should invariably lead to strong correlations between elemental ratios and isotope values, which is not the case for the chitin extract in this study. Because the cores are retrieved from a bat guano cave, insectivorous bat guano is dominantly composed of finely commutated insect exoskeletons (McFarlane et al., 2002), and the C:N and N:H ratios are close to theoretical chitin, it follows that the chitin extract is indeed natural chitin from insects deposited by bats through the Holocene, with much of the protein degraded. Chitin is a biopolymer considered to be resistant to biodegradation

(e.g., Miller et al., 1991). However, in aqueous sediments chitin breaks down rapidly in the presence of bacteria and chitinase (Poulick et al., 1985; Stankiewitz et al., 1998). In terrestrial regions, chitin is more resistant, especially in arid regions where chitin is effectively mummified (Mizutani et al., 1992a; Shahack-Gross et al., 2004). Experiments on sub-fossil insect cuticles indicate that chitin is rarely found beyond 100,000 years (Briggs, 1999), even in insects trapped in amber, although the presence of chitin has been found back to 25 m.y.a (Stankiewitz et al., 1997). The nature of preservation can be dependent on the depositional environment (Briggs, 1999). When chitin degradation occurs it is associated with an increase in aliphatic compounds (Briggs, 1999). The results from this study confirm this conclusion, as there is a general increase in the amount of solvent extract recovered in the older portions of the core. However, $\delta^{13}C$ values, and to a more limited extent δD values, indicate that the solvent extract may be a good biomarker if it is accepted that the chitin extract is original material. Nonetheless, $\delta^{13}C$ and δD values of the chitin extract are considered the most reliable for environmental interpretation, especially when selecting only samples with C:N ratios between 6 and 8.

C-4.3 Radiocarbon dates

Radiocarbon dating was performed on TOC. Washing samples with alkaline treatment resulted in the dissolution of the organic sample, and therefore only acid treatment was employed at Gliwice radiocarbon facilities (N. Piotrowska, personal communication). Two of eight radiocarbon dates appear too young, and may have been contaminated, for which polysaccarides are notably susceptible through the Maillard reaction (Hodgins et al., 2001), although this process is found to not effect chitin (Tripp et al., 2004). The other dates are monotonic and show a reasonably constant deposition rate except at the transition where very rapid deposition occurred. As dates were performed on TOC, and not explicitly on a chitin extract, there may be some cause for concern. However, a number of reasons suggest 96-04 core dates are reliable. First, dates for 96-04 are monotonic and performed at two radiocarbon laboratories. Second, the transition is dated at the end of the Younger Dryas, a time known for abrupt global climate change (e.g., Peteet, 1995), and unlikely a chance event. Third, $\delta^{13}C$ values for

the chitin extract mirror those of the guano extract (TOC), suggesting the same age among various extracts. Fourth, observed stratigraphy suggest carbon transfer (old or young) did not occur (N. Piotrowska, personal communication). Additionally, two independent studies have found only acid/solvent treatment necessary on insect cuticles to obtain radiocarbon dates consistent with radiocarbon dates on more traditional substances (peat/ cellulose) in a well-constrained depositional environment (Hodgins et al., 2001; Tripp et al., 2004). Finally, this method (dating TOC) is commonly performed in the literature. Nonetheless, it would be advisable to compare dates on different chemical extracts to support or refute this reasoning.

C-5 Conclusions

1) Diagenesis is not likely a significant influence on $\delta^{13}C$ or δD values of chemical extracts. Although diagenetic influences cannot be completely ruled out, both the covariations among various extracts, the lack of significant covariation between elemental ratios and isotope values for the chitin extract, and the lack of significant differences between elemental ratios and age attest to a lack of diagenetic influence.
2) The chitin extract is the best chemical derivative as elemental ratios can be used as a guide to diagenesis or contamination. Improved confidence is achieved by selecting only material with C:N elemental weight ratios between 6 and 8. Solvent extracts are likely secondarily derived, although the strong and significant covariation with the chitin extract, at least for $\delta^{13}C$ values, suggests that the solvent extract may nonetheless be a satisfactory biomarker. The guano extract isotopic profiles are the least useful as they are too influenced by the proportion of lipids present.
3) In particular, the transition in $\delta^{13}C$ and δD values is likely environmentally induced change. Even if diagenetically influenced, the timing at the end of the Younger Dryas likely points to a climatically driven signal.
4) Radiocarbon dates on TOC are generally reliable, but it would be desirable to test this conclusion by examining radiocarbon dates on different extracts from the same sample.

5) In future studies, a number of improvements can be attempted. First, better standard controls for δD_n values are required. Second, additional chemical techniques can be attempted. For example, a better density separation technique, use of a chitin solvent, or a mild treatment of a de-proteination step may improve results and confidence of isotopic analyses. Finally, better confidence in elemental ratios will provide more confidence in chemical homogeneity and substance.